

Asymmetric Transition Metal-Catalyzed Allylic Substitution Reactions

Thesis submitted in accordance with the requirements of the
University of Liverpool for the degree of Doctor in Philosophy

Elizabeth Adair Clizbe

April 2010

**Asymmetric Transition Metal-Catalyzed Allylic
Substitution Reactions**

Elizabeth Adair Clizbe

Abstract

The metal-catalyzed allylic substitution reaction has been studied using a wide array of transition metal complexes, and represents an important sp^3 cross-coupling reaction for the construction of tertiary and quaternary carbon-carbon and carbon-heteroatom bonds. Although a variety of transition metal complexes now provide enantiomerically enriched acyclic secondary allylic amines in a highly regioselective manner with more conventional nitrogen pronucleophiles, the examination of charge-separated derivatives has not been forthcoming. It was envisaged that aza-ylides would be excellent stabilized pronucleophiles in the allylic amination reaction due to their low basicity. We have developed a regio- and enantiospecific rhodium-catalyzed allylic amination reaction utilizing the aza-ylide of 1-aminopyridinium iodide as the pronucleophile. Further investigations focused on expanding the process to other aza-ylides, which prompted the development of a highly regio- and enantioselective iridium-catalyzed allylic amination using *S,S*-diphenylsulfilimine as the pronucleophile. This study demonstrates the ability to tune the reactivity of the aza-ylides depending on the catalyst.

The asymmetric α -alkylation of ketone enolates represents one of the most important and challenging carbon-carbon bond forming reactions in organic synthesis. Although, the asymmetric α -alkylation of ketone enolates has utilized chiral auxiliaries for stereoinduction, recent developments have been made in the enantioselective palladium-catalyzed allylic alkylation reaction using unstabilized ketone enolates. We envisioned that utilizing a chiral phosphite in conjunction with Wilkinson's catalyst would create a chiral environment sufficient at inducing enantioselectivity. In this context, we have developed an enantioselective rhodium-catalyzed allylic allylation of α -alkoxy prochiral ketones using a monodentate chiral phosphite ligand, which avoids the necessity for pre-activation of the ketone.

Acknowledgements

I would not be where I am today if it were not for a countless number of individuals. I would like to thank all the educators that I have had throughout the years. I would not have the same level of knowledge and appreciation if it were not for their dedication to teaching. I am especially indebted to my research advisor, P. Andrew Evans for the opportunity that he bestowed upon me to be a part of a wonderful research environment. I am grateful for all of the advice and guidance he has given me throughout the years, helping me grow as a chemist.

I am forever grateful to all the colleagues (professors, staff, and students) that I have had at both Indiana University and The University of Liverpool. I would also like to acknowledge all of the Evans' group members, both past and present. You are all a second family to me. No matter what curves were thrown our way, we kept pushing on with the support of one another. The knowledge that was shared is invaluable, and the times that we have had together are unforgettable.

Finally, I would like to thank my family and friends for their endless love, support and encouragement. I would especially like to thank my mom for showing me that you can accomplish anything if you set your mind to it and for never voicing hesitations that I might be taking on too much. She is always there supporting me through the good times and bad, and all the hours on the phone and e-mails shared are priceless. I would not have been able to do it without her.

Table of Contents

<i>Abstract</i>	ii
<i>Acknowledgments</i>	iii
<i>List of Schemes</i>	viii
<i>List of Tables</i>	xi
<i>List of Figures</i>	xiii
<i>List of Abbreviations</i>	xiv

Chapter 1 ASYMMETRIC ALLYLIC AMINATION

1.1	Introduction	1
1.2	Metal-Catalyzed Stereoselective Allylic Amination	1
1.2.1	Introduction to Mechanism	1
1.2.2	Dynamic Kinetic Asymmetric Transformations (DKAT)	
	Reactions	3
1.2.2.1	Symmetrical Substrates in DKAT Reactions	3
1.2.2.2	Unsymmetrical Substrates in DKAT Reactions	9
1.2.3	Enantioselective Metal-Catalyzed Allylic Amination Reactions	12
1.2.3.1	Intramolecular Enantioselective Allylic Amination	
	Reactions	13
1.2.3.2	Intermolecular Enantioselective Allylic Amination	
	Reactions	15
1.3	Stereospecific Metal-Catalyzed Allylic Amination Reactions	27
1.4	Organocatalytic Allylic Amination Reactions	33
1.5	C-H Activation	35
1.5.1	Intramolecular C-H Activation Reactions	35
1.5.2	Intermolecular C-H Activation Reactions	36
1.5.3	Diamination	36
1.6	Hydroamination	37
1.6.1	Addition to Allenes	38
1.6.1.1	Intramolecular Addition to Allenes	38
1.6.1.2	Intermolecular Addition to Allenes	39

1.6.2	Addition to Conjugated Olefins	40
1.7	Rearrangements	41
1.7.1	[2.3]-Sigmatropic Rearrangements	41
1.7.2	[3.3]-Sigmatropic Rearrangements	43
1.8	Final Remarks	47
1.9	References	48

Chapter 2 REGIO- AND ENANTIOSPECIFIC RHODIUM-CATALYZED ALLYLIC AMINATION WITH AZA-YLIDES

2.1	Introduction	55
2.2	Origin of Regioselectivity and Enantiospecificity	55
2.3	Regioselective and Enantiospecific Rhodium-Catalyzed Allylic Amination Utilizing an Aza Ylide Nucleophile	58
2.3.1	Introduction	58
2.3.2	Use of Ylide Pronucleophiles	59
2.3.3	Optimization and Scope of the Rhodium-Catalyzed Allylic Amination Reaction	60
2.4	Cleavage of Nitrogen-Nitrogen bonds	65
2.4.1	Background	65
2.4.2	Conversion to Free Amine	67
2.4.3	One-Pot Deprotection Utilizing Catalytic Base	68
2.5	Optimization of the Regiospecific Rhodium-Catalyzed Allylic Amination Reaction Utilizing Catalytic Base	72
2.6	Conclusion	76
2.7	Experimental	77
2.8	References	94
	Appendix 2.1	98

Chapter 3 REGIO- AND ENANTIOSELECTIVE IRIIDIUM-CATALYZED ALLYLIC AMINATION

3.1	Introduction	103
3.2	Origin of Stereoselectivity	103

3.2.1	Regioselectivity and Memory Effect	103
3.2.2	Enantioselectivity	107
3.3	Iridium-Catalyzed Allylic Amination Reaction utilizing a Sulfilimine Nucleophile	110
3.3.1	Introduction	110
3.3.2	Reaction Optimization	110
3.3.3	Substrate Scope	112
3.3.4	Optimization of Alkyl Substrates	113
3.4	Cleavage of Sulfilimine Bond	116
3.4.1	Background	116
3.4.2	Conversion to the Free Amine	117
3.5	Conclusion	118
3.6	Experimental	118
3.7	References	140

Chapter 4 ENANTIOSELECTIVE RHODIUM-CATALYZED ALLYLATION OF α -ALKOXY KETONE ENOLATES

4.1	Introduction	143
4.1.1	Transition Metal-Catalyzed Allylation Reactions	143
4.1.2	Pronucleophile Scope	143
4.1.3	Non-Metal Allyl Methods for Performing Enantioselective and Diastereoselective Allylations	144
	4.1.3.1 Chiral Auxiliary-Based Allylations	144
	4.1.3.2 Enantioselective Palladium-Catalyzed Allylations	146
4.2	Rhodium-Catalyzed Allylic Substitution: Mechanistic Background	151
4.2.1	Introduction	151
4.2.2	Pre-Catalyst Composition: Effect of the Trimethyl Phosphite Modifier	153
4.3	Rhodium-Catalyzed Enantioselective Allylation	155
4.3.1	Hypothesis	155
4.3.2	Reaction Optimization	156
4.3.3	Substrate Scope	157
4.3.4	Enolate Geometry	160

4.3.5	Baeyer-Villiger	161
4.3.5.1	Background	161
4.3.5.2	Application Towards Rhodium-Catalyzed Allylation	162
4.4	Conclusions	163
4.5	Experimental	163
4.6	References	184

List of Schemes

Chapter 1 ASYMMETRIC ALLYLIC AMINATION

Scheme 1.1	<i>Metal-Catalyzed Allylic substitution pathway.</i>	2
Scheme 1.2	<i>Various pathways for the formation of enantiomerically enriched products through the transition-metal catalyzed allylic substitution.</i>	3
Scheme 1.3	<i>Regioselectivity in transition metal-catalyzed allylic substitution reactions.</i>	9
Scheme 1.4	<i>Possible intermediates in the metal-catalyzed allylic substitution reaction.</i>	12
Scheme 1.5	<i>Ni-mediated allylic amination towards the synthesis of L-vinylglycine.</i>	15
Scheme 1.6	<i>Synthesis of tetrahydropyridine 68 through iridium-catalyzed allylic amination/RCM.</i>	18
Scheme 1.7	<i>Iridium-catalyzed allylic amination with ammonia.</i>	22
Scheme 1.8	<i>Synthesis of (S)-vigabatrin utilizing iridium-catalyzed allylic amination.</i>	23
Scheme 1.9:	<i>Two-Step synthesis of (S)-nicotine.</i>	26
Scheme 1.10	<i>Mechanism of rhodium-catalyzed substitution.</i>	28
Scheme 1.11	<i>Construction of cis- and trans-2,5-disubstituted pyrrolines.</i>	29
Scheme 1.12	<i>Synthesis of dihydrobenzo[b]indolines via Rh-catalyzed allylic amination/RCM/radical cyclization.</i>	30
Scheme 1.13	<i>Key step in the preparation of Batzelladine D.</i>	32
Scheme 1.14	<i>Rhodium-catalyzed allylic amination reaction with an aza-ylide pronucleophile.</i>	33
Scheme 1.15	<i>Synthesis of Boc-protected γ-amino nitrile via organocatalysis.</i>	34
Scheme 1.16	<i>Use of the diamination reaction enroute to tetraamine 147.</i>	37
Scheme 1.17	<i>P receptor antagonist (+)-CP-99,994</i>	37

Scheme 1.18	<i>Synthesis of (S)-valine 174 through a [3.3]-sigmatropic rearrangement.</i>	44
Scheme 1.19	<i>Key step in the synthesis of lentiginosine.</i>	45
Chapter 2.	REGIO AND ENANTIOSPECIFIC RHODIUM-CATALYZED ALLYLIC AMINATION WITH AZA-YLIDES	
Scheme 2.1	<i>Regioselectivity in rhodium-catalyzed allylic substitution.</i>	56
Scheme 2.2	<i>Proposed mechanism for the rhodium-catalyzed allylic substitution reaction.</i>	58
Scheme 2.3	<i>Confirmation of absolute stereochemistry</i>	68
Chapter 3	REGIO- AND ENANTIOSELECTIVE IRIIDIUM-CATALYZED ALLYLIC AMINATION	
Scheme 3.1	<i>“Memory effect” in the iridium-catalyzed allylic substitution</i>	105
Scheme 3.2	<i>Effects of olefin geometry in the iridium-catalyzed allylic substitution reaction.</i>	106
Scheme 3.3	<i>Iridium-phosphoramidite ligand complexes</i>	108
Scheme 3.4	<i>Mechanistic pathway for the enantioselective iridium-catalyzed allylic amination using phosphoramidite ligand L-3.</i>	109
Scheme 3.5	<i>Acid and base hydrolysis of sulfilimine (-)-31.</i>	117
Chapter 4	ENANTIOSELECTIVE RHODIUM-CATALYZED ALLYLATION OF α-ALKOXY KETONE ENOLATES	
Scheme 4.1	<i>Diastereoselective allylation towards the synthesis of (+) morinol B.</i>	146
Scheme 4.2	<i>Construction of (S)-oxybutynin intermediate 29 via palladium-catalyzed allylic allylation.</i>	150
Scheme 4.3	<i>Reaction profile for the metal-catalyzed allylic alkylation reaction with acyclic 3-substituted propenyl derivatives.</i>	152
Scheme 4.4	<i>Results of in situ modification of Wilkinson’s catalyst with P(OMe)₃.</i>	153

Scheme 4.5	<i>Preparation of E- and Z-silyl enol ethers of 38.</i>	160
Scheme 4.6	<i>Rhodium-allylation starting from silyl enol ethers.</i>	161
Scheme 4.7	<i>Baeyer-Villiger oxidation of α-alkoxyketones.</i>	162
Scheme 4.8	<i>Preparation of alcohol 52.</i>	163

List of Tables

Chapter 1 ASYMMETRIC ALLYLIC AMINATION

Table 1.1	<i>Enantioselective allylic amination utilizing sulfur ligands.</i>	5
------------------	---	---

Chapter 2. REGIO AND ENANTIOSPECIFIC RHODIUM-CATALYZED ALLYLIC AMINATION WITH AZA-YLIDES

Table 2.1.	<i>Examination of various aza-ylides in the regioselective rhodium-catalyzed allylic amination reaction ($R = Ph(CH_2)_2$)</i>	60
Table 2.2.	<i>Optimization of the regioselective rhodium-catalyzed allylic amination reaction using 1-aminopyridinium iodide ($R = Ph(CH_2)_2$)</i>	61
Table 2.3	<i>Examination of the acid quench of the amination reaction ($R = Ph(CH_2)_2$).^a</i>	62
Table 2.4	<i>Scope of the regioselective rhodium-catalyzed allylic amination reaction with the 1-aminopyridinium ylide.</i>	64
Table 2.5	<i>Reductive-cleavage to afford chiral amine (S)-23j.</i>	67
Table 2.6	<i>Optimization of the rhodium-catalyzed allylic amination reaction utilizing catalytic potassium carbonate ($R = Ph(CH_2)_2$)</i>	69
Table 2.7.	<i>Optimization of one-pot allylic amination and reductive cleavage ($R = Ph(CH_2)_2$).</i>	70
Table 2.8.	<i>Optimization of the regioselective rhodium-catalyzed allylic amination reaction using 1-aminopyridinium iodide ($R = Ph(CH_2)_2$).</i>	72
Table 2.9	<i>Scope of the regioselective rhodium-catalyzed allylic amination reaction with the 1-aminopyridinium ylide and catalytic DBU.</i>	73
Table 2.10	<i>Enantiospecificity over time in the rhodium-catalyzed allylic amination reaction utilizing catalytic DBU.</i>	74
Table 2.11	<i>Enantiospecific rhodium-catalyzed allylic amination: time course dependence of the enantiospecificity ($R = BnOCH_2$).</i>	75

Table 2.12	<i>Effect of concentration on the enantiospecific rhodium-catalyzed allylic substitution reaction (R = BnOCH₂).</i>	76
-------------------	--	----

Chapter 3 REGIO- AND ENANTIOSELECTIVE IRIIDIUM-CATALYZED ALLYLIC AMINATION

Table 3.1	<i>Optimization of the regio- and enantioselective iridium-catalyzed allylic amination reaction using S,S-diphenylsulfilimine.</i>	111
Table 3.2	<i>Scope of the enantioselective iridium-catalyzed allylic amination reaction with S,S-diphenyl sulfilimine.</i>	113
Table 3.3	<i>Optimization of the regio- and enantioselective iridium-catalyzed allylic amination reaction with alkyl substrates.</i>	115
Table 3.4	<i>Scope of the enantioselective iridium-catalyzed allylic amination reaction with alkyl derivatives.</i>	116

Chapter 4 ENANTIOSELECTIVE RHODIUM-CATALYZED ALLYLATION OF α -ALKOXY KETONE ENOLATES

Table 4.1	<i>Optimization of the enantioselective rhodium-catalyzed allylic alkylation reaction.</i>	157
Table 4.2	<i>Scope of the enantioselective rhodium-catalyzed allylic alkylation reaction with the α-alkoxy lithium enolates.</i>	159

List of Figures

Chapter 1 **ASYMMETRIC ALLYLIC AMINATION**

- Figure 1.1** *Phosphorus based ligands used in palladium-catalyzed asymmetric allylic amination.* 4
- Figure 1.2** *Phosphorus based ligands used with unsymmetrical substrates.* 10
- Figure 1.3** *Phosphorus based ligands used in the enantioselective allylic amination reaction.* 13

Chapter 2. **REGIO AND ENANTIOSPECIFIC RHODIUM-CATALYZED ALLYLIC AMINATION WITH AZA-YLIDES**

- Figure 2.1.** *Relative stability of various ylides based on field and resonance stability.* 59

Chapter 3 **REGIO- AND ENANTIOSELECTIVE IRIIDIUM-CATALYZED ALLYLIC AMINATION**

- Figure 3.1** *Commonly used phosphoramidite ligands.* 107

Chapter 4 **ENANTIOSELECTIVE RHODIUM-CATALYZED ALLYLATION OF α -ALKOXY KETONE ENOLATES**

- Figure 4.1** *Rhodium allyl phosphonate complex by NMR.* 155

List of Abbreviations

$[\alpha]_D^t$	specific rotation at temperature t and wavelength of sodium D line
Å	angstrom
Ac	acetate
Acac	acetylacetonato
Ar	aryl
APT	attached proton test
BINAP	2,2'-bis(diphenylphosphino)-1-1'-binaphthyl
BINOL	1,1'-bi-2-naphthol
BIPHEP	biphenylphosphine
Bn	benzyl
BOC	<i>tert</i> -butoxycarbonyl
BSA	<i>N,O</i> -Bis(trimethylsilyl)acetamide
ⁿ Bu	butyl
^t Bu	<i>tert</i> -butyl
Bz	benzoyl
c	concentration
°C	degrees Celsius
<i>cee</i>	conservation of enantiomeric excess
CI	chemical ionization
cod	1,5-cyclooctadiene
dba	dibenzylideneacetone
dbcot	dibenzo[<i>a,e</i>]cyclooctatetraene
DCM	dichloromethane
DEAD	diethyl azodicarboxylate
DIAD	diisopropyl azodicarboxylate
δ	NMR chemical shift in parts per million
DBU	1,8-diazobicyclo[5.4.0]undec-7-ene
DMAP	4-dimethylaminopyridine
DMF	dimethylformamide

DMSO	dimethyl sulfoxide
dppe	bisdiphenylphosphinoethane
<i>ds</i>	diastereoselectivity
EA	ethyl acetate
<i>ee</i>	enantiomeric excess
EI	electron ionization
<i>ent</i>	enantiomer
eq	equation
Et	ethyl
equiv.	equivalent
eV	electronvolt
FC	flash chromatography
FTIR	Fourier transform infra-red
g	gram
^c Hex	<i>cyclo</i> -hexyl
HMDS	bis(trimethylsilyl)amide
HPLC	high performance liquid chromatography
HRMS	high resolution mass spectrometry
Hz	hertz
<i>I</i>	spin quantum number
IR	infrared
<i>J</i>	coupling constant
<i>k</i>	rate constant
LDA	lithium diisopropylamine
Lg	leaving group
Ln	ligand set
M	molar
Mbs	4-methoxybenzenesulfonyl
Me	methyl
mg	milligram
MHz	megahertz
mL	millilitre
mmol	millimol
NMO	4-methylmorpholine <i>N</i> -oxide

NMR	nuclear magnetic resonance
Ns	4-nitrobenzenesulfonyl
Ph	phenyl
PMB	<i>para</i> -methoxybenzyl
PMP	<i>para</i> -methoxyphenyl
ppm	parts per million
ⁱ Pr	<i>iso</i> -propyl
ⁿ Pr	propyl
Pyr	pyridine
RT	room temperature
TBAT	tetrabutylammonium triphenyldifluorosilicate
TBD	1,5,6-triazabicyclo[4.4.0]dec-1-ene
TBS	<i>tert</i> -butyldimethylsilyl
TFA	trifluoroacetamide
TEA	triethylamine
Tf	trifluoromethanesulfonyl
THF	tetrahydrofuran
TIPS	triisopropylsilyl
Tol	toluene
TLC	thin layer chromatography
TMS	trimethylsilyl
Tr	triphenylmethyl
Ts	toluenesulfonyl
UV	ultraviolet
μL	microliter

Chapter 1

Asymmetric Allylic Amination

1.1 Introduction

Allylic amines are synthetically important intermediates, which explains the considerable efforts to develop new methodologies for the construction of this ubiquitous motif.¹ Although allylic amines are present in some biologically active natural products, they are more often used as building blocks since the olefin can be transformed into a wide array of various functionalities. The transition metal-catalyzed allylic amination reaction provides a particularly useful method for the synthesis of allylic amines, since it provides a direct and general method for a variety of useful amine pronucleophiles.² This review will focus on the synthetic advances in asymmetric allylic amination reactions using acyclic precursors since Jørgenson and Johannsen's review in 1998 through 2009.^{1a} The transition metal-catalyzed allylic substitution reaction will be included along with other synthetic methods, *i.e.* as sigmatropic rearrangements and hydroamination reactions.

1.2 Metal-Catalyzed Stereoselective Allylic Amination

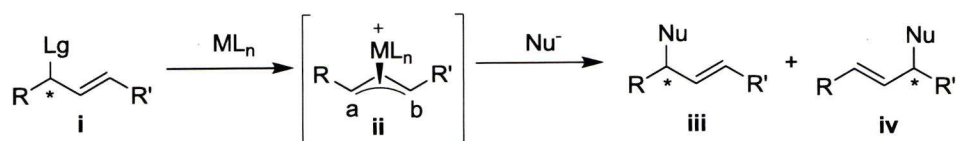
1.2.1 Introduction to Mechanism

The regio- and stereochemical outcome of metal-catalyzed allylic substitution reactions depend largely on the metal employed. Each metal presents its own challenges, for instance, palladium has a tendency to afford linear substitution products, and in the iridium-catalyzed reactions, high selectivities are generally only obtained with electronically biased substrates. Substrates can also provide a unique

set of challenges for the allylic substitution reaction. Historically, obtaining high levels of selectivity during the substitution of cyclic allylic alcohol derivatives has relied on symmetry. Therefore, this review will focus on the challenges and development made in preparing allylic amines, wherein the electrophile is acyclic.

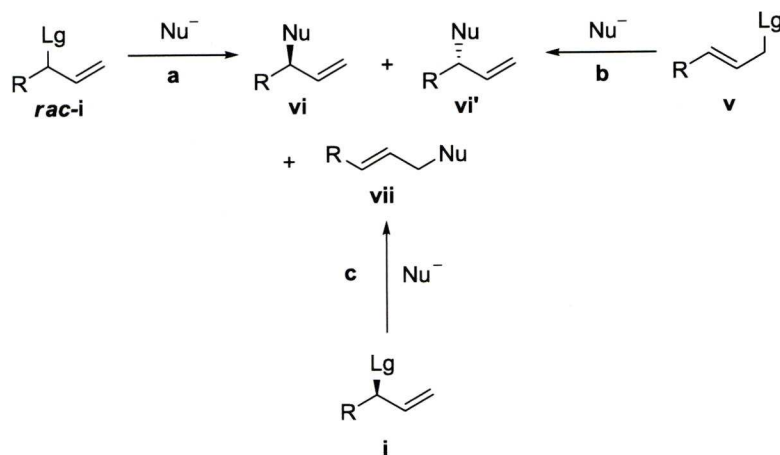
Oxidative addition of the transition metal into the allylic starting material affords a η^3 -allyl intermediate **ii** (Scheme 1.1). The nucleophile can then attack at either termini of the η^3 -allyl intermediate, affording products **iii** and **iv**, after reductive elimination of the metal. If the termini are the same, a symmetrical η^3 -allyl species is generated, which eliminates the issue of regioselectivity since products **iii** and **iv** are identical, albeit termini **a** and **b** are enantiotopic.

Scheme 1.1 Metal-catalyzed allylic substitution pathway.



When the substitution on the olefin is removed ($R'=H$), the transition-metal catalyzed allylic substitution reaction can proceed through three general pathways (Scheme 1.2).² Each pathway has the ability to afford either **vi** or **vi'** along with the linear isomer **vii**. During a dynamic kinetic asymmetric transformation (Pathway a), a racemic branched allylic alcohol derivative *rac*-**i** is converted into an enantiomerically pure product. In contrast to kinetic resolutions, the theoretical yield for this transformation is 100%. On the other hand, enantioselective processes employ achiral allylic alcohol derivatives **v** (Pathway b). A further possibility is the use of enantiomerically enriched substrates to furnish chiral nonracemic products in a stereospecific process (Pathway c).

Scheme 1.2 Various pathways for the formation of enantiomerically enriched products through the transition-metal catalyzed allylic substitution.



1.2.2 Dynamic Kinetic Asymmetric Transformation (DKAT) Reactions

1.2.2.1 Symmetrical Substrates in DKAT Reactions

As Scheme 1.1 demonstrates, regiochemical issues are alleviated by employing symmetrical substrates in the metal-catalyzed allylic substitution reaction. The termini of the symmetrical η^3 -allyl species are enantiotopic, thereby allowing an enantioselective reaction wherein the ligand metal complex determines the point of attack in a pseudosymmetrical intermediate to afford one enantiomer selectively.

Many classes of phosphorus based chiral ligands have been employed in metal-catalyzed allylic substitution reactions (Figure 1.1).³⁻¹⁰ C_2 -symmetrical ligands are generally well studied in asymmetric allylic substitution reactions. C_2 symmetry reduces the number of possible chiral metal-complexes formed and improves the facial selectivity of the reacting reagent on the metal.¹¹ Non C_2 -symmetrical ligands are also viable for asymmetric induction and often rely on the electronic influence of the ligands to direct the nucleophilic addition. The reaction conditions vary depending on the ligand, with high enantioselectivities being obtained at various

temperatures, concentrations and solvents. The majority of the ligands contain chirality derived from a chiral group attached to the phosphorus atom; however, the chirality can also be located directly on the phosphorus atom.

Figure 1.1 Phosphorus based ligands used in palladium-catalyzed asymmetric allylic amination.

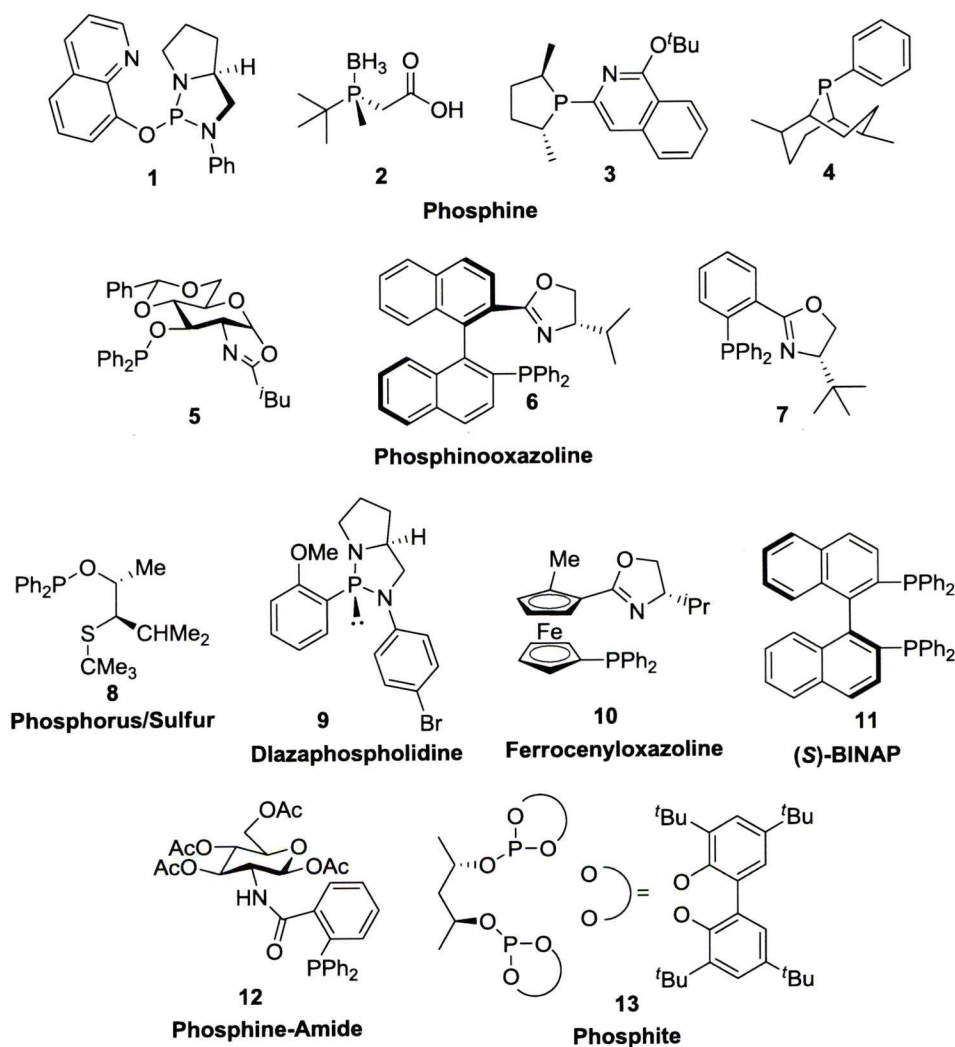
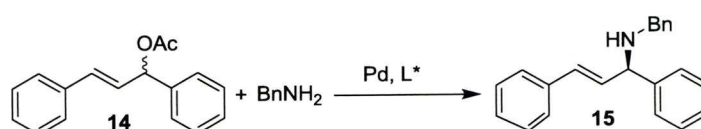


Table 1.1 compares the palladium-catalyzed allylic amination reaction of 1,3-diphenylpropenylacetate with benzyl amine in the presence of various chiral phosphorus-based ligands. The ligands are efficient at a range of temperatures to afford allylamine **15** in high yield with excellent enantiomeric excess. For example, Buono and co-workers introduced phosphine ligands bearing chirality on the phosphorus atom, *i.e.* **1**.^{3a,3b} These ligands were efficient in the palladium-catalyzed allylic amination reaction with various amine nucleophiles at low temperatures to

afford allylic amines with up to 94% enantiomeric excess. Treatment of **14** with benzylamine under optimized reaction conditions afforded the allylic amine **15** with 93% enantiomeric excess (entry 1). This demonstrated that ligands containing the chirality located on the binding atom are able to induce enantioselectivity in the allylic substitution reaction. Kann and co-workers also utilized a phosphorus-chirogenic ligand in the identical reaction and obtained **14** with 94% enantiomeric excess using ligand **2** (Table 1.1, entry 2).^{3c}

Table 1.1 Enantioselective allylic amination utilizing phosphorus-based ligands.



Entry	Pd (mol %)	Ligand (mol %)	Temp. (°C)	Yield (%)	ee (%)
1	[Pd(allyl)Cl] ₂ (2)	1 (8)	-10	95 ^a	93
2	[Pd(allyl)Cl] ₂ (2)	2 (8)	5	100 ^a	94
3	Pd ₂ (dba)·CHCl ₃ (0.5)	3 (1)	25	100 ^a	99
4	[Pd(allyl)Cl] ₂ (2)	8 (2.8)	-20	96	99
5	[Pd(allyl)Cl] ₂ (1.5)	5 (3.3)	22	72	95
6	[Pd(allyl)Cl] ₂ (2)	12 (4)	50	86	97
7	[Pd(allyl)Cl] ₂ (1)	6 (2.5)	40	99	92
8	[Pd(dba)Cl] ₂ (2.5)	9 (10)	22	80	95
9	[Pd(allyl)Cl] ₂ (1.5)	10 (3)	22	99	97
10	[Pd(OAc)Cl] ₂ (5)	(<i>R</i>)- 11 (10)	25	98 ^a	93
11	[Pd(allyl)Cl] ₂ (0.5)	13 (1.1)	22	100 ^a	96

^a% Conv.

Evans and co-workers utilized a non *C*₂-symmetrical phosphorus/sulphur bidentate ligand **8** in the palladium-catalyzed allylic amination of 1,3-diphenylpropenyl acetate **14** with benzylamine. The reaction benefited from low temperature and afforded allylic amine **15** in excellent yield and with 99% enantiomeric excess. (Table 1.1, entry 4).^{4a} Other phosphorus/sulfur ligands have

shown promising enantioselectivity; however, the yields are generally lower than with ligand **8**.^{4b-d}

Sugar based groups are attractive substrates to incorporate into chiral ligands due to their wide availability. Furthermore, the multiple hydroxyl functionality also allows for functional group manipulation. Uemura and co-workers utilized D-glucosamine to prepare new chiral phosphine-oxazoline ligands for use in the palladium-catalyzed asymmetric allylic amination reaction (Table 1.1, entry 5).^{5a} Treatment of **14** with benzylamine in the presence of [Pd(allyl)Cl]₂ and ligand **5**, provided the allylic amine **15** in excellent yield and with 95% enantiomeric excess. Whilst the enantioselectivity did not improve from previous reports, these new ligands were efficient at room temperature and were able to catalyze the allylic alkylation of more challenging substrates.

Sinou and co-workers took advantage of D-glucosamine for the rapid synthesis of phosphine-amide ligands, *i.e.* **12**, for use in the palladium-catalyzed allylic amination.^{6a} The reaction of 1,3-diphenylpropenyl acetate with benzylamine afforded the corresponding allylamine **15** in high yield and with 97% enantiomeric excess (Table 1.1, entry 6). A deacetylated version of the ligand was also examined, however this proved completely unreactive.

Pregosin and co-workers demonstrated that ligands containing a BINAP-like backbone were efficient in the palladium-catalyzed allylic amination reaction (Table 1.1, entry 7).^{5b} The reaction of acetate **14** with benzylamine in the presence of the palladium complex of phosphinooxazoline ligand **6** afforded amine **15** in 99% yield and with 92% enantiomeric excess. The reaction conditions proved efficient for numerous nitrogen nucleophiles affording the corresponding allylamine with >90% enantiomeric excess.

Wills and Breeden have developed diazaphospholidine ligands, *i.e.* **9**, and have shown that the monodentate ligands are efficient in the palladium-catalyzed allylic amination reaction.^{8a} Incorporating 2-(aminomethyl)pyrrolidine into the backbone provided higher rigidity, which in the reaction of 1,3-diphenylpropenyl acetate and the sodium salt of benzylamine furnished allylamine **15** in high yield and with 95%

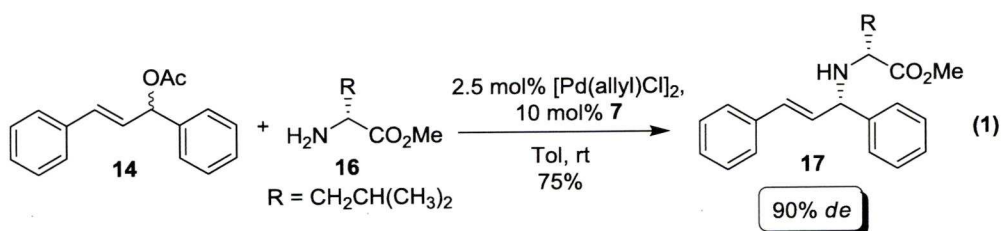
enantiomeric excess (Table 1.1, entry 8). Additional reactions with various nitrogen nucleophiles all proceeded in high yield and with excellent enantioselectivities demonstrating the feasibility of the diazaphosphilidine ligand in the asymmetric allylic amination reaction.

Another class of P,N-ligands that has proven attractive are the ferrocenylphosphine ligands, as exemplified by **10**. Although early investigations utilized the ferrocenyloxazoline ligands with disubstitution on the same cyclopentadienyl (Cp) ring,^{7a} Hou and co-workers developed complexes that have central, axial, and planar chirality, by using 1,1'-P,N-2'-substitution.^{7b} These ligands were employed in the allylic amination of 1,3-diphenylpropenyl acetate **14** with benzylamine to afford **15** in 99% yield and with 97% enantiomeric excess (Table 1.1, entry 9). By varying the substitution patterns on the ferrocene, it was determined that planar chiral groups were important in controlling enantioselectivity and the absolute configuration of the products.

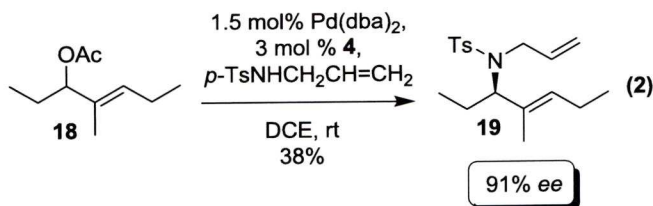
BINAP ligands have proven to be efficient ligands for enantioselective allylic substitution reactions. Sinou and co-workers have demonstrated high enantioselectivity in this process utilizing (*R*)-BINAP **11** with palladium in a biphasic water-organic solvent system. The reaction required the addition of surfactant to increase the solubility of the organic molecules in water.^{9b} For example, the reaction of allylic acetate **14** and benzyl amine proceeded with 98% conversion to afford the allylic amine **15** with 93% enantiomeric excess (Table 1.1, entry 10).

Diéguez and co-workers designed a series of diphosphite ligands, such as **13**, and investigated their reactivity in the palladium-catalyzed allylic substitution reaction.^{10b} The examination of the backbone, size of the chelate ring and substitution demonstrated that ligands forming an eight-membered chelate ring were optimal and that having a bulky substituent in the *ortho*- or *para*- position of the phenyl rings resulted in increased reactivity and enantioselectivity. For example, the reaction of 1,3-diphenylpropenyl acetate with benzylamine in the presence of the palladium complex with ligand **13** proceeded to afford the allylamine **15** in excellent yield and with 96% enantiomeric excess (entry 11).

Williams and co-workers examined chiral amino esters as nucleophiles in the palladium-catalyzed allylic amination reaction.^{5c} Initial studies utilized bisdiphenylphosphinoethane (dppe) as the ligand, however, the reaction of 1,3-diphenylpropenyl acetate **14** with L-leucine methyl ester **16** furnished the amine with only 70% diastereomeric excess (eq. 1). Utilizing chiral phosphinooxazoline ligand **7** resulted in decreased diastereoselectivity due to a mismatch in ligand and nucleophile. However, when D-leucine was employed, a significant increase in diastereoselectivity was observed and amine **17** was afforded in 75% yield and with 90% diastereomeric excess. This study demonstrates that chiral amine nucleophiles can be used to afford products with high levels of diastereoselectivity.



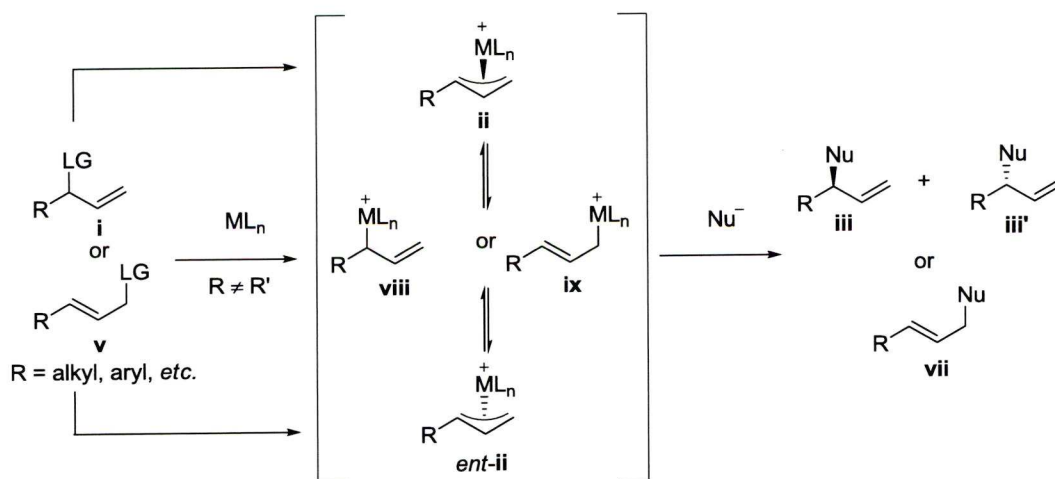
High levels of enantioselectivity can also be obtained with nonaromatic substrates. Hamada and co-workers developed a monodentate phosphine ligand containing a phosphabicyclo[3.3.1]nonane backbone **4** and utilized it in the palladium-catalyzed allylic amination reaction (eq. 2).^{3c} For example, the allylic amination of allylic acetate **18** proceeded in modest yield, albeit with excellent enantioselectivity (91%). This result demonstrates that high enantioselectivity can be induced in nonaromatic alkyl substrates.



1.2.2.2 Unsymmetrical Substrates in DKAT Reactions

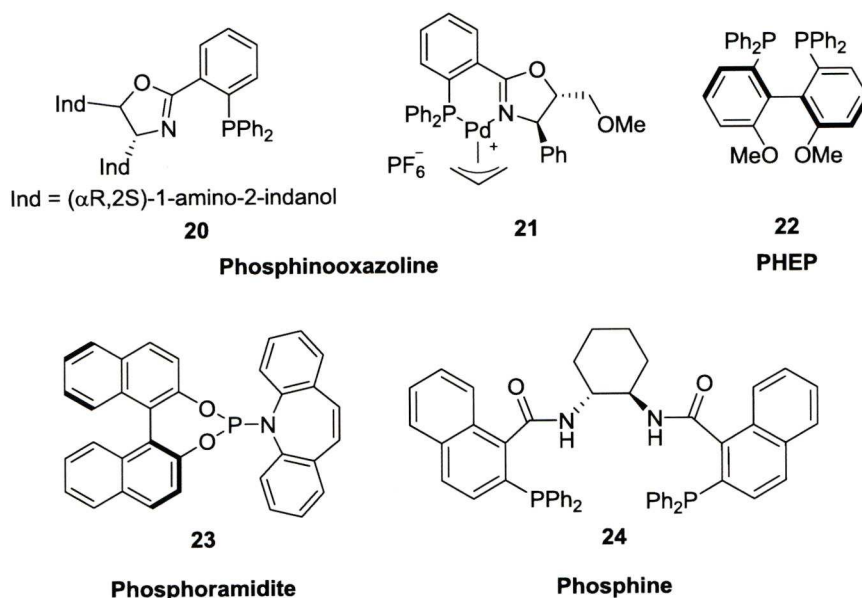
Unsymmetrical substrates provide an added challenge for the transition-metal catalyzed allylic substitution reaction. Along with having to control enantioselectivity, the ability to control regioselectivity has proven extremely challenging. Scheme 1.3 illustrates the complications present when using unsymmetrical substrates. Oxidative addition into **i** or **v** generates the η^3 -allyl intermediates **ii** or *ent*-**ii**, depending on which face of the molecule the metal binds. The η^3 -allyl intermediates are able to interconvert through the σ -species **viii** and **ix** via π - σ - π isomerization. The nucleophilic attack will then occur at either the more abundant species or the more reactive intermediate to afford the products. The reaction is capable of furnishing three separate compounds; both enantiomers of the branched substrate **iii** as well as the linear adduct **vii**.

Scheme 1.3 Regioselectivity in transition metal-catalyzed allylic substitution reactions.

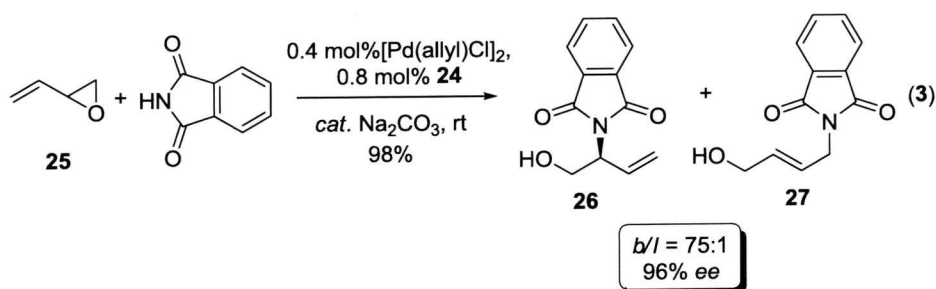


There has been considerable effort applied to developing catalysts that control the regioselectivity in the metal-catalyzed allylic substitution reaction in order to reduce the complexity. Like the symmetrical substrates, various phosphorus based ligands have been utilized (Figure 1.2).

Figure 1.2 Phosphorus based ligands used with unsymmetrical substrates.

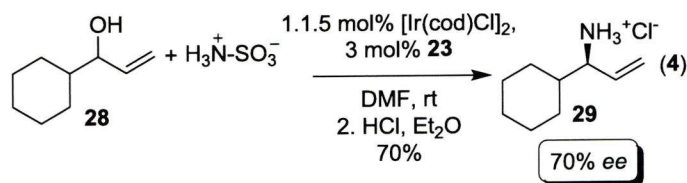


The majority of the transition-metal catalyzed allylic substitution reactions utilize allylic alcohol derivatives such as carbonates and acetates as starting materials. In 2000, Trost and co-workers reported using allylic epoxides as the electrophile in palladium-catalyzed allylic substitution (eq. 3).^{3h} Studies demonstrated that a low catalyst loading of 2.5 mol% and a trace amount of base was sufficient for smooth turnover. For example, treatment of epoxide **25** with phthalimide under the optimized reaction conditions afforded branched product **26** in 98% yield and with 96% enantiomeric excess. Nevertheless, this approach is somewhat limited to the electrophile, which detracts from its generality.

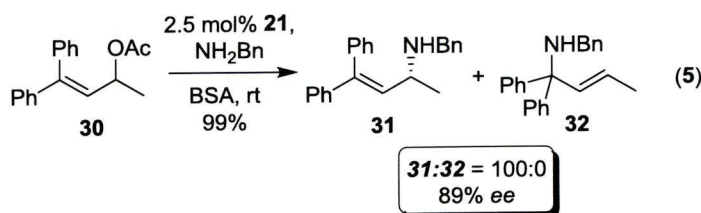


Carreira and co-workers developed a new phosphoramidite ligand to facilitate the direct allylic amination of branched allylic alcohols utilizing sulfamic acid as an ammonia equivalent (eq. 4).³² Initial attempts on the *tert*-butyl cinnamyl carbonate

were unsuccessful. However, a small amount of product was isolated from the branched moiety and unexpectedly from the free alcohol. Further ligand development led to the alkene containing derivative **23** which afforded the branched free amine (isolated as the HCl salt) with complete conversion and no observable side products. For example, treatment of 1-cyclohexylprop-2-en-1-ol **28** under the optimized conditions afforded the hydrochloride ammonia salt **29** in 70% yield and with 70% enantiomeric excess, which could be improved to 93% after recrystallization. Studies found that with prolonged reaction times the amine was converted to the sulfamic ester. Although the enantioselectivity is suboptimal, this represents an ingenious method of conducting a dual activated allylic amination.



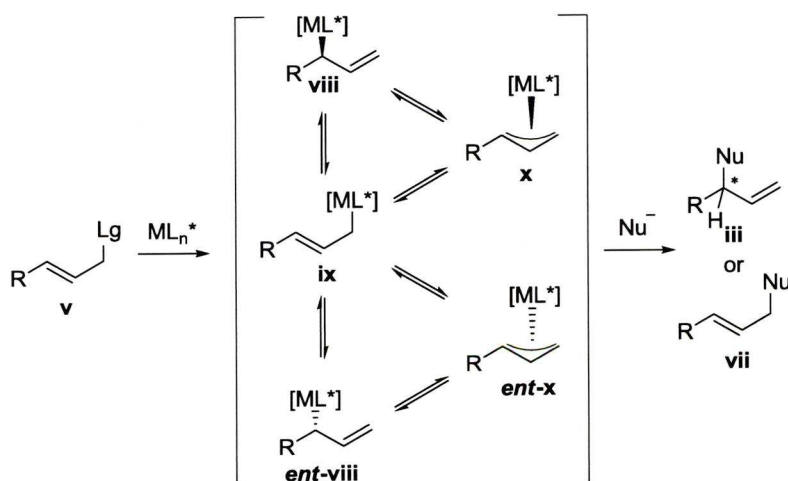
Pericàs and co-workers developed a new class of phosphinooxazoline ligands for the palladium-catalyzed allylic amination reaction.^{5g} These ligands proved to be more efficient than other PHOX ligands with a range of amine nucleophiles; however, bulkier nucleophiles require longer reaction times. For example, when allylic acetate **30** was treated with benzylamine in the presence of metal complex **21**, the enantiomerically enriched amine **31** was formed as a single regioisomer in near quantitative yield and with 89% enantiomeric excess (eq. 5). When the ligand was attached to a solid support resin, the reactions were slower, though they proceeded with excellent yield and enantioselectivities.



1.2.3 Enantioselective Metal-Catalyzed Allylic Amination Reactions

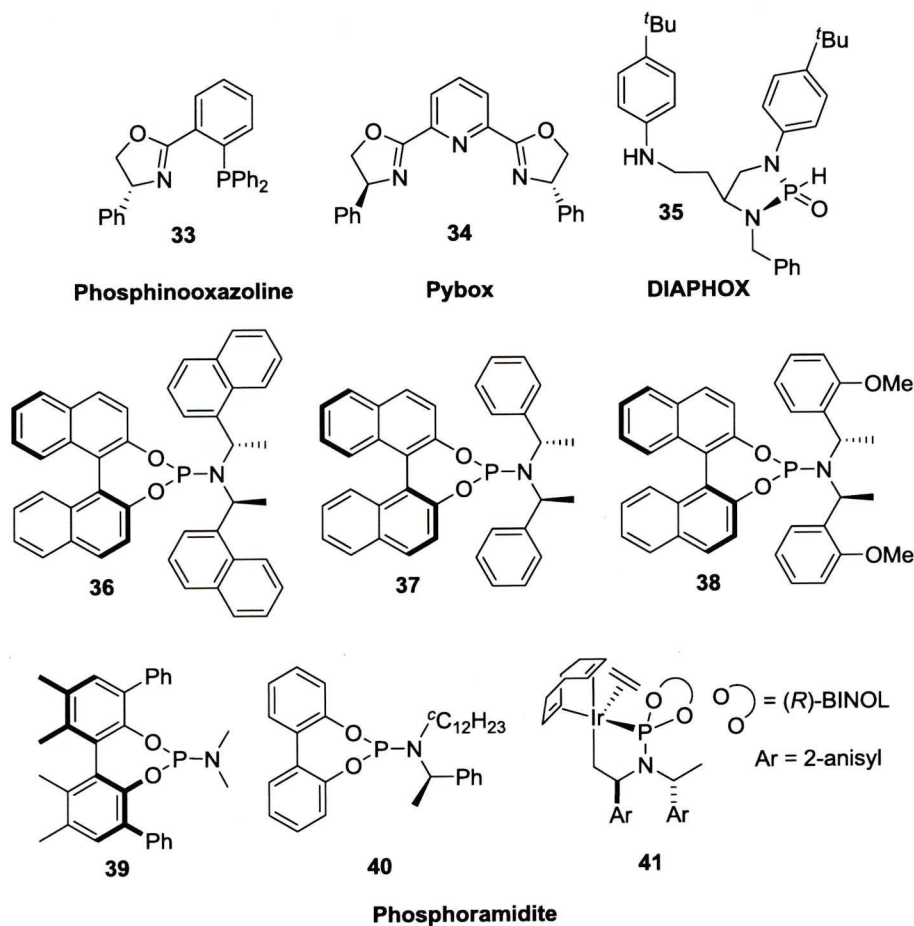
The enantioselective version of the allylic substitution reaction is attractive since it employs achiral allylic alcohol derivatives. Intra- and intermolecular variants have been employed to prepare a wide array of chiral nonsymmetrical substrates using various nucleophiles. Oxidative addition of the metal into **v** affords the σ -allyl complex **ix** which can isomerize to the secondary σ -allyl complexes **viii** or *ent*-**viii** through the π -allyl complex **x** or *ent*-**x** via a σ - π - σ isomerization (Scheme 1.4). The rate of isomerization is dependent on the metal used. For example, studies have demonstrated that in contrast to palladium systems, the σ - π - σ isomerization of the iridium-allyl complex is slow at room temperature.

Scheme 1.4 Possible intermediates in the metal-catalyzed allylic substitution reaction.



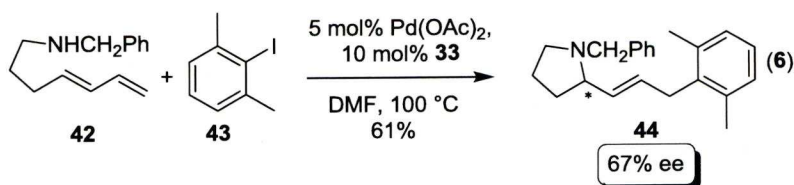
A variety of phosphorus based ligands have been utilized for this type of reaction; however, the phosphoramidite ligands, which were first described by the groups of Alexakis and Feringa are the most widely used.¹⁸ The phosphoramidites are attractive ligands since they are modular, making them easy to modify. Iridium is the most widely used metal in the enantioselective allylic amination reaction and is efficient at low catalyst loadings.

Figure 1.3 Phosphorus based ligands used in the enantioselective allylic amination reaction.



1.2.3.1 Intramolecular Enantioselective Allylic Amination Reactions

In 1999, Helmchen and Flubacher described a novel domino Heck-allylic amination reaction to afford chiral allylic pyrrolidines and piperidines using a phosphinooxazoline ligand (eq. 6).^{5e} Aryl triflates were required for the Heck reaction in order to obtain high enantioselectivities (up to 80%), although the reaction times were rather long and only moderate yields were achieved. The aryl iodide afforded products with lower enantioselectivities; however, the yields were generally higher. For instance, treatment of the diene **42** with aryl iodide **43** under the optimal reaction conditions afforded the allylic pyrrolidine **44** in 61% yield and with 67% enantiomeric excess.

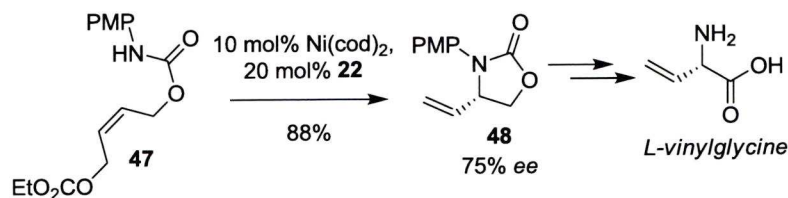


Ojima and Shi used phosphoramidite ligand **39** in the intramolecular palladium-catalyzed allylic amination reaction to prepare biologically important tetrahydroisoquinolines.^{19c} This work demonstrated that increasing the bulk of the 3 and 3'-substituents on the backbone increased the enantioselectivity, albeit to a limit since the *tert*-butyl group is simply too bulky and displayed decreased enantioselectivity. For example, treatment of **45** under the optimized reaction conditions proceeded in complete conversion to afford protected allylamine **46** with 95% enantiomeric excess (eq. 7). It was also noted that the *N*-trifluoroacetyl-protected derivatives provide higher enantioselectivities to the *p*-toluenesulfonyl-protected variants.

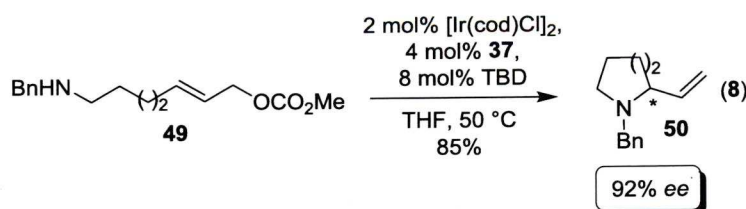


The first asymmetric nickel-mediated allylic amination reaction was reported by Berkowitz and Maiti (Scheme 1.5).^{9c} Although later studies showed the PHOX ligands to be superior, the initial *in situ* enzymatic screening (ISES) led to the identification of the MeO-BIPHEP ligand **22**, which afforded the nitrogen heterocycles in good to excellent yield and with moderate to good enantioselectivity. The key step in the synthesis of L-vinylglycine was the nickel-mediated allylic amination reaction of **47** to afford the amination product **48** in 88% yield and with excellent enantioselectivity after one recrystallization.

Scheme 1.5 Ni-mediated allylic amination towards the synthesis of *L*-vinylglycine.



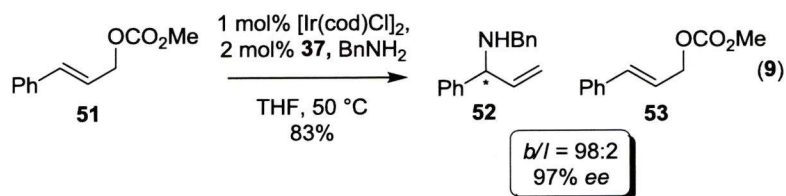
In 2004, Helmchen and co-workers described the first intramolecular enantioselective iridium-catalyzed allylic amination for the synthesis of 5- and 6-membered amines (eq. 8).^{19a} The iridium complex with a phosphinooxazoline ligand facilitated the amination of the branched allylic acetates in high yields and moderate to high enantioselectivities. The enantioselectivity proved to be temperature dependent, with increased temperatures improving the selectivity, presumably because it allows for faster isomerisation of the Ir-allyl complex. Moreover, phosphoramidite **37** afforded the cyclized amine in improved enantioselectivity over the phosphinooxazoline ligands albeit with prolonged reaction time. The rate and enantioselectivity were increased when the catalyst was activated with 1,5,7-triazabicyclo[4.4.0]undec-5-ene (TBD). For example, treatment of allylic carbonate **49** under the optimal reaction conditions, afforded *N*-benzyl-2-vinyl-piperidine in 85% yield and with 92% enantiomeric excess. As expected, the intramolecular reaction is much faster than the intermolecular variant.



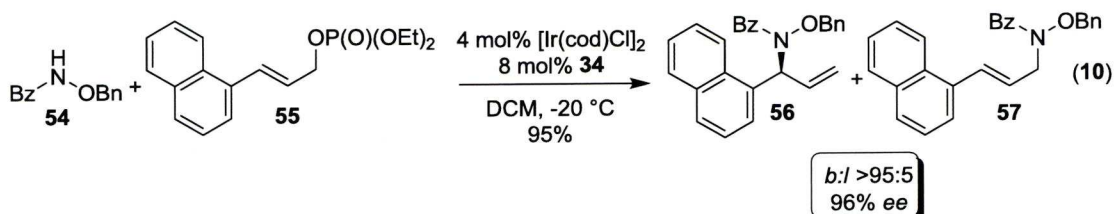
1.2.3.2 Intermolecular Enantioselective Allylic Amination Reactions

Hartwig and Ohmura examined phosphoramidite ligands for the iridium-catalyzed allylic amination of achiral carbonates with various nitrogen nucleophiles.²⁰ Reactions with primary amines and cyclic secondary amines proceed with excellent

enantioselectivity at room temperature and in high enantioselectivity for the branched amines over the linear and diamine products (eq. 9). For example, treatment of methyl cinnamyl carbonate **51** with diethylamine under the optimized reaction conditions, afforded the branched amine **52** in 83% yield and with 97% enantiomeric excess. The reaction conditions also proved efficient for inducing enantioselectivity in non-aromatic substrates, albeit with lower regioselectivity.

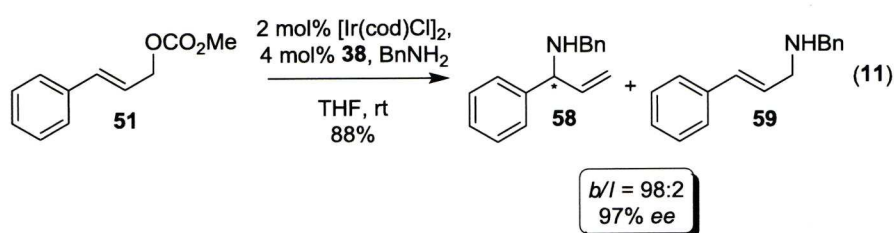


Structurally rigid pybox ligands have not been extensively examined in the context of the asymmetric allylic substitution reaction, despite their proven ability in other asymmetric reactions. Takemoto and co-workers described these ligands in the allylic amination of linear cinnamyl phosphates with various hydroxylamines (eq. 10).¹⁶ The reactions proceed in the presence of a weak base to afford the corresponding amine products in excellent yield and enantioselectivity. The regioselectivity was variable with the highest selectivities obtained for substrates containing bulkier aryl substituents on the phosphate. For example, treatment of the 1-naphthyl substituted phosphate **55** with hydroxylamine **54** in the presence of $[\text{Ir}(\text{cod})\text{Cl}]_2$ and the pybox ligand **34**, furnished the allylic amine in 95% yield and with 96% enantiomeric excess. Even though the reaction proceeds at times with lower regioselectivity, this study demonstrates that the pybox ligand is effective at inducing enantioselectivity in the iridium-catalyzed allylic amination reaction.

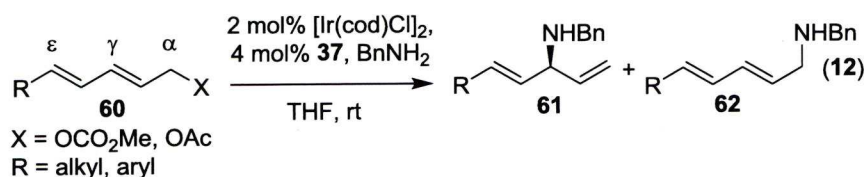


Alexakis and co-workers designed a third generation phosphoramidite ligand **38** which incorporated an *ortho*-methoxy substituent onto the phenyl rings of the amine component.²¹ These ligands proved efficient in the copper-catalyzed enantioselective

allylic alkylation reaction as well as the asymmetric iridium-catalyzed allylic amination. For example, treatment of methyl cinnamyl carbonate with benzyl amine under optimized reaction conditions afforded the branched amine **58** in 88% yield with 98:2 regioselectivity and with 97% enantiomeric excess (eq. 11). The examination of the reaction kinetics of various ligands indicated a difference in rates for the *para*-methoxy and *ortho*-methoxy analogues. Interestingly, the *para*-substituted variant has an induction period, which was ascribed to a chelation effect. The ligand containing an *ortho*-methoxy substituent displayed an absence of this induction period.

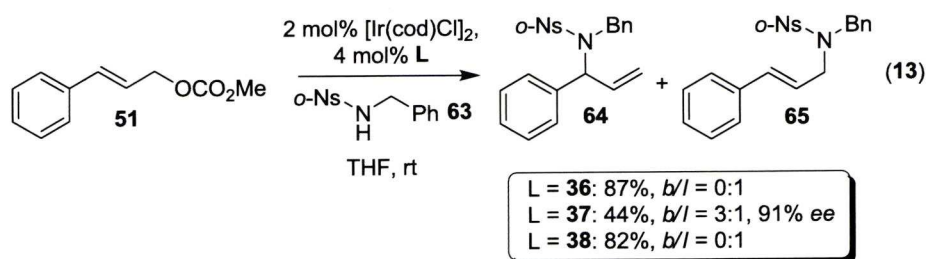


Iridium-catalyzed allylic substitution reactions have been most successful with cinnamyl alcohol derivatives, whereas the alkyl derivatives generally afford lower regioselectivities. Helmchen and Lipowsky expanded the utility of the iridium-catalyzed allylic amination reaction to the amination of dienyl esters **60** with benzylamine using the phosphoramidite ligand **37**.²² (eq. 12). Aryl and alkyl substituted dienyl esters were successfully aminated in good yields and high regio- and enantioselectivity. Interestingly, nucleophilic addition occurs at the α - and γ -positions rather than the ϵ position suggesting that the iridium-allyl complex forms regioselectively.



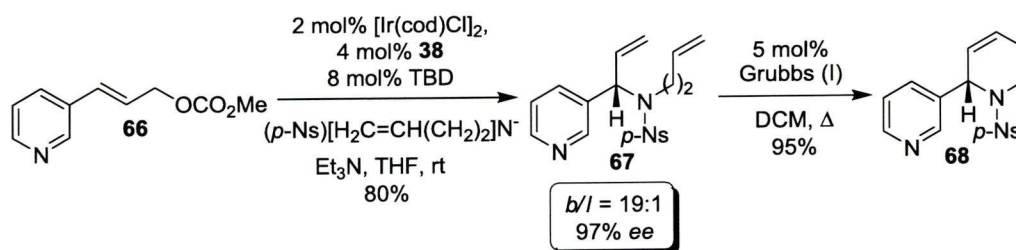
Helmchen's group also examined anionic *N*-nucleophiles in the iridium-catalyzed allylic substitution reaction utilizing phosphoramidite ligands.²³ Nucleophiles were chosen that would furnish protected amines, since it would eliminate the need for a protection step during synthesis. Interestingly, when *N*-(*o*-Ns)-NHCH₂Ph was used

as the nucleophile, there was a significant steric effect observed with the ligands (eq. 13). Sterically demanding ligands **36** and **38** afforded solely the linear product **65** in high yield, while ligand **37** furnished a mixture of branched and linear products in lower yield (44%). The issue of regioselectivity was circumvented by utilizing *p*-nosylamides as the nucleophile, which afforded the corresponding amination products in regioselectivity up to 16:1. The regioselectivities could be further improved by performing the reaction in the absence of base (up to 32:1).



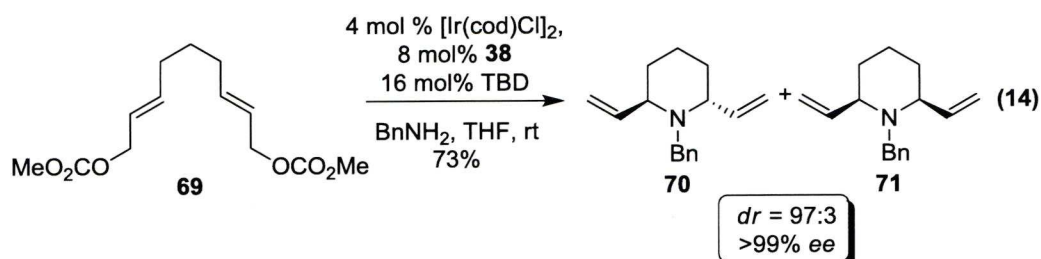
This methodology was applied to the synthesis of (+)-(*R*)- and (-)-(*S*)-nicotine (Scheme 1.6). Treatment of methyl carbonate **66** with (*p*-Ns)[H₂C=CH(CH₂)₂]⁻ under optimized reaction conditions afforded diene **67** in 80% yield and with 97% enantiomeric excess. Diene **67** was then converted to the tetrahydropyridine **68** in excellent yield *via* a ring closing metathesis reaction, which provided the key intermediate for these tobacco alkaloids.²⁴

Scheme 1.6 Synthesis of tetrahydropyridine **68** through iridium-catalyzed allylic amination/RCM.

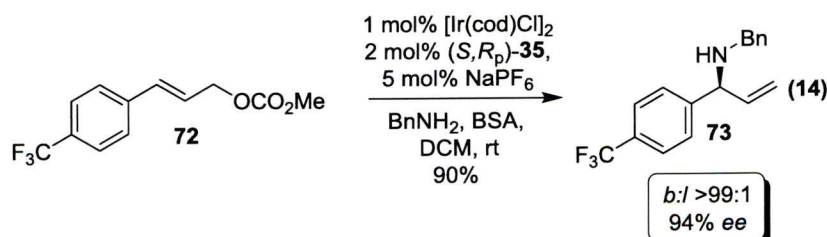


Helmchen's group further expanded the iridium-catalyzed allylic amination reaction to include a sequential inter- and intramolecular amination from bisalkenes to afford 5- and 6-membered *N*-heterocycles with excellent enantioselectivity and high diastereoselectivity (eq. 14).^{19b} For example, the reaction of bisalkene **69** with

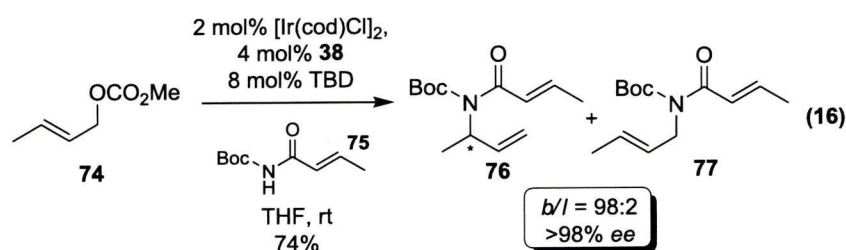
benzylamine afforded the benzyl protected 2,6-*trans*-piperidine **70** in 73% yield, with a diastereoselectivity of 97:3 and complete enantioselectivity ($\geq 99\%$ *ee*). The diastereo- and enantioselectivity are high since the catalyst controls both aminations to provide double stereochemical induction.



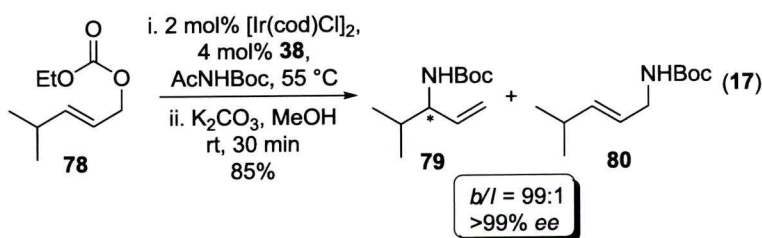
Hamada and co-workers described the utility of diaminophosphine oxide (DIAPHOXs) ligands in the palladium-catalyzed allylic amination reaction and expanded its use to the asymmetric iridium-catalyzed variant (eq. 15).¹⁷ Benzylamine was treated with a series of cinnamyl carbonates, and all proceeded in high yield and with excellent regio- and enantioselectivity. Interestingly, the more challenging electron withdrawing substituents were efficient substrates for this transformation. For example, treatment of the 4-(trifluoromethyl)-phenyl substituted cinnamyl carbonate **72** under the optimal conditions afforded the amine **73** in 90% yield and with 94% enantiomeric excess. The reaction proceeded well with other alkylamines, albeit morpholine resulted in decreased enantioselectivity (65% *ee*). Linear alkyl substrates were also examined, which afforded the branched amine in good yield but with a diminished enantioselectivity (up to 68% *ee*). These studies demonstrate that the DIAPHOXs ligands are effective at inducing high levels of enantioselectivity in the iridium-catalyzed amination reaction, even for the more challenging electron deficient substrates.



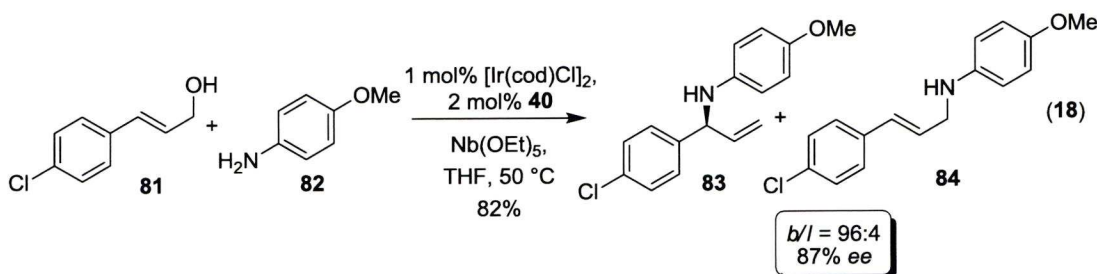
Helmchen and co-workers used the iridium-catalyzed asymmetric amination reaction to form the enantiomerically enriched Boc-protected amides in a single step, which facilitates the formation of α,β -unsaturated γ -lactams.²⁷ The reaction proceeded under salt free conditions depending on the nature of the allylic carbonate when utilizing the N-Boc amide **75**. For example, when the methyl derivative **74** was employed, the reaction furnished amide **76** in 74% yield, with excellent regioselectivity and enantiomeric excess (eq. 16).



Han and Singh developed a general method for the one pot asymmetric iridium-catalyzed allylic amination followed by *in situ* deprotection of *N*-Ac, *N*-Boc and *N*-Cbz compounds.³³ The di-benzyl imidodicarboxylate, *N*-acetyl *N*-*tert*-butyl carbamate, in addition to other disubstituted imidodicarboxylates, react with cinnamyl and aliphatic ethyl carbonates to afford the branched free amides in excellent regio- and enantioselectivities (eq. 17). For example, treatment of carbonate **78** with *N*-acetyl *N*-*tert*-butyl carbamate afforded the *N*-Boc allylic amine **79** in 85% yield with excellent enantiomeric excess ($\geq 99\%$), after *in situ* deprotection of the acetate. Substrates containing α -branched, protected hydroxy alkyl groups, electron rich aromatics and heteroatoms substituents were all tolerated affording the corresponding amines in high yield and with high regio- and enantioselectivity.



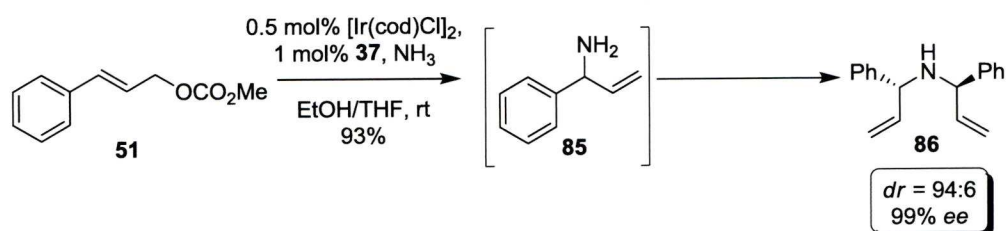
Hartwig and co-workers explored the synthetic utility of free terminal alcohols as the electrophile in the iridium-catalyzed allylic amination, which provides a more atom economical and expeditious approach.²⁸ Preliminary studies explored a variety of Lewis acids, in which Nb(OEt)₅ was optimal, albeit as a stoichiometric additive. Various allylic alcohols were treated with anilines in the presence of the phosphoramidite **40** (eq. 18)²⁹ to generate branched amines in high yield and selectivity with electron-rich and electron-poor aryl derivatives, although halo- and ortho-substituted anilines proceeded with lower yield. For example, treatment of the 4-Cl derivative **81** with aniline **82** under the optimized reaction conditions afforded the amination product **83** in 82% yield with high regio- and enantioselectivity (*b/l* = 96:4, 87% *ee*). Additionally, aliphatic amines were obtained with high enantioselectivities, but also with lower yield and regioselectivity. Triphenylborane also serves as a suitable Lewis acid, affording the branched amine with moderate to high yield and with high regio- and enantioselectivities.



The ability to affect the allylic amination with ammonia represents an important goal for this area, since it would provide allylic amines without the necessity to deprotect, which can be problematic. Hartwig and co-workers reported the first example of the iridium-catalyzed allylic amination reaction to afford diallylamines, which can be subjected to ring-closing metathesis to provide C₂-symmetric pyrrolidines (Scheme 1.7).³¹ The allylic amination of the methyl cinnamyl carbamate **51** with the iridium complex of **37** with a 2M ammonia solution, afforded the diallylamine **86** in 93% yield, with excellent diastereo- and enantioselectivity (94:6 *dr*, 99% *ee*), in which none of the monoallylated product observed. A number of inexpensive ammonia equivalents have also emerged. For example, the potassium salt of trifluoroacetamide was an efficient nucleophile for the amination of alkyl and aryl cinnamyl carbonates, including electron-poor substrates. The reaction proceeded

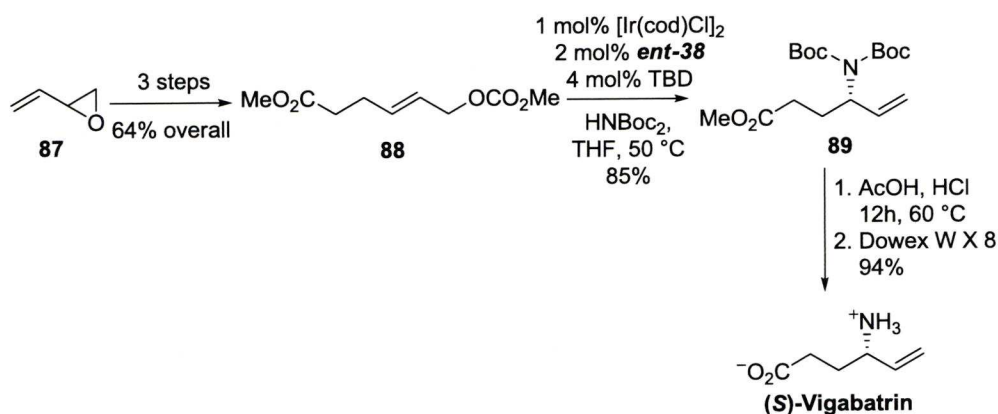
with excellent yield (59-93%) and enantioselectivity (92-98%). In a related study, LiNBoc₂ was examined, which also proceeded in good yield and with high regio- and enantioselectivities. Unfortunately, α -branched aliphatic substrates result in lower yield (45%), but with high regioselectivity (*b/l* = 89:1); however, excellent enantioselectivity (97% *ee*) was obtained with none of the mono-amination product observed.

Scheme 1.7 Iridium-catalyzed allylic amination with ammonia.

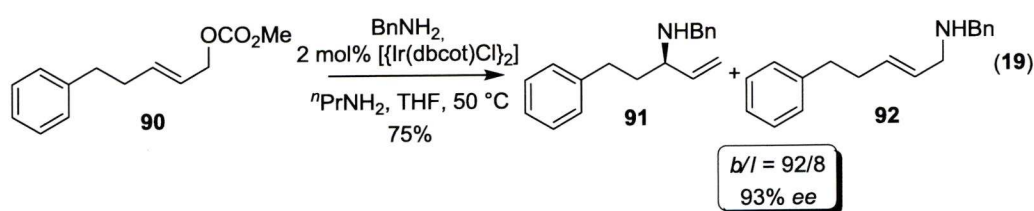


Helmchen and co-workers studied the feasibility of having oxygen-protected functionality on the sidechain of allylic carbonates in the iridium-catalyzed allylic amination reaction.³⁴ Studies showed that the alcohol had to be protected since the presence of a free hydroxyl group decreased the enantioselectivity, albeit the regioselectivity was high in the reactions with benzylamine and 4-methoxyaniline. Alternatively, when the hydroxyl group was protected, the products were obtained with low regio- and moderate to high enantioselectivity with benzylamine. Improved regioselectivities were observed with 4-methoxyaniline, and the reaction with HN(CHO)Boc under salt free conditions provided optimal results. This chemistry was then utilized in the key step to prepare (*S*)-vigabatrin, an antiepilepsy drug, in 5 steps (Scheme 1.8). Treatment of carbonate **88** under the optimized reaction conditions afforded the amination product **89** in 85% yield and with 98% enantiomeric excess. Deprotection of **89** afforded (*S*)-vigabatrin in 95% yield over the two steps.

Scheme 1.8 Synthesis of (*S*)-vigabatrin utilizing iridium-catalyzed allylic amination.

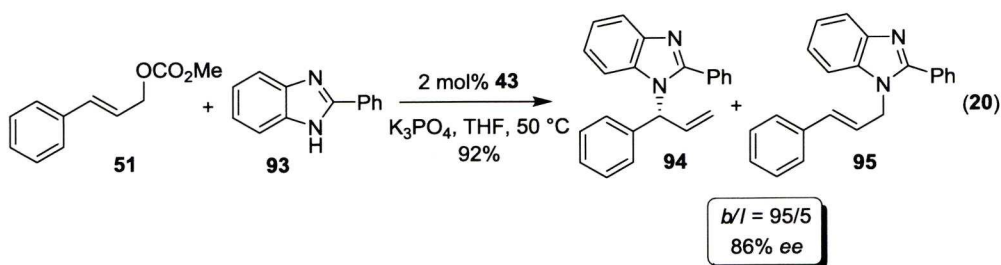


Helmchen and co-workers modified the iridium catalyst for the asymmetric allylic amination reaction by replacing the cycloocta-1,5-diene (cod) ligand with dibenzo[*a,e*]cyclooctatetraene (dbcot), which allowed the reaction to be undertaken under aerobic conditions.³⁴ A comparison of the dbcot ligand with cod indicated that (a) the dbcot bound more strongly to iridium, (b) dbcot is a better electron acceptor, and (c) that the dbcot-iridium complex does not undergo C-H activation at the dbcot amine moiety. The reaction of cinnamyl methyl carbonate with benzylamine in the presence of $[\{\text{Ir}(\text{dbcot})\text{Cl}\}_2]$ proceeded in high yield and with excellent regio- and enantioselectivities in the presence of oxygen at 50 °C. This catalyst complex also proved to be efficient with linear substrates (eq. 19). Treatment of the allylic carbonate **90** under the optimized conditions, furnished the allylic amine **91** in 75% yield with excellent regio- and enantioselectivity (*b/l* = 92:8, 93% *ee*). Although the regioselectivities were occasionally lower with the dbcot ligand, the fact that the reaction can be performed in the presence of oxygen is an important advance for the iridium-catalyzed allylic substitution reaction.



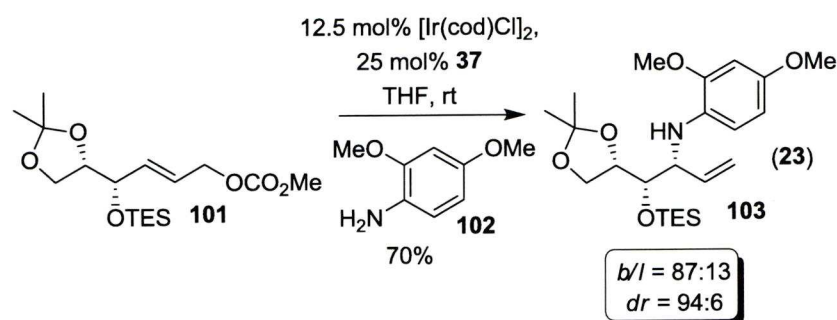
Hartwig and Stanley reported the first use of imidazole, benzimidazole, and purine nucleophiles in the iridium-catalyzed allylic amination reaction with $[\text{Ir}(\text{cod})(\kappa^2\text{-$

37)(ethylene)] catalyst (**43**).³⁶ The reactions afforded the enantiomerically enriched branched allylamines in high yield with excellent regio- and enantioselectivities (eq. 20). The reaction was applicable to both electron-rich and electron-poor cinnamyl substrates. For instance, treatment of the allylic carbonate **51** with benzimidazole **93** under the optimal conditions, afforded amine **94** in 92% yield and with 86% enantiomeric excess.



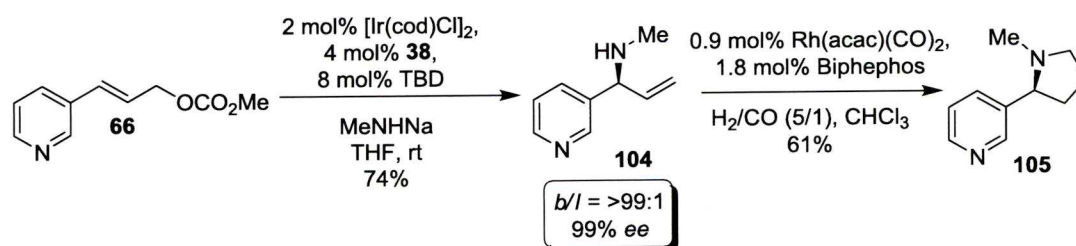
Hartwig and co-workers also investigated modifying the iridium catalyst used in the allylic amination reaction in order to make it more stable to excess ammonia.³⁸ Previous studies demonstrated that standard complexes made from $[\text{Ir}(\text{cod})\text{Cl}]_2$ and phosphoramidite ligands were unstable to excess ammonia and result in an achiral catalyst or a catalytic species that was completely inactive. Iridium complex **43** was found to be stable to 2000 equivalents of ammonia. Preliminary studies demonstrated that 100 equivalents of ammonia furnished the mono-amination product with 9:1 selectivity over the diamination compound. Electron rich and electron poor cinnamyl derivatives, in addition to straight chain and branched aliphatic substrates provide good to moderate yield and excellent enantioselectivity ($\geq 95\%$) after *in situ* protonation with HCl. The trityloxy-substituted allylic carbonate **96** afforded amine **97** in 53% yield and 97% enantiomeric excess (eq. 21). This compound is a potentially useful synthetic intermediate since it contains a 1,2-aminoalcohol moiety. This work represents the first monoallylation of ammonia with an iridium-catalyzed allylic amination reaction. In addition, a new ethylene catalyst has been reported, which will allow further development of the direct amination with ammonia.

protecting group, the iridium-catalyzed amination proceeded in good yield, with moderate b/l ratio, and a *syn/anti* ratio of 94:6. The *anti*-1,2-aminoalcohol was also prepared utilizing the ligand of opposite configuration in 58% yield, *b/l* = 73:27 and *dr* = 90:10 favoring the *anti*-diastereoisomer. These studies represent a convenient method for the synthesis of 1,2-aminoalcohols. Further studies are underway to improve the generality of this reaction, especially in complex molecules.



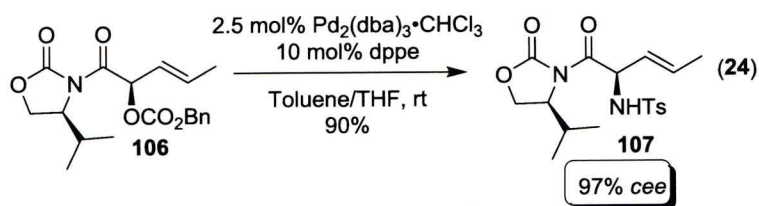
Helmchen and co-workers later combined the asymmetric iridium-catalyzed allylic amination with rhodium-catalyzed hydroformylation to afford 2-substituted pyrrolidines.²⁵ The synthesis of (*S*)-nicotine **105** was shortened (Scheme 1.9) and the synthesis of the indole alkaloid 225C, which was isolated from the venom of a species of fire ants, was accomplished using this methodology. Intramolecular hydroaminomethylation afforded the 2-substituted pyrrolidines in moderate to good yields, without racemization using $\text{Rh}(\text{acac})(\text{CO})_2$ and the chiral ligand, Biphephos. This sequence was utilized to synthesis (*S*)-nicotine in two steps in 61% overall yield and with $\geq 99\%$ enantiomeric excess.

Scheme 1.9: Two-Step synthesis of (*S*)-nicotine.



1.3 Stereospecific Metal-Catalyzed Allylic Amination Reactions

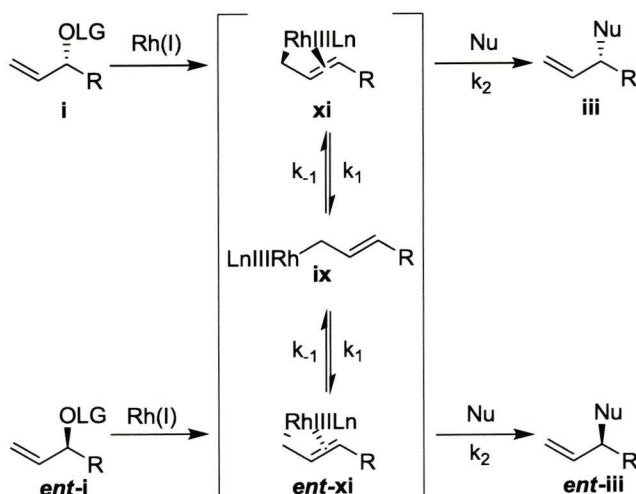
Nakai and co-workers prepared allylic carbonates *via* an asymmetric α -oxylation of a dienolate and subjected them to a palladium-catalyzed allylic substitution reaction, to afford *p*-toluenesulfonyl-protected amines in high yield (eq. 24).⁴¹ The allylic substitution reaction of **106** was catalyzed by $\text{Pd}_2(\text{dba})_3 \cdot \text{CHCl}_3$ -dppe and proceeded regioselectively to afford the γ -amino compounds with retention of configuration with >85% conservation of enantiomeric excess. The products are useful intermediates in the synthesis of natural and unnatural molecules.



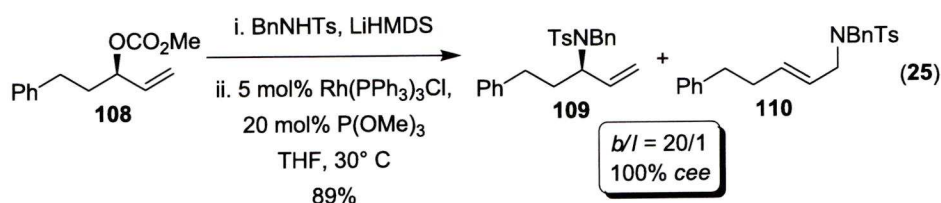
The first regioselective rhodium-catalyzed allylic substitution reactions were reported by Tsuji and co-workers in 1984 utilizing both Rh(I) and Rh(II) complexes modified with alkyl phosphines.^{2a} In contrast to the palladium-catalyzed reaction, this system displays a “memory effect,” with the nucleophile adding to the original position of the leaving group, which suggests the reaction does not proceed through a traditional fluxional π -allyl intermediate. Evans and Nelson suggested the formation of a stable enyl intermediate, which contains both σ and π components.⁴²

Scheme 1.10 outlines the proposed reaction pathway. Hence, the allylic carbonates **i** or *ent-i* undergo oxidative addition with Rh(I) to provide the enyl intermediate **xi** or *ent-xi*. Nucleophilic attack can then occur in a regio- and stereospecific manner to afford the product **iii** or *ent-iii*. The reaction occurs *via* a double inversion process, to afford overall retention of stereochemistry. The enantiomeric outcome implies that the rate of nucleophilic addition (k_2) is faster than the π - σ - π isomerization (k_{-1} or k_1).

Scheme 1.10 Mechanism of rhodium-catalyzed substitution.



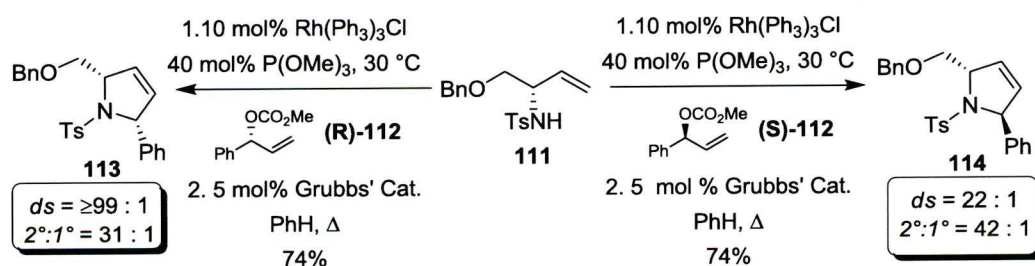
Evans and co-workers investigated the rhodium-catalyzed allylic amination using phosphite-modified Wilkinson's catalyst $[\text{Rh}(\text{PPh}_3)_3\text{Cl}]$ and *N*-toluenesulfonyl benzylamine as the pronucleophile (eq. 25).⁴³ Initial studies showed the lithium anion was optimal for yield and regioselectivity, as compared to the potassium and sodium salts. The reaction proved to be general, with high regioselectivity and enantiospecificity obtained with a wide array of substrates. For example, the reaction of methyl carbonate **108** with the lithium anion of *N*-tosyl benzylamine afforded the branched amine **109** and the linear isomer **110** in 89% yield, 20:1 *b/l* ratio with complete chirality transfer (100% *cee*). The absolute configuration was determined by the reaction of carbonate **108** with *o*-nitrobenzenesulfonyl benzylamine to afford the branched amine, which was then converted to (*R*)-homophenylalanine. It was also determined that the reaction proceeds with net retention of configuration, which is consistent with the intermediacy of an *enyl* ($\sigma + \pi$) organorhodium intermediate.



The Evans group combined the stereospecific rhodium-catalyzed allylic amination reaction with ring-closing metathesis (RCM) to prepare disubstituted monocyclic azacycles (Scheme 1.11).⁴⁴ The amination with *N*-*p*-toluenesulfonyl alkenylamines

proceeded in high yields and with excellent regioselectivity. The ring-closing metathesis afforded 5- to 7-membered azacycles in 84-94% yield. This methodology was applied to the synthesis of 2,5-disubstituted pyrrolidines through a sequential diamination, ring-closing metathesis sequence. In this case, the nucleophile was changed to *N*-*p*-toluene-sulfonyl *p*-methoxybenzylamine and treated with carbonate **112** under the optimal conditions, to afford the branched amine in 86% yield with 70:1 regioselectivity. After deprotection of the PMB group, the allylic sulfonamide **111** was subjected to a second rhodium-catalyzed allylic amination. Treatment with using (*R*)-**112**, furnished the diene with $\geq 99:1$ diastereospecificity, whereas the enantiomer (*S*)-**112** was afforded with lower, albeit useful, diastereospecificity. *ds* = 22:1. The difference in specificity was attributed to matched and mismatched reactions. The dienes were then subjected to RCM with Grubbs' catalyst to afford the *cis*- and *trans*-2,5-disubstituted pyrrolines in 86% and 87% yield, respectively. This methodology provides a highly specific strategy for the formation of either diastereoisomer.

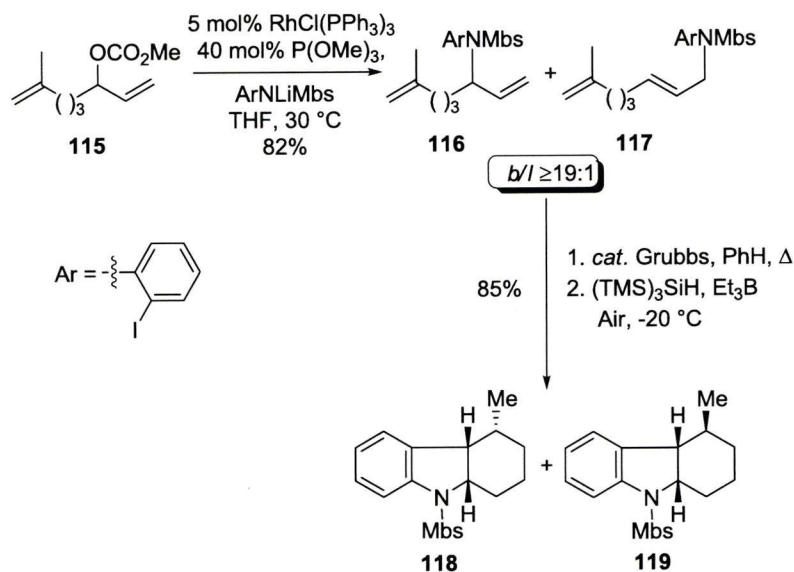
Scheme 1.11 Construction of *cis*- and *trans*-2,5-disubstituted pyrrolines.



Evans and co-workers also used the rhodium-catalyzed allylic amination methodology for the synthesis of dihydroquinolines and dihydrobenzo[*b*]indolines with high diastereoselectivities.⁴⁵ Formation of the dihydroquinolines followed the same sequence of reactions as the previous example with the amination product from *N*-4-methoxybenzenesulfonyl toluidine being subjected to ring closing metathesis. The dihydrobenzo[*b*]indolines were prepared through the rhodium-catalyzed allylic amination with 2-iodo-(*N*-4-methoxybenzenesulfonyl)aniline followed by ring-closing metathesis then a radical cyclization to afford the indolines in high diastereoselectivity (Scheme 1.12). For example, the reaction of carbonate **115** afforded the amination product in 82% yield with high regioselectivity. Amine **116**

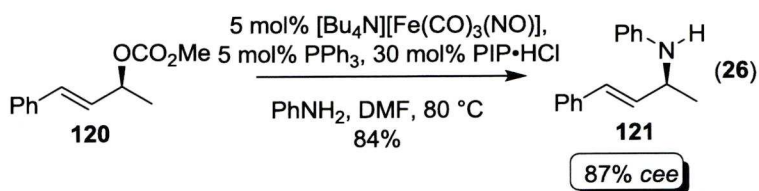
was then subjected to ring-closing metathesis followed by radical cyclization to afford indolines **118** and **119** in 85% yield favouring **118**.

Scheme 1.12 Synthesis of dihydrobenzo[*b*]indolines *via* Rh-catalyzed allylic amination/RCM/radical cyclization.



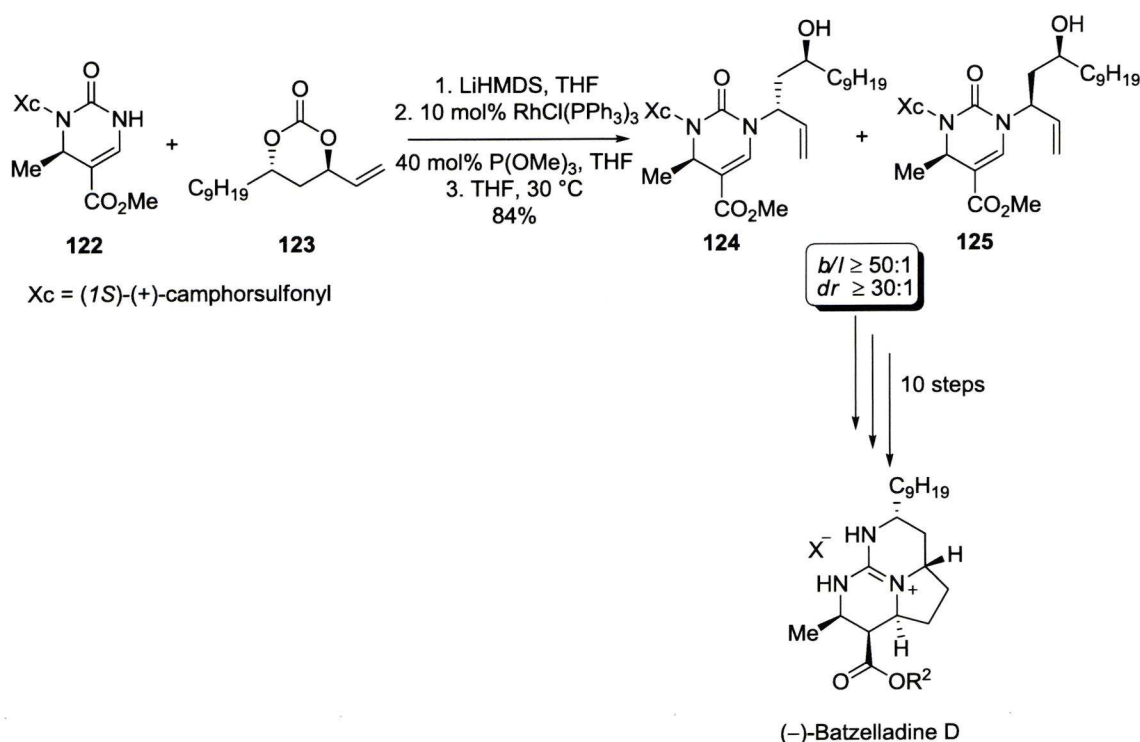
Bernd Plietker reported the regioselective iron-catalyzed allylic amination with $[\text{Bu}_4\text{N}][\text{Fe}(\text{CO})_3(\text{NO})]$ (eq. 26).⁴⁶ Preliminary studies with electron-poor secondary amines led to decomposition of the catalyst and low conversion. However, aniline and a tertiary carbonate provided the branched amine with moderate conversion but with high selectivity. When the reaction conditions were applied to secondary carbonates the yield was low (36%) due to catalyst decomposition. It was discovered that the addition of piperidinium chloride ($\text{Pip}\cdot\text{HCl}$) suppressed the catalyst decomposition and increased the yield. This allowed the anilines to be produced in high yield and with excellent regioselectivity favouring attack at the less sterically hindered carbon. *Meta*- and *para*-substituted anilines were effective nucleophiles in the reaction, with all examples proceeding with excellent regioselectivity. The amination was performed on enantiomerically enriched carbonates with two equivalents of aniline to afford the allylic amines with retention of configuration. For instance, when carbonate **120** was aminated with aniline, amine **121** was isolated in 84% yield and with 87% conservation of enantiomeric excess. This represents the

first iron-catalyzed allylic amination, and further investigation into a CO-free iron catalyst is underway.



Evans and co-workers reported the regio- and enantiospecific rhodium-catalyzed allylic amination of unsymmetrical chiral nonracemic allylic alcohol derivatives with *N*³-benzoyl thymine, and applied this methodology to the synthesis of a new conformationally rigid nucleoside.⁴⁷ The methodology was then applied to the total synthesis of batzelladine D (Scheme 1.13).⁴⁸ Treatment of cyclic carbonate **123** with 3,4-dihydropyrimidin-2(1H)-one **122** afforded the amination product **124** in 84% yield and with excellent regio- and diastereoselectivity (*dr* \geq 30:1, *b/l* \geq 50:1). batzelladine D was then prepared in 10 further steps including tributyltin hydride cyclization to furnish the second six-membered ring, and a reductive cyclization to afford batzelladine D.

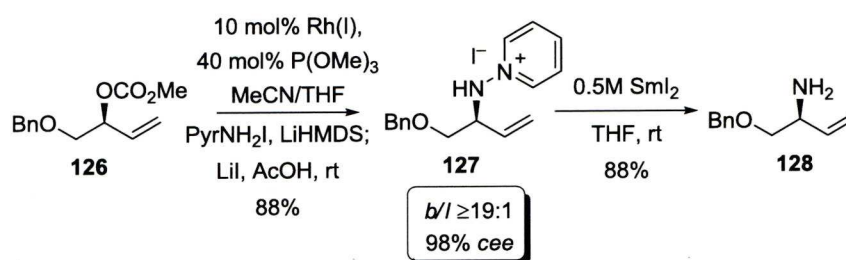
Scheme 1.13 Key step in the preparation of Batzelladine D.



Evans and Clizbe investigated the use of aza-ylides as pronucleophiles in the rhodium-catalyzed allylic amination reaction (Scheme 1.14).⁴⁹ It was anticipated that the aza-ylide would be more reactive as compared to the sulfur and phosphorus derivatives because they are only field stabilized, as compared to field and resonance stabilized. Since the nucleophile is an ylide, this process was not dependent on the counterion. Treatment of the anion of 1-aminopyridinium iodide, formed with different alkali metal salts as bases, furnished the amination adduct, albeit the potassium and sodium salts do not proceed to completion. Although the reaction with the lithium salt proceeds to completion, the isolated yield was initially moderate. It was determined that there was an equilibrium between the salt and the ylide and thus quenching the reaction with sodium iodide and acetic acid provided optimal yield. The reaction is applicable to a wide array of substrates, which provide excellent yield and regioselectivity. Scheme 1.14 outlines the determination of the stereochemical course of the reaction. Treatment of enantiomerically enriched allylic carbonate **126** with 1-aminopyridinium iodide under the optimized reaction conditions afforded the amination product **127** in 88% yield. The amination product **127** was subjected to a samarium diiodide deprotection which furnished the free

amine in 88% yield. Conversion to the known sulfonamide of **128** provided proof of absolute stereochemistry and it also revealed the reaction proceeded with retention of configuration. A one-pot amination/deprotection sequence was developed in order to afford the free amine directly in 74% yield from the allylic carbonate, although a significant amount of racemization was observed on the enantiomerically enriched substrate.

Scheme 1.14 Rhodium-catalyzed allylic amination reaction with an aza-ylide pronucleophile.

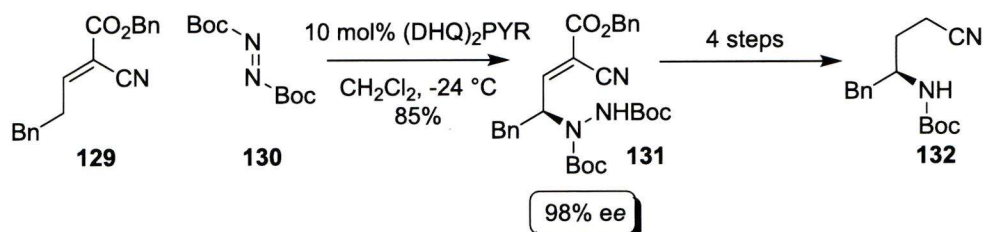


1.4. Organocatalytic Allylic Amination Reactions

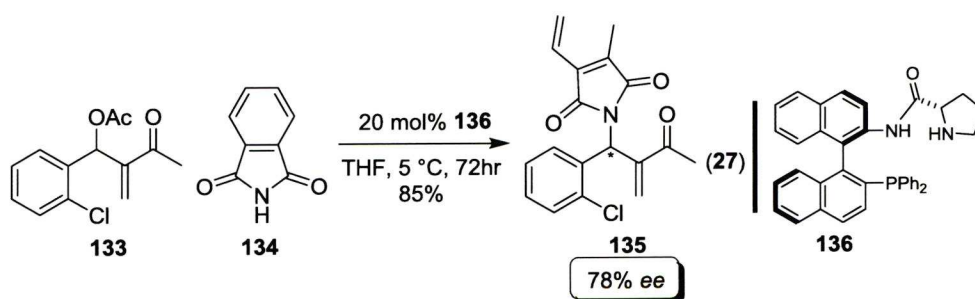
Organocatalyzed reactions are attractive since they avoid metals which can be toxic and expensive. Jørgensen and co-workers demonstrated the first enantioselective metal-free allylic amination using alkylidene cyanoacetates and dialkyl azodicarboxylates (Scheme 1.15).⁵⁰ In order for electrophilic addition to the allylic C-H bond to be successful, a number of problems with regioselectivity, diamination, and racemization had to be overcome. Initial results were poor, for example, the monomeric catalysts like quinine provide a mixture of α -, γ -, and diamination products at room temperature. Interestingly, the γ -amination product was the sole product when dimeric catalysts were used at lower temperature. For example, treatment of cyanoacetate **129** with azodicarboxylate **130** under optimal conditions afforded allylamine **131** in 85% yield and with 98% enantiomeric excess. The tolerance of γ -substitution on the cyanoacetate was high, with a range of substrates proving successful, including protected hydroxyl alkyl, branched alkyl, and allyl groups. All examples proceeded in high yield and excellent

enantioselectivity. The double bond in the product could be reduced and also act as the dienophile in the Diels-Alder reaction with 2,3-dimethyl-1,3-butadiene, to afford the cyclized product in 86% yield. The amination product **131** was also transformed into the Boc-protected γ -amino nitrile **132** in 4 steps.

Scheme 1.15 Synthesis of Boc-protected γ -amino nitrile *via* organocatalysis.



Shi and co-workers developed a series of mono- and bisphosphine catalysts, as well as phosphine-amide ligands, and applied them to the allylic amination of Morita-Baylis-Hillman acetates, as exemplified by **133** (eq. 27).⁵¹ It was determined that the organocatalyst **136**, prepared from L-proline, was optimal at a 20 mol% loading in THF at 5 °C, to afford the chiral amine in 90% yield and 53% *ee* when phthalimide was used as the nucleophile. The expanded scope included substrates containing electron-donating and withdrawing groups on the phenyl ring. Substrates containing a strongly electron withdrawing group (*i.e.* *m*-NO₂, *p*-CF₃, and *p*-CN) provided higher enantioselectivities than the electron donating substrates. The ortho substituted substrate **133** provided the highest enantioselectivity (78% *ee*). Although the enantioselectivity is modest in most examples, ligand **136** has great promise as an organocatalyst in the asymmetric allylic substitution reaction.

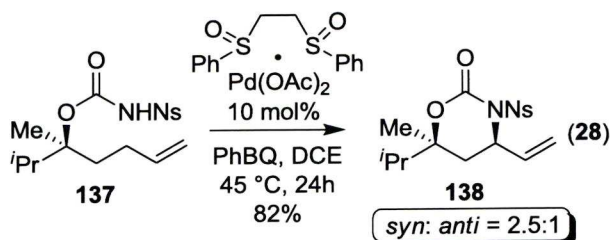


1.5 C-H Activation

The direct formation of a C-N bond from an unfunctionalized C-H bond is of significant interest for the formation of nitrogen-containing building blocks in organic synthesis. This has been accomplished through the activation of the C-H bond by transition metals. The intramolecular variant is generally more efficient than the intermolecular equivalent, with the intermolecular version generally requiring a large excess of the alkane to obtain complete conversion.

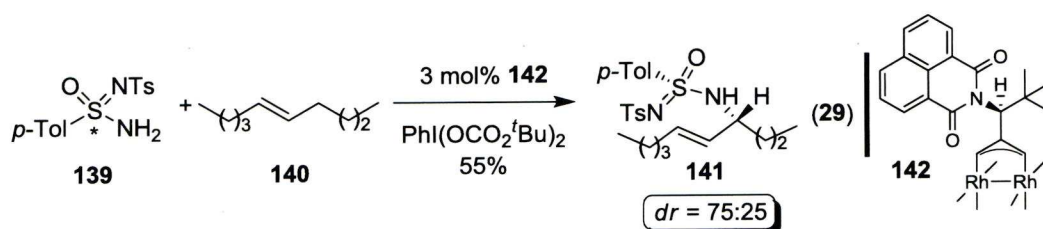
1.5.1 Intramolecular C-H Activation

White and Rice looked at intramolecular C-H amination of *N*-nosyl carbamates to prepare *syn*-1,3-amino alcohols with a Pd/sulfoxide catalyst.⁵² Initial studies demonstrated the acidity of the pronucleophile to be important, with more acidic compounds increasing the reactivity (eq. 28). However, if the substrate was too acidic the nucleophilicity decreased. The optimal nucleophile was found to be *N*-nosyl carbamate. The reaction proved to be general with a variety of substrates proceeding with good diastereoselectivity favouring the *syn*-adduct in high yield. Substrates containing an ester or ketone proceeded without difficulty, as well the quaternary carbamate **137** which afforded the cyclized product **138** in 82% yield and 2.5:1 diastereoselectivity. The *N*-nosyl carbamate proved to be more efficient in the preparation of 1,2-amino alcohol since the rate of reaction is much faster.



1.5.2 Intermolecular C-H Activation

Chiral dirhodium tetracarboxylate catalyst **142**, utilized by Dauban and co-workers, facilitates the intermolecular C-H amination to provide enantiomerically enriched allylic and benzylic sulfonimidamides (eq. 29).^{53,54} Previously, copper-catalyzed reactions proved efficient at inducing high levels of enantioselectivity; however, in this example rhodium provides higher diastereoselectivity than the corresponding copper catalyzed reactions. The allylic compounds afforded products in good to high yield but with moderate diastereoselectivity; however, utilizing benzylic compounds furnished products with increased diastereoselectivity. For example, the cyclopentene **140** provides the allylic sulfonamide **141** in 72% yield and only 3:1 diastereoselectivity.

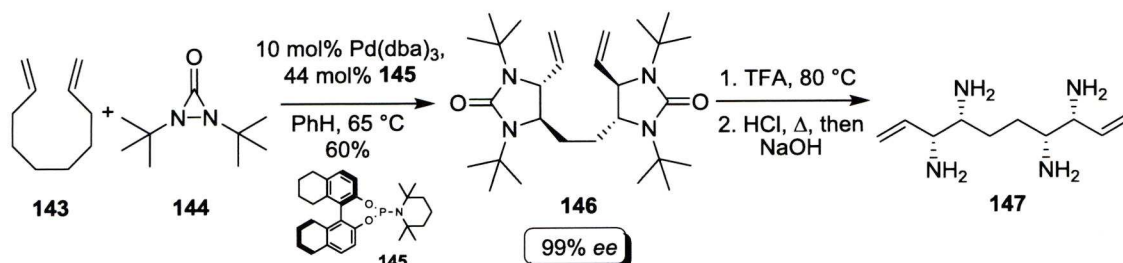


1.5.3 Diamination

Shi and co-workers described the asymmetric diamination of terminal olefins at the allylic and homoallylic carbons with di-*tert*-butyldiaziridinone *via* a palladium-catalyzed C-H amination using the phosphoramidite ligand **145** (Scheme 1.16).^{55,56} Interestingly, two of these ligands bind to the palladium regardless of the ratio of ligand. Various terminal olefins, including substrates containing heteroatoms, branching and a second internal olefin, provide good to high yield and excellent enantioselectivity. If two terminal olefins are present, a second diamination reaction occurred affording a tetraamine after deprotection in moderate yield and excellent enantioselectivity. For example, treatment of diene **143** with Pd(*dba*)₃ and

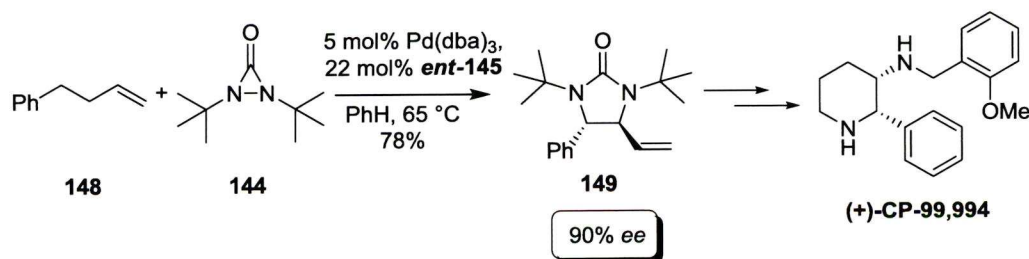
phosphoramidite ligand **145** afforded protected tetraamine **146** in 60% yield. This reaction provides an efficient route to 1,2-diamines.

Scheme 1.16 Use of the diamination reaction enroute to tetraamine **147**.



This methodology was applied to the synthesis of P receptor antagonist (+)-CP-99,994 (Scheme 1.17). The antagonist was prepared in 13 steps from terminal olefin **148** in 20% overall yield. The key step was the diamination of **148** which afforded the protected diamine **149** in 78% yield and with 90% enantiomeric excess.⁵⁶

Scheme 1.17: P receptor antagonist (+)-CP-99,994



1.6 Hydroamination

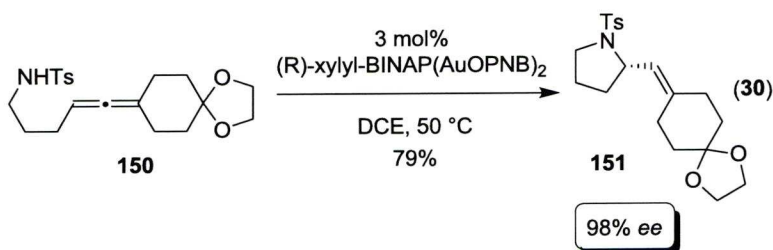
Hydroamination involves the activation of an N-H bond by a late transition metal to form a metal-amide or metal-imide complex.⁵⁹ As with the C-H activation reaction, the intermolecular variant is much more difficult, albeit the intramolecular version has been well studied. The reaction proceeds with the formal addition of an

N-H bond across an alkene or alkyne, with the chirality in the product being introduced either through a chiral catalyst or from the substrate.

1.6.1 Addition to Allenes

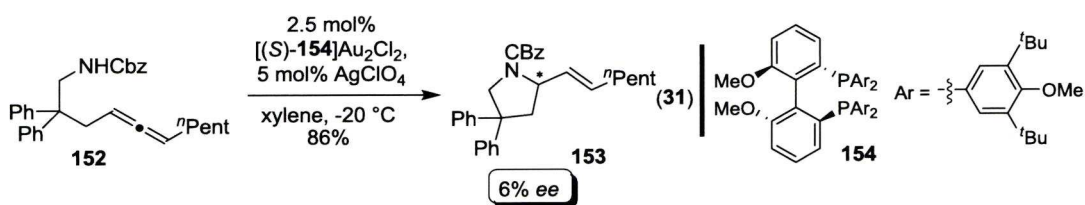
1.6.1.1 Intramolecular Addition to Allenes

Toste and co-workers employed gold phosphine complexes to facilitate an intramolecular hydroamination of allenes, forming vinyl pyrrolidines and piperidines (eq. 30).⁵⁸ During the optimization of the reaction a prominent counterion effect was observed whereby the larger the counter-ion of the added silver salt, the higher the enantioselectivity. The larger counter-ions initially caused low yields; however, adding a silver salt with an electron withdrawing benzoate increased the yield without lowering the enantioselectivity. The reaction also proceeded in high yields and enantioselectivity with cyclic and linear alkanes. For example, treatment of allene **150** with the gold catalyst, afforded allylamine **151** in 79% yield and with 98% enantiomeric excess. Electronic changes caused the reaction to become sluggish and require longer reaction times and/or higher temperature. It was also demonstrated that the tether could contain substitution, although the reaction conditions required additional modification to achieve complete conversion. When the substrate contained a dimethyl α - to the amine, the reaction needed to be run in nitromethane at 50 °C which afforded the pyrrolidine in 76% and with 96% *ee*.



Widenhoefer and co-workers also observed that silver salts caused a dramatic effect on the rate of the asymmetric intramolecular hydroamination of *N*-allenyl

carbamates (eq 31).⁵⁹ Interestingly, a 1:2 mixture of [(*S*)-**154**] Au_2Cl_2 : AgClO_4 caused a 1000-fold increase in the rate of the reaction, compared to other silver salts like AgOTf and AgBF_4 . The reaction was efficient with several carbamate and carboxamide derivatives and were dependent on the substitution at the C2 position. The reaction preceeded with low enantioselectivity when the diphenyl was not present, and disubstitution of the terminal allene was tolerated. Whereas monosubstitution afforded only 6% enantiomeric excess as in the reaction of carbamate **152**.



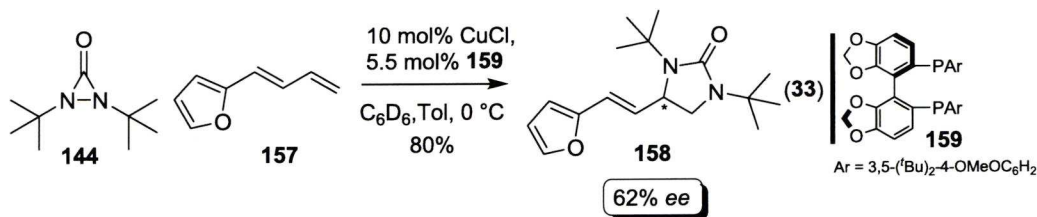
1.6.1.2 Intermolecular Addition to Allenes

The intramolecular hydroamination reaction has been well studied compared to the intermolecular variant. Yamamoto and Nishina have studied the gold-catalyzed intermolecular hydroamination with aryl⁶⁰ and aliphatic⁶¹ amines as well as probing the mechanism. Studies support that the gold complexes react first with the amine and then to the allene due to an observed induction period as well as a drop in yield if the gold is not mixed with the amine first. It is believed that the gold-amine complex approaches the less hindered side of the allene and then the amine is transferred to the less substituted terminal carbon. For example, in the reaction of **155** the nitrogen is transferred to the carbon with the methyl substituent rather than the phenyl, to provide the allylic amine in 68% yield and with 94% conservation of enantiomeric excess (eq. 32). Interestingly, the product of a morpholine addition was obtained in just 57% *cee*, presumably because of the higher reaction temperature ($80\text{ }^\circ\text{C}$). In the case of aniline, alkyl and aryl substituents are tolerated. 1,3-disubstituted compounds react similar to monosubstituted compounds, but 1,1-disubstituted compounds afford trace amounts of products.



1.6.2 Addition to Conjugated Olefins

Shi and co-workers investigated the copper-catalyzed diamination of conjugated dienes to compliment their work with Pd-catalyzed diamination.^{62,63} The copper-catalyzed reaction had been reported to proceed selectively at the terminal olefin, which was envisioned to proceed through a radical intermediate making the development of an enantioselective process challenging. In this context, bisphosphine ligands with CuCl proved optimal for inducing enantioselectivity, which provided the diamination product with good enantioselectivity (up to 74%) which could be improved with recrystallization ($\geq 99\%$). For example, treatment of diene **157** with the chiral copper complex of ligand **159** afforded the protected diamine **158** in 80% yield and with 62% enantiomeric excess (eq. 33). Aryl and alkyl substrates were tolerated, *cis*-alkenes isomerize to afford solely the *trans*-product, and 1,1'-disubstituted compounds gave slightly higher enantioselectivities. This work also demonstrated a chiral copper phosphoric acid complex catalyzes this process, albeit with slightly lower enantioselectivity.⁶⁵

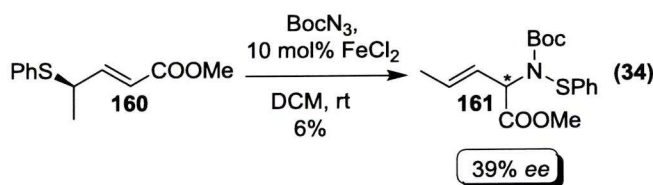


1.7 Rearrangements

Sigmatropic rearrangements provide a convenient method for preparing enantiomerically enriched allylamines through a transfer of chirality in the substrate.⁶⁵ The reaction proceeds through a cyclic intermediate and can be uncatalyzed; however, Lewis acids or even transition have been used to catalyze the rearrangements.

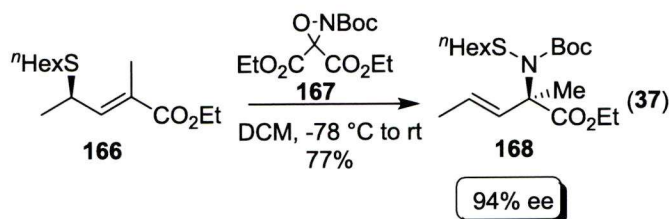
1.7.1 [2,3]-Sigmatropic Rearrangements

Bach and Körber reported the first synthesis of *N*-Boc *N*-allylamines from allyl sulfides *via* an imidation/[2,3]-sigmatropic rearrangement sequence (eq. 34).⁶⁶ The reactions were performed at room temperature using catalytic FeCl₂ and BocN₃ as the nitrene source affording the rearranged allylamine in moderate to good yield. Alkyl and oxygen containing substituents demonstrated that α -branching, hydroxyl, ethers and esters are tolerated, albeit the esters are produced in much lower yield. The stereospecific rearrangement of the enantiomerically enriched sulfide **160**, provided the allylic amine **161** in 6% yield and with only 39% *ee*. The low enantioselectivity was attributed to the product racemizing, which prompted the examination of a substrate in which the ester was replaced with a methyl group; however, the reaction still afforded product with poor stereoselectivity (39% *ee*) albeit in slightly higher yield (32%).



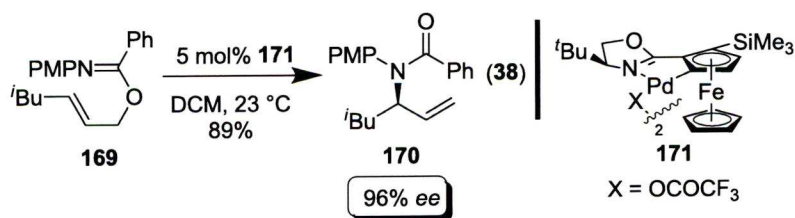
Saito and co-workers utilized the [2,3]-sigmatropic rearrangement of hydroxylamines to afford *N*-(hydroxyl)allylamines in generally good yield.⁶⁷ Interestingly, only the (*E*)-geometry of 1,2-disubstituted olefins provided a good

low yield of amine was attributed to steric factors, and gratifyingly, when *n*-hexyl sulfide was used, the desired amine was isolated in high yield and with excellent transfer of chirality (>95% *cee*). The application of this process to the generation of a chiral quarternary stereogenic center using substrate **166**, provided the *N*-Boc hexylsulfinyl allylamine **168** in 77% yield and with 94% enantiomeric excess.



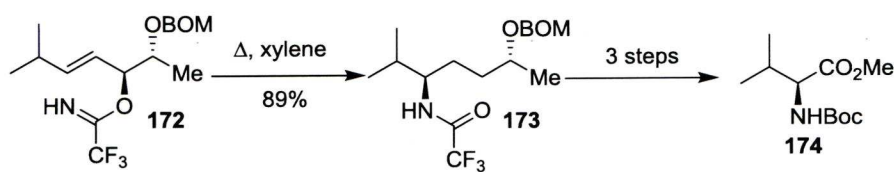
1.7.2 [3,3]-Sigmatropic Rearrangement

Overman and co-workers reported the [3,3]-sigmatropic rearrangement of allylic imidates to prepare allylic amines (eq. 38).⁷¹ Preliminary studies used palladium-diamine or palladium-bisoxazoline complexes as ligand. In 1999, ferrocenyl-oxazoline ligands were reported to catalyze the reaction with high efficiency with enantioselectivity up to 96%. In all cases the *Z*-stereoisomer of the imidate rearranges with higher enantioselectivity than the corresponding *E*-variant. For example, treatment of imidate **169** with catalyst **171** afforded allylic amine **170** in 89% yield and with 96% enantiomeric excess. When the *E*-isomer of **169** was employed, the amine was furnished in higher yield (97%); however, the enantioselectivity decreased to 84%. The reaction was tolerant of straight chain and branched alkyl substituents off the olefin, however aryl derivatives afforded lower enantioselectivity. The use of the ferrocenyl palladium complexes for the rearrangement of the imidates afforded the highest selectivities at the time.



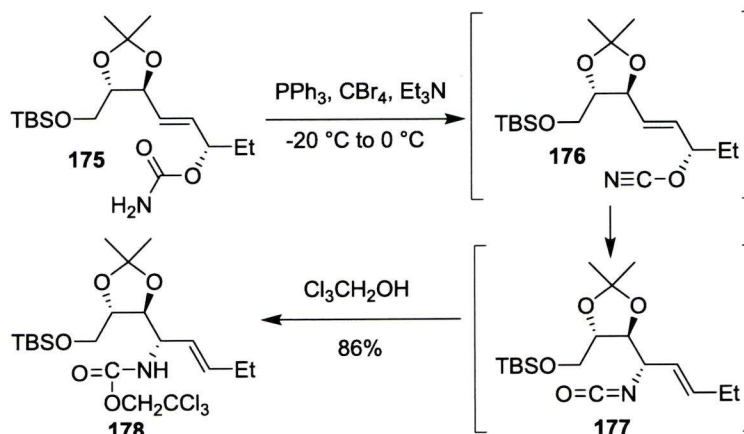
Thomas and co-workers used the [3.3]-sigmatropic rearrangement of chiral trifluoroacetimidates to afford trifluoroacetimides as intermediates for the preparation of α -amino acid derivatives.^{72,73} Preliminary reactions with trichloroacetimidates provided extended reaction times and low yields. Changing the acetimidate to the trifluoro- variant **172** reduced the reaction time by half and furnished the acetimide **173** in 89% yield as a single stereoisomer. Sodium borohydride reduction furnished the free amine in 75% yield. The synthesis of (*R*)- and (*S*)-valine **174** demonstrates that remote stereocenters do not influence the 1,3-chirality transfer (Scheme 1.18). This rearrangement was used as the key step in the synthesis of antifungal nucleoside thymine polyoxin C in which the reaction proceeded in 90% yield selectively.

Scheme 1.18 Synthesis of (*S*)-valine **174** through a [3.3]-sigmatropic rearrangement.

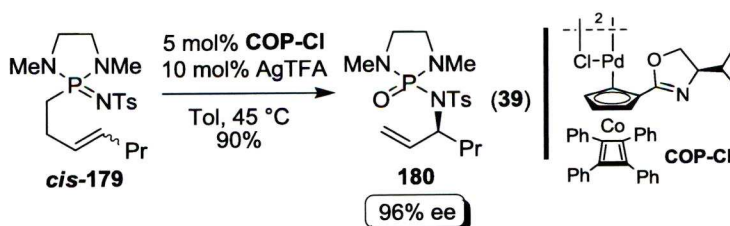


The synthesis of the amyloglucosidase inhibitor, lentiginosine was reported by Ichikawa and co-workers from L-tartaric acid using the rearrangement of a cyanate as the key step (Scheme 1.19).^{74,75} The previously developed methodology demonstrated that allyl cyanates undergo the [3.3]-sigmatropic rearrangement to afford allyl isocyanates, which could be transformed into the acetamide and finally hydrolyzed to the free amine. This process proceeds with complete transfer of chirality to the newly formed C-N bond. In the key step for the synthesis of lentiginosine the allyl cyanate was prepared from carbamate **175** which rearranges to isocyanate **177**. The isolation of isocyanate led to a decrease in yield so the crude mixture was treated with 2,2,2-trichloroethanol to afford the carbamate **178** in 86% yield from **175**. The group has also utilized this methodology to prepare pachastrissamine, a cytotoxic anhydrophingosine, from L-tartaric acid.⁷⁷

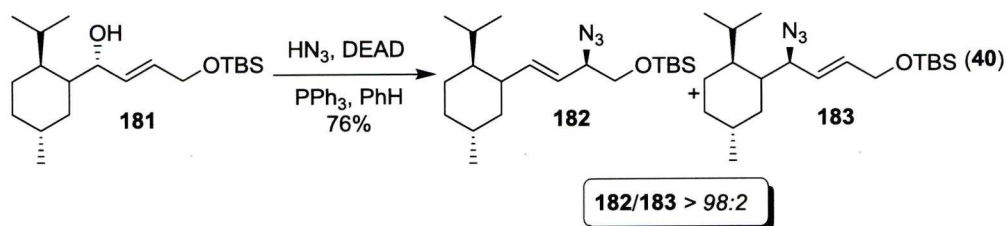
Scheme 1.19 Key step in the synthesis of lentiginosine.



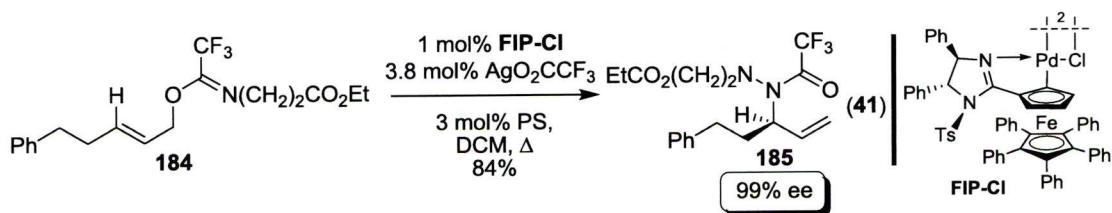
Batey and Lee presented the first example of an oza-phospha-oxa-Cope rearrangement for a synthesis of producing asymmetric allylic amines using $\text{PdCl}_2(\text{MeCN})_2$ as catalyst (eq. 39).⁷⁸ The use of phospholindines allows more variation than phosphorimidates, and therefore more of a chance to control reactivity and selectivity. The rearrangements proceeded in high yield and β -substituted compounds as well as those generated from secondary alcohols were tolerated. However, γ,γ -disubstituted substrates afford no product, and more hindered substrates proceed slower. Additionally, the *E*-olefins react with nearly complete chirality transfer (from 95% *ee* to 91% *ee*); whereas, the *Z*-olefins are no longer stereospecific (from 95% to 70%). A diastereoselective variant with a chiral auxiliary was also examined; however, the process provides poor selectivity. An enantioselective version has also been developed using a chiral cobalt oxazoline palladacycle (COP-Cl) using silver salts suppress side reactions. The *cis*-olefins were more efficient, providing enantioselectivity up to 96%. For example rearrangement of *cis*-**179** afforded the allylic amine **180** in 90% yield. This is a great improvement for the [3,3]-sigmatropic rearrangement, since it circumvents the necessity for chiral starting materials.



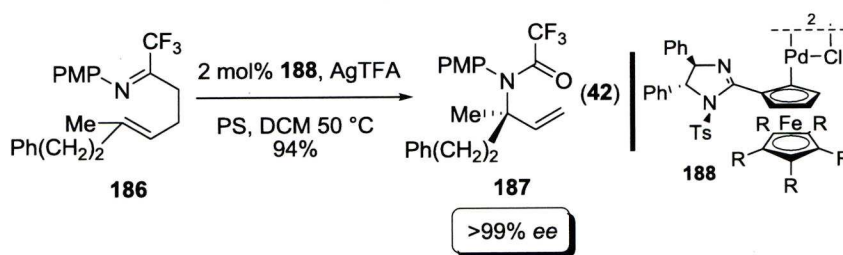
Spino and co-workers subjected auxillary containing chiral allylic alcohols to hydrazoic acid under Mitsunobu conditions and saw a [3,3]-sigmatropic rearrangement occur (eq. 40).⁷⁹ The rearrangement of allylic azides have been reported previously; however, there is usually a regioselectivity issue. The reaction with hydrazoic acid afforded only the rearrangement product in high yield, with only small amounts of the S_N2 product. The reaction proved efficient with branched substituents as well as silyl-protected alcohols. For example treatment of allylic alcohol **181** under the optimized reaction conditions afforded allylic azides **182** and **183** in 76% yield and with high regioselectivity (**182/183** >98:2). When the olefin was in conjugation with a phenyl, the regioselectivity was lower. The auxiliary could be readily removed to afford amino acids or *N*-heterocycles.



Peters and co-workers reported the first use of aza-Claisen rearrangements of *N*-aryl and *N*-alkyl-substituted trifluoroacetimidates to afford secondary allylic amines (eq. 40).⁸⁰ The rearrangement was tested with a series of substrates catalyzed by palladium. For example, rearrangement of trifluoroacetimidate **184** afforded 84% of **185**. When unbranched alkyl substituents were on the trifluoroacetamide, catalyst loadings as low as 0.2 mol% were used; however, when the steric bulk increased, loadings up to 1-2 mol% were required though the yield was generally lower. Whereas, the reaction completely fails for α -branched alkyls. Removal of the trifluoroacetamide group under standard conditions afforded the secondary amine in good yield.



In related studies, the same group examined forming enantiomerically enriched quaternary centers using this methodology.⁸¹ Until this point, all methods utilized to form quaternary centers *via* the aza-Claisen reaction were performed in a non-enantioselective manner. The poor results were attributed to the slow formation of the quaternary center due to steric reasons. It was demonstrated that by employing the ferrocenyl catalyst **188**, 3,3-disubstituted allylic trifluoroacetimidates rearranged to furnish quaternary amine centers in high yield and with excellent enantiomeric excess. For example the rearrangement of **186** in the presence of 2 mol% **188** afforded **187** in 94% yield and with >99% enantiomeric excess. The catalyst loading could be lowered to 0.5 mol%; however a dramatic increase in reaction time occurred. These studies represent a significant advancement in the formation of enantiomerically enriched tertiary amine compounds.



1.8 Final Remarks

The reactions presented in this review represent the advances made towards the synthesis of enantiomerically enriched allylic amines in the past decade. There has been significant advances on the transition-metal catalyzed allylic amination reaction with the introduction of new ligands and metal complexes. New developments in organocatalysts and related methodology has not advanced to the same degree, but promises to provide a range of complementary methods. Additional advances will continually have to deal with increasing the substrate scope rather than the simple demonstration of the process, which will promote the development of new catalysts.

1.9 References

1. For general reviews on allylic amination
 - (a) Johannsen, M.; Jørgensen, K. A. *Chem. Rev.* **1998**, *98*, 1689.
 - (b) Jørgensen, K. A. *Modern Amination Methods*; Ricci, A., Ed.; Wiley-VCH: Weinheim, Germany, 2000; Chapter 1, 1-35.
2. For reviews on transition-metal catalyzed allylic substitution reactions:
 - (a) Miyabe, H.; Takemoto, Y. *Synlett* **2005**, *11*, 1641.
 - (b) Leahy, D. K.; Evans, P. A. *In Modern Rhodium-Catalyzed Organic Reactions*; Evans, P. A., Ed.; Wiley-VCH: Weinheim, Germany, 2005; Chapter 10, pp 191-214
 - (c) Lu, Z.; Ma, S. *Angew. Chem. Int. Ed.* **2008**, *47*, 258.
 - (d) Helmchen, G.; Dahnz, A.; Dübon, P.; Schelwies, M.; Weihofen, M. *Chem. Commun.* 2007, 675.
3. Use of Phosphine Ligands:
 - (a) Constantieux, T.; Brunel, J.-M.; Labande, A.; Buono, G. *Synlett* **1998**, 1998, 49.
 - (b) Muchow, G.; Brunel, J. M.; Maffei, M.; Pardigon, O.; Buono, G. *Tetrahedron* **1998**, *54*, 10435.
 - (c) Dolben, F.; Johansson, M. J.; Antonsson, T.; Kann, N. *Synlett* **2006**, *20*, 3389.
 - (d) Birkholz, M.-N.; Dubrovina, N. V.; Shuklov, I. A.; Holz, J.; Paciello, R.; Waloch, C.; Breit, B.; Börner, A. *Tetrahedron Asymm.* **2007**, *18*, 2055.
 - (e) Hamada, Y.; Seto, N.; Takayanagi, Y.; Nakano, T.; Hara, O. *Tetrahedron Lett.* **1999**, *40*, 7791.
 - (f) Uozumi, Y.; Tanaka, J.; Shibatomi, K. *Org. Lett.*, **2004**, *6*, 281.
 - (g) Trost, B. M.; Malhotra, S.; Olson, D. E.; Maruniak, A.; Du Bois, J. *J. Am. Chem. Soc.*, **2009**, *131*, 4190
 - (h) Trost, B. M.; Bunt, R. C.; Lemoine, R. C.; Calkins, T. L. *J. Am. Chem. Soc.* **2000**, *122*, 5968.
 - (i) Trost, B. M.; Lee, C. B. *J. Am. Chem. Soc.* **2001**, *123*, 3687.
 - (j) Trost, B. M.; Horne, D. B.; Woltering, M. J. *Chem. Eur. J.* **2006**, *12*, 6607.
4. Use of Sulfur/Phosphine Ligands:

- (a) Evans, D. A.; Campos, K. R.; Tedrow, J. S.; Michael, F. E.; Gagne, M. R. *J. Org. Chem.* **1999**, *64*, 2994.
 - (b) Hiroi, K.; Suzuki, Y.; Kawagishi, R. *Tetrahedron. Lett.* **1999**, *40*, 715.
 - (c) Nakano, H.; Okuyama, Y.; Yanagida, M.; Hongo, H. *J. Org. Chem.* **2001**, *66*, 620.
 - (d) Chen, J.; Lang, F.; Li, D.; Cun, L.; Zhu, J.; Deng, J.; Liao, J. *Tetrahedron Asymm.* **2009**, *20*, 1953.
5. Use of Phosphinooxazoline Ligands:
- (a) Yonehara, K.; Hashizume, T.; Mori, K.; Ohe, K.; Uemura, S. *J. Org. Chem.* **1999**, *64*, 9374.
 - (b) Selvakumar, K.; Valentini, M.; Wörle, M.; Progosin, P. S. *Organometallics*, **1999**, *18*, 1207.
 - (c) Humphries, M. E.; Clark, B. P. Regini, S.; Acemoglu, L.; Williams, J. M. J. *Chirality* **2003**, *15*, 190.
 - (d) Benetsky, E.; Safronov, A.; Grishina, T.; Petrovskii, P.; Davankov, V.; Gavrilov, K. *Russ. Chem. Bull. Int. Ed.* **2006**, *55*, 2187.
 - (e) Flubacher, D; Helmchen G. *Tetrahedron Lett.* **1999**, *40*, 3867.
 - (f) Berkowitz, D. B.; Shen, W.; Maiti, G. *Tetrahedron Asymm.* **2004**, *15*, 2945.
 - (g) Popa, D.; Marcos, R.; Sayalero, S.; Vidal-Ferran, A.; Pericàs, M. A. *Adv. Synth. Catal.* **2009**, *351*, 1539.
6. Use of Phosphine-Amide Ligands:
- (a) Tollabi, M.; Framery, E.; Goux-Henry, C.; Sinou, D. *Tetrahedron Asymm.* **2003**, *14*, 3329.
 - (b) Glegola, K.; Midrier, C; Framery, E.; and Pietrusiewicz, K. M. *Phosphorus, Sulfur Silicon Relat. Elem.* **2009**, *184*, 1065
7. Use of Ferrocenylphosphine Ligands:
- (a) Malone, Y. M.; Guiry, P. J. *J. Organomet. Chem.* **2000**, *603*, 110.
 - (b) Deng, W.-P.; You, S.-L.; Hou, X.-L.; Dai, L.-X.; Yu, Y.-H.; Xia, W., Sun, J. *J. Am. Chem. Soc.* **2001**, *123*, 6508.
8. Use of Diazaphospholidine Ligands:
- (a) Breeden, S. and Wills, M. *J. Org. Chem.* **1999**, *64*, 9735.
 - (b) Edwards, C. W.; Shipton, M. R.; Alcock, N. W.; Clase, H.; Wills, M. *Tetrahedron* **2003**, *59*, 6473.
9. Use of BINAP Ligands:

- (a) Wang, Y.; Ding, K. *J. Org. Chem.* **2001**, *66*, 3238.
 - (b) Rabeyrin, C.; Sinou, D. *Tetrahedron. Asymm.* **2003**, *14*, 3891.
 - (c) Ohta, T.; Sasayama, H.; Nakajima, O.; Kurahashi, N.; Furii, T.; Furukawa, I. *Tetrahedron Asymm.* **2003**, *14*, 537.
 - (d) Nagano; T. Kobayashi, S. *J. Am. Chem. Soc.* **2009**, *131*, 4200.
 - (e) Berkowitz, D. B.; Maiti, G. *Org. Lett.* **2004**, *6*, 2661
 - (f) Faller, J. W.; Wilt, J. C. *Org. Lett.* **2005**, *7*, 633.
 - (g) Faller, J. W.; Wilt, J. C. *Organometallics*, **2005**, *24*, 5076.
10. Use of Phosphite Ligands:
- (a) Brunel, J. M.; Faure, B. *J. Mol. Catal. A: Chem.* **2004**, *212*, 61.
 - (b) Diéguez, M.; Pàmies, Claver, C. *J. Org. Chem.*, **2005**, *70*, 3363.
 - (c) Lyubimov, A. N.; Davankov, V. A.; Kucherenko, A. S.; Zlotin, S. G.; Zheglov, S. V.; Gavrilov, K. N.; Petrovskii, P. C. *Russ. Chem. Bull.* **2005**, *54*, 2558.
 - (d) Benetsky, E. B.; Zheglov, S. V.; Grishina, T. B.; Macaev, F. Z.; Bet, L. P.; Davankov, V. .; Gavrilov, K. N. *Tetrahedron Lett.* **2007**, *48*, 8326.
 - (e) Lyubimov, S. E.; Tyutyunov, A. A.; Vologzhanin, P. A.; Safronov, A. S.; Petrovskii, P. V.; Kalinin, V. N.; Gavrilov, K. N.; Davankov, V. A. *J. Organomet. Chem.* **2008**, *693*, 3321.
11. Reviews on the use of C_2 -symmetric ligands:
- (a) Pfaltz, A.; Drury, W. J., III *Proc. Natl. Acad. Sci.* **2004**, *101*, 5723
 - (b) Desimoni, G.; Faita, G.; Jørgensen, K. A. *Chem. Rev.* **2006**, *106*, 3561.
 - (c) Fraile, J. M.; García, J. I.; Gissibl, A.; Mayoral, J. A.; Pires, E.; Reiser, O.; Roldán, M.; Villalba, I. *Chem. Eur. J.* **2007**, *13*, 8830.
12. (a) Nemoto, T.; Hamada, Y. *Chem Rec.* **2007**, *7*, 150.
 (b) Nemoto, T. *Chem. Pharm Bull.* **2008**, *56*, 1213.
13. Nemoto, T.; Masuda, T.; Akimoto, Y.; Fukuyama, T.; Hamada, Y. *Org. Lett.* **2005**, *7*, 4447.
14. Nemoto, T.; Fukuyama, T.; Yamamoto, E.; Tamura, S.; Fukuda, T.; Matsumoto, T.; Akimoto, Y.; Hamada, Y. *Org Lett.* **2007**, *9*, 927.
15. Nemoto, T.; Tamura, S.; Sakamoto, T.; Hamada, Y. *Tetrahedron. Asymm.* **2008**, *19*, 1751.
16. Miyabe, H.; Matsumura, A.; Moriyama, K.; Takemoto, Y. *Org. Lett.* **2004**, *6*, 4631.

17. Nemoto, T.; Sakamoto, T.; Matsumoto, T.; Hamada, Y. *Tetrahedron Lett.*, **2006**, 47, 8737.
18. (a) de Vries, A. H. M.; Meetsma, A.; Feringa, B. L. *Angew. Chem. Int. Ed.* **1996**, 36, 2374.
 (b) Van den Beuken, E. K.; Meetsma, A.; Huub, K.; Spek, A. L.; Feringa, B. L. *Inorg. Chim. Acta* **1997**, 264, 171.
 (c) Polet, D.; Alexakis, A.; Tissot-Croset, K.; Corminboeuf, C.; Ditrich, K. *Chem. Eur. J.* **2006**, 12, 3596.
19. (a) Welter, C.; Koch, O.; Lipowsky, G.; Helmchen, G. *Chem. Commun.* **2004**, 896.
 (b) Welter, C.; Dahnz, A.; Brunner, B.; Streiff, S.; Dübon, P.; Helmchen, G. *Org. Lett.* **2005**, 7, 1239.
 (c) Shi, Ce; Ojima, I. *Tetrahedron* **2007**, 63, 8563.
20. Ohmura, T.; Hartwig, J. F. *J. Am. Chem. Soc.* **2002**, 124, 15164.
21. Tissot-Croset, K.; Polet, D.; Alexakis, A. *Angew. Chem. Int. Ed.* **2004**, 43, 2426.
22. Lipowsky G.; Helmchen G. *Chem. Commun.* **2004**, 116.
23. Weihofen, R.; Dahnz, A.; Tverskoy, O.; Helmchen, G. *Chem. Commun.* **2005**, 3541.
24. Welter, C.; Moreno, R. M.; Streiff, S.; Helmchen, G. *Org. Biomol. Chem.* **2005**, 3, 3266.
25. Dübon, P.; Farwick, A.; Helmchen, G. *Synlett* **2009**, 1413.
26. Weihofen, R.; Tverskoy, O.; Helmchen, G. *Angew. Chem. Int. Ed.* **2006**, 45, 5546.
27. Spiess, S.; Berthold, C.; Weihofen, R.; Helmchen, G. *Org. Biomol. Chem.* **2007**, 2357.
28. Yamashita, Y.; Gopalarathnam, A.; Hartwig, J. F. *J. Am. Chem. Soc.* **2007**, 129, 7508.
29. Leitner, A.; Shekhar, S.; Pouy, M. J.; Hartwig, J. F. *J. Am. Chem. Soc.* **2005**, 127, 15506.
30. Lee, J. H.; Shin, S.; Kang, J.; Lee, S.-G. *J. Org. Chem.* **2007**, 72, 7443.
31. Pouy, M. J.; Leitner, A.; Weix, D. J.; Ueno, S.; Hartwig, J. F. *Org. Lett.* **2007**, 9, 3949.
32. Defieber, C.; Ariger, M. A.; Moriel, P.; Carreira, E. M. *Angew. Chem. Int. Ed.* **2007**, 46, 3139.

33. Singh, O. V.; Han, H. *Tetrahedron Lett.* **2007**, *48*, 7094.
34. Spiess, S.; Welter, C.; Frank, G.; Taquet, J.-P.; Helmchen, G. *Angew. Chem. Int. Ed.* **2008**, *47*, 7652.
35. Gnam, C.; Franck, G.; Miller, N.; Stork, T.; Groedner, K.; Helmchen, F. *Synthesis* **2008**, *20*, 3331.
36. Stanley, L. M.; Hartwig, J. F. *J. Am. Chem. Soc.* **2009**, *131*, 8971.
37. Weix, D. J.; Marković, D.; Ueda, M.; Hartwig, J. F. *Org. Lett.* **2009**, *11*, 2944.
38. Pouy, M. J.; Stanley, L. M.; Hartwig, J. F. *J. Am. Chem. Soc.* **2009**, *131*, 11312.
39. Ichikawa, Y.; Yamamoto, S.-I.; Kotsuki, H.; Nakano, K. *Synlett*, **2009**, *14*, 2281.
40. Nakanishi, S.; Okamoto, K.; Yamaguchi, H.; Takata, T. *Synthesis*, **1998**, 1735.
41. Sugiura, M.; Yagi, Y.; Wei, S.-Y.; Nakai, T. *Tetrahedron Lett.* **1998**, *39*, 4351.
42. Evans, P. A.; Nelson, J. D. *J. Am. Chem. Soc.* **1998**, *120*, 5581.
43. Evans, P. A.; Robinson, J. E.; Nelson, J. D. *J. Am. Chem. Soc.* **1999**, *121*, 6761.
44. Evans, P. A.; Robinson, J. E. *Org. Lett.* **1999**, *1*, 1929.
45. Evans, P. A.; Robinson, J. E.; Moffett, K. K. *Org. Lett.* **2001**, *3*, 3269.
46. B. Plietker, *Angew. Chem. Int. Ed.* **2006**, *45*, 6053.
47. Evans, P. A.; Lai, K. W.; Zhang, H.-R.; Huffman, J. C. *Chem. Commun.* **2006**, 844.
48. Evans, P. A.; Qin, J.; Robinson, J. E.; Bazin, B. *Angew. Chem. Int. Ed.* **2007**, *119*, 7561.
49. Evans, P. A.; Clizbe, E. A. *J. Am. Chem. Soc.* **2009**, *131*, 8722.
50. Poulsen, T. B.; Alemparte, C.; Jørgensen, K. A. *J. Am. Chem. Soc.* **2005**, *127*, 11614.
51. Ma, G.-N.; Cao, S.-H.; Shi, M. *Tetrahedron. Asymm.* **2009**, *20*, 1086.
52. Rice, G. T.; White, M. C. *J. Am. Chem. Soc.* **2009**, *131*, 11707.
53. Liang, C.; Robert-Peillard, F.; Fruit, C.; Müller, P.; Dodd, R. H.; Dauban, P. *Angew. Chem. Int. Ed.* **2006**, *45*, 4641.
54. Liang, C.; Collet, F.; Robert-Peillard, F.; Müller, P.; Dodd, R. H.; Dauban, P. *J. Am. Chem. Soc.* **2008**, *130*, 343.
55. Du, H.; Zhao, B.; Shi, Y. *J. Am. Chem. Soc.* **2008**, *130*, 8590.
56. Fu, R.; Zhao, B.; Shi, Y. *J. Org. Chem.* **2009**, *74*, 7577.
57. (a) Patil, N. T.; Lutete, L. M.; Wu, H.; Pahadi, N. K.; Gridnev, I. D.; Yamamoto, Y. *J. Org. Chem.* **2006**, *71*, 4270.

- (b) Aillaud, I.; Collin, J.; Hannedouche, J.; Schulz, E. *J. Chem. Soc. Dalton Trans.* **2007**, 5105.
- (c) Bongers, N.; Krause, N. *Angew. Chem. Int. Ed.* **2008**, 47, 2178.
- (d) Dzhemilev, U. M.; Tolstikov, G. A.; Khusnutdinov, R. I. *Russ. J. Org. Chem.* **2009**, 45, 957.
58. LaLonde, R. L.; Sherry, B. D.; Kang, E. J.; Toste, F. D. *J. Am. Chem. Soc.* **2007**, 129, 2454.
59. Zhang, Z.; Bender, C. F.; Widenhoefer, R. A. *Org. Lett.* **2007**, 9, 2887.
60. Nashina, N.; Yamamoto, Y. *Angew. Chem. Int. Ed.* **2006**, 45, 3314.
61. Nishina, N.; Yamamoto, Y. *Tetrahedron* **2009**, 65, 1799.
62. Du, H.; Zhao, B.; Yuan, W.; Shi, Y. *Org. Lett.* **2008**, 10, 4231.
63. Zhao, B.; Du, H.; Shi, Y. *J. Org. Chem.* **2009**, 74, 8392.
64. Fustero, S.; Soler, J. G.; Barolomé, A.; Roselló, S. *Org. Lett.* **2003**, 5, 2707.
65. Somfaie, P.; Panknin, O. *Synlett* **2007**, 8, 1190.
66. Bach, T.; Körber, C. *J. Org. Chem.* **2000**, 65, 2358.
67. Ishikawa, T.; Kawakami, M.; Fukui, M.; Yamashita, A.; Urano, J.; Saito, S. *J. Am. Chem. Soc.* **2001**, 123, 7734.
68. Murakami, M.; Uchida, T.; Saito, B.; Katsuki, T. *Chirality* **2003**, 15, 116.
69. Armstrong, A.; Challinor, L.; Cooke, R. S.; Moir, J. H.; Treweek, N. R. *J. Org. Chem.* **2006**, 71, 4028.
70. Armstrong, A.; Challinor, L.; Moir, J. H. *Angew. Chem. Int. Ed.* **2007**, 46, 5369.
71. Donde, Y.; Overman, L. E. *J. Am. Chem. Soc.* **1999**, 121, 2933.
72. Savage, I.; Thomas, E. J.; Wilson, P. D. *J. Chem. Soc., Perkin Trans. 1* **1999**, 3291.
73. Chen, A.; Thomas, E. J.; Wilson, P. D. *J. Chem. Soc., Perkin Trans. 1* **1999**, 3305.
74. Ichikawa, Y.; Ito, T.; Nishiyama, T.; Isobe, M. *Synlett* **2003**, 7, 1034.
75. Ichikawa, Y.; Ito, T.; Isobu, M. *Chem. Eur. J.* **2005**, 11, 1949.
76. Ichikawa, Y.; Yamaoka, T.; Nakano, K.; Kotsuki, H. *Org. Lett.* **2007**, 9, 2989.
77. Ichikawa, Y.; Matsunaga, K.; Masuda, T.; Kotsuki, H.; Nakano, K. *Tetrahedron* **2008**, 64, 11313.
78. Lee, E. E.; Batey, R. A. *J. Am. Chem. Soc.* **2005**, 127, 14887.
79. Gagnon, D.; Lauzon, S.; Godbout, C.; Spino, C. *Org. Lett.* **2005**, 7, 4769.
80. Xin, Z.-Q.; Fischer, D. F.; Peters, R. *Synlett* **2008**, 10, 1495.

81. Fischer, D. F.; Barakat, A.; Xin, Z.-q.; Weiss, M. E.; Peters, R. *Chem. Eur. J.* **2009**, *15*, 8722.
82. O'Brien, P.; Rosser, C. M.; Caine, D. *Tetrahedron Lett.* **2003**, *44*, 6613.
83. O'Brien, P.; Rosser, C. M.; Caine, D. *Tetrahedron*, 2003, *59*, 9779.

Chapter 2

Regio- and Enantiospecific Rhodium-Catalyzed Allylic Amination with Aza-Ylides

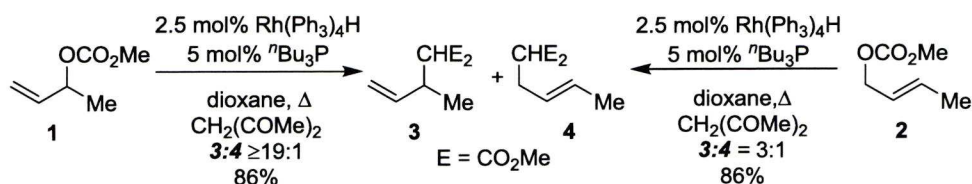
2.1 Introduction

As highlighted in the introductory review, a significant amount of effort has been applied towards the synthesis of chiral allylamines. Amines are a very important class of compounds in organic synthesis, as they are found in both natural and unnatural biologically active compounds. Allylamines are specifically targeted because in addition to occurring in natural compounds, the olefin can be transformed in a number of ways to further enhance the synthetic utility of the substrate.¹ The transition-metal catalyzed allylic amination reaction has proven very efficient for the construction new carbon-nitrogen bonds with high levels of stereocontrol through either a dynamic kinetic resolution or an enantioselective reaction.²

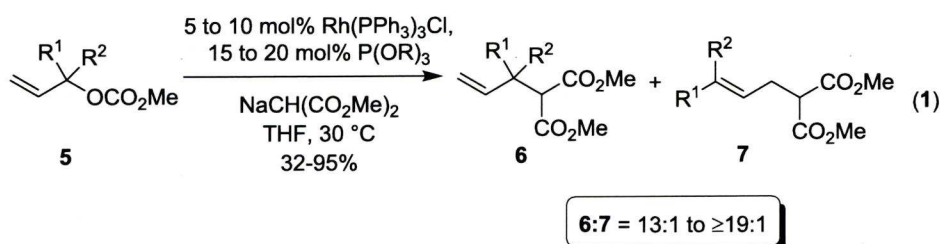
2.2 Origin of Regioselectivity and Enantiospecificity

In 1984, Tsuji and co-workers described the first regioselective rhodium-catalyzed allylic alkylation reaction using both rhodium(I) and rhodium(II) complexes modified with P^nBu_3 (Scheme 2.1).³ This work demonstrated that rhodium, unlike palladium, displayed a memory effect with respect to the alkylation at the position of the leaving group. For example, the reaction of secondary allylic carbonate **1** was shown to favour the secondary product in $\geq 19:1$; however, the linear derivative provided the linear product as the major adduct, albeit with a regioselectivity of only 3:1. The difference in regioselectivity suggests that the rhodium-catalyzed allylic alkylation reaction does not proceed through a conventional π -allyl intermediate.

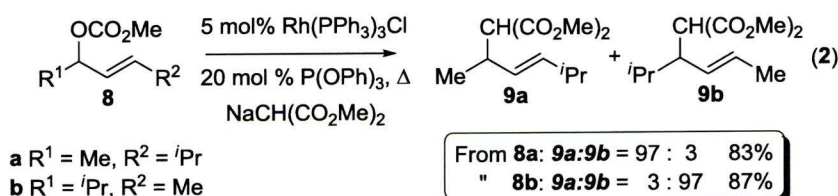
Scheme 2.1 Regiospecificity in rhodium-catalyzed allylic substitution.



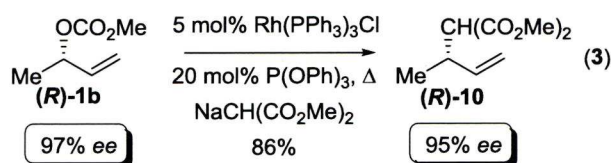
Evans and Nelson demonstrated that Wilkinson's catalyst, modified with triorganophosphites, catalyzed the allylic alkylation of secondary and tertiary allylic carbonates with the sodium enolate of dimethyl malonate (eq 1).⁴ This catalyst afforded higher regioselectivities (up to $\geq 19:1$) and demonstrated an increased reaction rate as compared to the catalyst system employed by Tsuji. This reaction has also proven to be remarkably general.



Additional studies probed substituted allylic carbonates which were known to afford fluxional π -allyl intermediates.⁵ For example, the alkylation of **8a** afforded allylic products **9a/b** in good yield (83%) and excellent regioselectivity (**9a:9b** = 97:3) favouring substitution at the least hindered termini (eq. 2). Interestingly, the isomeric carbonate **8b** furnished isomer **9b** as the major product in excellent regioselectivity. These results implied that the reaction intermediate may be a σ -complex, since palladium complexes often provide the same product irrespective of the starting material.

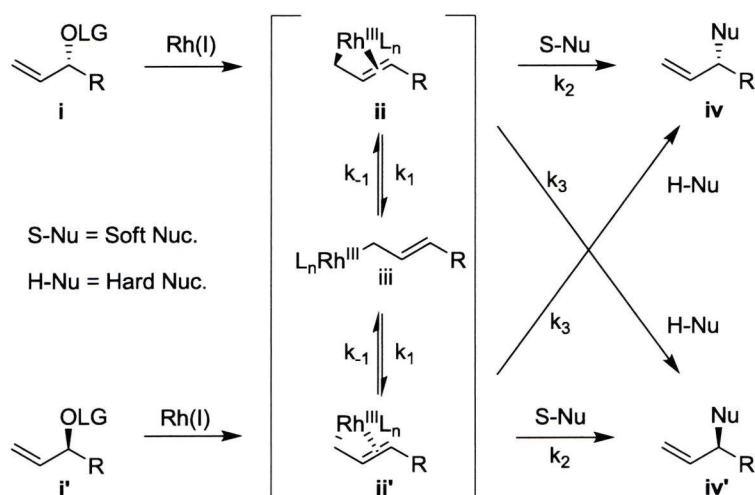


It was rationalized that if the reaction proceeded through a σ -complex, the alkylation of enantiomerically enriched allylic carbonate **(R)-1b** would result in the racemic product. Interestingly, however, the reaction afforded the secondary product with 95% *ee* (eq. 3). This demonstrates that there is no rapid C-C bond rotation in the intermediate, and implies that the reaction may proceed through an *enyl* ($\sigma + \pi$) intermediate in which both σ and π components are present in the same metal-allyl intermediate.



Scheme 2.2 outlines the proposed pathway for the rhodium-catalyzed allylic substitution reaction. Beginning from **i** or **i'** the rhodium oxidatively adds on the opposite face to the leaving group, affording *enyl* intermediate **ii** or **ii'**. $\text{S}_{\text{N}}^{2'}$ addition of a stabilized nucleophile can then take place in a regio- and enantiospecific manner with inversion of stereochemistry, furnishing the product **iv** or **iv'** with net retention of configuration. This occurs as long as nucleophilic attack (k_2) is faster than the π - σ - π isomerization ($k_2 \gg k_1$ or k_{-1}). Inversion of configuration can occur *via* nucleophilic addition to the metal center followed by reductive elimination ($k_3 \gg k_2$). This generally occurs with hard, unstabilized, nucleophiles.

Scheme 2.2 Proposed mechanism for the rhodium-catalyzed allylic substitution reaction.



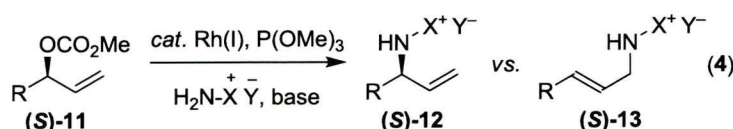
2.3 Regioselective and Enantiospecific Rhodium-Catalyzed Allylic Amination Utilizing an Aza-Ylide Nucleophile.

2.3.1 Introduction

The transition-metal catalyzed allylic amination reaction represents a powerful tool for the asymmetric synthesis of allylamines.¹ Although there have been significant advances in this area, the ability to develop a generalized carbon-nitrogen bond forming cross-coupling reaction has been impeded by the ability to control regioselectivity in unsymmetrical substrates. The removal of protecting groups can be a significant challenge and the judicious choice of pronucleophile has proven critical. Hence, the use of a highly reactive ammonia equivalent, which could easily undergo deprotection to afford the free amine, would add a significant contribution to this field.

2.3.2 Use of Ylide Pronucleophiles

A comprehensive screen of the literature revealed that whilst a great deal of research had been undertaken with conventional nitrogen nucleophiles, the use of a charge-separated derivative had not been realized.⁶ To this end, we envisaged that aza-ylide nucleophiles would prove efficient in the rhodium-catalyzed allylic amination reaction due to their low basicity and high nucleophilicity (eq 4).⁷



It was hypothesized that the nucleophilicity of the aza-ylide could be tuned by the careful selection of stabilizing groups. Interestingly, there is a distinct difference in stability between phosphorus, sulphur, and nitrogen aza-ylides (Figure 2.1).^{8,9} The group 3 element variants, phosphorus and sulphur, have access to the empty d-orbitals and are therefore both resonance and field stabilized. In comparison, the nitrogen variants do not have access to the empty d-orbital and are only field stabilized making them less stable. Hence, we reasoned that the nitrogen aza-ylides would be considerably more reactive than the sulphur or phosphorus variants.

Figure 2.1. Relative stability of various ylides based on field and resonance stability.

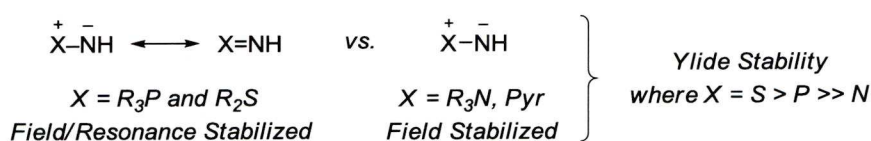
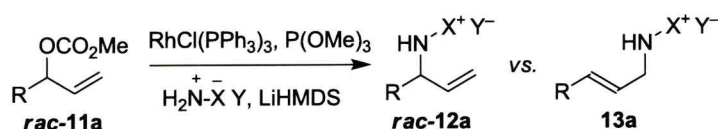
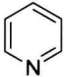


Table 2.1 shows the preliminary evaluation of various aza-ylides in the allylic amination reaction. Treatment of **rac-11a** ($R = \text{Ph}(\text{CH}_2)_2$) with the sulfonium or phosphonium aza-ylides (entries 1-3) in the presence of trimethyl phosphite modified Wilkinson's catalyst, did not provide any of the desired product, with complete recovery of starting material. Further studies illustrated that the halide counterion in

the salt was inconsequential to reactivity (entries 2 and 3). Gratifyingly, the aza-ylide generated from commercially available 1-aminopyridinium iodide furnished the product **rac-12a** in 71% yield and with excellent regioselectivity (*b/l* \geq 19:1) (entry 4). This clearly demonstrates the effect of the ylide stabilizing group on nucleophilicity.

Table 2.1. Examination of various aza-ylides in the regioselective rhodium-catalyzed allylic amination reaction ($R = \text{Ph}(\text{CH}_2)_2$).^a



Entry	X =	Y =	<i>rac-12a</i> : <i>13a</i> ^{b,c}	Yld (%) ^d
1	SPh ₂	Cl	-	NR
2	PPh ₃	Br	-	NR
3	PPh ₃	I	-	NR
4		"	\geq 19:1	71

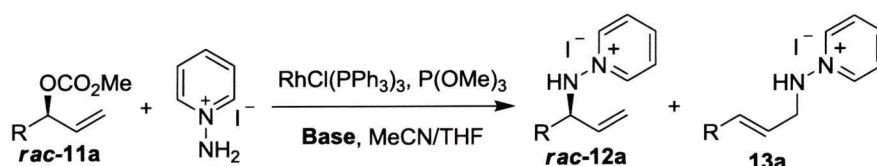
^aAll reactions were carried out on a 0.25 mmol reaction scale using 10 mol% RhCl(PPh₃)₃ modified with 40 mol% P(OMe)₃ and 1.1 equiv. of the lithium anion of the ylide salt in MeCN/THF (1.5:1) at room temperature. ^bRegioselectivity was determined by 500 MHz ¹H NMR on the crude reaction mixtures. ^cThe linear product **13a** was prepared independently *via* Pd(0) catalysis. ^dIsolated yields.

2.3.3 Optimization and Scope of the Rhodium-Catalyzed Allylic Amination Reaction.

Previous studies within the group on the rhodium-catalyzed allylic substitution reaction demonstrated that the alkali-metal salt of the pronucleophile had an effect on the efficiency and selectivity of the reaction.¹⁰ The lithium counterion generally afforded products with the highest yields and regioselectivities, which was attributed to the low basicity and high solubility of the pronucleophile. In the case of 1-aminopyridinium iodide, the resulting nucleophile is an ylide and therefore the reaction should have very little dependency on the counterion, provided the base is

strong enough to generate the ylide. Table 2.2 (entries 1-3) illustrates the examination of the alkali metal counterion, which, as suspected, did not have an effect on the regioselectivity of the reaction. However, the sodium and potassium derivatives afford slightly lower yield due to the recovery of a small amount of the allylic carbonate.

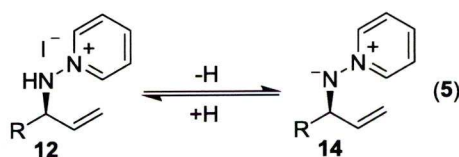
Table 2.2. Optimization of the regioselective rhodium-catalyzed allylic amination reaction using 1-aminopyridinium iodide (R= Ph(CH₂)₂).



Entry	Base	<i>rac-12a</i> : <i>13a</i> ^{b,c}	Yld (%) ^d
1	LiHMDS	≥19:1	71
2	NaHMDS	"	68 ^e
3	KHMDS	"	65 ^e
4	K ₂ CO ₃	"	68 ^e
5	DBU	"	39

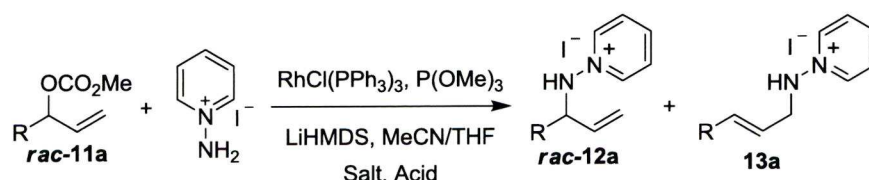
^aAll reactions were carried out on a 0.25 mmol reaction scale using 10 mol% RhCl(PPh₃)₃ modified with 40 mol% P(OMe)₃ and 1.1 equiv. of the lithium anion of the ylide salt in MeCN/THF (1.5:1) at room temperature. ^bRegioselectivity was determined by 500 MHz ¹H NMR on the crude reaction mixtures. ^cThe linear product **13a** was prepared independently *via* Pd(0) catalysis. ^dIsolated yields. ^eRecovered **rac-11a** (5-10%).

Further studies examined the effects of inorganic and tertiary amine bases. Potassium carbonate (Table 2.2, entry 4) afforded a similar yield to LiHMDS, although further studies demonstrated it was less general. Additionally, the tertiary amine 1,8-diazabicyclo[5.4.0]undec-7-ene (DBU) proved to be less efficient, furnishing only 39% of **12a** even though no starting material was recovered.



Although the reaction is generally clean and consumes the starting material, the lower yields were attributed to the formation of methoxide from the decarboxylation of the methyl carbonate leaving group. The lithium methoxide can then presumably deprotonate **12** to generate aza-ylide **14** which cannot be isolated *via* flash chromatography (eq. 5). It was hypothesized that the overall yield could be improved with the addition of acid upon completion of the reaction, to ensure all of the product was protonated. In order to ensure the salt was reforming as the iodide, lithium iodide was added along with the acids. Gratifyingly, a significant increase in yield was observed with addition of both formic acid and acetic acid (entries 2 and 3). Although the amination was complete in all cases, decreased yields were observed with weaker acids such as phenol and methanol (entries 4 and 5). This supports the idea that protonation of the product is crucial for isolation. Finally, although HI could be added directly, the yield was slightly lower (entry 6).

Table 2.3 Examination of the acid quench of the amination reaction (R = Ph(CH₂)₂).^a

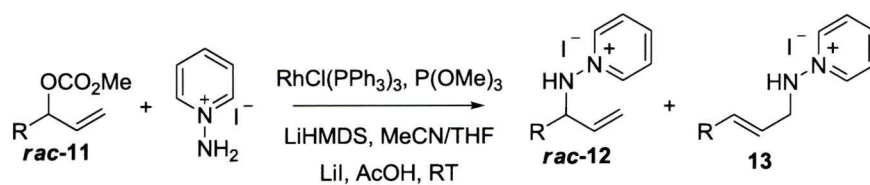


Entry	Salt	Acid	Acid pka	Yld (%) ^b
1	-	-	-	71
2	LiI	Formic Acid	3.77	87
3	"	Acetic Acid	4.76	89
4	"	Phenol	9.95	66
5	"	Methanol	15.5	52
6	-	HI	-11	74

^aAll reactions were carried out on a 0.25 mmol reaction scale using 10 mol% RhCl(PPh₃)₃ modified with 40 mol% P(OMe)₃ and 1.1 equiv. of the lithium anion of the ylide salt in MeCN/THF (1.5:1) at room temperature. ^bIsolated yields.

Table 2.4 summarizes the application of the optimized conditions (Table 2.3, entry 3) to a variety of racemic secondary allylic carbonates. The regioselectivity proved tolerant to a wide array of allylic alcohol derivatives. For example, linear (entries 1-5) and branched alkyl substituents (entries 6-9) afford excellent regiocontrol, in which the branching is inconsequential in terms of regioselectivity. This is contradictory to previous work with *N*-sulfonamide nucleophiles which displayed a decrease in secondary selectivity for substrates containing α -substitution. Additional studies demonstrated that benzyl and *tert*-butyldimethylsilyl protected hydroxymethyl and ethyl derivatives also provide excellent selectivity (entries 10-13), as do aryl substrates (entries 14 and 15).

Table 2.4 Scope of the regioselective rhodium-catalyzed allylic amination reaction with the 1-aminopyridinium ylide.^a



Entry	Allylic carbonate rac-11 R =		rac-12:13 ^{b,c}	Yld (%) ^d
1	$\text{Ph}(\text{CH}_2)_2$	a	$\geq 19:1$	89
2	Me	b	$\geq 19:1$	76
3	ⁿ Pr	c	$\geq 19:1$	87
4	ⁿ Bu	d	$\geq 19:1$	87
5	$\text{CH}_2=\text{CH}(\text{CH}_2)_2$	e	$\geq 19:1$	73
6	ⁱ Pr	f	$\geq 19:1$	79
7	^c Hex	g	$\geq 19:1$	75
8	ⁱ Bu	h	$\geq 19:1$	86
9	PhCH_2	i	$\geq 19:1$	78
10	BnOCH_2	j	$\geq 19:1$	88
11	$\text{BnO}(\text{CH}_2)_2$	k	$\geq 19:1$	84
12	TBSOCH_2	l	$\geq 19:1$	84
13	$\text{TBSO}(\text{CH}_2)_2$	m	$\geq 19:1$	86
14	Ph	n	$\geq 19:1$	81
15	Naphthyl	o	$\geq 19:1$	89

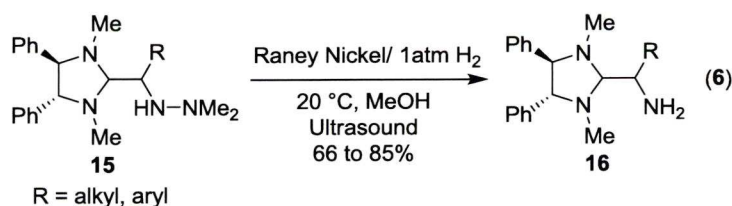
^aAll reactions were carried out on a 0.25 mmol reaction scale using 10 mol% $\text{RhCl}(\text{PPh}_3)_3$ modified with 40 mol% $\text{P}(\text{OMe})_3$ and 1.1 equiv. of the lithium anion of the ylide salt in MeCN/THF (1.5:1) at room temperature. ^bRegioselectivity was determined by 500 MHz ^1H NMR on the crude reaction mixtures. ^cThe linear products **13** was prepared independently *via* $\text{Pd}(0)$ catalysis. ^dIsolated yields.

2.4 Cleavage of Nitrogen-Nitrogen bonds.

2.4.1 Background

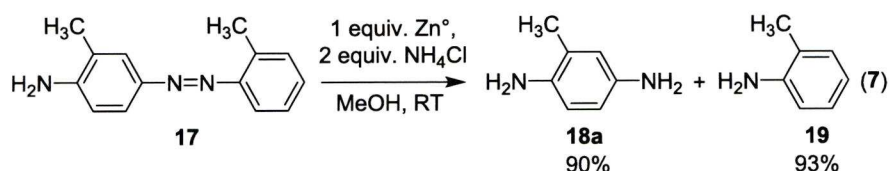
The use of hydrazines for the installation of a nitrogen atom is common.¹¹ However the cleavage of the nitrogen-nitrogen bond to afford a free amine is not trivial and often requires harsh reaction conditions. The reductive hydrazine cleavage is often accomplished through hydrogenation, hydride cleavage and single electron transfer reduction.¹²⁻¹⁶

Sodium metal and lithium/ammonia cleave hydrazine bonds though this is incompatible with some functionality.^{12,13} Additionally, Raney-Nickel has been employed under an atmosphere of hydrogen. Generally the reaction is conducted at 30-50 °C with 3-50 atm of hydrogen,¹⁴ and although the method is fairly general, reaction times can be long for sterically hindered compounds. Alexakis and co-workers reported an improved method involving an ultrasound bath, (eq. 6)^{14b} which avoids the requirement of elevated temperatures. Moreover, the reaction is compatible with sterically hindered hydrazines (*i.e.* R = ^tBu), which afford the amines in moderate yield. For example the treatment of **15a** (R = ^tBu) under the optimal conditions furnished the free amine **16a** in 85% yield.^{14d}

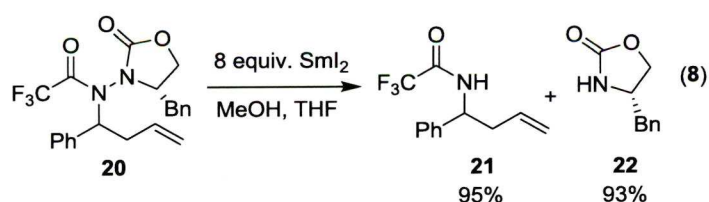


The reductive cleavage of various nitrogen-nitrogen bonds using zinc dust is also an efficient method.¹⁵ This method is attractive not only due to its functional group compatibility, but also for the low cost of zinc dust. Gowda and co-workers described an adaptation of this method, which employed ammonium chloride and zinc dust to reductively cleave aryl azo compounds to anilines in high yield and with a relatively short reaction time.^{15g} Symmetrical substrates all worked in excellent

yield and the reaction was tolerant of halogens, protected hydroxyl groups, esters, alkyls, and carboxylic acids. The unsymmetrical substrates provide two anilines in high yields. For instance, treatment of azo compound **17** with zinc dust afforded anilines **18a** and **19** in excellent yield (90% and 93% respectively).



Another relatively popular method utilizes samarium diiodide, and was first described by Kagan and co-workers in 1980.^{16a} Molander and Flowers, in addition to others, have described the reactivity and selectivity of SmI₂ along with the effect of solvents and co-solvents.¹⁶ Tetrahydrofuran is often the optimal solvent since most organic material is soluble. However, solvents such as benzene, acetonitrile and dimethoxyethane have also been employed and have a dramatic effect on reactivity. The addition of co-solvents such as methanol, hexamethylphosphoramide (HMPA) and 1,3-dimethyl-3,4,5,6-tetrahydro-2(1H)-pyrimidinone (DMPU) also has a significant effect on the reaction rate, presumably by solvating and ligating the samarium metal differently, thereby changing the structure of the active reducing agent and enabling it to be tuned to a specific reaction.

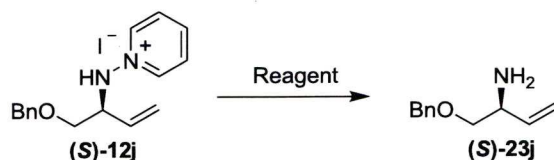


Friestad and Ding demonstrated the importance of an additive in the cleavage of trifluoroacetyl-activated hydrazines (eq. 8).^{16k} Treatment of **20** with SmI₂ alone afforded the trifluoroacetamide in 68% yield. However, the yield was increased with the addition of HMPA or methanol to 83 and 95% respectively, and the oxazolidinone **22** was recovered in 93% yield in the latter case.

2.4.2 Conversion to Free Amine

Preliminary work focused on the examination of various methods for conversion of (**S**)-**12j** to the free amine (Table 2.5). For example, treatment with Raney-Nickel afforded only recovery of the starting material (entry 1), whereas zinc and acetic acid (entry 2) was more promising. This was an appealing option because the cleavage could be performed sequentially in a one-pot process with the amination reaction. However, these conditions proved to be inconsistent with the amine generally afforded in 15-49% yield. Amine (**S**)-**23j** was isolated, initially in moderate yield, when samarium (II) iodide was used as a 0.1M solution in THF. A screen of solvents such as acetonitrile and methanol, and the use of additives such as HMPA and DBU, demonstrated that THF without additives was optimal, providing the amine in 88% yield when a 0.5M solution was used in the presence of excess samarium metal (entry 3).

Table 2.5 Reductive-cleavage to afford chiral amine (**S**)-**23j**.



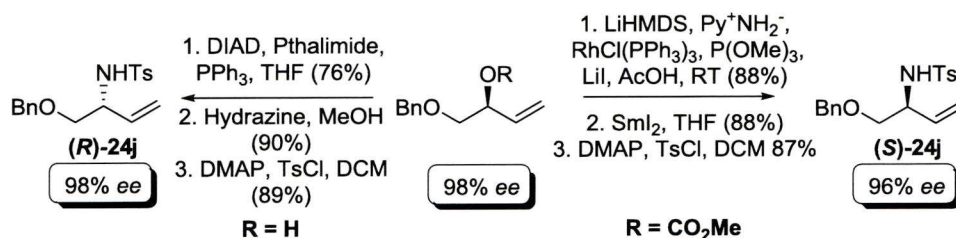
Entry	Reagent	Yld (%) ^a
1	Raney-Nickel	NR
2	Zn/AcOH	15-49
3	SmI ₂	88

^aIsolated Yields.

The stereochemical outcome of the reaction was investigated by treating allylic carbonate (**S**)-**11j** (98% *ee*) with the ylide of 1-aminopyridinium iodide under the optimized reaction conditions (Scheme 2.3). The pyridinium salt was treated with samarium (II) iodide and the furnished amine was protected as the *p*-toluenesulfonamide to afford (**S**)-**24j**. The enriched allylic alcohol was treated under standard Mitsunobu conditions to afford the enantiomerically enriched phthalamide.

Treatment of the phthalamide with hydrazine afforded the free amine, which was then protected to afford the sulfonamide (**(R)**-24j. Comparison of the enantiomers of the known sulfonamide (**(S)**-24j *via* HPLC as well as rotation, revealed the reaction proceeded with retention of configuration which is in agreement with previous studies utilizing soft nucleophiles.

Scheme 2.3 Confirmation of absolute stereochemistry.



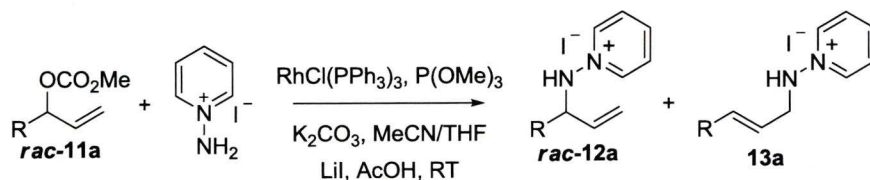
2.4.3 One-Pot Deprotection Utilizing Catalytic Base

Since the zinc/acetic acid protocol (Table 2.5, entry 2) could be undertaken in a one-pot process, it was further examined. It was envisioned that the cleavage would be more efficient in the absence of the excess base present from the amination reaction. This is particularly relevant since the methyl carbonate leaving group provides a source of methoxide. Since we had already attributed the initially low yields to the formation of methoxide, it was surmised that it should be a strong enough base to deprotonate 1-aminopyridinium iodide. Although in the absence of base the reaction did not afford any product, and the analogous process with catalytic LiHMDS was significantly more effective, albeit with the recovery of a small amount of starting material.

In order to further improve the conversion, potassium carbonate was utilized, which had provided complete conversion when used stoichiometrically. Table 2.6 summarises the examination of substoichiometric quantities of base. Gratifyingly, the amination went to full conversion using 0.25 equivalents of base when the

temperature was increased to 30 °C. Although the base could be lowered even further (0.1 equiv.), this presented practical problems on a small scale.

Table 2.6 Optimization of the rhodium-catalyzed allylic amination reaction utilizing catalytic potassium carbonate (R = Ph(CH₂)₂).^a

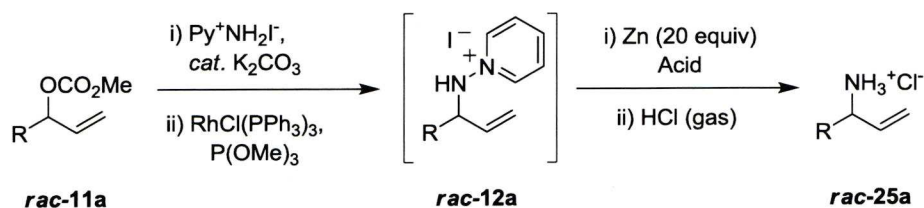


Entry	K ₂ CO ₃ (Equiv.)	Temp.	Conv. (%) ^b
1	1.1	RT	100
2	0.50	"	83
3	0.25	"	77
4	0.25	30	100
5	0.10	"	100

^aAll reactions were carried out on a 0.25 mmol reaction scale using 10 mol% $\text{RhCl(PPh}_3)_3$ modified with 40 mol% P(OMe)_3 and 1.2 equiv. 1-aminopyridinium iodide in MeCN/THF (1.5:1). ^bConversion was determined by 500 MHz ¹H NMR on the crude reaction mixtures.

With the newly optimized conditions in hand, the *in situ* cleavage could be further examined. A comprehensive survey of the literature revealed numerous sources of acid have been employed with zinc to promote nitrogen bond cleavage.¹⁶ Interestingly, ammonium formate gave a complex mixture of compounds, whereas both trifluoroacetic acid and acetic acid afforded the amine in low yield. Gratifyingly, the combination of zinc with ammonium chloride furnished the HCl salt in 74% yield from allylic carbonate **rac-11a** (entry 6).

Table 2.7. Optimization of one-pot allylic amination and reductive cleavage (R = Ph(CH₂)₂).

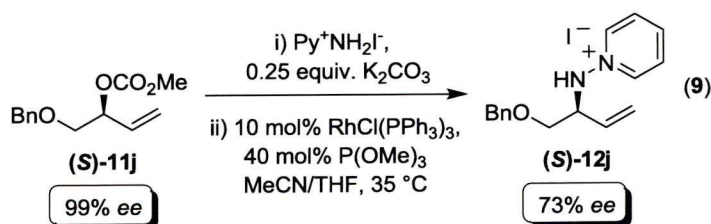


Entry	Acid	Equiv.	Temp (°C)	Yld (%) ^b
1	NH ₄ HCO ₂	20	22	Mixture
2	TFAA	2	"	20
3	AcOH	"	"	22
4	"	4	"	27
5	NH ₄ Cl	10	"	68
6	"	"	35	74

^aAll reactions were carried out on a 0.25 mmol reaction scale using 10 mol% RhCl(PPh₃)₃ modified with 40 mol% P(OMe)₃, 0.25 equiv K₂CO₃, and 1.2 equiv. 1-aminopyridinium iodide in MeCN/THF (1.5:1). Upon TLC completion, zinc and acid were added and temperature increased to 45 °C.

^bIsolated Yields.

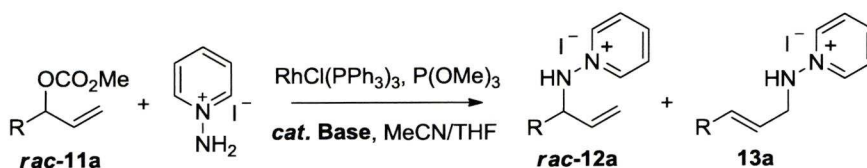
The allylic amination was performed on (**S**)-**11j** (R = BnOCH₂) in order to determine enantiospecificity when using catalytic base (eq 9). Unfortunately, product (**S**)-**12j** was afforded in only 74% *cee* as compared to 98% *cee* with stoichiometric LiHMDS. Although this nicely demonstrates the ability to utilize 1-aminopyridinium iodide as an ammonia equivalent in a one-pot process, the lower enantiospecificity significantly detracts from its synthetic utility, and thus warranted further investigation.



2.5 Optimization of the Regiospecific Rhodium-Catalyzed Allylic Amination Reaction Utilizing Catalytic Base.

Several bases were examined using catalytic amounts in order to ascertain the specific problem (Table 2.8). As previously stated, the use of 0.25 equiv. LiHMDS at room temperature and at elevated temperature afforded azanide **rac-12a** in low yield with the recovery of starting material (entries 1 and 2). The examination of inorganic carbonate bases (entries 3 and 4) afforded 85 and 88% of **rac-12a** at 35 °C. Gratifyingly, 1,8-diazabicyclo[5.4.0]undec-7-ene (DBU) afforded the product in 92% yield.

Table 2.8. Optimization of the regioselective rhodium-catalyzed allylic amination reaction using 1-aminopyridinium iodide ($R = \text{Ph}(\text{CH}_2)_2$).^a



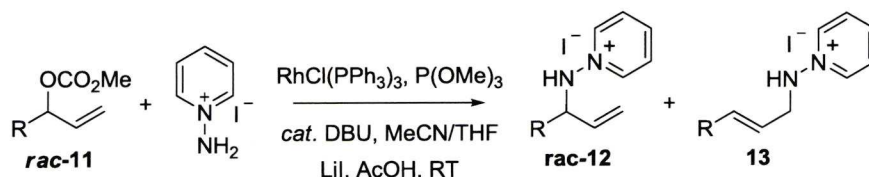
Entry	Base	Temperature	Yield (%) ^b
1	LiHMDS	22	29
2	"	35	57
3	Cs_2CO_3	"	85
4	K_2CO_3	"	88
5	<i>i</i> PrNEt	"	72
6	DBU	"	92

^aAll reactions were carried out on a 0.25 mmol reaction scale using 10 mol% $\text{RhCl}(\text{PPh}_3)_3$ modified with 40 mol% $\text{P}(\text{OMe})_3$, 0.25 equiv. base, and 1.2 equiv. 1-aminopyridinium iodide in MeCN/THF (1.5:1). ^b Isolated yields.

The generality of this reaction was determined by examination of the same series of substrates, as outlined in Table 2.9, which demonstrates that the reaction was tolerant of α - and β -branching (entries 5-7), as well as protected hydroxyl derivatives (entries 9 and 10). In all cases the regioselectivity was excellent ($rs \geq 19:1$) and the

yields were generally higher than in the stoichiometric reaction conditions utilizing LiHMDS.

Table 2.9 Scope of the regioselective rhodium-catalyzed allylic amination reaction with the 1-aminopyridinium ylide and catalytic DBU.^a



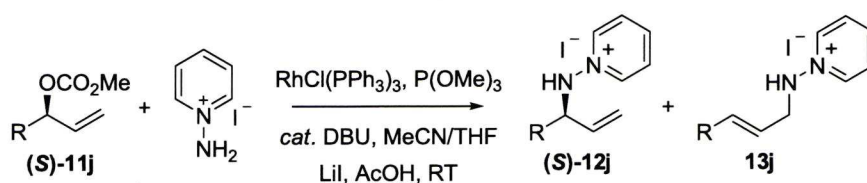
Entry	Allylic carbonate rac-11 R =		rac-12:13 ^{b,c}	Yld (%) ^d
1	Ph(CH ₂) ₂	a	≥19:1	92
2	Me	b	≥19:1	84
3	ⁿ Pr	c	≥19:1	87
4	CH ₂ =CH(CH ₂) ₂	e	≥19:1	82
5	ⁱ Pr	f	≥19:1	83
6	^c Hex	g	≥19:1	76
7	ⁱ Bu	h	≥19:1	84
8	PhCH ₂	i	≥19:1	89
9	BnOCH ₂	j	≥19:1	87
10	TBSOCH ₂	l	≥19:1	76
11	Ph	n	≥19:1	80
12	Naphthyl	o	≥19:1	93

^aAll reactions were carried out on a 0.25 mmol reaction scale using 10 mol% $\text{RhCl(PPh}_3)_3$ modified with 40 mol% P(OMe)_3 1.2 equiv. of 1-aminopyridinium iodide, and 0.25 equiv. DBU in MeCN/THF (1.5:1) at room temperature. ^bRegioselectivity was determined by 500 MHz ¹H NMR on the crude reaction mixtures. ^cThe linear product **13** was prepared independently *via* Pd(0) catalysis. ^dIsolated yields.

Although the reaction was generally more efficient, it demonstrated the same enantiospecificity (74% *ee*) observed previously with potassium carbonate. In order to ascertain whether the loss of enantiomeric purity was occurring at the start of the reaction or gradually over time, the reaction was stopped at partial conversion as outlined in Table 2.10. Interestingly, the initial conversion, is much faster than

expected (entries 1 and 2), and then slows quite dramatically throughout the course of the reaction. The most surprising observation is that the stereospecificity is excellent at the outset and diminishes with conversion, with no obvious evidence for epimerization of the product.

Table 2.10 Enantiospecificity over time in the rhodium-catalyzed allylic amination reaction utilizing catalytic DBU ($R = \text{BnOCH}_2$).^a

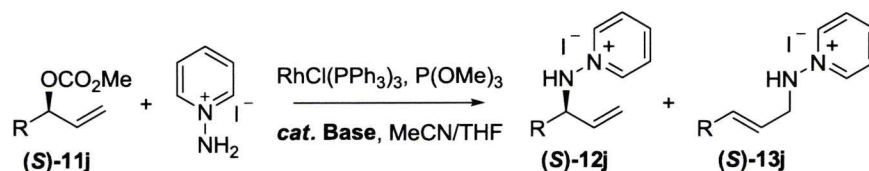


Entry	Time (mins)	Conv. (%) ^b	cee (%) ^c
1	5	18	90
2	30	50	83
3	60	65	83
4	180	100	74
5	360	100	72

^aAll reactions were carried out on a 0.25 mmol reaction scale using 10 mol% $\text{RhCl(PPh}_3)_3$ modified with 40 mol% P(OMe)_3 1.2 equiv. of 1-aminopyridinium iodide, and 0.25 equiv. DBU in MeCN/THF (1.5:1) at 30 °C ^bConversion was determined by 500 MHz ^1H NMR on the crude reaction mixtures. Enantioselectivity was determined on the tosylate derivative.

Many bases were screened in an attempt to raise the enantiospecificity, in which only DBU, cesium carbonate and potassium carbonate achieved full conversion (Table 2.11, entries 1-3). Nevertheless, the same trend prevails, in which higher stereospecificity is achieved at lower conversion (entries 5, 6 and 8). Another interesting feature is that sodium and lithium salts of both hydroxide and methoxide (entry 6 vs 7 and 8 vs 9) provide complementary results in which the latter always proceeds with lower conversion and higher stereospecificity.

Table 2.11 Enantiospecific rhodium-catalyzed allylic amination: time course dependence of the enantiospecificity (R = BnOCH₂).^a

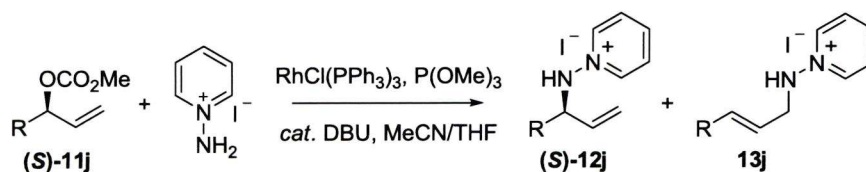


Entry	Base	Conv. (%) ^b	cee (%) ^c
1	DBU	100	74
2	K ₂ CO ₃	100	74
3	Cs ₂ CO ₃	100	73
4	LiHMDS	57	88
5	LDA	35	93
6	LiOH	35	93
7	NaOH	69	76
8	LiOMe	28	90
9	NaOMe	82	76

^aAll reactions were carried out on a 0.25 mmol reaction scale using 10 mol% RhCl(PPh₃)₃ modified with 40 mol% P(OMe)₃ 1.2 equiv. of 1-aminopyridinium iodide, and 0.25 equiv. base, in MeCN/THF (1.5:1) at 30 °C ^bConversion was determined by 500 MHz ¹H NMR on the crude reaction mixtures. ^cEnantioselectivity was determined on the tosylate derivative.

It was hypothesized that increasing the reaction concentration would increase the reaction rate and thus increase the conservation of enantiomeric excess. Entry 1 (Table 2.12) shows the previous result when reacting DBU at 30 °C at 0.1M at which 74% *cee* was obtained. A significant increase in enantiospecificity was observed when the reaction was carried out at 0.33M, which increased the specificity to 85% *cee*. Additional increases either led to a marginal increase or significant decrease.

Table 2.12 Effect of concentration on the enantiospecific rhodium-catalyzed allylic substitution reaction (R = BnOCH₂).^a



Entry	Conc.	Conv. (%) ^b	cee (%) ^c
1	0.1	100	74
2	0.33	100	83
3	0.5	100	85
4	1.0	100	66

^aAll reactions were carried out on a 0.25 mmol reaction scale using 10 mol% RhCl(PPh₃)₃ *modified* with 40 mol% P(OMe)₃ 1.2 equiv. of 1-aminopyridinium iodide, and 0.25 equiv. DBU in MeCN/THF (1.5:1) at 30 °C ^bConversion was determined by 500 MHz ¹H NMR on the crude reaction mixtures.

^cEnantioselectivity was determined on the tosylate derivative.

2.6 Conclusion

In conclusion, we have developed the first regio- and enantiospecific rhodium-catalyzed allylic amination reaction utilizing the aza-ylide derived from 1-aminopyridinium iodide. This study demonstrates the importance of the ylide-stabilizing group for obtaining the desired nucleophilicity. The aza-ylide also provides a commercially available ammonia equivalent, thereby illustrating its synthetic potential for the preparation of enantiomerically enriched primary allylic amines. This work presents a new class of pronucleophiles for the allylic substitution reaction and we anticipate this will lead to the utilization of related aza-ylides in metal-catalyzed cross-coupling reactions.

2.7 Experimental

General

Unless otherwise indicated, all reactions were carried out in flame-dried glassware, under an atmosphere of argon or nitrogen. Tetrahydrofuran (THF) was distilled from sodium benzophenone ketyl. All other starting materials were purchased from Acros, Aldrich, Alfa Aesar, or Fluorochem and used without further purification unless otherwise stated.

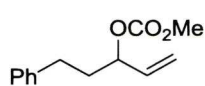
All carbonates were prepared using literature procedures and freshly distilled. Wilkinson's catalyst $[\text{RhCl}(\text{PPh}_3)_3]$ was prepared in 10 mmol batches.¹⁷ Trimethyl phosphites were distilled and stored over 4Å molecular sieves.

Primary amination standards were prepared by performing the amination reaction with tetrakis(triphenylphosphine)palladium (0) ($\text{Pd}(\text{PPh}_3)_4$). Thin layer chromatography (TLC) was performed on Whatman F₂₅₄ precoated silica gel plates. Visualization was accomplished with a UV light and/or a KMnO_4 solution. Flash chromatography (FC) was performed using either Merck Silica Gel 60 (230-400 mesh) or Whatman Silica Gel Purasil[®] 60Å (230-400 mesh). Solvents for extraction and FC were technical grade. Reported solvent mixtures for TLC and FC are volume/volume mixtures. Infrared spectra were obtained on a Perkin-Elmer spectrum 100 series FTIR spectrometer. Peaks are reported in cm^{-1} with the following relative intensities: vs (very strong), s (strong), m (medium) and w (weak). Mass spectra were performed at either the Indiana University Mass Spectrometry Center, the University of Liverpool Mass Spectrometry Center or the EPSRC National Mass Spectrometry Service Centre, Swansea. High-resolution electron-impact (EI, ionization voltages of 70 eV), chemical ionization (CI, reagent gas CH_4 or NH_3) were obtained on either an Autospec, ZAB 2SE, Kratos MS-80, VG 7070E double focusing magnetic sector mass spectrometer equipped with a solid probe inlet, a Quattro II, MAT 95, or MAT 900. The electrospray ionization (ESI) mass spectra were obtained on a Waters micromass LCT mass spectrometer. ^1H and ^{13}C NMR

were recorded on a Bruker AV 500 MHz NMR spectrometer in the indicated deuterated solvents, which were obtained from Cambridge Isotope Labs. For ^1H NMR, CDCl_3 was set to 7.26 ppm (CHCl_3 singlet). For ^{13}C NMR, CDCl_3 was set to 77.16 ppm (CDCl_3 center of triplet). ^1H data are reported in the following order: chemical shift in ppm (δ) (multiplicity, which are indicated by br (broadened), s (singlet), d (doublet), t (triplet), q (quartet), m (multiplet)); assignment of 2nd order pattern, if applicable; coupling constants (J , Hz); integration. values for All ^{13}C NMR spectra data using the descriptor *o* and *e* refer to whether the peak is odd or even respectively, and correlate to an attached proton test (ATP) experiment.

All liquid chromatographs were obtained on the Agilent 1200 series HPLC, equipped with a variable wavelength UV detector. The instrument was fitted with either a CHIRALCELTM AD-H column (Diacel, 4.6 mm x 25 cm) or CHIRALCELTM OD column (Diacel, 4.6 mm x 25 cm).

General synthesis of allylic carbonates:



Methyl 5-phenylpent-1-en-3-yl carbonate *rac*-11a.

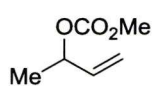
5-Phenylpenten-3-ol (1.62 g, 10 mmol) was weighed into a flame-dried 50 mL round bottom flask under an atmosphere of argon, and dissolved in 20 mL of anhydrous methylene chloride. The reaction flask was then cooled to 0 °C, followed by the addition of DMAP (1.49 g, 12 mmol) in one portion from a weighing vial. After 15 minutes, methylchloroformate (1.16 mL, 15 mmol) was then added dropwise. Following the addition, the reaction was allowed to warm to RT with stirring until the allylic alcohol derivative was consumed, TLC control. The reaction was then cooled to 0 °C, and quenched by addition of saturated NH_4Cl solution. The reaction was partitioned between methylene chloride and saturated aqueous NH_4Cl solution then the organic layers were combined, washed with saturated aqueous NaCl solution, dried (MgSO_4), filtered, and concentrated *in vacuo* to afford a crude oil. Flash column chromatography on silica gel (eluting with 5% EA/HEX gradient) produced the desired allylic carbonate ***rac*-11a**, as a light yellow oil. Kugelrohr distillation at 119 °C (3.0 mm Hg) in 93% yield (2.05 g).

¹H NMR (500 MHz, CDCl₃) δ 7.34-7.30 (m, 2H), 7.25-7.20 (m, 3H), 5.87 (ddd, *J* = 17.2, 10.6, 6.8 Hz, 1H), 5.36 (dt, *J* = 17.2, 1.2 Hz, 1H), 5.28 (dt, *J* = 10.6, 1.1 Hz, 1H), 5.12 (quartet, *J* = 6.6 Hz, 1H), 3.80 (s, 3H), 2.79-2.66 (m, 2H), 2.13-2.04 (m, 1H), 2.01-1.92 (m, 1H).

¹³C NMR (125 MHz, CDCl₃) δ 155.31 (e), 141.19 (e), 135.82 (o), 128.57 (o), 128.46 (o), 126.14 (o), 117.91 (e), 78.57 (o), 54.78 (o), 35.95 (e), 31.35 (e).

IR (Neat) 3089 (w), 3058 (w), 3028 (w), 2955 (w), 2927 (w), 2857 (w), 1744 (s), 1442 (m), 1259 (s), 935 (m), 791 (m), 699 (m) cm⁻¹.

HRMS (CI, [M]⁺) calc for C₁₃H₁₆O₃ 220.1099, found 220.1087.



But-3-en-2-yl methyl carbonate *rac*-11b¹⁹

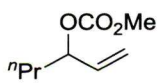
Prepared according to the general synthesis of allylic carbonates and displaying the following properties.

¹H NMR (500 MHz, CDCl₃) δ 5.84 (ddd, *J* = 17.3, 10.5, 6.4 Hz, 1H), 5.30-5.27 (m, 1H), 5.20-5.13 (m, 2H), 3.75 (s, 3H), 1.35 (d, *J* = 6.6 Hz, 3H).

¹³C NMR (125 MHz, CDCl₃) δ 155.21 (e), 137.15 (o), 116.63 (e), 75.31 (o), 54.68 (o), 20.09 (o).

IR (Neat) 2987 (w), 2959 (w), 1744 (s), 1443 (m), 1335 (m), 1256 (s), 1043 (m), 939 (m), 896 (m), 792 (m) cm⁻¹.

HRMS (CI, [M+NH₄]⁺) calcd for C₆H₁₄O₃N 148.0968, found 148.0968.



Hex-1-en-3-yl methyl carbonate *rac*-11c²⁰

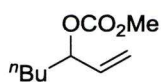
Prepared according to the general synthesis of allylic carbonates and displaying the following properties.

¹H NMR (500 MHz, CDCl₃) δ 5.78 (ddd, *J* = 17.3, 10.5, 6.8 Hz, 1H), 5.28 (d, *J* = 17.2 Hz, 1H), 5.19 (d, *J* = 10.5 Hz, 1H), 5.04 (q, 6.7 Hz, 1H), 3.76 (s, 3H), 1.72-1.64 (m, 1H), 1.60-1.53 (m, 1H), 1.42-1.30 (m, 2H), 0.91 (t, *J* = 7.4 Hz, 3H).

¹³C NMR (125 MHz, CDCl₃) δ 155.41 (e), 136.15 (o), 117.48 (e), 79.11 (o), 54.72 (o), 36.36 (e), 18.36 (e), 13.89 (o)

IR (Neat) 2960 (w), 2937 (w), 2876 (w), 1745 (s), 1442 (m), 1254 (s), 1088 (w), 955 (m), 940 (m), 792 (m) cm⁻¹.

HRMS (CI, [M+NH₄]⁺) calcd for C₈H₁₈O₃N 176.1281, found 176.1277.



Hept-1-en-3-yl methyl carbonate *rac*-11d²¹

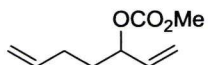
Prepared according to the general synthesis of allylic carbonates and displaying the following properties.

¹H NMR (500 MHz, CDCl₃) δ 5.78 (ddd, *J* = 17.3, 10.5, 6.9 Hz, 1H), 5.26 (d, *J* = 17.2 Hz, 1H), 5.17 (d, *J* = 10.5 Hz, 1H), 5.01 (quartet, *J* = 6.7 Hz, 1H), 3.74 (s, 3H), 1.72-1.63 (m, 1H), 1.62-1.53 (m, 1H), 1.36-1.24 (m, 4H), 0.86 (t, *J* = 6.7 Hz, 3H).

¹³C NMR (125 MHz, CDCl₃) δ 155.35 (e), 136.15 (o), 117.39 (e), 79.25 (o), 54.62 (o), 33.96 (e), 27.14 (e), 22.48 (e), 13.98 (o).

IR (Neat) 2958 (w), 2927 (w), 2863 (w), 1746 (s), 1442 (m), 1257 (s), 963 (m), 932 (m), 792 (m) cm⁻¹.

HRMS (CI, [M+NH₂]) calcd for C₉H₁₈O₃N 188.1281, found 188.1283.



Hepta-1,6-dien-3-yl methyl carbonate *rac*-11e

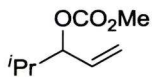
Prepared according to the general synthesis of allylic carbonates and displaying the following properties.

¹H NMR (500 MHz, CDCl₃) δ 5.84-5.76 (m, 2H), 5.31 (d, *J* = 17.2 Hz, 1H), 5.33 (d, *J* = 10.5 Hz, 1H), 5.09-4.98 (m, 3H), 3.77 (s, 3H), 2.14-2.10 (m, 2H), 1.85-1.78 (m, 1H), 1.74-1.67 (m, 1H).

¹³C NMR (125 MHz, CDCl₃) δ 155.34 (e), 137.46 (o), 135.90 (o), 117.80 (e), 115.46 (e), 78.64 (o), 54.78 (o), 33.45 (e), 29.27 (e).

IR (Neat) 3081 (w), 2997 (w), 2956 (w), 2927 (w), 2851 (w), 1746 (s), 1442 (m), 1259 (s), 936 (m), 916 (m), 692 (m) cm⁻¹.

HRMS (CI, [M+NH₄]⁺) calcd for C₉H₁₈O₃N 188.1281, found 188.1283.



Methyl 4-methylpent-1-en-3-yl carbonate *rac*-11f

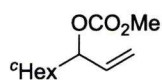
Prepared according to the general synthesis of allylic carbonates and displaying the following properties.

¹H NMR (500 MHz, CDCl₃) δ 5.76 (ddd, *J* = 17.4, 10.5, 7.0 Hz, 1H), 5.28 (dt, *J* = 17.3, 1.3 Hz, 1H), 5.24 (dt, *J* = 10.5, 1.2 Hz, 1H), 4.83 (t, *J* = 6.7 Hz, 1H), 3.76 (s, 3H), 1.90 (octet, *J* = 6.7 Hz, 1H), 0.93 (d, *J* = 6.8 Hz, 3H), 0.91 (d, *J* = 7.2 Hz, 3H).

¹³C NMR (125 MHz, CDCl₃) δ 155.50 (e), 134.32 (o), 118.50 (e), 83.96 (o), 54.73 (o), 31.95 (o), 17.44 (o).

IR (Neat) 3087 (w), 2965 (m), 2876 (w), 1753 (s), 1648 (w), 1443 (m), 1032 (m) cm⁻¹.

HRMS (ESI, $[M]^+$) calcd for $C_8H_{14}O_3$ 158.0943, found 158.0940.



1-Cyclohexylprop-2-en-1-yl methyl carbonate *rac*-11g

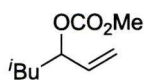
Prepared according to the general synthesis of allylic carbonates and displaying the following properties.

1H NMR (500 MHz, $CDCl_3$) δ 5.77 (ddd, $J = 17.3, 10.4, 7.1$ Hz, 1H), 5.27 (dd, $J = 17.3, 0.9$ Hz, 1H), 5.23 (d, $J = 10.6$ Hz, 1H), 4.84 (t, $J = 7.0$ Hz, 1H), 3.77 (s, 3H), 1.81-1.62 (m, 5H), 1.61-1.54 (m, 1H), 1.26-1.09 (m, 3H), 1.05-0.96 (m, 2H).

^{13}C NMR (125 MHz, $CDCl_3$) δ 155.55 (e), 124.71 (o), 118.38 (e), 83.51 (o), 54.72 (o), 41.59 (o), 28.54 (e), 28.45 (e), 26.41 (e), 26.00 (e), 25.95 (e).

IR (Neat) 2927 (m), 2854 (m), 1745 (s), 1441 (m), 1253 (s), 960 (m), 941 (m), 928 (m), 791 (m) cm^{-1} .

HRMS (CI, $[M+NH_4]^+$) calcd for $C_{11}H_{22}NO_3$ 216.1594, found 216.1597.



Methyl 5-methylhex-1-en-3-yl carbonate *rac*-11h

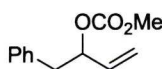
Prepared according to the general synthesis of allylic carbonates and displaying the following properties.

1H NMR (500 MHz, $CDCl_3$) δ 5.77 (ddd, $J = 17.2, 10.5, 6.9$ Hz, 1H), 5.29 (d, $J = 17.2$ Hz, 1H), 5.18 (d, $J = 10.4$ Hz, 1H), 5.11 (quartet, $J = 6.9$ Hz, 1H), 3.76 (s, 3H), 1.72-1.60 (m, 2H), 1.43-1.35 (m, 1H), 0.92 (d, $J = 6.5$ Hz, 3H), 0.91 (d, $J = 6.5$ Hz, 3H).

^{13}C NMR (125 MHz, $CDCl_3$) δ 155.40 (e), 136.44 (o), 117.45 (e), 77.85 (o), 54.73 (o), 43.29 (e), 24.43 (o), 22.83 (o), 22.44 (o).

IR (Neat) 2959 (m), 2932 (w), 2873 (w), 1742 (s), 1442 (m), 1259 (vs), 909 (s), 731 (vs) cm^{-1} .

HRMS (CI, $[M+NH_4]^+$) calcd for $C_9H_{20}NO_3$ 190.1438, found 190.1437.



Methyl 1-phenylbut-3-en-2-yl carbonate *rac*-11i²²

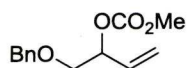
Prepared according to the general synthesis of allylic carbonates and displaying the following properties.

1H NMR (500 MHz, $CDCl_3$) δ 7.31-7.26 (m, 2H), 7.24-7.21 (m, 3H), 5.82 (ddd, $J = 17.3, 10.6, 6.7$ Hz, 1H), 5.29-5.25 (m, 2H), 5.20 (d, $J = 9.6$, 1H), 3.74 (s, 3H), 3.03 (dd, A of ABX, $J_{AB} = 13.9, J_{AX} = 7.4$ Hz, 1H), 2.91 (dd, B of ABX, $J_{AB} = 13.9, J_{BX} = 6.3$ Hz, 1H).

^{13}C NMR (125 MHz, CDCl_3) δ 155.14 (e), 136.59 (e), 135.34 (o), 129.66 (o), 128.46 (o), 126.76 (o), 117.86 (e), 79.39 (o), 54.73 (o), 40.99 (e).

IR (Neat) 3087 (w), 3067 (w), 3027 (m), 2958 (m), 2850 (w), 1747 (s), 1445 (m), 1035 (m) cm^{-1} .

HRMS (CI, $[\text{M}]^+$) calcd for $\text{C}_{12}\text{H}_{18}\text{O}_3$ 224.1287, found 224.1289.



1-(Benzyloxy)but-3-en-2-yl methyl carbonate *rac*-11j

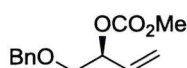
Prepared according to the general synthesis of allylic carbonates and displaying the following properties.

^1H NMR (500 MHz, CDCl_3) δ 7.38-7.35 (m, 4H), 7.32-7.27 (m, 1H), 5.84 (ddd, J = 17.2, 10.7, 6.4 Hz, 1H), 5.40 (dt, J = 17.3, 1.1 Hz, 1H), 5.34-5.31 (m, 1H), 5.29 (dt, J = 10.6, 1.1 Hz, 1H), 4.59 (d, A of AB, J_{AB} = 12.9 Hz, 1H), 4.57 (d, B of AB, J_{AB} = 12.3 Hz, 1H), 3.79 (s, 3H), 3.64-3.56 (m, 2H).

^{13}C NMR (125 MHz, CDCl_3) δ 155.30 (e), 137.91 (e), 132.78 (o), 128.51 (o), 127.83 (o), 127.75 (o), 118.88 (e), 77.48 (o), 73.35 (e), 71.23 (e), 54.90 (o).

IR (Neat) 3030 (w), 2956 (w), 2861 (w), 2192 (w), 1746 (s), 1442 (m), 1363 (w), 1339 (w), 1260 (s), 1095 (m), 989 (m), 939 (m), 790 (m), 738 (m), 698 (m) cm^{-1} .

HRMS (CI, $[\text{M}+\text{NH}_4]^+$) calcd for $\text{C}_{13}\text{H}_{20}\text{NO}_4$ 254.1392, found 254.1390.

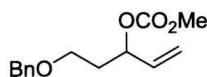


(*S*)-1-(Benzyloxy)but-3-en-2-yl methyl carbonate *S*-11j

Prepared according to the general synthesis of allylic carbonates and displaying the following properties.

^1H NMR (500 MHz, CDCl_3) δ 7.37-7.26 (m, 5H), 5.84 (ddd, J = 17.1, 10.6, 6.5 Hz, 1H), 5.40 (dt, J = 17.4, 1.2 Hz, 1H), 5.34-5.32 (m, 1H), 5.29 (dt, J = 10.6, 1.0 Hz, 1H), 4.59 (d, A of AB, J_{AB} = 12.3 Hz, 1H), 4.57 (d, B of AB, J_{AB} = 12.3 Hz, 1H), 3.79 (s, 3H), 3.63-3.36 (m, 2H).

IR (Neat) 3033 (w), 2956 (w), 2858 (w), 2190 (w), 1747 (s), 1439 (m), 1361 (w), 1339 (w), 1260 (s), 1096 (m), 989 (m), 940 (m), 791 (m), 738 (m), 698 (m) cm^{-1} .



5-(Benzyloxy)pent-1-en-3-yl methyl carbonate *rac*-11k

Prepared according to the general synthesis of allylic carbonates and displaying the following properties.

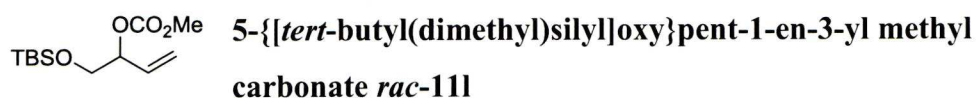
^1H NMR (500 MHz, CDCl_3) δ 7.36-7.31 (m, 4H), 7.30-7.26 (m, 1H), 5.81 (ddd, J = 17.2, 10.5, 6.8 Hz, 1H), 5.32 (dt, J = 17.2, 1.1 Hz, 1H), 5.38-5.34 (m, 1H), 5.27 (q, J

= 6.8, 1H), 5.22 (dt, $J = 10.6, 1.1$ Hz), 4.51 (d, A of AB, $J_{AB} = 20.3$ Hz, 1H), 4.47 (d, B of AB, $J_{AB} = 20.8$ Hz, 1H), 3.76 (s, 3H), 3.57-3.50 (m, 2H), 2.06-1.99 (m, 1H), 1.96-1.89 (m, 1H).

^{13}C NMR (125 MHz, CDCl_3) δ 155.18 (e), 138.32 (e), 135.78 (o), 128.45 (o), 127.76 (o), 127.68 (o), 117.72 (e), 76.42 (o), 73.12 (e), 65.94 (e), 54.72 (o), 34.48 (e).

IR (Neat) 3028 (w), 2956 (w), 2922 (w), 2860 (w) 1745 (s), 1451 (m), 1442 (m), 1259 (s), 1096 (m), 940 (m), 791 (m), 737 (m), 689 (m) cm^{-1} .

HRMS (ESI, $[\text{M}+\text{NH}_4]^+$) calcd for $\text{C}_{14}\text{H}_{22}\text{NO}_4$ 268.1543, found 268.1541.



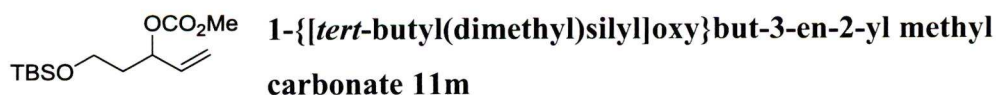
Prepared according to the general synthesis of allylic carbonates and displaying the following properties.

^1H NMR (500 MHz, CDCl_3) δ 5.81 (ddd, $J = 17.2, 10.7, 6.4$ Hz, 1H), 5.35 (dt, $J = 17.3, 1.3$ Hz, 1H), 5.25 (dt, $J = 10.7, 1.2$ Hz, 1H), 5.17-5.13 (m, 1H), 3.76 (s, 3H), 3.68 (d, $J = 5.8$ Hz, 2H), 0.86 (s, 9H), 0.04 (s, 3H), 0.04 (s, 3H)

^{13}C NMR (125 MHz, CDCl_3) δ 155.39 (e), 132.98 (o), 118.58 (e), 79.26 (o), 64.76 (e), 54.78 (o), 25.85 (o), 18.34 (e), -5.31 (o), -5.33 (o).

IR (Neat) 2956 (m), 2930 (m), 2858 (m), 1750 (s), 1443 (m), 1258 (vs), 1128 (m), 910 (m), 836 (s), 777 (s), 732 (s) cm^{-1} .

HRMS (CI, $[\text{M}+\text{Na}]^+$) calcd for $\text{C}_{12}\text{H}_{24}\text{O}_4\text{SiNa}$ 283.1342, found 283.1346.



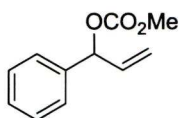
Prepared according to the general synthesis of allylic carbonates and displaying the following properties.

^1H NMR (500 MHz, CDCl_3) δ 5.81 (ddd, $J = 17.2, 10.7, 6.4$ Hz, 1H), 5.32 (d, $J = 17.8, 1\text{H}$), 5.25-5.21 (m, 2H), 3.72-3.64 (m, 2H), 1.95-1.88 (m, 1H), 1.85-1.77 (m, 1H), 0.86 (s, 9H), 0.04 (s, 3H), 0.04 (s, 3H).

^{13}C NMR (125 MHz, CDCl_3) δ 155.25 (e), 136.04 (o), 117.52 (e), 77.27 (o), 60.32 (e), 54.78 (o), 36.67 (e), 25.83 (o), -5.31 (o), -5.33 (o).

IR (Neat) 2956 (m), 2930 (m), 2858 (m), 1750 (s), 1443 (m), 1258 (vs), 1128 (m), 937 (m), 910 (m), 836 (s), 777 (s), 732 (s) cm^{-1} .

HRMS (ESI, $[\text{M}+\text{NH}_4]^+$) calcd for $\text{C}_{13}\text{H}_{30}\text{NO}_4\text{Si}$ 292.1939, found 292.1936.



Methyl 1-phenylprop-2-en-1-yl carbonate 11n²³

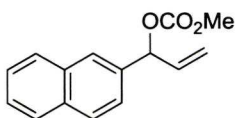
Prepared according to the general synthesis of allylic carbonates and displaying the following properties.

¹H NMR (500 MHz, CDCl₃) δ 7.39-7.35 (m, 4H), 7.34-7.30 (m, 1H), 6.09-6.07 (m, 1H), 6.04 (ddd, *J* = 16.7, 10.5, 6.1 Hz, 1H), 5.35 (d, *J* = 16.7 Hz, 1H), 5.28 (d, *J* = 10.0 Hz, 1H), 3.78 (s, 3H).

¹³C NMR (125 MHz, CDCl₃) δ 155.12 (e), 138.25 (e), 135.84 (o), 128.72 (o), 128.54 (o), 127.17 (o), 117.59 (e), 80.30 (o), 54.93 (o).

IR (Neat) 3034 (w), 2957 (w), 2851 (w), 1745 (s), 1441 (m), 1251 (m), 1200 (m), 970 (m), 924 (s), 790 (m), 764 (m), 698 (s) cm⁻¹.

HRMS (ESI, [M+NH₄]⁺) calcd for C₁₁H₁₆NO₃ 210.1125, found 210.1124.



Methyl 1-(naphthalene-2-yl)prop-2-en-1-yl carbonate 11o

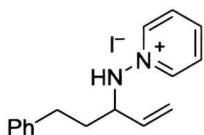
Prepared according to the general synthesis of allylic carbonates and displaying the following properties.

¹H NMR (500 MHz, CDCl₃) δ 7.86-7.81 (m, 4H), 7.51-7.46 (m, 3H), 6.25 (d, *J* = 6.0 Hz, 1H), 6.11 (ddd, *J* = 17.0, 10.6, 6.2 Hz, 1H), 5.40 (dt, *J* = 17.1, 1.3 Hz, 1H), 5.32 (dt, *J* = 10.4, 1.2 Hz, 1H), 2.79 (s, 3H).

¹³C NMR (125 MHz, CDCl₃) δ 155.17 (e), 135.81 (o), 135.69 (e), 133.34 (e), 133.24 (e), 128.65 (o), 128.27 (o), 127.83 (o), 126.51 (o), 126.47 (o), 126.43 (o), 124.78 (o), 117.89 (e), 80.47 (o), 55.04 (o).

IR (Neat) 3057 (m), 3020 (w), 2957 (w), 1445 (s), 1643 (m), 1446 (m), 1032 (m) cm⁻¹.

HRMS (ESI, [M]⁺) calcd for C₁₅H₁₄O₃ 242.0943, found 242.0955.



1-[(5-Phenylpent-1-en-3-yl)amino]pyridinium iodide *rac*-12a.

Representative Procedure for the Rhodium-Catalyzed Allylic

Amination: Trimethyl phosphite (12 μL, 0.10 mmol) was added to a red suspension of Wilkinson's catalyst (23.0 mg, 0.025 mmol) in anhydrous THF (1.0 mL). The mixture was then stirred under an atmosphere of argon at room temperature for *ca.* 15 minutes resulting in a light yellow homogeneous solution. In a separate flask, lithium bis(trimethylsilyl)amide (275 μL, 0.28 mmol) was added dropwise to a suspension of 1-aminopyridinium iodide (69.4 mg, 0.31 mmol) in anhydrous acetonitrile (1.5 mL) at room temperature and the

anion allowed to form over *ca.* 20 minutes resulting in a dark purple heterogeneous mixture. The catalyst solution was then added *via* Teflon[®] cannula to the anion, followed by the allylic carbonate **rac-11a** (55.2 mg, 0.25 mmol) *via* a tared 500 μ L gas-tight syringe. The reaction was allowed to stir at room temperature for *ca.* 18 hours (t.l.c. control). Lithium iodide (66.7 mg, 0.50 mmol) was then added to the reaction in one portion followed by acetic acid (30 μ L, 0.50 mmol) and stirred at room temperature for *ca.* 2 hours. The reaction mixture was concentrated *in vacuo* and the crude product pre-absorbed onto silica gel for purification *via* flash chromatography (eluting with 3.5% methanol/chloroform), decolorized with activated charcoal and recrystallized from dichloromethane/diethyl ether to afford aminopyridinium salt **rac-12a** (81.9 mg, 89%) as a pale yellow solid. Oils were further purified *via* flash chromatography (eluting with 1:1 acetone/hexane), whereas solids were recrystallized from dichloromethane/hexane.

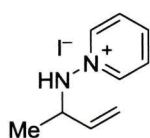
Color and State: Pale yellow solid; **mp** = 113-115 °C; *Selectivity:* **rac-12a/13a** \geq 19:1.

¹H NMR (500 MHz, CDCl₃) δ 9.22 (d, *J* = 6.6 Hz, 2H), 8.90 (dd, *J* = 7.5, 3.2 Hz, 1H), 8.35 (t, *J* = 7.8 Hz, 1H), 7.98-7.95 (m, 2H), 7.33-7.20 (m, 5H), 6.05-5.96 (m, 1H), 5.14 (d, *J* = 10.1 Hz, 1H), 4.88 (d, *J* = 17.2 Hz, 1H), 3.89-3.81 (m, 1H), 2.85-2.71 (m, 2H), 2.45-2.36 (m, 1H), 2.14-2.04 (m, 1H).

¹³C NMR (125 MHz, CDCl₃) δ 143.81 (o), 143.36 (o), 140.82 (e), 135.38 (o), 128.72 (o), 128.66 (o), 128.04 (o), 126.29 (o), 121.86 (e), 68.43 (o), 33.43 (e), 31.86 (e).

IR (Neat) 3104 (m), 3058 (m), 3022 (m), 2926 (m), 2856 (w), 1621 (m), 1602 (w), 1496 (m), 1476 (m), 1453 (s), 1261 (w), 1157 (w), 999 (m), 939 (m), 917 (s), 754 (m), 727 (s), 702 (vs), 675 (s) cm⁻¹.

HRMS (EI, [M-I]⁺) calcd for C₁₆H₁₉N₂ 239.1543, found 239.1543.



1-[(But-3-en-2-yl)amino]pyridinium iodide *rac*-12b.

Synthesized according to the general procedure outlined for 12a, showing the following properties:

Color and State: Yellow oil; *Selectivity:* **rac-12b/13b** \geq 19:1.

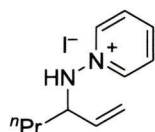
¹H NMR (500 MHz, CDCl₃) δ 9.30 (dd, *J* = 6.6, 1.1 Hz, 2H), 8.77 (d, *J* = 5.9 Hz, 1H), 8.42 (tt, *J* = 7.8, 1.2 Hz, 1H), 8.05-8.00 (m, 2H), 5.90 (ddd, *J* = 17.2, 10.1, 9.0

Hz, 1H), 5.06 (d, $J = 10.3$ Hz, 1H), 4.92 (d, $J = 17.2$ Hz, 1H), 4.07-3.99 (m, 1H), 1.53 (d, $J = 6.4$ Hz, 3H).

^{13}C NMR (125 MHz, CDCl_3) δ 144.18 (o), 143.97 (o), 136.68 (o), 128.28 (o), 120.38 (e), 63.91 (o), 18.62 (o).

IR (Neat) 3105 (s), 3051 (s), 2970 (s), 2930 (s), 1619 (vs), 1475 (s), 1458 (vs), 1422 (m), 1377 (m), 1330 (m), 1260 (m), 1159 (m), 1065 (s), 998 (s), 939 (vs), 896 (s), 788 (vs), 771 (vs), 698 (m), 674 (vs) cm^{-1} .

HRMS (EI, $[\text{M-I}]^+$) calcd for $\text{C}_9\text{H}_{13}\text{N}_2$ 149.1073, found 149.1077.



1-[(Hex-1-en-3-yl)amino]pyridinium iodide *rac*-12c.

Synthesized according to the general procedure outlined for 12a, showing the following properties:

Color and State: Yellow oil; *Selectivity:* ***rac*-12c/13c** $\geq 19:1$.

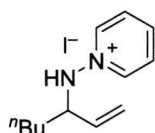
^1H NMR (500 MHz, CDCl_3) δ 9.26 (d, $J = 6.5$ Hz, 2H), 8.68 (d, $J = 5.9$ Hz, 1H), 8.41 (dt, $J = 7.8, 1.0$ Hz, 1H), 8.04-8.01 (m, 2H), 5.88 (dt, $J = 17.2, 9.7$ Hz, 1H), 5.08 (d, $J = 10.2$ Hz, 1H), 4.87 (d, $J = 17.1$ Hz, 1H), 3.87-3.80 (m, 1H), 2.04-1.95 (m, 1H), 1.78-1.66 (m, 1H), 1.50-1.34 (m, 2H), 0.94 (t, $J = 7.4$ Hz, 3H).

^{13}C NMR (125 MHz, CDCl_3) δ 144.12 (o), 143.56 (o), 135.74 (o), 128.07 (o), 121.48 (e), 69.09 (o), 34.11 (e), 19.23 (e), 13.95 (o).

IR (Neat) 3104 (m), 3048 (m), 3019 (m), 2959 (s), 2931 (s), 2872 (m), 1728 (w), 1620 (m), 1479

(m), 1454 (vs), 1257 (m), 1157 (m), 999 (m), 936 (vs), 778 (s), 676 (vs) cm^{-1} .

HRMS (EI, $[\text{M-I}]^+$) calcd for $\text{C}_{11}\text{H}_{17}\text{N}_2$ 177.1386, found 177.1390.



1-[(Hept-1-en-3-yl)amino]pyridinium iodide *rac*-12d.

Synthesized according to the general procedure outlined for 12a, showing the following properties:

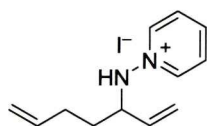
Color and State: Yellow oil; *Selectivity:* ***rac*-12d/13d** $\geq 19:1$.

^1H NMR (500 MHz, CDCl_3) δ 9.24 (d, $J = 5.7$ Hz, 2H), 8.61 (d, $J = 7.1$ Hz, 1H), 8.43 (t, $J = 7.8$ Hz, 1H), 8.06-8.03 (m, 2H), 5.86 (dt, $J = 17.1, 9.8$ Hz, 1H), 5.07 (dd, $J = 10.2, 0.8$ Hz, 1H), 4.87 (d, $J = 17.1$ Hz, 1H), 3.86-4.78 (m, 1H), 2.04-1.96 (m, 1H), 1.77-1.67 (m, 1H), 1.40-1.28 (m, 4H), 0.87 (t, $J = 7.1$ Hz, 3H).

¹³C NMR (125 MHz, CDCl₃) δ 143.98 (o), 143.65 (o), 135.69 (o), 128.16 (o), 121.51 (e), 69.23 (o), 31.82 (e), 28.05 (e), 22.47 (e), 14.10 (o).

IR (Neat) 3099 (m), 3014 (m), 2956 (vs), 2930 (vs), 2859 (m), 1619 (m), 1474 (s), 1454 (vs), 1259 (w), 1156 (w), 999 (m), 938 (s), 778 (s), 676 (vs) cm⁻¹.

HRMS (EI, [M-I]⁺) calcd for C₁₂H₁₉N₂ 191.1543, found 191.1537.



1-[(Hepta-1,6-dien-3-yl)amino]pyridinium iodide *rac*-12e.

Synthesized according to the general procedure outlined for 12a, showing the following properties:

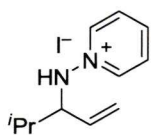
Color and State: Yellow oil; *Selectivity:* ***rac*-12e/13e** ≥19:1.

¹H NMR (500 MHz, CDCl₃) δ 9.24 (d, *J* = 5.7 Hz, 2H), 8.74 (d, *J* = 7.3 Hz, 1H), 8.42 (t, *J* = 7.8 Hz, 1H), 8.05-8.02 (m, 2H), 5.91 (dt, *J* = 17.1, 9.8, 1H), 5.80 (ddt, *J* = 17.1, 10.4, 6.6 Hz, 1H), 5.10 (dd, *J* = 10.2, 1.0 Hz, 1H), 5.05 (dd, *J* = 17.2, 1.6 Hz, 1H), 5.00 (d, *J* = 10.3 Hz, 1H), 4.88 (d, *J* = 17.1 Hz, 1H), 3.91-3.82 (m, 1H), 2.28-2.18 (m, 1H), 2.18-2.10 (m, 2H), 1.89-1.80 (m, 1H).

¹³C NMR (125 MHz, CDCl₃) δ 143.99 (o), 143.31 (o), 137.20 (o), 135.37 (o), 127.91 (o), 121.61 (e), 115.94 (e), 68.45 (o), 30.91 (e), 29.82 (e).

IR (Neat) 3099 (s), 3058 (s), 3016 (s), 2927 (s), 1640 (m), 1623 (m), 1476 (s), 1452 (s), 1421 (m), 1260 (w), 1156 (w), 1050 (w), 997 (s), 915 (vs), 775 (s), 726 (vs), 675 (vs) cm⁻¹.

HRMS (EI, [M-I]⁺) calcd for C₁₂H₁₇N₂ 189.1392, found 189.1395.



1-[(4-Methylpent-1-en-3-yl)amino]pyridinium iodide *rac*-12f.

Synthesized according to the general procedure outlined for 12a, showing the following properties:

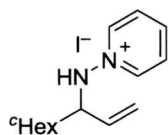
Color and State: Pale orange solid; **mp** = 86-87 °C; *Selectivity:* ***rac*-12f/13f** ≥19:1.

¹H NMR (500 MHz, CDCl₃) δ 9.24 (d, *J* = 6.3 Hz, 2H), 8.70 (d, *J* = 7.1 Hz, 1H), 8.37 (t, *J* = 7.8 Hz, 1H), 8.00-7.97 (m, 2H), 5.94 (dt, *J* = 17.2, 9.9 Hz, 1H), 5.12 (d, *J* = 10.2 Hz, 1H), 4.85 (d, *J* = 17.2 Hz, 1H), 3.55 (dt, *J* = 9.4, 6.9 Hz, 1H), 2.36 (octet, *J* = 6.7 Hz, 1H), 1.11 (d, *J* = 6.7 Hz, 3H), 1.01 (d, *J* = 6.9 Hz, 3H).

¹³C NMR (125 MHz, CDCl₃) δ 144.23 (o), 143.28 (o), 133.78 (o), 127.90 (o), 122.10 (e), 75.18 (o), 30.49 (o), 20.23 (o), 18.79 (o).

IR (Neat) 3103 (m), 2957 (vs), 2925 (vs), 2871 (s), 1736 (m), 1621 (m), 1455 (s), 1259 (m), 1158 (w), 999 (m), 934 (m), 772 (m), 676 (s) cm^{-1} .

HRMS (EI, $[\text{M-I}]^+$) calcd for $\text{C}_{11}\text{H}_{17}\text{N}_2$ 177.1386, found 177.1382.



1-[(1-Cyclohexylprop-2-en-1-yl)amino]pyridinium iodide *rac*-12g.

Synthesized according to the general procedure outlined for 12a, showing the following properties:

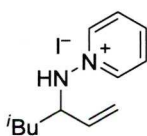
Color and State: Pale yellow solid; **mp** = 186-188 °C; **Selectivity:** *rac*-12g/13g $\geq 19:1$.

^1H NMR (500 MHz, CDCl_3) δ 9.24 (d, J = 5.8 Hz, 2H), 8.75 (d, J = 7.6 Hz, 1H), 8.34 (t, J = 7.8 Hz, 1H), 7.98-7.95 (m, 2H), 5.96 (dt, J = 17.2, 9.9 Hz, 1H), 5.10 (dd, J = 10.2, 1.0 Hz, 1H), 4.80 (d, J = 17.2 Hz, 1H), 3.55 (dt, J = 9.4, 7.5 Hz, 1H), 2.10-1.96 (m, 2H), 1.88-1.81 (m, 1H), 1.79-1.64 (m, 3H), 1.39-1.23 (m, 2H), 1.20-1.08 (m, 2H), 1.02 (dq, J = 12.4, 3.4 Hz, 1H).

^{13}C NMR (125 MHz, CDCl_3) δ 144.14 (o), 143.06 (o), 134.35 (o), 127.84 (o), 121.66 (e), 74.73 (o), 39.79 (o), 30.49 (e), 29.52 (e), 26.43 (e), 25.90 (e), 25.89 (e).

IR (Neat) 3103 (m), 3059 (m), 3008 (m), 2927 (m), 2915 (m), 2850 (m), 1623 (w), 1529 (w), 1481 (m), 1453 (m), 1157 (m), 1004 (m), 944 (s), 773 (s), 674 (vs) cm^{-1} .

HRMS (EI, $[\text{M-I}]^+$) calcd for $\text{C}_{14}\text{H}_{21}\text{N}_2$ 217.1699, found 217.1698.



1-[(5-Methylhex-1-en-3-yl)amino]pyridinium iodide *rac*-12h.

Synthesized according to the general procedure outlined for 12a, showing the following properties:

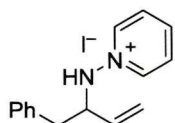
Color and State: Pale yellow solid; **mp** = 102-105 °C; **Selectivity:** *rac*-12h/13h $\geq 19:1$.

^1H NMR (500 MHz, CDCl_3) δ 9.28 (d, J = 5.9 Hz, 2H), 8.82 (d, J = 7.4 Hz, 1H), 8.37 (t, J = 7.8 Hz, 1H), 8.00-7.97 (m, 2H), 5.92 (dt, J = 17.2, 9.7 Hz, 1H), 5.04 (d, J = 10.1 Hz, 1H), 4.84 (d, J = 17.2 Hz, 1H), 3.91-3.83 (m, 1H), 1.93-1.84 (m, 1H), 1.80-1.67 (m, 2H), 0.98 (d, J = 6.4 Hz, 3H), 0.93 (d, J = 6.3 Hz, 3H).

^{13}C NMR (125 MHz, CDCl_3) δ 144.03 (o), 143.44 (o), 135.82 (o), 128.06 (o), 121.26 (e), 67.77 (o), 40.77 (e), 24.86 (o), 23.38 (o), 21.96 (o).

IR (Neat) 3080 (vs), 3048 (s), 2999 (s), 2953 (vs), 2923 (vs), 2868 (s), 1720 (w), 1620 (m), 1456 (vs), 1467 (vs), 1270 (s), 991 (s), 931 (vs), 779 (vs), 678 (vs) cm^{-1} .

HRMS (EI, $[\text{M-I}]^+$) calcd for $\text{C}_{12}\text{H}_{19}\text{N}_2$ 191.1543, found 191.1548.



1-[(1-Phenylbut-3-en-2-yl)amino]pyridinium iodide *rac*-12i.

Synthesized according to the general procedure outlined for **12a**, showing the following properties:

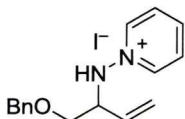
Color and State: Yellow oil; *Selectivity:* ***rac*-12i/13i** $\geq 19:1$.

^1H NMR (500 MHz, CDCl_3) δ 9.24 (d, $J = 5.8$ Hz, 2H), 9.03 (d, $J = 7.1$ Hz, 1H), 8.36 (t, $J = 7.8$ Hz, 1H), 7.98-7.96 (m, 2H), 7.35-7.31 (m, 2H), 7.29-7.23 (m, 2H), 7.22-7.17 (m, 1H), 5.95 (dt, $J = 17.2, 9.7$ Hz, 1H), 5.01 (d, $J = 10.3$ Hz, 1H), 4.76 (d, $J = 17.1$ Hz, 1H), 4.14 (quint, $J = 7.6$ Hz, 1H), 3.46 (dd, A of ABX, $J_{\text{AB}} = 13.7$, $J_{\text{AX}} = 6.0$ Hz, 1H), 3.04 (dd, B of ABX, $J_{\text{AB}} = 13.7$, $J_{\text{BX}} = 7.9$ Hz, 1H).

^{13}C NMR (125 MHz, CDCl_3) δ 143.87 (o), 143.55 (o), 136.73 (e), 134.77 (o), 129.91 (o), 128.52 (o), 128.12 (o), 126.87 (o), 121.96 (e), 70.29 (o), 38.76 (e).

IR (Neat) 3101 (m), 3020 (s), 2957 (s), 2924 (s), 2853 (m), 1728 (m), 1620 (m), 1475 (s), 1453 (vs), 1265 (s), 1156 (w), 1074 (m), 939 (s), 780 (m), 733 (s), 699 (vs), 674 (vs) cm^{-1} .

HRMS (EI, $[\text{M-I}]^+$) calcd for $\text{C}_{15}\text{H}_{17}\text{N}_2$ 225.1386, found 225.1385.



1-[[1-(Benzyloxy)but-3-en-2-yl]amino]pyridinium iodide *rac*-12j.

Synthesized according to the general procedure outlined for **12a**, showing the following properties:

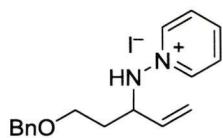
Color and State: Yellow oil; *Selectivity:* ***rac*-12j/13j** $\geq 19:1$.

^1H NMR (500 MHz, CDCl_3) δ 9.26 (d, $J = 6.6$ Hz, 2H), 8.76 (d, $J = 6.1$ Hz, 1H), 8.30 (dt, $J = 7.8, 1.1$ Hz, 1H), 7.93-7.90 (m, 2H), 7.32-7.23 (m, 5H), 6.00-5.91 (m, 1H), 5.27-5.20 (m, 2H), 4.53 (d, A of AB, $J_{\text{AB}} = 11.9$ Hz, 1H), 4.50 (d, B of AB, $J_{\text{AB}} = 11.8$ Hz, 1H), 4.32-4.24 (m, 1H), 3.92 (dd, A of ABX, $J_{\text{AB}} = 10.3$, $J_{\text{BX}} = 7.4$ Hz, 1H), 3.77 (dd, B of ABX, $J_{\text{AB}} = 10.4$, $J_{\text{BX}} = 4.1$ Hz, 1H).

^{13}C NMR (125 MHz, CDCl_3) δ 144.34 (o), 143.52 (o), 137.47 (e), 131.97 (o), 128.56 (o), 128.21 (o), 128.05 (o), 127.91 (o), 122.45 (e), 73.67 (e), 71.15 (e), 66.68 (o).

IR (Neat) 3099 (m), 3053 (m), 3022 (m), 2957 (s), 2925 (vs), 2856 (m), 1732 (m), 1621 (m), 1472 (s), 1454 (vs), 1439 (s), 1263 (m), 1113 (vs), 1099 (vs), 1077 (s), 997 (m), 942 (m), 913 (m), 745 (vs), 700 (vs), 676 (vs) cm^{-1} .

HRMS (EI, $[\text{M-I}]^+$) calcd for $\text{C}_{16}\text{H}_{19}\text{N}_2\text{O}$ 255.1492, found 255.1483.



1-[[5-(Benzyloxy)pent-1-en-3-yl]amino]pyridinium iodide *rac*-12k.

Synthesized according to the general procedure outlined for 12a, showing the following properties:

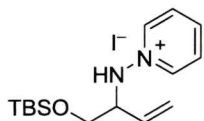
Color and State: Pale yellow solid; **mp** = 97-99 °C; **Selectivity:** *rac*-12k/13k ≥19:1.

¹H NMR (500 MHz, CDCl₃) δ 9.11 (d, *J* = 5.8 Hz, 2H), 8.85 (d, *J* = 8.0 Hz, 1H), 8.34 (t, *J* = 7.8 Hz, 1H), 7.96-7.93 (m, 2H), 7.37-7.32 (m, 4H), 7.32-7.27 (m, 1H), 6.01 (dt, *J* = 17.1, 9.8 Hz, 1H), 5.09 (dd, *J* = 10.1, 0.9 Hz, 1H), 4.88 (d, *J* = 17.1 Hz, 1H), 4.52 (s, 2H), 4.14-4.06 (m, 1H), 3.75 (ddd, *J* = 9.8, 6.3, 4.7 Hz, 1H), 3.60 (ddd, *J* = 9.6, 7.8, 4.4 Hz, 1H), 2.37-2.28 (m, 1H), 2.09-2.00 (m, 1H).

¹³C NMR (125 MHz, CDCl₃) δ 143.50 (o), 143.13 (o), 138.31 (e), 135.13 (o), 128.59 (o), 128.22 (o), 128.06 (o), 127.90 (o), 121.47 (e), 73.22 (e), 66.38 (o), 66.19 (e), 32.40 (e).

IR (Neat) 3099 (m), 3053 (m), 3017 (m), 2948 (m), 2863 (m), 1620 (m), 1475 (m), 1453 (s), 1366 (m), 1258 (w), 1202 (w), 1096 (s), 1075 (s), 998 (m), 938 (m), 918 (s), 734 (s), 699 (vs), 675 (vs) cm⁻¹.

HRMS (EI, [M-I]⁺) calcd for C₁₇H₂₁N₂O 269.1648, found 269.1648.



1-[[1-[[*tert*-Butyl(dimethyl)silyl]oxy]but-3-en-2-yl]amino]pyridinium iodide *rac*-12l.

Synthesized according to the general procedure outlined for 12a, showing the following properties:

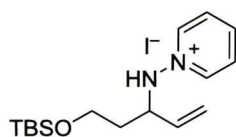
Color and State: Off-white solid; **mp** = 129-132 °C; **Selectivity:** *rac*-12/13 ≥19:1.

¹H NMR (500 MHz, CDCl₃) δ 9.26 (dd, *J* = 6.7, 1.1 Hz, 2H), 8.67 (d, *J* = 5.5 Hz, 1H), 8.42 (tt, *J* = 7.8, 1.1 Hz, 1H), 8.02 (dd, *J* = 7.0, 7.6 Hz, 2H), 5.95 (ddd, *J* = 17.3, 10.3, 8.5 Hz, 1H), 5.25 (d, *J* = 10.4 Hz, 1H), 5.20 (d, *J* = 17.3 Hz, 1H), 4.11-4.04 (m, 1H), 4.00 (dd, A of ABX, *J*_{AB} = 10.8, *J*_{AX} = 6.5 Hz, 1H), 3.90 (dd, B of ABX, *J*_{AB} = 10.8, *J*_{BX} = 4.3 Hz, 1H), 0.85 (s, 9H), 0.07 (s, 3H), 0.06 (s, 3H).

¹³C NMR (125 MHz, CDCl₃) δ 144.59 (o), 143.81 (o), 132.32 (o), 128.06 (o), 122.54 (e), 68.96 (o), 64.48 (e), 26.07 (o), 18.47 (e), -5.02 (o), -5.08 (o).

IR (Neat) 3105 (w), 3019 (m), 2951 (m), 2928 (m), 2856 (m), 1621 (m), 1471 (s), 1438 (m), 1388 (m), 1342 (w), 1255 (s), 1117 (m), 1087 (s), 1058 (s), 1005 (m), 948 (m), 874 (m), 833 (vs), 773 (vs), 671 (vs) cm^{-1} .

HRMS (EI, $[\text{M-I}]^+$) calcd for $\text{C}_{15}\text{H}_{27}\text{N}_2\text{OSi}$ 279.1887, found 279.1874.



1-[(5-{*tert*-Butyl(dimethyl)silyl}oxy}pent-1-en-3-yl)amino]pyridinium iodide *rac*-12m.

Synthesized according to the general procedure outlined for 12a, showing the following properties:

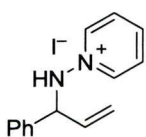
Color and State: Pale yellow solid; **mp** = 132-134 °C; *Selectivity:* ***rac*-12m/13m** $\geq 19:1$.

^1H NMR (500 MHz, CDCl_3) δ 9.24 (d, J = 6.0 Hz, 2H), 9.00 (d, J = 7.7 Hz, 1H), 8.36 (t, J = 7.8 Hz, 1H), 8.00-7.97 (m, 2H), 6.06 (dt, J = 17.2, 9.7 Hz, 1H), 5.13 (d, J = 10.2 Hz, 1H), 4.90 (d, J = 17.0 Hz, 1H), 4.15-4.07 (m, 1H), 3.89-3.82 (m, 1H), 3.73-3.65 (m, 1H), 2.31-2.22 (m, 1H), 2.04-1.95 (m, 1H), 0.88 (s, 9H), 0.06 (s, 3H), 0.05 (s, 3H).

^{13}C NMR (125 MHz, CDCl_3) δ 143.23 (o), 142.84 (o), 135.28 (o), 128.02 (o), 121.32 (e), 66.28 (o), 59.08 (e), 35.06 (e), 26.08 (o), 18.39 (e), -5.14 (o), -5.18 (o).

IR (Neat) 3085 (vs), 3043 (m), 3008 (m), 2951 (vs), 2927 (vs), 2881 (m), 2856 (m), 1616 (w), 1520 (w), 1467 (s), 1254 (s), 1101 (vs), 937 (w), 835 (vs), 778 (vs), 680 (w) cm^{-1} .

HRMS (EI, $[\text{M-I}]^+$) calcd for $\text{C}_{16}\text{H}_{29}\text{N}_2\text{OSi}$ 293.2044, found 293.2037.



1-[(1-Phenylprop-2-en-1-yl)amino]pyridinium iodide *rac*-12n.

Synthesized according to the general procedure outlined for 12a, showing the following properties:

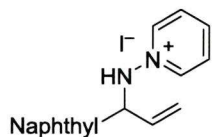
Color and State: Yellow solid; **mp** = 145-147 °C; *Selectivity:* ***rac*-12n/13n** $\geq 19:1$.

^1H NMR (500 MHz, CDCl_3) δ 9.22 (dd, J = 6.7, 1.1 Hz, 2H), 9.05 (d, J = 5.4 Hz, 1H), 8.29 (t, J = 7.8 Hz, 1H), 7.88-7.85 (m, 2H), 7.46-7.42 (m, 2H), 7.34-7.27 (m, 3H), 6.25 (ddd, J = 17.3, 10.2, 7.2 Hz, 1H), 5.34 (d, J = 17.1 Hz, 1H), 5.29 (d, J = 10.3 Hz, 1H), 5.10 (t, J = 6.2 Hz, 1H).

^{13}C NMR (125 MHz, CDCl_3) δ 144.85 (o), 143.90 (o), 136.44 (e), 134.42 (o), 129.31 (o), 129.10 (o), 128.44 (o), 127.91 (o), 120.85 (e), 70.93 (o).

IR (Neat) 3089 (m), 3024 (m), 2931 (w), 2866 (w), 1619 (m), 1478 (m), 1446 (m), 1157 (m), 1013 (m), 943 (vs), 779 (s), 756 (s), 698 (vs), 679 (vs) cm^{-1} .

HRMS (EI, $[\text{M-I}]^+$) calcd for $\text{C}_{14}\text{H}_{15}\text{N}_2$ 211.1235, found 211.1241.



1-([1-(2-Naphthyl)prop-2-en-1-yl]amino)pyridinium iodide *rac*-12o.

Synthesized according to the general procedure outlined for 12a, showing the following properties:

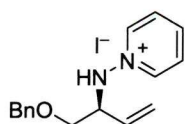
Color and State: Pale yellow solid; **mp** = 103-105 °C; *Selectivity:* ***rac*-12n/13n** $\geq 19:1$.

^1H NMR (500 MHz, CDCl_3) δ 9.23 (d, J = 5.9 Hz, 2H), 8.90 (d, J = 6.1 Hz, 1H), 8.07 (t, J = 7.8 Hz, 1H), 7.92 (s, 1H), 7.80-7.72 (m, 3H), 7.71-7.66 (m, 3H), 7.47-7.40 (m, 2H), 6.27 (ddd, J = 17.5, 10.2, 7.8 Hz, 1H), 5.30-5.27 (m, 1H), 5.27 (d, J = 17.4 Hz, 1H), 5.20 (d, J = 10.3 Hz, 1H).

^{13}C NMR (125 MHz, CDCl_3) δ 144.52 (o), 143.69 (o), 134.36 (o), 133.86 (e), 133.23 (e), 133.10 (e), 129.04 (o), 128.30 (o), 128.04 (o), 127.77 (o), 126.81 (o), 126.64 (o), 125.71 (o), 121.05 (e), 70.88 (o).

IR (Neat) 3051 (m), 2958 (m), 1720 (w), 1684 (w), 1625 (m), 1477 (m), 1450 (m), 1265 (s), 1117 (m), 997 (m), 939 (m), 897 (m), 862 (m), 823 (m), 730 (vs), 700 (s) cm^{-1} .

HRMS (EI, $[\text{M-I}]^+$) calcd for $\text{C}_{18}\text{H}_{17}\text{N}_2$ 261.1392, found 261.1391.

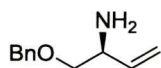


1-([(S)-1-(Benzyloxy)but-3-en-2-yl]amino)pyridinium iodide (*S*)-12j.

Color and State: Yellow oil; *Selectivity:* (***S*-12j/13j**) $\geq 19:1$; *Chiral HPLC analysis* (Daicel AD-H column) *cee* $\geq 98\%$;

$[\alpha]_{\text{D}}^{20}$ -1.5 (c = 1.16, CHCl_3).

^1H NMR (500 MHz, CDCl_3) δ 9.23 (d, J = 6.5 Hz, 2H), 8.79 (d, J = 6.1 Hz, 1H), 8.27 (dt, J = 7.8, 1.1 Hz, 1H), 7.90-7.88 (m, 2H), 7.34-7.25 (m, 5H), 5.99-5.90 (m, 1H), 5.26-5.22 (m, 2H), 4.53 (d, A of AB, J_{AB} = 12.1 Hz, 1H), 4.50 (d, B of AB, J_{AB} = 11.9 Hz, 1H), 4.30-4.22 (m, 1H), 3.92 (dd, A of ABX, J_{AB} = 10.3, J_{BX} = 7.5 Hz, 1H), 3.77 (dd, B of ABX, J_{AB} = 10.3, J_{BX} = 4.0 Hz, 1H).



(2S)-1-(Benzyloxy)but-3-en-2-amine (S)-23j.

A solution of samarium diiodide (5.22 mL, 2.6 mmol, 0.5M in THF) was added to the aminopyridinium salt (S)-12j (55.1 mg, 0.22 mmol) at room temperature under an atmosphere of argon. The dark blue-green solution was allowed to stir at room temperature for *ca.* 16 hours (t.l.c. control). The mixture was then pre-absorbed onto silica gel and purified by flash chromatography (eluting with ethyl acetate) to afford (S)-4 (34.1 mg, 88%) as a yellow oil:

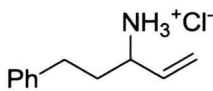
$[\alpha]_{\text{D}}^{20} -11.3$ ($c = 1.10$, CHCl_3), lit.¹⁸ $[\alpha]_{\text{D}} -16.5$ ($c = 1.2$, CHCl_3);

¹H NMR (500 MHz, CDCl_3) δ 7.36-7.31 (m, 4H), 7.30-7.25 (m, 1H), 5.82 (ddd, $J = 17.3, 10.5, 6.2$ Hz, 1H), 5.24 (dt, $J = 17.3, 1.4$ Hz, 1H), 5.11 (dt, $J = 10.5, 1.3$ Hz, 1H), 4.54 (s, 2H), 3.64-3.59 (m, 1H), 3.50 (dd, A of ABX, $J_{\text{AB}} = 9.1, J_{\text{AX}} = 4.1$ Hz, 1H), 3.30 (dd, B of ABX, $J_{\text{AB}} = 9.1, J_{\text{BX}} = 8.0$ Hz, 1H), 1.72 (bs, 2H);

¹³C NMR (125 MHz, CDCl_3) δ 139.09 (o), 138.23 (e), 128.47 (o), 127.76 (o), 127.74 (o), 115.36 (e), 75.02 (e), 73.31 (e), 53.91 (o);

IR (Neat) 3376 (w), 3063 (w), 3030 (w), 2982 (w), 2855 (m), 1643 (w), 1587 (m), 1454 (m), 1364 (m), 1205 (w), 1092 (vs), 1077 (vs), 993 (s), 919 (s), 860 (s), 736 (vs), 698 (vs) cm^{-1} ;

HRMS (EI, $[\text{M}+\text{H}]^+$) calcd for $\text{C}_{11}\text{H}_{16}\text{NO}$ 178.1232, found 178.1226.



5-Phenylpent-1-en-3-amine hydrochloride *rac*-25.

Trimethyl phosphite (24.0 μL , 0.20 mmol) was added to a red suspension of Wilkinson's catalyst (45.7 mg, 0.05 mmol) in anhydrous THF (2.0 mL), and the mixture was stirred under an atmosphere of argon at room temperature for *ca.* 15 minutes resulting in a light yellow homogeneous solution. In a separate flask, anhydrous acetonitrile (3.0 mL) was added to potassium carbonate (7.6 mg, 0.06 mmol) and 1-aminopyridinium iodide (133.2 mg, 0.60 mmol) under an atmosphere of argon. The anion was allowed to form for 30 minutes at 30 °C to afford a pale purple heterogeneous solution. The catalyst solution was then added *via* Teflon[®] cannula to the anion followed by the addition of the allylic carbonate *rac*-11a (110.4 mg, 0.50 mmol) *via* a tared 500 μL gas-tight syringe and allowed to stir at 30 °C for *ca.* 18 hours (t.l.c. control). Activated zinc dust (328 mg, 5.0 mmol) and ammonium chloride (265 mg, 5.0 mmol) were added *via* a tared vial and the reaction mixture stirred for *ca.* 15 minutes, before an additional amount of activated zinc dust

(304 mg, 4.7 mmol) was added. The flask was then warmed to 40 °C and stirred for 2 hours (t.l.c. control). The reaction mixture was filtered through a pad of celite and washed with dichloromethane before being concentrated *in vacuo* to half its volume. The reaction mixture was then partitioned between 1M sodium carbonate and chloroform. The combined organic layers were dried (Na₂SO₄), filtered, and concentrated *in vacuo* to afford a crude oil. The mixture was preabsorbed onto silica gel and purified by flash chromatography (eluting with 6.5% acetone/hexanes). The product was then decolorized with charcoal and filtered through a pad of celite washing with dichloromethane. Hydrochloride gas (freshly made by dropping sulfuric acid onto calcium(II) chloride) was then bubbled through the filtered solution until a white precipitate formed. The mixture was then filtered to obtain **rac-23** (73.3 mg, 74%) as an off-white solid:

Color and State: white solid **mp** = 184-185 °C;

¹H NMR (500 MHz, CDCl₃) δ 8.59 (bs, 3H), 7.29-7.22 (m, 3H), 7.21-7.15 (m, 2H), 5.89 (ddd, *J* = 17.2, 10.3, 8.0 Hz, 1H), 5.44 (d, *J* = 17.2 Hz, 1H), 5.33 (d, *J* = 10.5 Hz, 1H), 3.74-3.65 (m, 1H), 2.78-2.62 (m, 2H), 2.28-2.17 (m, 1H), 2.11-2.01 (m, 1H);

¹³C NMR (125 MHz, CDCl₃) δ 140.05 (e), 133.28 (o), 128.71 (o), 128.59 (o), 126.45 (o), 121.44 (e), 54.21 (o), 34.82 (e), 31.50 (e);

IR (Neat) 3003 (m), 2888 (s), 2724 (m), 1649 (w), 1602 (m), 1512 (s), 1454 (m), 1429 (m), 1368 (w), 1049 (w), 988 (m), 937 (m), 765 (m), 746 (m), 700 (vs) cm⁻¹;

HRMS (EI, [M-Cl]⁺) calcd for C₁₁H₁₆N 162.1283, found 162.1284.

2.3 References

- For general reviews on allylic amination:
 - Johannsen, M.; Jørgensen, K. A. *Chem. Rev.* **1998**, *98*, 1689.
 - Jørgensen, K. A. *Modern Amination Methods*; Ricci, A., Ed.; Wiley-VCH: Weinheim, Germany, 2000; Chapter 1, pp 1-35.
- For recent reviews on transition-metal catalyzed allylic substitution reactions, see:
 - Trost, B. M.; Crawley, M. L. *Chem. Rev.* **2003**, *103*, 2921.
 - Miyabe, H.; Takemoto, Y. *Synlett* **2005**, *11*, 1641.

- (c) Leahy, D. K.; Evans, P. A. *In Modern Rhodium-Catalyzed Organic Reactions*; Evans, P. A., Ed.; Wiley-VCH: Weinheim, Germany, 2005; Chapter 10, pp 191-214
- (d) Lu, Z.; Ma, S. *Angew. Chem. Int. Ed.* **2008**, *47*, 258.
- (e) Helmchen, G.; Dahnz, A.; Dübon, P.; Schelwies, M.; Weihofen, M. *Chem. Commun.* **207**, 675.
3. Tsuji, J.; Minami, I.; Shimizu, I. *Tetrahedron Lett.* **1984**, *25*, 5157.
 4. Evans, P. A.; Nelson, J. D. *Tetrahedron Lett.* **1998**, *39*, 1725.
 5. Evans, P. A.; Nelson, J. D. *J. Am. Chem. Soc.* **1998**, *120*, 5581.
 6. For leading examples of *intermolecular* enantioselective metal-catalyzed allylic amination reactions with various nitrogen pronucleophiles, see:
 - (a) Hayashi, T.; Kishi, K.; Yamamoto, A.; Ito, Y. *Tetrahedron Lett.* **1990**, *31*, 1743.
 - (b) You, S.-L.; Zhu, X.-Z.; Luo, Y.-M.; Hou, X.-L.; Dai, L.-X. *J. Am. Chem. Soc.* **2001**, *123*, 7471.
 - (c) Ohmura, T.; Hartwig, J. F. *J. Am. Chem. Soc.* **2002**, *124*, 13164.
 - (d) Lipowsky, G.; Helmchen, D. *Chem. Commun.* **2004**, 116.
 - (e) Tissot-Croset, K.; Polet, D.; Alexakis, A. *Angew. Chem. Int. Ed.* **2004**, *43*, 2426.
 - (f) Miyabe, H.; Matsumura, A.; Moriyama, K.; Takemoto, Y. *Org. Lett.* **2004**, *6*, 4631.
 - (g) Yamashita, Y.; Gopalarathnam, A.; Hartwig, J. F. *J. Am. Chem. Soc.* **2007**, *129*, 7508.
 - (h) Miyabe, K.; Yoshida, K.; Reddy, V. K.; Takemoto, Y. *J. Org. Chem.* **2009**, *74*, 305 and pertinent references cited therein.
 7. Evans, P. A.; Clizbe, E. A. *J. Am. Chem. Soc.* **2009**, *131*, 8722.
 8. (a) *Nitrogen, Oxygen and Sulfur Ylide Chemistry: A Practical Approach to Chemistry*; Clark, J. S., Ed.; Oxford Univ. Press: Oxford, 2002.
 - (b) *Phosphorus Ylides; Chemistry and Application in Organic Synthesis*; Kolodiazhnyi, O. I.; Wiley-VCH: Weinheim, 1999.
 9. For discussion of the stability of various ylides, see:
 - (a) Naito, T.; Nagase, S.; Yamataka, J. *J. Am. Chem. Soc.* **1994**, *116*, 10080.
 - (b) Cheng, J.-P.; Liu, B.; Zhao, Y.; Sun, Y.; Zhang, X.-M.; Lu, Y. *J. Org. Chem.* **1999**, *64*, 604.

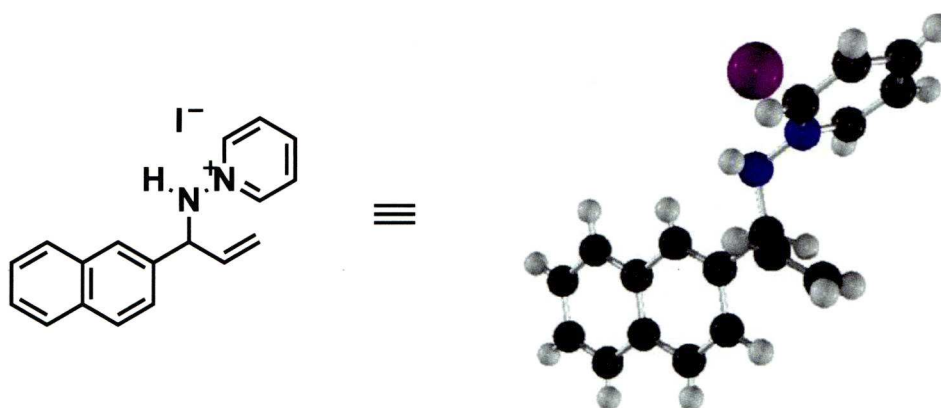
- (c) Aggarwal, V. K.; Harvery, J. N.; Robiette, R. *Angew. Chem. Int. Ed.* **2005**, *44*, 5468.
10. For examples of the stereospecific *intermolecular* rhodium-catalyzed allylic amination reactions, see:
- (a) Evans, P. A.; Robinson, J. E.; Nelson, J. D. *J. Am. Chem. Soc.* **1999**, *121*, 6761.
- (b) Evans, P. A.; Robinson, J. E. *Org. Lett.* **1999**, *1*, 1929.
- (c) Evans, P. A.; Robinson, J. E.; Moffett, K. K. *Org. Lett.* **2001**, *3*, 3269.
- (d) Evans, P. A.; Lai, K. W.; Zhang, J.-R.; Huffman, J. C. *Chem. Commun.* **2006**, 844.
- (e) Evans, P. A.; Qin, J.; Robinson, J. E.; Bazin, B. *Angew. Chem. Int. Ed.* **2007**, *46*, 7417.
11. For examples of the regioselective allylic amination with hydrazine derivatives, see:
- (a) Matunas, R.; Lai, A. J.; Lee, C. *Tetrahedron* **2005**, *61*, 6298.
- (b) Johns, A. M.; Liu, Z.; Hartwig, J. F. *Angew. Chem. Int. Ed.* **2007**, *46*, 7259.
12. Mellor, J. M.; Smith, N. M. *J. Chem. Soc., Perkin Trans. 1* **1984**, 2927.
13. Denmark, S. E.; Nicaise, O.; Edwards, J. P. *J. Org. Chem.* **1990**, *55*, 6219.
14. (a) C. Ainsworth *J. Am. Chem. Soc.* **1956**, *78*, 1636.
- (b) Alexakis, A.; Lensen, N.; Mangeney, P. *Synlett* **1991**, *9*, 625.
- (c) Nugent, T. C.; Wakchaure, V. N.; Ghosh, A. K.; Mohanty, R. R. *Org. Lett.* **2005**, *7*, 4967.
- (d) Alexakis, A.; Lensen, N.; Tranchier, J.-P.; Mangeney, P.; Feneau-Dupont, J.; Declercq, J. P. *Synthesis*, **1995**, 1038.
15. (a) Lunn, G.; Sanson, E. B.; *J. Org. Chem.* **1984**, *49*, 3470.
- (b) Martínez-Barrasa, V.; Delgado, F.; Burgos, C.; García-Navío, J. L.; Izquierdo, M. L.; Alvarez-Builla, J. *Tetrahedron*, **2000**, *56*, 2481.
- (c) Gowda, S.; Abiraj, K.; Gowda, D. C. *Tet. Lett.* **2002**, *43*, 1329.
- (d) Lin, W.; Zhang, X.; He, Z.; Jin, Y.; Gong, L.; Mi, A. *Synth. Commun.* **2002**, *32*, 3279.
- (e) Prasad, H. S.; Gowda, S.; Abiraj, K.; Gowda, D. C. *Synth. React. Inorg. Met.-Org. Chem.* **2003**, *33*, 717.
- (f) Gowda, S.; Kempe, B. K.; Gowda, D. C. *Synth. React. Inorg. Met.-Org. Chem.* **2003**, *33*, 281.

- (g) Sridhara, M. B.; Srinivasa, G. R.; Gowda, D. C. *Synth. Commun.* **2004**, *34*, 1441.
- (h) Srinivasa, G. R.; Abiraj, K.; Gowda, D. C. *Synth. React. Inorg. Met.-Org.-Chem.* **2004**, *34*, 223.
- (i) Smith, C. R. *Synlett*, **2009**, *9*, 1522.
16. (a) Girard, P.; Namy, J.L.; Hagan, H. B. *J. Am. Chem. Soc.* **1980**, *102*, 2693.
- (b) Hasegawa, E.; Curran, D. P. *J. Org. Chem.* **1993**, *58*, 5008.
- (c) Shabangi, M.; Flowers, R. A., II *Tetrahedron. Lett.* **1997**, *38*, 1137
- (d) Shabangi, M.; Sealy, J. M.; Fuchs, J. R.; Flowers, R. A., II *Tetrahedron Lett.* **1998**, *39*, 4429.
- (e) Kuhlman, M. L.; Flowers, R. A., II *Tetrahedron Lett.* **2000**, *41*, 8049.
- (f) Ogawa, C.; Sugiura, M.; Kobayashi, S. *J. Org. Chem.* **2002**, *67*, 5359.
- (g) Banik, B. K.; *Eur. J. Org. Chem.* **2002**, 2431.
- (h) Kim, M.; Knettle, B. W.; Dahlén, A.; Hilmeson, G.; Flowers, R. A., II *Tetrahedron* **2003**, *59*, 10397
- (i) Chopade, P. R.; Davis, T. A.; Prasad, E.; Flowers, R. A., II *Org. Lett.* **2004**, *6*, 2685.
- (j) Suri, J. T.; Steiner, D. D.; Barbas, C. F., III *Org. Lett.* **2005**, *7*, 3885
- (k) Friestad, G. K.; Korapala, C. S.; Ding, H. *J. Org. Chem.* **2006**, *71*, 281.
17. For preparation of Wilkinson's catalyst see:
- (a) Osborn, J. A.; Jardine, F. H.; Young, J. F.; Wilkinson, G. *J. Chem. Soc. A* **1966**, 1711
- (b) Griffith, W. P.; Swars, K.; Eds. *Gmelin Handbook of Coordination Compounds, Rhodium Supplement*; Springer-Verlag: Berlin, **1984**
18. Rama Rao, A. V.; Bose, D. S.; Gurjar, M. K.; Ravindranathan, T. *Tetrahedron* **1989**, *45*, 7031.
19. Vrieze, D. C.; Hoge, G. S; Hoerter, P. Z.; Van Haitsma, J. T.; Samas, B. M. *Org. Lett.* **2009**, *11*, 3140.
20. Bongin, A.; Cardillo, G.; Oregna, M.; Porz, G.; Sandri, S. *J. Org. Chem.* **1982**, *47*, 4626.
21. Trost, B. M.; Tanoury, G. J.; Lautens, M.; Chan, C.; Mac Pherson, D. T. *J. Am. Chem. Soc.* **1994**, *116*, 4255.
22. Hon, Y.-S.; Devulapally, R. *Tetrahedron Lett.* **2009**, *50*, 2831.

23. Kinoshita, N.; Marx, K. H.; Tanaka, K.; Tsubaki, K.; Kawabata, T.; Yoshikai, N.; Nakamura, E.; Fuji, K. *J. Org. Chem.* **2004**, 69, 7960.

Appendix 2.1

Crystal and diffraction data for *rac*-12o



Summary

The sample studied here, MSC05257, was submitted by Elizabeth Clizbe of Professor P. Andrew Evans' research group in the Indiana University Department of Chemistry. Data were collected on a Bruker Platform goniometer equipped with a Bruker SMART 6000 CCD area detector. Seven 180-degree omega frame runs were measured, and reflections out to a maximum of 60 degrees in 2θ were harvested. Centrosymmetric space group $P2_1/c$ was selected based on metric symmetry and systematic absences, and this group was confirmed by successful structure solution and refinement.

Data collection, structure solution, and refinement of this structure all proved challenging, and all members of the IUMSC scientific staff worked on aspects of the

problem. All of the several crystals examined were twinned to a greater or lesser degree, and the atomic arrangement additionally causes the diffraction pattern to prominently exhibit a subcell of the true unit cell. The combination of twinning and pseudosymmetry also make the data unusually permissive of incorrect (but somewhat reasonable) chemical models, and several such were rejected before the correct model was found.

The structure contains one unique pair of $C_{18}H_{17}N_2^+$ and I^- ions. A final difference Fourier map was clean, with a maximum intensity of $1.131\ e^-/\text{\AA}^3$ near the iodine atom.

TABLE 1. Crystal and diffraction data for *rac*-12o

Crystal Information

<i>Chemical formula</i>	$C_{18}H_{17}IN_2$
<i>Formula weight</i>	388.24 Da
<i>Crystal description</i> colorless plate,	$0.15 \times 0.15 \times 0.04\text{ mm}$
<i>Temperature</i>	128(2) K
<i>Symmetry</i> Monoclinic,	$P2_1/c$
<i>Unit cell (from 912 reflections, $3.803 \leq \theta \leq 33.702^\circ$)</i>	
<i>a</i> 17.287(5) Å α 90.00°	
<i>b</i> 8.552(2) Å β 91.16(7)°	
<i>c</i> 11.053(3) Å γ 90.00°	
<i>Cell volume</i>	1633.7(8) Å ³
<i>Z</i> 4	
<i>Density (calc.)</i>	1.578 g/cm ³
<i>Linear Absorption Coefficient</i>	1.955 mm ⁻¹
<i>F(000)</i> 768	

Data Collection

<i>Diffractometer</i> Bruker Platform goniometer w/ SMART 6000	
<i>Radiation</i> Mo K α ,	0.71073 Å
<i>Reflections collected</i>	48095
<i>Data range</i>	$3.80 \leq \theta \leq 30.00^\circ$
<i>Index ranges</i> $-24 \leq h \leq 24$; $-12 \leq k \leq 12$; $-15 \leq \ell \leq 15$	
<i>Independent reflections</i>	4751 ($R_{\text{int}} = 0.0831$)
<i>Observed Reflections</i>	$(I > 2\sigma(I))$ 2873

Solution and Refinement

<i>Absorption correction type</i> Semi-empirical based on equivalent reflections	
<i>Transmission factors</i> <i>n/a</i>	

Structure solution Direct methods
Refinement method Full-matrix least-squares on F₂
Data / restraints / parameters 4751 / 0 / 259
R(F, observed data)* 0.0405
R_w(F₂, all refinement data)† 0.0755
Goodness of fit (F₂, all refinement data)‡ 0.958
Maximum Δ/σ, final cycle 0.002
Largest difference peak and hole 1.131 and −1.300 e[−]/Å³

* $R(F) = \Sigma(|F_o| - |F_c|) / \Sigma|F_o|$
† $R_w(F_2) = \{\Sigma[w(F_{o2} - F_{c2})^2] / \Sigma[w(F_{o2})^2]\}^{1/2}$
‡ Goodness of fit = $\{\Sigma[w(F_{o2} - F_{c2})^2] / (N_{obs} - N_{param})\}^{1/2}$

TABLE 2. ATOMIC COORDINATES (×104) AND EQUIVALENT ISOTROPIC DISPLACEMENT PARAMETERS (×103)*

Atom	x	y	z	U _{eq}
C(1)	8982(3)	4201(6)	5589(4)	28(1)
C(2)	9423(3)	4690(6)	6560(5)	33(1)
C(3)	9081(3)	5360(5)	7596(4)	28(1)
C(4)	9512(3)	5873(6)	8617(5)	35(1)
C(5)	9161(3)	6482(6)	9601(5)	38(1)
C(6)	8351(3)	6600(6)	9623(5)	33(1)
C(7)	7906(3)	6123(5)	8639(4)	26(1)
C(8)	8266(3)	5505(5)	7606(4)	24(1)
C(9)	7823(3)	4980(5)	6574(4)	24(1)
C(10)	8164(2)	4355(5)	5589(4)	24(1)
C(11)	7712(3)	3760(5)	484(4)	27(1)
C(12)	7920(3)	4629(6)	3352(4)	30(1)
C(13)	8268(4)	3996(7)	2427(5)	38(1)
N(14)	6878(2)	3805(5)	4752(4)	21(1)
N(15)	6438(2)	3140(5)	3784(4)	20(1)
C(16)	6139(3)	4032(6)	2873(5)	22(1)
C(17)	5715(3)	3334(7)	1969(5)	26(1)
C(18)	5613(3)	1727(7)	1961(5)	23(1)
C(19)	5926(3)	846(6)	2904(5)	23(1)
C(20)	6326(3)	1580(5)	3824(5)	22(1)
I(21)	5999(1)	7465(1)	447(1)	22(1)

TABLE 3. BOND LENGTHS (Å) AND ANGLES (°)

C(1)—C(2)	1.369(7)	C(1)—C(10)	1.421(6)
C(2)—C(3)	1.420(7)	C(3)—C(4)	1.410(7)
C(3)—C(8)	1.413(6)	C(4)—C(5)	1.360(8)
C(5)—C(6)	1.405(7)	C(6)—C(7)	1.381(7)
C(7)—C(8)	1.414(7)	C(8)—C(9)	1.433(6)
C(9)—C(10)	1.358(6)	C(10)—C(11)	1.524(6)
C(11)—N(14)	1.478(6)	C(11)—C(12)	1.505(7)
C(12)—C(13)	1.313(7)	N(14)—N(15)	1.419(6)

N(15)—C(20)	1.349(5)	N(15)—C(16)	1.357(6)
C(16)—C(17)	1.365(8)	C(17)—C(18)	1.385(6)
C(18)—C(19)	1.387(7)	C(19)—C(20)	1.369(7)
C(1)—H(1)	1.02(5)	C(2)—H(2)	0.86(4)
C(4)—H(4)	0.87(5)	C(5)—H(5)	0.96(5)
C(6)—H(6)	0.99(5)	C(7)—H(7)	0.98(5)
C(9)—H(9)	0.82(5)	C(11)—H(11)	1.05(5)
C(12)—H(12)	1.05(7)	C(13)—H(13A)	0.85(6)
C(13)—H(13B)	0.98(6)	N(14)—H(14)	0.64(4)
C(16)—H(16)	0.85(5)	C(17)—H(17)	0.85(4)
C(18)—H(18)	0.91(5)	C(19)—H(19)	0.92(4)
C(20)—H(20)	0.94(4)		
C(2)—C(1)—C(10)	120.7(4)	C(1)—C(2)—C(3)	121.4(4)
C(4)—C(3)—C(2)	23.2(4)	C(4)—C(3)—C(8)	118.5(5)
C(2)—C(3)—C(8)	118.3(4)	C(5)—C(4)—C(3)	121.5(5)
C(4)—C(5)—C(6)	120.1(5)	C(7)—C(6)—C(5)	120.3(5)
C(6)—C(7)—C(8)	120.0(5)	C(7)—C(8)—C(3)	119.6(4)
C(7)—C(8)—C(9)	121.5(4)	C(3)—C(8)—C(9)	118.8(4)
C(10)—C(9)—C(8)	121.9(4)	C(9)—C(10)—C(1)	118.9(4)
C(9)—C(10)—C(11)	123.4(4)	C(1)—C(10)—C(11)	117.6(4)
N(14)—C(11)—C(12)	113.9(4)	N(14)—C(11)—C(10)	108.5(4)
C(12)—C(11)—C(10)	111.9(4)	C(13)—C(12)—C(11)	124.4(5)
N(15)—N(14)—C(11)	110.4(4)	C(20)—N(15)—C(16)	121.8(5)
C(20)—N(15)—N(14)	116.6(4)	C(16)—N(15)—N(14)	121.6(4)
N(15)—C(16)—C(17)	119.2(5)	C(16)—C(17)—C(18)	120.4(6)
C(19)—C(18)—C(17)	119.1(6)	C(20)—C(19)—C(18)	119.5(5)
N(15)—C(20)—C(19)	120.0(5)		
C(2)—C(1)—H(1)	119(2)	C(10)—C(1)—H(1)	120(2)
C(1)—C(2)—H(2)	123(3)	C(3)—C(2)—H(2)	115(3)
C(5)—C(4)—H(4)	117(3)	C(3)—C(4)—H(4)	121(3)
C(4)—C(5)—H(5)	121(3)	C(6)—C(5)—H(5)	118(3)
C(7)—C(6)—H(6)	120(3)	C(5)—C(6)—H(6)	120(3)
C(6)—C(7)—H(7)	119(3)	C(8)—C(7)—H(7)	121(3)
C(10)—C(9)—H(9)	124(3)	C(8)—C(9)—H(9)	114(3)
N(14)—C(11)—H(11)	112(2)	C(12)—C(11)—H(11)	106(2)
C(10)—C(11)—H(11)	105(2)	C(13)—C(12)—H(12)	116(4)
C(11)—C(12)—H(12)	119(4)	C(12)—C(13)—H(13A)	115(4)
C(12)—C(13)—H(13B)	118(4)	H(13A)—C(13)—H(13B)	128(5)
N(15)—N(14)—H(14)	106(4)	C(11)—N(14)—H(14)	109(4)
N(15)—C(16)—H(16)	118(3)	C(17)—C(16)—H(16)	123(3)
C(16)—C(17)—H(17)	119(3)	C(18)—C(17)—H(17)	121(3)
C(19)—C(18)—H(18)	122(3)	C(17)—C(18)—H(18)	119(3)
C(20)—C(19)—H(19)	116(3)	C(18)—C(19)—H(19)	124(3)
N(15)—C(20)—H(20)	115(3)	C(19)—C(20)—H(20)	125(3)

TABLE 4. ANISOTROPIC THERMAL PARAMETERS ($\times 103$)*

<i>Atom</i>	U_{11}	U_{22}	U_{33}	U_{23}	U_{13}	U_{12}
C(1)	24(2)	32(2)	29(3)	7(2)	7(2)	1(2)
C(2)	18(2)	37(3)	45(3)	12(2)	6(2)	-1(2)
C(3)	23(2)	24(2)	37(3)	7(2)	-2(2)	0(2)
C(4)	25(3)	33(3)	47(3)	4(2)	-10(2)	-3(2)
C(5)	44(4)	27(2)	43(3)	-2(2)	-16(3)	-5(2)
C(6)	39(3)	20(2)	40(3)	-2(2)	-5(2)	-2(2)
C(7)	26(3)	18(2)	34(3)	-1(2)	-1(2)	0(2)
C(8)	26(2)	14(2)	31(2)	5(2)	0(2)	2(2)
C(9)	16(2)	20(2)	35(3)	9(2)	1(2)	3(2)
C(10)	23(2)	21(2)	27(2)	5(2)	4(2)	-1(2)
C(11)	22(2)	25(2)	34(3)	4(2)	4(2)	1(2)
C(12)	36(3)	23(2)	31(3)	0(2)	4(2)	-2(2)
C(13)	49(3)	32(3)	35(3)	-3(2)	12(2)	-8(3)
N(14)	23(2)	16(2)	25(2)	-5(2)	1(2)	4(2)
N(15)	21(2)	20(2)	20(2)	-1(2)	2(2)	7(2)
C(16)	20(3)	20(2)	28(3)	1(2)	7(2)	1(2)
C(17)	23(3)	28(3)	27(3)	7(2)	8(2)	7(2)
C(18)	21(3)	24(3)	24(3)	-2(2)	3(2)	3(2)
C(19)	20(2)	22(3)	28(3)	-1(2)	6(2)	2(2)
C(20)	24(3)	13(2)	28(3)	3(2)	9(2)	5(2)
I(21)	27(1)	16(1)	23(1)	0(1)	2(1)	-4(1)

TABLE 5. HYDROGEN ATOM COORDINATES ($\times 103$) AND ISOTROPIC DISPLACEMENT PARAMETERS ($\times 103$)

<i>Atom</i>	<i>x</i>	<i>y</i>	<i>z</i>	U_{eq}
H(1)	925(3)	374(5)	485(4)	23(12)
H(2)	992(3)	462(5)	659(3)	6(10)
H(4)	1002(3)	588(6)	861(4)	29(14)
H(5)	945(3)	674(5)	1033(4)	29(13)
H(6)	810(3)	704(6)	1034(4)	35(14)
H(7)	735(3)	626(6)	865(4)	30(13)
H(9)	736(3)	513(5)	663(4)	15(11)
H(11)	791(2)	260(6)	436(3)	25(11)
H(12)	775(4)	580(8)	325(6)	80(20)
H(13A)	835(4)	302(7)	250(5)	60(20)
H(13B)	837(4)	466(7)	173(5)	55(18)
H(14)	677(3)	451(5)	479(4)	10(13)
H(16)	626(3)	499(6)	286(4)	31(14)
H(17)	554(3)	389(5)	139(4)	14(12)
H(18)	530(3)	130(6)	138(4)	29(15)
H(19)	590(2)	-22(5)	295(4)	10(10)
H(20)	656(3)	107(5)	449(4)	13(11)

Chapter 3

Regio- and Enantioselective Iridium-Catalyzed Allylic Amination

3.1 Introduction

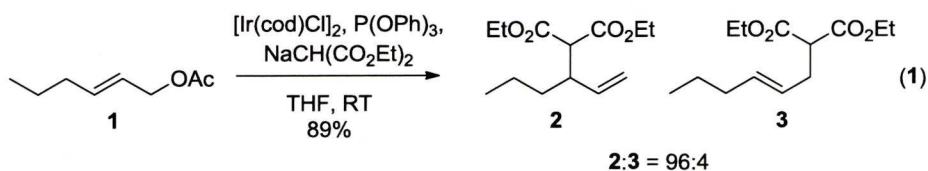
As outlined in Chapters 1 and 2, the transition metal-catalyzed allylic amination reaction is an important method for the preparation of enantiomerically enriched allylic amines. The iridium-catalyzed allylic substitution reaction provides a complementary approach for this type of reaction since achiral substrates are readily converted to the enantiomerically enriched amines.¹ This approach is efficient at low catalyst loadings and has provided a convenient method for the construction of an array of allylic fragments using various pronucleophiles in an intra- and intermolecular fashion. Nevertheless, a significant limitation with the iridium-catalyzed allylic substitution reaction is that it is generally limited to electronically biased substrates, where electron poor aryl groups and alkyl derivatives afford lower yields and regioselectivities. Since the recent accomplishments in the iridium-catalyzed allylic amination reaction were previously outlined, the preliminary development of the iridium-catalyzed allylic substitution reaction will be described.

3.2 Origin of Stereoselectivity

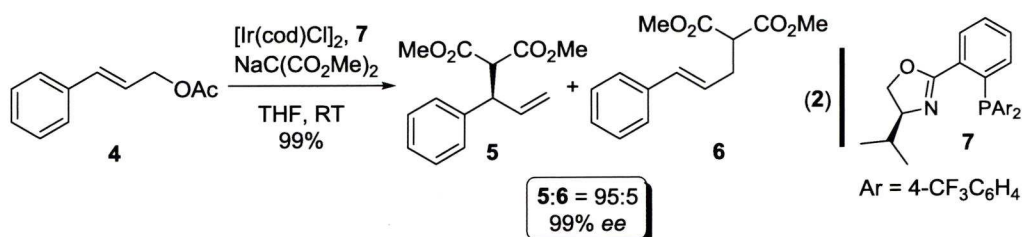
3.2.1 Regioselectivity and Memory Effect

Iridium complexes are frequently used as models for intermediates in catalytic reactions due to their low reactivity. Although these complexes have been well established for the hydrogenation of alkenes,² it was not until 1997 that an iridium complex was utilized in the allylic substitution reaction. Takeuchi and Kashio

reported a regioselective iridium-catalyzed allylic substitution of alkyl and aryl allylic alcohol derivatives with the sodium salt of diethyl malonate (eq. 1).³ A ligand study demonstrated that phosphorus ligands significantly improve the regioselectivity of the reaction with triphenyl phosphite being optimal, affording the branched products in high yield and with excellent regioselectivity (*b/l* up to 99:1). For example, treatment of (*E*)-2-hexenyl acetate **1** with sodium diethyl malonate in the presence of [Ir(cod)Cl]₂ and P(OPh)₃ afforded the substituted products **2** and **3** in 89% yield and with excellent regioselectivity (*b/l* = 96:4). This methodology demonstrates that similar to rhodium, the iridium-catalyzed allylic substitution reaction is highly regioselective for branched substrates.

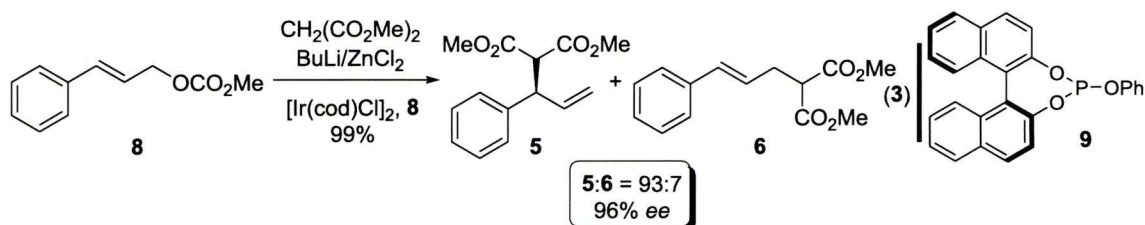


In the same year, Helmchen and Jenssen reported the first enantioselective allylic alkylation using phosphinooxazoline (PHOX) ligands (eq 2).⁴ Treatment of cinnamyl allylic acetate **4** with sodium dimethyl malonate under the optimized reaction conditions afforded the alkylated product **5** in 99% yield, with excellent regioselectivity (*b/l* = 95:5) and enantiomeric excess (91% *ee*). The high selectivity was transcribed to the substituent on the electrophile preferentially sitting away from the aryl of the phosphinooxazoline ligand in the intermediate complex. The regioselectivity can also be explained by the preferential attack of the nucleophile at the terminus of the π -allyl system which is *trans* to the phosphorus.



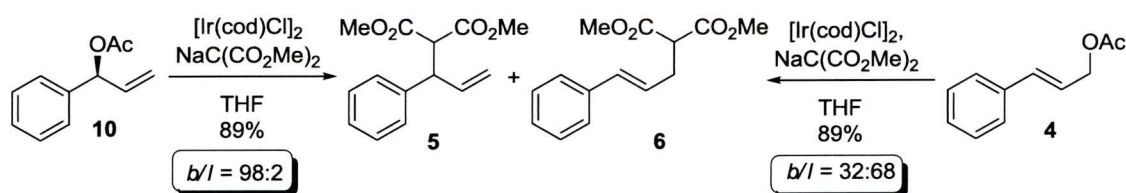
Further investigation revealed that strong π -acceptor monodentate phosphoramidite⁵ and chiral phosphite ligands⁶ provide higher levels of selectivity than the phosphinooxazoline ligands. For example, the reaction of methyl cinnamyl

carbonate **8** with the zinc anion of dimethyl malonate in the presence of the iridium complex of chiral phosphite **9**, afforded alkylation products **5** and **6** in 99% yield, with excellent regio- (*b/l* = 93:7) and enantioselectivity (96% *ee*) (eq. 3).



Additional studies demonstrated that the level of regioselectivity was dependent on the nature of the starting material. For example, when branched allylic acetate **10** (scheme 3.1) was treated with sodium dimethyl malonate under the optimized conditions, the substitution products were isolated in 89% yield and with high regioselectivity favouring the branched substrate (*b/l* = 98:2).^{5,9} However, when the corresponding linear acetate **4** was subjected to identical conditions, the reaction proceeded with a partial reversal of regioselectivity (*b/l* = 32:68), favouring the linear product **6**. These results suggest that, like rhodium, the iridium-catalyzed allylic substitution reaction has a “memory effect” and does not proceed through a π -allyl complex, but rather through a σ -allyl or an *enyl* intermediate.⁹

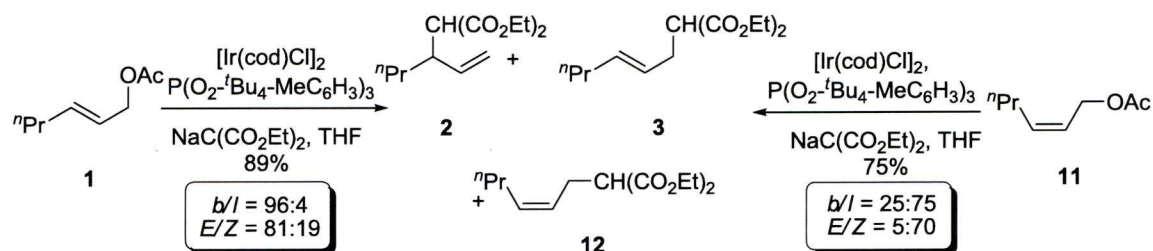
Scheme 3.1 “Memory effect” in the iridium-catalyzed allylic substitution



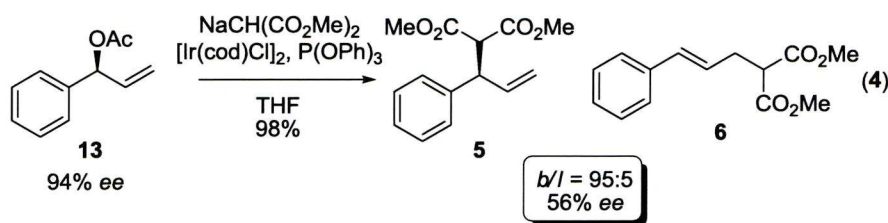
Further studies have demonstrated that the olefin geometry of the starting material also has a significant impact on the regiochemical outcome.⁶ For instance, when the *E*-allylic alcohol derivative is utilized, branched substrates are obtained with high selectivity. However, when the corresponding *Z*-isomer is utilized, the linear substrates are favoured and the olefin geometry is retained (Scheme 3.2). For example, treatment of *E*-allylic acetate **1** with sodium diethyl malonate under

optimized conditions furnished the alkylation products **2**, **3** and **12** in 89% overall yield and with excellent regioselectivity ($b/l = 96:4$). The linear substrates **3** and **12** were isolated with an E/Z ratio of 81:19. On the other hand, when the Z -allylic acetate **11** was employed, the products **2**, **3** and **12** were isolated in 75% overall yield and with a high regioselectivity favouring the linear substrates **3** and **12** ($b/l = 25:75$). The linear substrates **3** and **12** were obtained with high retention of the Z -confirmation ($E/Z = 5:70$). This retention of olefin geometry is attributed to the slow σ - π - σ isomerization of the metal-allyl intermediate.

Scheme 3.2 Effects of olefin geometry in the iridium-catalyzed allylic substitution reaction.



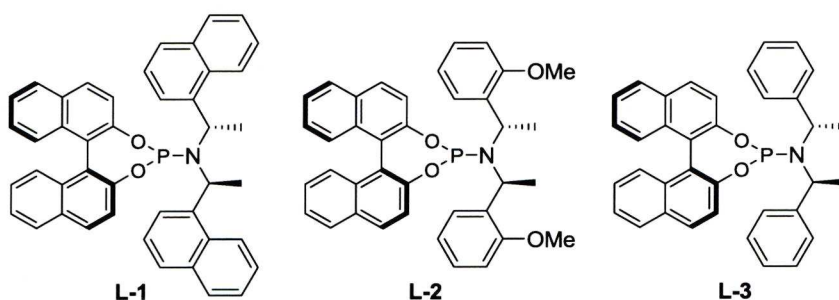
Studies by Helmchen demonstrated that the utilization of an enantiomerically enriched acetate in the iridium-catalyzed allylic substitution reaction, using an achiral ligand, furnished products with partial retention of stereochemistry (eq. 4).^{5,9} For example, allylic substitution of the chiral nonracemic allylic acetate **13** (94% ee) furnished the branched product **5** with 56% enantiomeric excess.⁷ However, regioselectivities of $\geq 99:1$ and enantioselectivity of up to 86% could be obtained using a chiral phosphoramidite ligand in conjunction with a racemic carbonate. Branched starting materials were crucial for obtaining high levels of enantioselectivity, since linear substrates afforded significantly lower yields and selectivity.



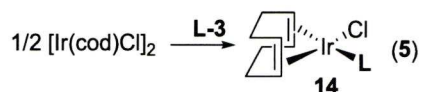
3.2.2 Enantioselectivity

Phosphoramidite ligands (Figure 3.1) have become the ligand of choice for the iridium-catalyzed allylic substitution reaction.⁹ They are attractive ligands since they are modular, making them easy to modify, and new variants have proven highly efficient in affording products with high levels of regio- and enantioselectivity.¹⁰

Figure 3.1 Commonly used phosphoramidite ligands.

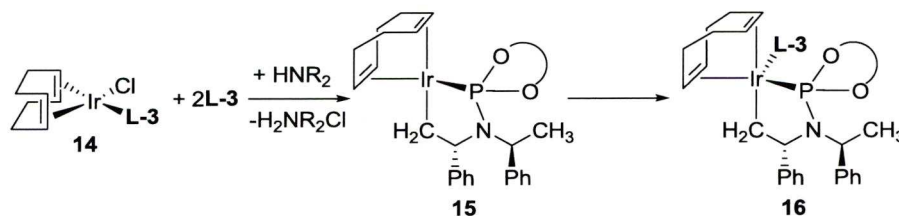


A great deal of effort has gone into studying the mechanism and kinetics of the iridium-catalyzed allylic substitution reaction.¹¹ Helmchen reported the formation of a square-planar complex when $[\text{Ir}(\text{cod})\text{Cl}]_2$ was treated with phosphinooxazoline **7**.^{11a} Hartwig later reported the corresponding square-planar complex **14** with phosphoramidite ligand **L-3**. When methyl cinnamyl carbonate **8** was treated with benzylamine in the presence of compound **14**, product formation was slow compared to the reaction involving the *in situ* generated catalyst. This suggests that while complex **14** is effective in catalyzing the reaction, it is not involved in the catalytic pathway under optimized reaction conditions.^{11b}



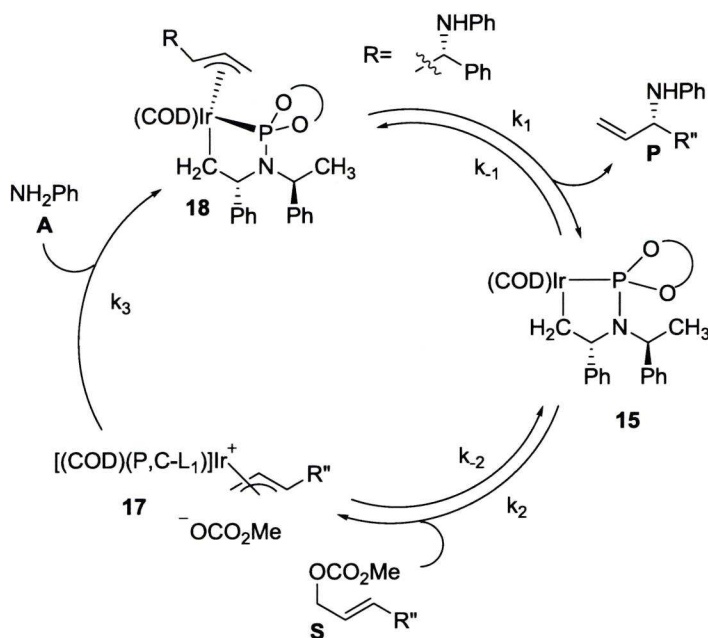
Treatment of the square-planar complex **14** with base at room temperature provided trace amounts of a new iridium complex. The yield of this complex could be dramatically increased when **14** was treated with two equivalents of the phosphoramidite ligand in the presence of base. The new complex was characterized by NMR and X-ray crystallography to provide the trigonal bipyramidal complex **16**, which arises from the cyclometalation of the phosphoramidite ligand at the methyl group, followed by the coordination of a second phosphoramidite ligand (Scheme 3.3). The complex was then examined in an allylic substitution reaction to ascertain its ability to catalyze this type of process. Treatment of methyl cinnamyl carbonate **8** with benzylamine in the presence of **16**, furnished the corresponding branched amine in 81% yield and with 97% enantiomeric excess.

Scheme 3.3 Iridium-phosphoramidite ligand complexes



Hartwig and Marković further examined the kinetics of the iridium-catalyzed allylic amination reaction in order to probe for possible intermediates.^{11d} Many of the assumptions made about the mechanism were based on the palladium-catalyzed process, since so little data had been collected on the iridium-catalyzed version.³¹ ³¹P NMR data was collected on the reactions of methyl cinnamyl carbonate **8** with various amines to identify possible intermediates. These studies concluded that the allylic carbonate adds reversibly to the iridium metalocycle **15** to form the π -allyl intermediate **17** (Scheme 3.4). This is followed by irreversible addition of the amine nucleophile to form allylamine complex **18**, which undergoes reductive elimination to generate the amination product **P**, and reform the iridium metalocycle **15**.

Scheme 3.4 Mechanistic pathway for the enantioselective iridium-catalyzed allylic amination using phosphoramidite ligand **L-3**.



Hartwig also made observations about the coordination of the allyl fragment to the iridium complex in order to gain insight into the origin of enantioselectivity.^{11d} The stability of the diastereomeric allylamine complexes can be related to the enantioselectivity obtained in the reaction. The Hammond postulate implies that the relative stability of the iridium-allylamine complexes should relate to the rates of formation of the two enantiomers. These results demonstrate that when the nucleophile is aniline, the allylamine product with (*R*)-configuration binds 70 times weaker than the (*S*)-variant when (*S,S,S*)-**L-3** is utilized. If the binding constants directly correspond to the relative rates of formation, the amine would theoretically be formed with 97% enantiomeric excess. The reaction of methyl cinnamyl carbonate with aniline afforded the (*S*)-amine (*S*)-**P** with 96% enantiomeric excess, which is within experimental error. These studies allowed for the identification of a unique mode of catalyst activation as well as an insight into the origin of the enantioselectivity.

3.3 Iridium-Catalyzed Allylic Amination Reaction Utilizing a Sulfilimine Nucleophile

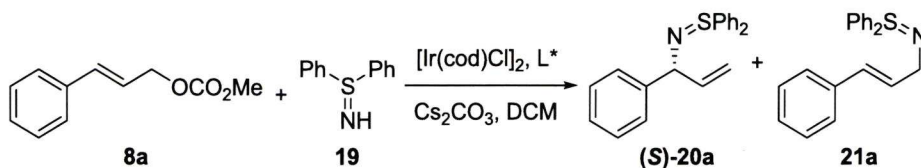
3.3.1 Introduction

Following our success in using 1-aminopyridinium iodide for the rhodium-catalyzed allylic substitution reaction, we sought to examine other nitrogen ylides in this type of reaction. Our aim was to develop an enantioselective variant to complement the stereospecific reaction. It was reasoned that *S,S*-diphenylsulfilimine would be an effective nucleophile since it naturally contains ylide character, and a survey of the literature indicates that the sulfur-nitrogen bond is relatively labile. Hence, the cleavage of the sulfilimine should be relatively straightforward, and afford the requisite amine.

3.3.2 Reaction Optimization

Table 3.1 summarizes the development of the regio- and enantioselective iridium-catalyzed allylic amination reaction using *S,S*-diphenylsulfilimine as the pronucleophile.¹¹ We envisioned that the reaction would proceed in the absence of base as it is reported that the sulfilimine exists with up to 40-60% ylide character.¹³ However, treatment of the methyl cinnamyl carbonate **8a** with *S,S*-diphenylsulfilimine **19** in the absence of base furnished the allylic sulfilimine (*S*)-**20a** in low yield, albeit in $\geq 19:1$ regioselectivity (entry 1). A marginal improvement in yield (27%) was observed with the introduction of a base (entry 2). Gratifyingly, increasing the reaction concentration afforded the branched allylic sulfilimine (*S*)-**20a** in 88% yield with 98% enantiomeric excess (entry 3), albeit with modest regioselectivity (*b/l* = 11:1).

Table 3.1 Optimization of the regio- and enantioselective iridium-catalyzed allylic amination reaction using *S,S*-diphenylsulfilimine.^a



Entry	L*	Cs ₂ CO ₃ (equiv.)	Conc. (M)	Yld (%) ^b	(<i>S</i>)- 20a / 21a ^c	<i>ee</i> (%)
1	L-1	-	0.1	18	≥ 19:1	93
2	“	1.1	“	27	16:1	> 99
3	“	“	0.33	88	11:1	98
4	L-2	“	“	57	5:1	95
5	L-3	“	“	10	2:1	98
6 ^e	L-1	“	“	87	≥19:1	> 99
7 ^e	“	0.25	“	87	≥19:1	97
8	“	-	“	79	≥19:1	96

^aAll reactions were carried out on a 0.25 mmol reaction scale using 2 mol% [Ir(cod)Cl]₂, 4 mol% **L-1**, 0.25 equiv. Cs₂CO₃, and 1.1 equiv. of *S,S*-diphenylsulfilimine in DCM at 35 °C. Isolated yields.

^cRegioselectivity was determined by 500 MHz ¹H NMR on the crude reaction mixtures.

^dEnantioselectivity was determined by chiral HPLC analysis on the corresponding trifluoroacetamide. ^eCesium carbonate was dried under vacuum at 80 °C overnight.

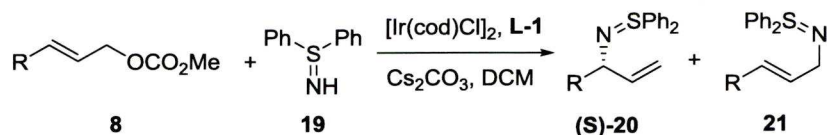
Further optimization focused on varying the phosphoramidite ligand. Interestingly when **L-2** or **L-3** were employed, the reaction did not proceed to completion and the regioselectivity was very poor (Table 3.1, entries 4 and 5). A consistent trend in this reaction was the variable regioselectivity. Hence, considering the only difference between entries 1 and 2 was the introduction of cesium carbonate, we hypothesized that trace amounts of water was the most likely cause of this inconsistency. Gratifyingly, drying of the cesium carbonate led to significantly improved and consistent regioselectivity (entry 6), while the yield and enantioselectivity were maintained. Subsequent studies demonstrated that catalytic base could be employed with similar results (entry 7). Treatment of methyl cinnamyl carbonate **8a** in the absence of base at the higher concentration provided the allylic sulfilimine (**(S)-20a**) in 79% yield and in 96% enantiomeric excess (entry 8). Although, this result is a great improvement on the 18% yield originally

obtained, catalytic base was required to ensure the reaction proceeds to completion (entry 7).

3.3.3 Substrate Scope

Table 3.2 summarizes the application of the optimized reaction conditions (Table 3.1, entry 7) to a variety of cinnamyl allylic carbonates. The regioselectivity proved tolerant of a wide array of cinnamyl alcohol derivatives. For example, electron rich aromatics (entries 2-5) afford the corresponding sulfilimine in high yield and with excellent regioselectivity. The enantioselectivity of these reactions is also high (>90% *ee*) in all cases except for the *ortho* substituted variants (entries 2 and 8). As is typical in iridium-catalyzed allylic amination, the electron deficient substrates (entries 6 and 7) proceeded in lower yield; albeit still with excellent enantioselectivity (96% *ee*), and surprisingly, the regioselectivity remained high. The reaction was also tolerant of the 2-naphthyl substituent which proceeded in 89% yield and with 96% enantiomeric excess (entry 9). Unfortunately, the expansion to alkyl substituted derivatives provided none of the sulfilimine product (entry 10).

Table 3.2 Scope of the enantioselective iridium-catalyzed allylic amination reaction with *S,S*-diphenyl sulfilimine.^a

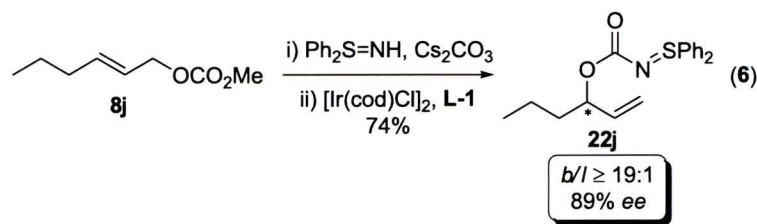


Entry	R =		Yld (%) ^b	(S)-20/21^c	ee (%) ^d
1	Ph	8a	87	≥ 19:1	97
2	2-MeOC ₆ H ₄	8b	87	≥ 19:1	74
3	3-MeOC ₆ H ₄	8c	85	≥ 19:1	94
4	4-MeOC ₆ H ₄	8d	80	≥ 19:1	95
5	4-MeC ₆ H ₄	8e	90	≥ 19:1	95
6	4-ClC ₆ H ₄	8f	78	≥ 19:1	96
7	4-CF ₃ C ₆ H ₄	8g	70	≥ 19:1	96
8	2,4-(MeO) ₂ C ₆ H ₃	8h	83	≥ 19:1	69
9	2-Naphthyl	8i	89	≥ 19:1	96
10	ⁿ Pr	8j	-	-	-

^aAll reactions were carried out on a 0.25 mmol reaction scale using 2 mol% $[\text{Ir}(\text{cod})\text{Cl}]_2$, 4 mol% **L-1**, 0.25 equiv. Cs_2CO_3 , and 1.1 equiv. of *S,S*-diphenylsulfilimine in DCM at 35 °C. ^b Isolated yields. ^cRegioselectivity was determined by 500 MHz ¹H NMR on the crude reaction mixtures. ^dEnantioselectivity was determined by chiral HPLC analysis on the corresponding trifluoroacetamide.

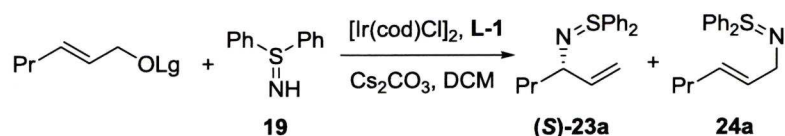
3.3.4 Optimization of Alkyl Substrates

Although the reaction of (*E*)-2-hexenyl carbonate **8j** did not afford any sulfilimine product (Table 3.2, entry 10), the carbonate was completely consumed furnishing the sulfilimine carbamate **23j**, which was obtained in 74% yield and with 89% enantiomeric excess (eq. 6).



Although the formation of the carbamate **22j** is very interesting, it was envisioned that this could be circumvented by alteration of the leaving group on the allylic alcohol (Table 3.3). The reaction of the methyl and *tert*-butyl carbonate derivatives under the optimized reaction conditions proceeded in >80% conversion and afforded the carbamate as the sole product (entries 1 and 2). However, changing the leaving group to an acetate provided a modest improvement, with a trace amount of product detected by ^1H NMR after 3.5 hours (entry 3). Extending the reaction time afforded up to 50% of the sulfilimine, but the reaction failed to reach full conversion (entries 4 and 5). Although the more electron withdrawing trifluoroacetamide did not provide an improvement (entry 6), a significant increase in the formation of sulfilimine (70%) was observed when using 4-fluorophenyl acetate (entry 7). Gratifyingly, the more electrophilic 3-fluorophenyl acetate leaving group afforded complete conversion to sulfilimine (**S**)-**23a** (entry 8). However, in contrast to the aryl examples, the reaction required stoichiometric amounts of base to affect complete conversion.

Table 3.3 Optimization of the regio- and enantioselective iridium-catalyzed allylic amination reaction with alkyl substrates.^a

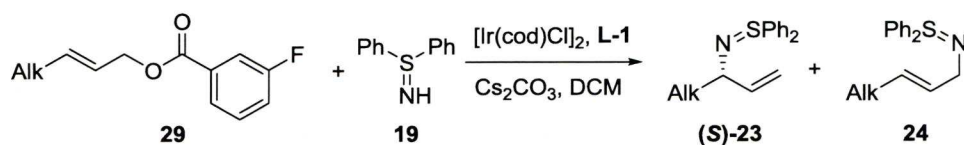


Entry	OLg		Time (hr)	(<i>S</i>)-23a (%) ^b
1	CO ₂ Me	8a	3.5	0
2	CO ₂ ^t Bu	25	"	0
3	Ac	26	"	≤ 20 ^c
4	"	"	5	≤ 50 ^c
5	"	"	14	≤ 50 ^c
6	TFA	27	"	50
7	C(O)4-FC ₆ H ₄	28	"	70
8	C(O)3-FC ₆ H ₄	29	"	100 ^d
9	"	"	6	100 ^e

^aAll reactions were carried out on a 0.25 mmol reaction scale using 2 mol% [Ir(cod)Cl]₂, 4 mol% **L-1**, 1.0 equiv. Cs₂CO₃, and 1.1 equiv. of *S,S*-diphenylsulfilimine in DCM at 35 °C. ^b% Formation of sulfilimine determine by 500MHz ¹H NMR. ^c Accurate results could not be deteremined due to volatility of starting material. ^d Sulfilimine isolated in 75%. ^e Sulfilimine isolated in 73%.

A preliminary study investigated the generality of the revised conditions using other alkyl substrates (Table 3.4). The reaction was tolerant of linear alkyl substituents (entries, 1,2 and 5) and a protected hydroxyl group (entry 6). However, no reaction occurred when α- or β-branched substrates (entries 2 and 3) were used. Treatment of the carbonate **29e** with *S,S*-diphenyl sulfilimine in the presence of the iridium complex of **L-1** afforded the branched sulfilimine in 85% yield and with 98% enantiomeric excess (entry 5). These results demonstrate the feasibility of using this methodology with alkyl substituted derivatives, which are traditionally more challenging.

Table 3.4 Scope of the enantioselective iridium-catalyzed allylic amination reaction with alkyl derivatives.^a



Entry	Alk =		Yld (%) ^b	(S)-23/ 24 ^c	ee (%) ^d
1	Pr	29a	75	≥ 19:1	95
2	Bu	29b	82	≥ 19:1	98
3	ⁱ Pr	29c	-	-	-
4	ⁱ Bu	29d	-	-	-
5	Ph(CH ₂) ₂	29e	85	≥ 19:1	98
6	BnO(CH ₂) ₂	29f	79	≥ 19:1	ND

^aAll reactions were carried out on a 0.25 mmol reaction scale using 2 mol% [Ir(cod)Cl]₂, 4 mol% L-1, 1.0 equiv. Cs₂CO₃, and 1.1 equiv. of *S,S*-diphenylsulfilimine in DCM at 35 °C. ^b% Isolated Yield.

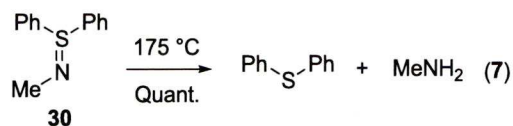
^cRegioselectivity was determined by 500 MHz ¹H NMR on the crude reaction mixtures.

^dEnantioselectivity was determined by chiral HPLC analysis on the corresponding trifluoroacetamide.

3.4 Cleavage of Sulfilimine Bond

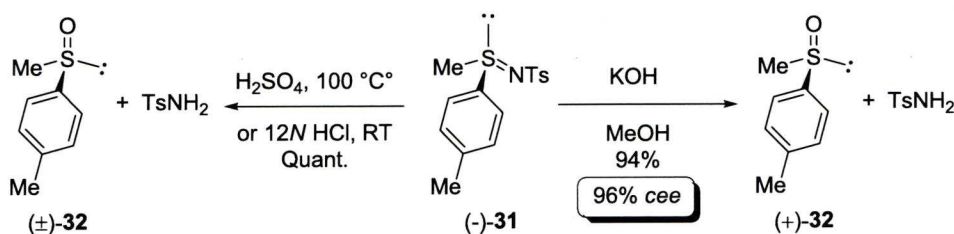
3.4.1 Background

There are many examples of the preparation of sulfides and chiral sulfoxides from the cleavage of chiral sulfilimines.¹⁴ Thermal decomposition is a common method employed for the cleavage of sulfilimine bonds, since the sulfilimines afford the corresponding sulfide, ammonia, or an amine upon heating. However, some sulfilimines prove to be more stable and require elevated temperature for the cleavage. For example, *S,S*-diphenyl-*N*-methylsulfilimine **30** can only be cleaved at 175 °C (eq. 7).¹⁵



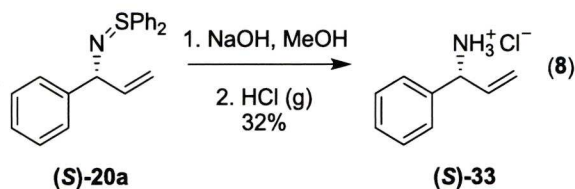
Acid and base hydrolysis are also efficient methods for cleaving the sulfilimine bond to provide the corresponding sulfoxide and amine. Treatment of the chiral sulfilimine (-)-**31** with concentrated sulfuric acid at 100 °C, or 12 *N* HCl at room temperature, furnished the sulfoxide and amine in quantitative yield (Scheme 3.5).¹⁶ The sulfoxide however was isolated as the racemate. Replacing the acid with methanolic potassium hydroxide afforded sulfoxide (+)-**32** with inversion of stereochemistry in 94% yield.

Scheme 3.5 Acid and base hydrolysis of sulfilimine (-)-**31**.



3.4.2 Conversion to the Free Amine

Initial attempts focused on the thermal decomposition of sulfilimine product (*S*)-**20a**. Unfortunately, heating the sulfilimine (*S*)-**20a** in benzene at 80 °C or toluene at 110 °C afforded none of the amine product, but only recovered starting material. Surprisingly, no olefin isomerization was detected. Alternatively, treatment of (*S*)-**20a** with methanolic hydroxide proceeded with only partial conversion to afford 32% of allylic amine (*S*)-**33** as the hydrochloride salt after treatment with aqueous hydrochloric acid.



3.5 Conclusion

The iridium-catalyzed allylic amination reaction with *S,S*-diphenylsulfilimine pronucleophiles demonstrates the aza-ylide may be tuned by the judicious choice of stabilizing groups. This pronucleophile was efficient for the allylic amination of aryl and alkyl substituted allylic alcohol derivatives, which is in contrast to related iridium-catalyzed allylic amination reactions. We envision that this amination work will further stimulate the examination of ylide nucleophiles in the metal-catalyzed allylic substitution reactions.

3.6 Experimental

Unless otherwise indicated, all reactions were carried out in flame-dried glassware, under an atmosphere of argon or nitrogen. Dichloromethane (DCM) was dried by passing through activated alumina columns. All other starting materials were purchased from Acros, Aldrich, Alfa Aesar, Strem, or Fluorochem and used without further purification unless otherwise stated.

All carbonates were prepared using literature procedures.

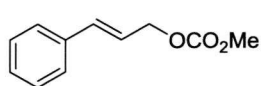
Allylic leaving groups were synthesized according to known procedures.

Thin layer chromatography (TLC) was performed on Whatman F₂₅₄ precoated silica gel plates. Visiulation was accomplished with a UV light and/or a KMnO₄ solution. Flash chromatography (FC) was performed using either Merck Silica Gel 60 (230-400 mesh) or Whatman Silica Gel Purasil[®] 60Å (230-400 mesh). Solvents for extraction and FC were technical grade. Reported solvent mixtures for TLC and FC are volume/volume mixtures. Infrared spectra were obtained on a Perkin-Elmer

spectrum 100 series FTIR spectrometer Peaks are reported in cm^{-1} with the following relative intensities: vs (very strong), s (strong), m (medium) and w (weak). Mass spectra were performed at either the University of Liverpool Mass Spectrometry Center or the EPSRC National Mass Spectrometry Service Centre, Swansea. High-resolution electron-impact (EI, ionization voltages of 70 eV), chemical ionization (CI, reagent gas CH_4 or NH_3) were obtained on either an Autospec, ZAB 2SE, Kratos MS-80, VG 7070E double focusing magnetic sector mass spectrometer equipped with a solid probe inlet, a Quattro II, MAT 95, or MAT 900. The electrospray ionization (ESI) mass spectra were obtained on a Waters micromass LCT mass spectrometer. ^1H and ^{13}C NMR were recorded on a Bruker AV 500 MHz NMR spectrometer in the indicated deuterated solvents, which were obtained from Cambridge Isotope Labs. For ^1H NMR, CDCl_3 was set to 7.26 ppm (CHCl_3 singlet). For ^{13}C NMR, CDCl_3 was set to 77.16 ppm (CDCl_3 center of triplet). ^1H data are reported in the following order: chemical shift in ppm (δ) (multiplicity, which are indicated by br (broadened), s (singlet), d (doublet), t (triplet), q (quartet), m (multiplet)); assignment of 2nd order pattern, if applicable; coupling constants (J , Hz); integration values for all ^{13}C NMR spectra data using the descriptor *o* and *e* refer to whether the peak is odd or even respectively, and correlate to an attached proton test (APT) experiment.

All liquid chromatographs were obtained on the Agilent 1200 series HPLC, equipped with a variable wavelength UV detector. The instrument was fitted with either a CHIRALCELTM AD-H column (Diacel, 4.6mm x 25cm) or CHIRALCELTM OD column (Diacel, 4.6mm x 25cm).

All liquid chromatographs were obtained on the Agilent 1200 series HPLC, equipped with a variable wavelength UV detector. The instrument was fitted with either a CHIRALCELTM AD-H column (Diacel, 4.6mm x 25cm) or CHIRALCELTM OD column (Diacel, 4.6mm x 25cm).



Methyl (2E)-3-phenylprop-2-en-1-yl carbonate 8a²²

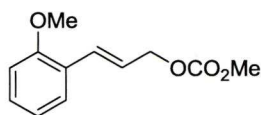
Prepared according to general synthesis of allylic carbonates outlined in chapter 2.

^1H (500 MHz, CDCl_3) δ 7.40 (d, J = 7.6 Hz, 2H), 7.35-7.32 (m, 2H), 7.29-7.26 (m, 1H), 6.70 (d, J = 15.8 Hz, 1H), 6.31 (dt, J = 15.8, 6.5 Hz, 1H), 4.80 (dd, J = 6.3, 1.1 Hz, 2H), 3.81 (s, 3H).

^{13}C (125 MHz, CDCl_3) δ 155.75 (e), 136.11 (e), 134.86 (o), 128.71 (o), 128.28 (o), 126.77 (o), 122.51 (o), 68.49 (e), 54.91 (o).

IR 30.28 (w), 2957 (w), 1742 (s), 1441 (m), 1251 (s), 1119 (m), 1044 (w)

HRMS: (ESI $[\text{M}+\text{Na}]^+$): calc'd for $\text{C}_{11}\text{H}_{12}\text{O}_3\text{Na}$ 215.0684, found 215.0686.



(2E)-3-(2-methoxyphenyl)prop-2-en-1-yl methyl carbonate
8b

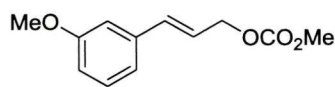
Prepared according to general synthesis of allylic carbonates outlined in chapter 2.

^1H NMR (500 MHz, CDCl_3) δ 7.43 (dd, $J = 7.7, 1.6$ Hz, 1H), 7.26-7.23 (m, 1H), 7.02 (d, $J = 16.1$ Hz, 1H), 6.94-6.91 (m, 1H), 6.87 (d, $J = 8.2$ Hz, 1H), 6.33 (dt, $J = 16.0, 6.6$ Hz, 1H), 4.80 (dd, $J = 6.6, 1.3$ Hz, 2H), 3.84 (s, 3H), 3.80 (s, 3H).

^{13}C NMR (125 MHz, CDCl_3) δ 157.04 (e), 155.79 (e), 130.05 (3), 129.36 (o), 127.34 (o), 125.11 (o), 124.10 (o), 120.71 (o), 110.94 (o), 69.14 (e), 55.48 (o), 54.84 (o).

IR (neat) 3008 (w), 2956 (w), 2839 (w), 1744 (s), 1598 (m), 1489 (m), 1439 (m), 1379 (m), 1257 (s), 1244 (s), 1177 (m), 1122 (m), 1027 (m) cm^{-1} .

HRMS: (ESI $[\text{M}+\text{Na}]^+$): calc'd for $\text{C}_{12}\text{H}_{14}\text{O}_4\text{Na}$ 245.0790, found 245.0789.



(2E)-3-(3-methoxyphenyl)prop-2-en-1-yl methyl carbonate 8c

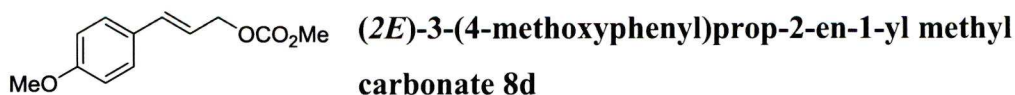
Prepared according to general synthesis of allylic carbonates outlined in chapter 2.

^1H NMR (500 MHz, CDCl_3) δ 7.29-7.25 (m, 1H), 7.01 (d, $J = 7.8$ Hz, 1H), 6.96-6.95 (m, 1H), 6.86-6.84 (m, 1H), 6.68 (d, $J = 15.9$ Hz, 1H), 6.32 (dt, $J = 16.0, 6.4$ Hz, 1H), 4.81 (dd, $J = 6.6, 1.5$ Hz, 2H), 3.83 (s, 3H), 3.82 (s, 3H).

^{13}C NMR (125 MHz, CDCl_3) δ 159.76 (e), 155.60 (e), 137.42 (e), 134.51 (o), 129.55 (o), 122.74 (o), 119.27 (o), 113.84 (o), 111.85 (o), 68.25 (e), 55.09 (o), 54.75 (o).

IR (neat) 3005 (w), 2957 (w), 1837 (w), 1743 (s), 1598 (m), 1580 (m), 1490 (m), 1440 (m), 1251 (s), 1156 (m), 1041 (m) cm^{-1} .

HRMS (ESI $[\text{M}+\text{Na}]^+$): calc'd for $\text{C}_{12}\text{H}_{14}\text{O}_4\text{Na}$ 245.0790, found 245.0787.



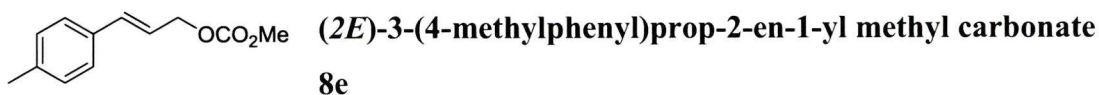
Prepared according to general synthesis of allylic carbonates outlined in chapter 2.

¹H NMR (500 MHz, CDCl₃) δ 7.34-7.32 (m, 2H), 6.86-6.85 (m, 2H), 6.64 (d, *J* = 15.6 Hz, 1H), 6.16 (dt, *J* = 15.9, 6.7 Hz, 1H), 4.77 (d, *J* = 6.4 Hz, 2H), 3.81 (s, 3H), 2.80 (s, 3H).

¹³C NMR (125 MHz, CDCl₃) δ 159.86 (e), 134.80 (o), 134.73 (e), 128.95 (e), 128.09 (o), 120.19 (o), 114.13 (o), 68.85 (e), 55.40 (o), 54.92 (o).

IR (neat) 3028 (w), 2957 (w), 1742 (s), 1441 (m), 1298 (m), 1251 (s), 943 (m) cm⁻¹.

HRMS (ESI [M+Na]⁺): calc'd for C₁₂H₁₄O₄Na 245.0790, found 245.0787.



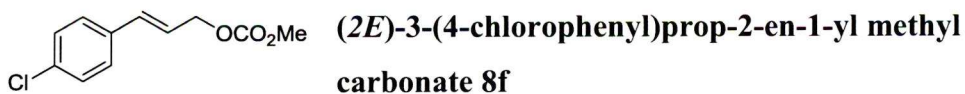
Prepared according to general synthesis of allylic carbonates outlined in chapter 2.

¹H NMR (500 MHz, CDCl₃) δ 7.29 (d, *J* = 8.0 Hz, 2H), 7.14 (d, *J* = 7.9 Hz, 2H), 6.66 (d, *J* = 15.9 Hz, 1H), 6.25 (dt, *J* = 15.9, 6.6 Hz, 1H), 4.78 (dd, *J* = 6.6, 1.1 Hz, 2H), 3.8 (s, 3H), 2.34 (s, 3H).

¹³C NMR (125 MHz, CDCl₃) δ 155.80 (e), 138.26 (e), 135.00 (o), 133.34 (e), 129.46 (o), 126.79 (o), 121.41 (o), 68.76 (e), 54.94 (o), 21.35 (o).

IR (neat) 3024 (w), 2948 (w), 1741 (s), 1440 (m), 1302 (m), 1247 (s), 941 (m) cm⁻¹.

HRMS (ESI [M+Na]⁺): calc'd for C₁₂H₁₄O₃Na 229.0841, found 229.0851.



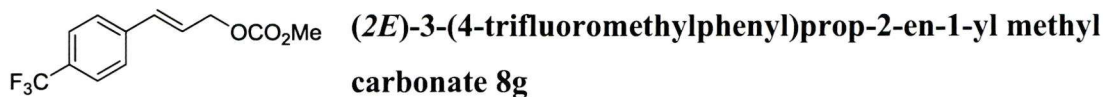
Prepared according to general synthesis of allylic carbonates outlined in chapter 2.

¹H NMR (500 MHz, CDCl₃) δ 7.36-7.27 (m, 4H), 6.63 (d, *J* = 16.0 Hz, 1H), 6.27 (dt, *J* = 15.9, 6.4 Hz, 1H), 4.78 (dd, *J* = 6.4, 1.2 Hz, 2H), 3.81 (s, 3H).

¹³C NMR (125 MHz, CDCl₃) δ 155.63 (e), 134.68 (e), 134.26 (e), 133.30 (o), 129.12 (o), 129.02 (o), 128.76 (o), 127.33 (o), 123.16 (o), 68.14 (e), 55.63 (o).

IR (neat) 3008 (w), 2958 (w), 1747 (s), 1702 (m), 1591 (m), 1492 (m), 1442 (m), 1257 (s), 1206 (m), 1090 (m), 1013 (m) cm⁻¹.

HRMS (ESI [M+Na]⁺): calc'd for C₁₁H₁₁O₃Na³⁵Cl 249.0294, found 249.0306.



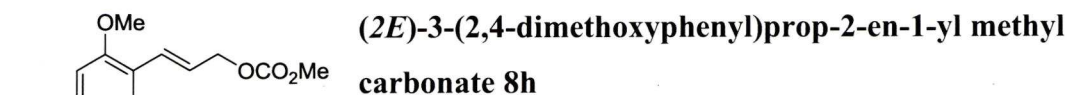
Prepared according to general synthesis of allylic carbonates outlined in chapter 2.

¹H NMR (500 MHz, CDCl₃) δ 7.56 (d, *J* = 8.3 Hz, 2H), 7.51 (d, *J* = 8.0 Hz, 2H), 6.74 (d, *J* = 16.1 Hz, 1H), 6.41 (dt, *J* = 15.9, 6.2 Hz, 1H), 4.85 (d, *J* = 6.2 Hz, 2H), 3.85 (s, 3H).

¹³C NMR (125 MHz, CDCl₃) δ 155.80 (e), 145.22 (e, q, ²*J*_{CF} = 36.1 Hz), 128.59 (o), 128.30 (e), 126.85 (o), 125.60 (o, q, ³*J*_{CF} = 3.5 Hz), 125.41 (o), 115.7 (e, q, ¹*J*_{CF} = 275.7 Hz), 67.07 (e), 54.85 (o).

IR (neat) 2960 (w), 2861 (w), 1747 (s), 1618 (m), 1443 (m), 1325 (s), 1263 (s), 1162 (m), 1115 (s), 1067 (s), 1018 (m) cm⁻¹.

HRMS (ESI [M+Na]⁺): calc'd for C₁₂H₁₁O₃NaF₃ 283.0558, found 283.0555.



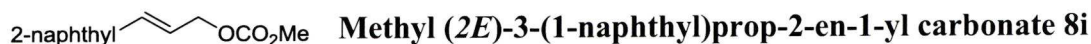
Prepared according to general synthesis of allylic carbonates outlined in chapter 2.

¹H NMR (500 MHz, CDCl₃) δ 7.34 (d, *J* = 8.4 Hz, 1H), 6.9 Hz, 6.9 Hz, 1H), 6.50-6.45 (m, 2H), 6.25 (dt, *J* = 16.2, 6.8 Hz, 1H), 4.80 (d, *J* = 7.0 Hz, 2H), 3.85 (s, 3H), 3.84 (s, 3H), 8.82 (s, 3H).

¹³C NMR (125 MHz, CDCl₃) δ 155.82 (e), 135.21 (e), 134.97 (e), 129.56 (e), 128.12 (o), 127.28 (o), 121.34 (o), 114.12 (o), 67.92 (e), 55.36 (o), 54.99 (o).

IR (neat) 3028 (w), 2957 (w), 1742 (s), 1441 (m), 1298 (m), 1251 (s), 943 (m) cm⁻¹.

HRMS (ESI [M+Na]⁺): calc'd for C₁₃H₁₆O₅Na 275.0895, found 275.0894.



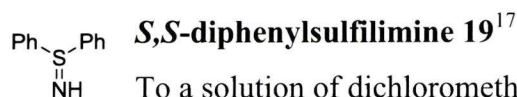
Prepared according to general synthesis of allylic carbonates outlined in chapter 2.

¹H NMR (500 MHz, CDCl₃) δ 7.84-7.79 (m, 4H), 7.63 (d, *J* = 8.9 Hz, 1H), 7.52-7.47 (m, 2H), 6.88 (d, *J* = 16.0 Hz, 1H), 6.46 (dt, *J* = 16.0, 6.4 Hz, 1H), 4.88 (d, *J* = 6.5 Hz, 2H), 3.86 (s, 3H).

^{13}C NMR (125 MHz, CDCl_3) δ 155.79 (e), 134.96 (o), 133.56 (e), 133.55 (e), 133.33 (e), 128.41 (o), 128.18 (o), 127.77 (o), 127.15 (o), 126.46 (o), 126.27 (o), 123.55 (o), 122.83 (o), 68.58 (e), 54.97 (o).

IR (neat) 3053 (w), 2992 (w), 2947 (w), 1736 (s), 1447 (m), 1382 (m), 1266 (s), 1226 (m) cm^{-1} .

HRMS (ESI, $[\text{M} + \text{Na}]^+$) calcd for $\text{C}_{15}\text{H}_{14}\text{O}_3\text{Na}$ 265.0841, found 265.0854



To a solution of dichloromethane (188 mL) under an argon atmosphere was added, diphenyl sulfide (6.3 mL, 37.5 mmol), 2,2,2-trifluoroacetamide (8.48g, 75 mmol), magnesium oxide (6.05g, 150 mmol), and rhodium(II) acetate dimer (0.24g, 0.563 mmol). After 15 minutes of stirring, iodobenzene diacetate (15.71g, 48.8 mmol) was added to the blue-green mixture. The reaction mixture was stirred for 14 hours at room temperature resulting in a brown suspension. The crude material was preabsorbed onto silica for flash chromatography through a short plug. The trifluoroacetamide was isolated as an orange oil eluting at 30% ethylacetate/hexane with a slight baseline impurity.

Semi pure trifluoroacetamide was dissolved in methanol (375 mL) and aqueous potassium hydroxide (2M, 113 mL) was added. Mixture stirred for 14 hours at room temperature. Mixture cooled to 0 °C and acidified to pH 2 with conc. hydrochloric acid and extracted with DCM (1x 300 mL). Aqueous layer was returned to 0 °C and basified to pH 14 with 2M NaOH. The basic aqueous layer was extracted with chloroform (4x 300 mL). Combined organic layers were dried using sodium sulphate, filtered, and concentrated *en vacuo* to afford 5.54g (74% over two steps) of pure diphenylsulfilimine as an off white solid.

^1H (500 HMz, CDCl_3) δ 7.60-7.58 (m, 4H), 7.48-7.44 (m, 6H), 1.53 (bs, 1H).

IR 3433 (m), 3110 (s), 1647 (m), 1578 (m), 1475 (s), 1439 (s), 1083 (m), 1068 (m), 932 (vs), 756 (m), 689 (s) cm^{-1} .



(*S*)-1,1' [N-(1-phenylprop-2-en-1-yl)sulfinimidoyl]dibenzene (*S*)-20a

Representative Procedure for the Iridium-Catalyzed Allylic Amination with aryl substrates: In a glovebox, **L-1** (6.3 mg, 0.01 mmol) and $[\text{Ir}(\text{cod})\text{Cl}]_2$ (3.6

mg, 0.005 mmol) were combined in a flame-dried RBF and fitted with a septa. In a second flame-dried RBF, *S,S*-diphenylsulfilimine (60.7mg, 0.30 mmol) and dried cesium carbonate (20.2 mg, 0.06 mmol) were combined. Both flasks were removed from the glovebox and fitted with an argon balloon. DCM (250 μ L) was added to the sulfilimine flask and warmed to 35 $^{\circ}$ C and stirred for *ca.* 15 minutes resulting in a heterogeneous colorless solution. DCM (500 μ L) was added to the catalyst flask and stirred for *ca.* 15minutes resulting in a light yellow homogeneous solution. The catalyst solution was then added *via* Teflon[®] cannula to the anion, followed by the allylic carbonate **8a** (48.9 mg, 0.25 mmol) *via* a tared 500 μ L gas-tight syringe. The reaction was allowed to stir at 35 $^{\circ}$ C for 6 hours (t.l.c. control). The reaction mixture was concentrated *in vacuo* and the crude product was pre-absorbed onto silica gel for purification *via* flash chromatography (eluting with 55% ethyl acetate/hexanes) to afford the allylic sulfilimine **20a** (69.4 mg, 89%) as a yellow oil.

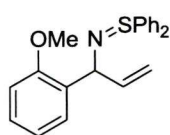
$[\alpha]_D^{20}$ -68.9 (*c* = 1.03, CHCl₃)

¹H NMR (500 MHz, CDCl₃) δ 7.58-7.56 (m, 2H), 7.52-7.50 (m, 2H), 7.43-7.40 (m, 3H), 7.37-7.33 (m, 5H), 7.23-7.20 (m, 2H), 7.14-7.11 (m, 1H), 5.99 (ddd, *J* = 17.1, 10.1, 6.8 Hz, 1H), 5.05 (d, *J* = 17.0 Hz, 1H), 4.91 (d, *J* = 10.1 Hz, 1H), 4.76 (d, *J* = 6.8 Hz, 1H).

¹³C NMR (125 MHz, CDCl₃) δ 145.93 (e), 143.83 (o), 141.81 (e), 141.80 (e), 130.50 (o), 130.42 (o), 129.14 (o), 129.07 (o), 128.12 (o), 127.91 (o), 127.79 (o), 127.39 (o), 126.27 (o), 112.88 (e), 67.83 (o).

IR (neat) 3057 (m), 3023 (m), 2925 (w), 1634 (w), 1598 (m), 1580 (m), 1475 (m), 1442 (s), 1302 (m), 1274 (m), 1077 (s), 1057 (s), 1022 (s), 912 (m), 742 (vs), 690 (vs) cm⁻¹.

HRMS (ESI, [M+H]⁺) calcd for C₂₁H₂₀NS 318.1316, found 318.1320.



(S)-1-{1-[(diphenyl- λ^4 -sulfanylidene)amino]prop-2-en-1-yl}-2-methoxybenzene (S)-20b

Synthesized according to the general procedure outlined for (S)-20a, showing the following properties:

$[\alpha]_D^{20}$ -26.7 (*c* = 1.06, CHCl₃).

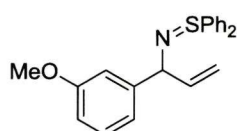
¹H NMR (500 MHz, CDCl₃) δ 7.54-7.52 (m, 3H), 7.48 (d, *J* = 6.8 Hz, 2H), 7.41-7.39 (m, 3H), 7.33-7.27 (m, 3H), 7.08 (dt, *J* = 7.8, 1.6 Hz, 1H), 6.84 (t, *J* = 7.5 Hz, 1H),

6.68 (d, $J = 8.2$ Hz, 1H), 6.04 (ddd, $J = 17.0, 10.4, 6.1$ Hz, 1H), 5.21 (d, $J = 5.8$ Hz, 1H), 5.13 (dt, $J = 17.0, 1.6$ Hz, 1H), 4.93 (d, $J = 10.1$ Hz, 1H), 3.62 (s, 3H).

^{13}C NMR (125 MHz, CDCl_3) δ 155.79 (e), 142.97 (o), 141.99 (e), 141.90 (e), 134.14 (e), 130.24 (o), 130.14 (o), 128.95 (o), 128.82 (o), 128.39 (o), 128.01 (o), 127.60 (o), 127.07 (o), 120.57 (o), 112.62 (e), 109.78 (o), 59.81 (o), 55.07 (o).

IR (neat) 3060 (w), 2926 (w), 2851 (w), 1635 (m), 1580 (w), 1475 (m), 1443 (s), 1245 (vs), 1067 (m), 1046 (m), 1032 (m), 919 (w), 745 (vs), 690(vs) cm^{-1} .

HRMS (ESI, $[\text{M}+\text{H}]^+$) $\text{C}_{22}\text{H}_{22}\text{NOS}$ 348.1422, found 348.1406.



(S)-1-{1-[(diphenyl- λ^4 -sulfanylidene)amino]prop-2-en-1-yl}-3-methoxybenzene (S)-20c

Synthesized according to the general procedure outlined for (S)-20a, showing the following properties:

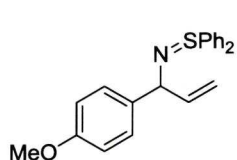
$[\alpha]_D^{20}$ -77.9 ($c = 1.09$, CHCl_3).

^1H NMR (500 MHz, CDCl_3) δ 7.58-7.56 (m, 2H), 7.53-7.51 (m, 2H), 7.41-7.40 (m, 3H), 7.35-7.33 (m, 3H), 7.12 (t, $J = 7.9$ Hz, 1H), 6.94-6.89 (m, 2H), 6.67 (dd, $J = 8.0, 2.3$ Hz, 1H), 5.99 (ddd, $J = 17.0, 10.2, 6.9$ Hz, 1H), 5.06 (dt, $J = 17.0, 1.4$ Hz, 1H), 4.92 (d, $J = 10.1$ Hz, 1H), 4.75 (d, $J = 6.7$ Hz, 1H), 3.69 (s, 3H).

^{13}C NMR (125 MHz, CDCl_3) δ 159.44 (e), 147.65 (e), 143.61 (o), 141.78 (e), 141.69 (e), 130.47 (o), 130.37 (o), 129.10 (o), 129.00 (o), 128.94 (o), 127.87 (o), 127.68 (o), 119.75 (o), 112.91 (e), 112.34 (o), 112.20 (o), 67.79 (o), 55.13 (o).

IR (neat) 3054 (w), 3000 (w), 2936 (w), 2833 (w), 1634 (w), 1596 (m), 1582 (m), 1475 (m), 1442 (m), 1314 (m), 1258 (s), 1147 (m), 1042 (s), 913 (m), 743 (vs), 689 (vs) cm^{-1} .

HRMS (ESI, $[\text{M}+\text{H}]^+$) calcd for $\text{C}_{22}\text{H}_{22}\text{NOS}$ 348.1422, found 348.1407.



(S)-1-{1-[(diphenyl- λ^4 -sulfanylidene)amino]prop-2-en-1-yl}-4-methoxybenzene (S)-20d

Synthesized according to the general procedure outlined for (S)-20a, showing the following properties:

$[\alpha]_D^{20}$ -41.6 ($c = 1.08$, CHCl_3).

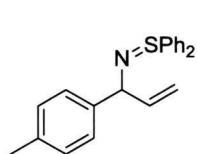
^1H NMR (500 MHz, CDCl_3) δ 7.58-7.56 (m, 2H), 7.52-7.50 (m, 2H), 7.42-7.39 (m, 3H), 7.38-7.32 (m, 3H), 7.25 (d, $J = 8.7$ Hz, 2H), 6.76 (d, $J = 8.6$ Hz, 2H), 5.96 (ddd,

$J = 17.0, 10.1, 6.9$ Hz, 1H), 5.01 (d, $J = 17.0$ Hz, 1H), 4.88 (dt, $J = 10.0, 0.7$ Hz, 1H), 4.72 (d, $J = 6.6$ Hz, 1H), 3.75 (s, 3H).

^{13}C NMR (125 MHz, CDCl_3) δ 158.01 (e), 143.96 (o), 141.78 (e), 141.75 (e), 130.45 (o), 130.35 (o), 129.08 (o), 129.02 (o), 128.31 (o), 127.88 (o), 127.69 (o), 113.43 (o), 112.53 (e), 67.09 (o), 55.28 (o).

IR (neat) 3058 (w), 3000 (w), 2930 (w), 2835 (w), 1673 (w), 1601 (m), 1580 (m), 1508 (s), 1475 (m), 1441 (m), 1243 (s), 1171 (m), 1032 (m), 1032 (m), 1023 (m), 915 (w), 825 (m), 741 (vs), 689 (vs) cm^{-1} .

HRMS (ESI, $[\text{M}+\text{H}]^+$) calcd $\text{C}_{22}\text{H}_{22}\text{NOS}$ 348.1422, found 348.1412.



(S)-1-{1-[(diphenyl- λ^4 -sulfanylidene)amino]prop-2-en-1-yl}-4-methylbenzene (S)-20e

Synthesized according to the general procedure outlined for (S)-20a, showing the following properties:

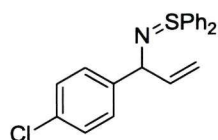
$[\alpha]_D^{20}$ -79.8 ($c = 1.07$, CHCl_3).

^1H NMR (500 MHz, CDCl_3) δ 7.59-7.57 (m, 2H), 7.53-7.51 (m, 2H), 7.41-7.39 (m, 3H), 7.38-7.33 (m, 3H), 7.24 (d, $J = 8.0$ Hz, 2H), 7.04 (d, $J = 7.9$ Hz, 2H), 5.97 (ddd, $J = 17.1, 10.1, 6.9$ Hz, 1H), 5.02 (dt, $J = 17.0, 1.4$ Hz, 1H), 4.88 (d, $J = 10.1$ Hz, 1H), 4.73 (d, $J = 6.8$ Hz, 1H), 2.29 (s, 3H).

^{13}C NMR (125 MHz, CDCl_3) δ 143.95 (o), 142.99 (e), 141.94 (e), 141.8 (e), 135.67 (e), 130.45 (o), 130.30 (o), 129.07 (o), 129.02 (o), 128.80 (o), 127.94 (o), 127.66 (o), 127.22 (o), 112.59 (e), 67.55 (o), 21.16 (o).

IR (neat) 3053 (w), 3003 (w), 2921 (w), 2851 (w), 2806 (w), 1633 (w), 1580 (w), 1508 (m), 1475 (m), 1442 (s), 1300 (w), 1061 (s), 1020 (s), 907 (s), 727 (vs), 688 (vs) cm^{-1} .

HRMS (ESI, $[\text{M}+\text{H}]^+$) calcd for $\text{C}_{22}\text{H}_{22}\text{NS}$ 332.1473, found 332.1487.



(S)-1-chloro-4-{1-[(diphenyl- λ^4 -sulfanylidene)amino]prop-2-en-1-yl}benzene (S)-20f

Synthesized according to the general procedure outlined for (S)-20a, showing the following properties:

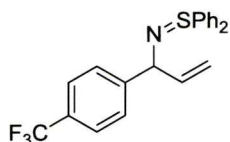
$[\alpha]_D^{20}$ -80.1 ($c = 1.10$, CHCl_3).

^1H NMR (500 MHz, CDCl_3) δ 7.56-7.54 (m, 2H), 7.51-7.48 (m, 2H), 7.43-7.40 (m, 3H), 7.37-7.32 (m, 3H), 7.27-7.24 (m, 2H), 7.17-7.14 (m, 2H), 5.94 (ddd, $J = 17.0$, 10.1, 6.9 Hz, 1H), 5.04 (dt, $J = 17.0$, 1.5 Hz, 1H), 4.93 (dt, $J = 10.1$, 1.4 Hz, 1H), 4.72 (d, $J = 6.8$ Hz, 1H).

^{13}C (125 MHz, CDCl_3) δ 144.48 (e), 143.42 (o), 141.52 (e), 141.46 (e), 131.70 (e), 130.56 (o), 130.53 (o), 129.18 (o), 129.11 (o), 128.72 (o), 128.07 (o), 127.75 (o), 127.74 (o), 113.22 (e), 67.12 (o).

IR (neat) 3056 (m), 2924 (w), 2846 (w), 1633 (w), 1580 (m), 1486 (s), 1475 (s), 1442 (s), 1403 (m), 1287 (m), 1087 (s), 1064 (s), 1014 (s), 914 (m), 810 (m), 743 (s), 690 (s) cm^{-1} .

HRMS (ESI, $[\text{M}+\text{H}]^+$) calcd for $\text{C}_{21}\text{H}_{19}\text{NS}^{35}\text{Cl}$ 352.0927, found 354.0897.



(S)-1-{1-[diphenyl- λ^4 -sulfanylidene]amino}prop-2-en-1-yl}-2,4-dimethoxybenzene (S)-20h

Synthesized according to the general procedure outlined for (S)-20a, showing the following properties:

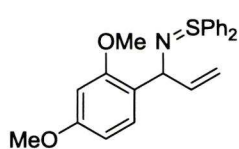
$[\alpha]_D^{20}$ -75.2 ($c = 1.02$, CHCl_3).

^1H NMR (500 MHz, CDCl_3) δ 7.58-7.53 (m, 2H), 7.51-7.47 (m, 2H), 7.44-7.41 (m, 5H), 7.37-7.32 (m, 4H), 7.29-7.24 (m, 1H), 5.98 (ddd, $J = 16.9$, 10.1, 6.8 Hz, 1H), 4.98 (d, $J = 10.1$ Hz, 1H), 4.80 (d, $J = 6.7$ Hz, 1H).

^{13}C NMR (125 MHz, CDCl_3) δ 136.04 (e), 135.01 (e, q, $^2J_{\text{CF}} = 35.2$ Hz) 130.96 (e), 130.84 (e), 130.73 (o), 129.31 (o), 129.21 (o), 128.61 (e, q, $^1J_{\text{CF}} = 281.6$ Hz), 127.89 (o), 127.74 (o), 127.71 (o), 125.01 (o), 125.00 (o, q, $^3J_{\text{CF}} = 3.9$ Hz), 113.79 (e), 67.50 (o).

IR (neat) 3061 (m), 2948 (w), 2842(w), 1630 (w), 1581 (m), 1492 (s), 1463 (s), 1440 (s), 1403 (m), 1285 (m), 1083 (s), 1062 (s), 1013 (s), 915 (m), 810 (m), 742 (s), 690 (s) cm^{-1} .

HRMS (ESI, $[\text{M}+\text{H}]^+$) calcd for $\text{C}_{22}\text{H}_{19}\text{F}_3\text{NS}$ 386.1185, found 386.1189.



(S)-1-{1-[diphenyl- λ^4 -sulfanylidene]amino}prop-2-en-1-yl}-2,4-dimethoxybenzene (S)-20h

Synthesized according to the general procedure outlined for (S)-20a, showing the following properties:

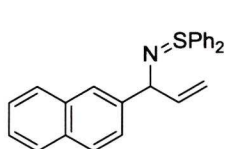
$[\alpha]_D^{20}$ -36.7 (c = 1.04, CHCl₃).

¹H NMR (500 MHz, CDCl₃) δ 7.54-7.52 (m, 2H), 7.49-7.47 (m, 2H), 7.41 (d, J = 8.4 Hz, 1H), 7.38-7.37 (m, 3H), 7.31-7.26 (m, 3H), 6.38 (dd, J = 8.5, 2.3 Hz, 1H), 6.27 (d, J = 2.4 Hz, 1H), 6.02 (ddd, J = 17.0, 10.2, 5.9 Hz, 1H), 5.13 (d, J = 5.8 Hz, 1H), 5.09 (dt, J = 17.0, 1.9 Hz, 1H), 4.92-4.89 (m, 1H), 3.74 (s, 3H), 3.58 (s, 3H).

¹³C NMR (125 MHz, CDCl₃) δ 159.13 (e), 156.77 (e), 143.12 (o), 142.05 (e), 141.94 (e), 130.19 (o), 130.12 (o), 128.91 (o), 128.86 (o), 128.80 (o), 127.89 (o), 127.58 (o), 126.82 (e), 112.34 (e), 103.96 (o), 97.92 (o), 59.62 (o), 55.33 (o), 55.02 (o).

IR(neat) 3056 (w), 2999 (w), 2952 (w), 2834 (w), 1608 (s), 1586 (s), 1499 (s), 1440 (s), 1415 (m), 1286 (s), 1205 (vs), 1153 (s), 1103 (m), 1035 (vs), 912 (m), 831 (m), 743 (vs), 689 (s) cm⁻¹.

HRMS (ESI, [M+H]⁺) calcd for C₂₃H₂₄NO₂S 378.1528, found 378.1530.



(S)-2-{1-[diphenyl- λ^4 -sulfanylidene]amino}prop-2-en-1-yl}naphthalene (S)-20i

Synthesized according to the general procedure outlined for (S)-20a, showing the following properties:

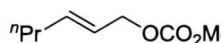
$[\alpha]_D^{20}$ -122.4 (c = 1.00, CHCl₃).

¹H NMR (500 MHz, CDCl₃) δ 7.77-7.75 (m, 2H), 7.73-7.69 (m, 2H), 7.60-7.58 (m, 2H), 7.53-7.51 (m, 2H), 7.48 (dd, J = 8.5, 1.6 Hz, 1H), 7.43-7.39 (m, 5H), 7.34-7.30 (m, 3H), 6.05 (ddd, J = 17.0, 10.2, 6.8 Hz, 1H), 5.09 (dt, J = 17.0, 1.4 Hz, 1H), 4.95 (d, J = 10.1 Hz, 1H), 4.92 (d, J = 6.6 Hz, 1H).

¹³C NMR (125 MHz, CDCl₃) δ 143.62 (o), 143.35 (e), 141.58 (e), 141.58 (e), 133.47 (e), 132.43 (e), 130.50 (o), 130.37 (o), 129.11 (o), 129.02 (o), 127.92 (o), 127.69 (o), 127.63 (o), 127.55 (o), 126.34 (o), 125.59 (o), 125.47 (o), 125.17 (o), 113.13 (e), 67.80 (o).

IR (neat) 3055 (m), 3008 (w), 2922 (w), 1631 (w), 1599 (m), 1580 (m), 1507 (m), 1475 (m), 1442 (m), 1303 (m), 1110 (m), 1065 (m), 1022 (m), 912 (m), 819 (m), 743 (s), 692 (s) cm⁻¹.

HRMS (ESI, $[M+H]^+$) calcd for $C_{25}H_{22}NS$ 368.1473, found 368.1459.

 **(2E)-hex-2-en-1-yl methyl carbonate 8a**

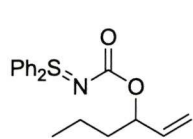
Prepared according to general synthesis of allylic carbonates outlined in chapter 2.

1H NMR (500 MHz, $CDCl_3$) δ 5.82-5.74 (m, 1H), 5.60-5.52 (m, 1H), 4.54 (dd, J = 6.6, 0.9 Hz, 2H), 3.75 (s, 3H), 2.01 (quartet, J = 7.1 Hz, 2H), 1.38 (sextet, J = 7.4 Hz, 2H), 0.87 (t, J = 7.4 Hz, 3H).

^{13}C NMR (125 MHz, $CDCl_3$) δ 155.77 (e), 137.32 (o), 123.43 (o), 68.76 (e), 54.71 (o), 34.35 (e), 22.04 (e), 13.67 (o).

IR 2959 (w), 2932 (m), 2875 (m), 1746 (s), 1442 (m), 1380 (w), 1252 (s), 971 (m), 942 (s), 792 (m).

HRMS (CI, $[M+NH_4]^+$) calcd for $C_8H_{18}O_3N$ 176.1281, found 176.1279.



hex-1-en-3-yl (diphenyl- λ^4 -sulfanylidene)carbamate 22

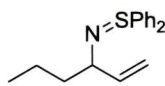
Chiral HPLC analysis (25 cm x 4.6 mm Chiralpak AD-H column, 15% isopropanol-hexane at 1.0 mL/min. flow rate, 210 nm; t_R (*minor*) 17.6 min., t_R (*major*) 19.7 min., 89% *ee*.

1H (500 MHz, $CDCl_3$) δ 7.74-7.71 (m, 4H), 7.50-7.43 (m, 6H), 5.84 (ddd, J = 17.3, 10.6, 6.6 Hz, 1H), 5.254 (dt, J = 17.2, 1.3 Hz, 1H), 5.14-5.08 (m, 2H), 1.73-1.66 (m, 1H), 1.58-1.51 (m, 1H), 1.44-1.29 (m, 2H), 0.88 (t, J = 7.4 Hz, 3H).

^{13}C (125 MHz, $CDCl_3$) δ 164.64 (e), 138.09 (o), 136.95 (o), 136.85 (o), 132.04 (o), 132.01 (o), 129.82 (o), 129.81 (o), 127.67 (o), 127.63 (o), 115.79 (e), 76.45 (o), 36.87 (e), 18.64 (e), 14.01 (o).

IR (neat) 3063 (w), 2958 (m), 2932 (m), 2871 (w), 1631 (s), 1580 (m), 1476 (m), 1445 (m), 1278 (vs), 1068 (m) cm^{-1} .

HRMS (ESI, $[M+Na]^+$) calcd for $C_{19}H_{21}NO_2Na$ 350.1191, found 350.1196.



(S)-1,1'-[N-(hex-1-en-3-yl)sulfinimidoyl]dibenzene 23a

Representative Procedure for the Iridium-Catalyzed Allylic Amination with alkyl substrates: In a glovebox, **L-1** (6.7 mg, 0.01 mmol) and $[Ir(cod)Cl]_2$ (3.6 mg, 0.005 mmol) were combined in a flame-dried RBF and fitted with a septa. In a second flame-dried RBF, *S,S*-diphenylsulfilimine (60mg, 0.32 mmol) and dried cesium carbonate (90.3 mg, 0.28 mmol) were combined. Both flasks were removed

from the glovebox and fitted with an argon balloon. DCM (250 μ L) was added to the sulfilimine flask and warmed to 35 $^{\circ}$ C and stirred for *ca.* 15 minutes resulting in a heterogeneous colorless solution. DCM (500 μ L) was added to the catalyst flask and stirred for *ca.* 15 minutes resulting in a light yellow homogeneous solution. The catalyst solution was then added *via* Teflon[®] cannula to the anion, followed by the allylic carbonate **8a** (39.6g, 0.25 mmol) *via* a tared 500 μ L gas-tight syringe. The reaction was allowed to stir at 35 $^{\circ}$ C for 6 hours (t.l.c. control). The reaction mixture was concentrated *in vacuo* and the crude product was pre-absorbed onto silica gel for purification *via* flash chromatography (eluting with 55% ethyl acetate/hexanes) to afford the allylic sulfilimine **(S)-23a** (53.2 mg, 75%) as a yellow oil.

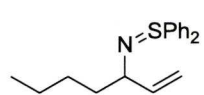
$[\alpha]_D^{20}$ -52.3 ($c = 0.99$, CHCl_3).

^1H NMR (500 MHz, CDCl_3) δ 7.60-7.56 (m, 4H), 7.41-7.39 (m, 6H), 5.76 (ddd, $J = 17.2, 10.0, 7.5$ Hz, 1H), 4.93 (dd, $J = 17.2, 1.1$ Hz, 1H), 4.82 (dd, $J = 10.1, 1.8$ Hz, 1H), 3.53 (q, $J = 7.1$ Hz, 1H), 1.54-1.42 (m, 2H), 1.34-1.22 (m, 2H), 0.81 (t, $J = 7.4$ Hz, 3H),

^{13}C NMR (125 MHz, CDCl_3) δ 144.83 (o), 143.33 (e), 142.55 (e), 130.41 (o), 130.27 (o), 129.13 (o), 129.04 (o), 127.65 (o), 127.39 (o), 112.22 (e), 65.45 (o), 41.05 (e), 19.78 (e), 14.17 (o).

IR (neat) 3059 (w), 2956 (m), 2928 (m), 2870 (m), 1635 (w), 1580 (m), 1475 (m), 1442 (s), 1303 (m), 1064 (s), 1022 (s), 997 (s), 909 (s), 742 (vs), 690 (vs) cm^{-1} .

HRMS (ESI, $[\text{M}+\text{H}]^+$) calcd for $\text{C}_{18}\text{H}_{22}\text{NS}$ 284.1473, found 284.1466.



(S)-1,1'-[N-(hex-1-en-3-yl)sulfinimidoyl]dibenzene (S)-23b

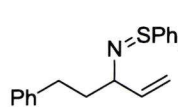
Synthesized according to the general procedure outlined for (S)-23a, showing the following properties:

^1H NMR (500 MHz, CDCl_3) δ 7.62-7.61 (m, 4H), 7.47-7.43 (m, 6H), 5.79 (ddd, $J = 17.1, 10.3, 7.7$ Hz, 1H), 4.96 (d, $J = 17.4$ Hz, 1H), 4.87 (dd, $J = 10.2, 1.6$ Hz, 1H), 3.54 (q, $J = 7.1$ Hz, 1H), 1.57-1.47 (m, 2H), 1.30-1.21 (m, 4H), 0.83 (t, $J = 7.1$ Hz, 3H).

^{13}C NMR (125 MHz, CDCl_3) δ 144.82 (e), 144.53 (e), 130.72 (o), 130.59 (o), 129.29 (o), 129.20 (o), 127.88 (o), 127.64 (o), 112.80 (e), 65.41 (o), 38.21 (e), 28.84 (e), 22.74 (e), 14.23 (o).

IR (neat) 3059 (w), 2955 (m), 2926 (m), 2855 (m), 1580 (w), 1475 (m), 1442 (s), 1303 (m), 1062 (s), 1022 (s), 909 (s), 742 (vs), 691 (vs) cm^{-1} .

HRMS (ESI, $[\text{M}+\text{H}]^+$) calcd for $\text{C}_{18}\text{H}_{22}\text{NS}$ 284.1473, found 284.1466.

 **(S)-1,1'-[N-(hex-1-en-3-yl)sulfinimidoyl]dibenzene (S)-23e**
Synthesized according to the general procedure outlined for (S)-23a, showing the following properties:

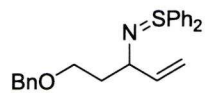
$[\alpha]_D^{20}$ -48.3 (c = 1.01, CHCl_3).

^1H NMR (500 MHz, CDCl_3) δ 7.67-7.60 (m, 4H), 7.46-7.43 (m, 6H), 7.37-7.26 (m, 5H), 5.83 (ddd, J = 17.4, 10.0, 7.4 Hz, 1H), 5.00 (d, J = 17.1 Hz, 1H), 4.87 (d, J = 10.2 Hz, 1H), 3.84 (q, J = 6.9 Hz, 1H), 3.61-5.56 (m, 1H), 3.54-3.49 (m, 1H), 1.96-1.84 (m, 2H).

^{13}C NMR (125 MHz, CDCl_3) δ 144.54 (o), 143.03 (e), 143.02 (e), 130.46 (o), 130.38 (o), 129.21 (o), 129.12 (o), 128.59 (o), 128.46 (e), 128.25 (o), 127.59 (o), 127.37 (o), 125.49 (o), 112.72 (e), 65.32 (o), 40.38 (e), 32.93 (e).

IR (neat) 3060 (m), 3025 (m), 2922 (m), 1636 (w), 1496 (m), 1474 (m), 1442 (s), 1302 (m), 1063 (s), 1022 (s), 910 (m), 742 (vs), 692 (vs) cm^{-1} .

HRMS (ESI, $[\text{M}+\text{H}]^+$) calcd for $\text{C}_{23}\text{H}_{24}\text{NS}$ 346.1424, found 346.1422.



(S)-1,1'-[N-(hex-1-en-3-yl)sulfinimidoyl]dibenzene (S)-23f
Synthesized according to the general procedure outlined for (S)-23a, showing the following properties:

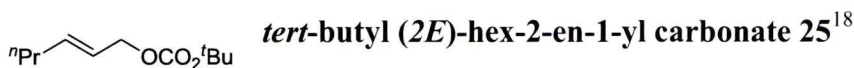
$[\alpha]_D^{20}$ -60.3 (c = 1.01, CHCl_3).

^1H (500 MHz, CDCl_3) δ 7.62-7.61 (m, 4H), 7.49-7.41 (m, 6H), 7.38-7.26 (m, 5H), 5.44 (ddd, J = 17.3, 10.2, 7.5 Hz, 1H), 5.01-4.98 (m, 1H), 4.88-4.86 (m, 1H), 4.40 (s, 2H), 3.85 (q, J = 7.0 Hz, 1H), 3.61-3.56 (m, 1H), 3.54-3.49 (m, 1H).

^{13}C (125 MHz, CDCl_3) δ 132.88 (e), 132.74 (e), 130.47 (o), 129.21 (o), 129.14 (o), 128.73 (e), 128.38 (o), 127.67 (o), 127.52 (o), 112.61 (e), 72.88 (e), 67.96 (e), 67.95 (e), 62.77 (o).

IR (neat) 3061 (w), 2924 (m), 2854 (m), 1580 (w), 1475 (m), 1443 (s), 1362 (w), 1092 (s), 1076 (s), 1022 (m), 913 (m), 742 (vs), 693 (vs) cm^{-1} .

HRMS (ESI, $[\text{M}+\text{H}]^+$) calcd for $\text{C}_{24}\text{H}_{26}\text{NOS}$ 376.1730, found 376.1728.



Prepared according to general synthesis of allylic carbonates outlined in chapter 2.

¹H NMR (500 MHz, CDCl₃) 5.79 (dt, *J* = 15.2, 6.8 Hz, 1H), 5.63-5.57 (m, 1H), 4.57 (d, *J* = 6.6 Hz, 2H), 2.06 (q, *J* = 6.9 Hz, 2H), 1.50 (s, 9H), 1.46-1.37 (m, 2H), 0.92 (t, *J* = 7.4 Hz, 3H).

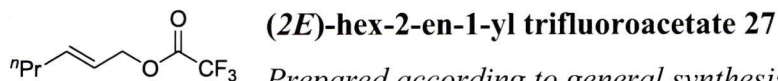
IR (neat) 2962 (m), 1933 (m), 1875 (m), 1738 (s), 1458 (m), 1369 (m), 1273 (s), 1251 (s), 1160 (s), 1104 (m), 1081 (m) cm⁻¹.



Prepared according to general synthesis of allylic carbonates outlined in chapter 2.

¹H NMR (500 MHz, CDCl₃) δ 5.82-4.76 (m, 1H), 4.61-5.55 (m, 1H), 4.53 (d, *J* = 6.2 Hz, 2H), 2.08 (s, 3H), 2.07-2.03 (m, 2H), 1.43 (sextet, *J* = 7.6 Hz, 2H), 0.92 (t, *J* = 7.3 Hz, 3H).

IR (neat) 2960 (m), 2932 (m), 2875 (w), 1739 (s), 1458 (m), 1380 (m), 1363 (m), 1226 (s), 1023 (m) cm⁻¹.



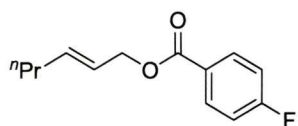
Prepared according to general synthesis of allylic carbonates outlined in chapter 2.

¹H NMR (500 MHz, CDCl₃) δ 5.93-5.87 (m, 1H), 5.62-5.56 (m, 1H), 4.77 (d, *J* = 6.9 Hz, 2H), 2.06 (q, *J* = 7.0 Hz, 2H), 1.42 (sextet, *J* = 7.5 Hz, 2H), 0.90 (t, *J* = 7.4 Hz, 3H).

¹³C NMR (125 MHz, CDCl₃) δ 158.12 (e, q, ²*J*_{CF} = 35.9 Hz), 128.75 (o), 128.32 (o), 114.37 (e, q, ¹*J*_{CF} = 289.9 Hz), 65.89 (e), 35.67 (e), 23.35 (e), 14.01 (o).

IR (neat) 2962 (m), 2916 (m), 2851 (m), 1679 (s), 1601 (m), 1464 (m), 1205 (s), 1153 (s), 1076 (m).

HRMS (CI, [M+NH₄]⁺) calcd for C₇H₁₃F₃NO 184.0944, found 184.0943.



(2E)-hex-2-en-1-yl 4-fluorobenzoate 28

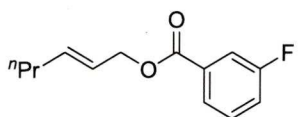
Prepared according to general synthesis of allylic carbonates outlined in chapter 2.

¹H NMR (500 MHz, CDCl₃) δ 7.87 (d, *J* = 7.7 Hz, 1H), 7.77-7.75 (m, 1H), 7.44 (dt, *J* = 8.0, 5.6 Hz, 1H), 7.30-7.26 (m, 1H), 5.91-5.86 (m, 1H), 5.73-5.67 (m, 1H), 4.79 (d, *J* = 6.5 Hz, 2H), 2.09 (q, *J* = 7.2 Hz, 2H), 1.46 (sextet, *J* = 7.4 Hz, 2H), 0.94 (t, *J* = 7.4 Hz, 3H).

¹³C NMR (125 MHz, CDCl₃) δ 165.84 (e, d, ¹*J*_{CF} = 256.3 Hz), 165.59 (e), 136.76 (o), 132.26 (o, d, ³*J*_{CF} = 9.2 Hz), 126.77 (e), 123.97 (o), 115.57 (o, d, ²*J*_{CF} = 22.2 Hz), 66.02 (e), 34.47 (e), 22.18 (e), 13.77 (o).

IR (neat) 2960 (m), 2932 (m), 2874 (m), 1717 (s), 1603 (m), 1508 (m), 1412 (m), 1265 (s), 1238 (s), 1153 (m), 1108 (m), 1089 (m) cm⁻¹.

HRMS (ESI, [M+Na]⁺) calcd for C₁₃H₁₅O₂FNa 245.0954, found 245.0952.



(2E)-hex-2-en-1-yl 3-fluorobenzoate 29a

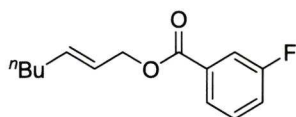
Prepared according to general synthesis of allylic carbonates outlined in chapter 2.

¹H NMR (500 MHz, CDCl₃) δ 7.87 (d, *J* = 7.9 Hz, 1H), 7.77-7.75 (m, 1H), 7.44 (dt, *J* = 7.9, 5.6 Hz, 1H), 7.30-7.22 (m, 1H), 5.91-5.86 (m, 1H), 5.73-5.67 (m, 1H), 4.79 (d, *J* = 6.5 Hz, 2H), 2.09 (q, *J* = 7.1 Hz, 2H), 1.46 (sextet, *J* = 7.5 Hz, 2H), 0.94 (t, *J* = 7.3 Hz, 3H).

¹³C NMR (125 MHz, CDCl₃) δ 165.17 (e), 165.15 (e), 162.55 (e, d, ¹*J*_{CF} = 247.5 Hz), 161.56 (e), 136.75 (o), 132.64 (e, d, ³*J*_{CF} = 7.3 Hz), 129.92 (o, d, ³*J*_{CF} = 7.9 Hz), 125.34 (o), 123.77 (o), 119.85 (o, d, ²*J*_{CF} = 21.1 Hz), 116.47 (o, d, ²*J*_{CF} = 22.7 Hz), 66.08 (e), 34.35 (e), 22.05 (e), 13.62 (o).

IR (neat) 2960 (m), 2932 (m), 1874 (m), 1721 (s), 2593 (m), 1487 (m), 1447 (m), 1268 (s), 1197 (s), 1154 (m), 1093 (m), 1066 (m) cm⁻¹.

HRMS (ESI, [M+Na]⁺) calcd for C₁₃H₁₅O₂FNa 245.0954, found 245.0951.



(2E)-hept-2-en-1-yl 3-fluorobenzoate 29b

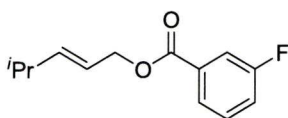
Prepared according to general synthesis of allylic carbonates outlined in chapter 2.

^1H NMR (500 MHz, CDCl_3) δ 7.87 (d, $J = 7.6$ Hz, 1H), 7.77-7.74 (m, 1H), 7.43 (dt, $J = 8.0, 5.6$ Hz, 1H), 5.72-5.66 (m, 1H), 5.92-5.86 (m, 2H), 5.72-5.66 (m, 1H), 4.79 (d, $J = 7.2$ Hz, 2H), 2.11 (q, $J = 7.2$ Hz, 2H), 1.44-1.32 (m, 4H), 0.93 (t, $J = 7.2$ Hz, 3H).

^{13}C NMR (125 MHz, CDCl_3) δ 165.43 (e), 165.40 (e), 162.66 (e, d, $^1J_{\text{CF}} = 247.3$ Hz), 137.22 (o), 132.74 (e, d, $^3J_{\text{CF}} = 7.4$ Hz), 130.06 (o, d, $^3J_{\text{CF}} = 7.4$ Hz), 125.46 (o), 123.58 (o), 120.03 (o, d, $^2J_{\text{CF}} = 21.1$ Hz), 116.64 (o, d, $^2J_{\text{CF}} = 23.0$ Hz), 66.26 (e), 32.10 (e), 31.14 (e), 22.34 (e), 14.03 (o).

IR (neat) 2958 (m), 2929 (m), 1860 (m), 1721 (s), 1592 (m), 1487 (m), 1447 (m), 1269 (s), 1197 (s), 1092 (m), 1066 (m) cm^{-1} .

HRMS (ESI, $[\text{M}+\text{Na}]^+$) calcd for $\text{C}_{14}\text{H}_{17}\text{FNaO}_2$ 259.1105, found 259.1107.



(2E)-4-methylpent-2-en-1-yl 3-fluorobenzoate 29c

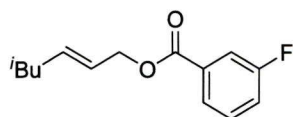
Prepared according to general synthesis of allylic carbonates outlined in chapter 2.

^1H NMR (500 MHz, CDCl_3) δ 7.85 (d, $J = 7.6$ Hz, 1H), 7.74-7.72 (m, 1H), 7.43-7.39 (m, 1H), 7.27-7.23 (m, 1H), 5.83 (d, $J = 15.4, 6.5$ Hz, 1H), 5.62 (dt, $J = 15.5, 6.5$ Hz, 1H), 4.76 (d, $J = 6.4$ Hz, 2H), 2.39-2.30 (m, 1H), 1.03 (s, 3H), 1.01 (s, 3H).

^{13}C NMR (125 MHz, CDCl_3) δ 165.42 (e), 162.72 (e, d, $^1J_{\text{CF}} = 254.3$ Hz), 143.86 (o), 132.73 (o, d, $^3J_{\text{CF}} = 7.0$ Hz), 130.06 (o, d, $^3J_{\text{CF}} = 8.0$ Hz), 128.63 (o), 125.46 (o), 120.03 (o, d, $^2J_{\text{CF}} = 21.0$ Hz), 116.71 (o, d, $^2J_{\text{CF}} = 23.1$ Hz), 66.35 (e), 30.94 (e), 22.11 (o).

IR (neat) 2961 (m), 2872 (w), 1720 (s), 1592 (m), 1487 (m), 1447 (m), 1268 (s), 1197 (s), 1092 (m), 1067 (m) cm^{-1} .

HRMS (ESI, $[\text{M}+\text{Na}]^+$) calcd for $\text{C}_{13}\text{H}_{15}\text{FNaO}_2$ 245.0948, found 245.0948.



(2E)-5-methylhex-2-en-1-yl 3-fluorobenzoate 29d

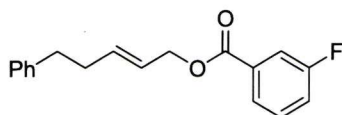
Prepared according to general synthesis of allylic carbonates outlined in chapter 2.

¹H NMR (500 MHz, CDCl₃) δ 7.85 (d, *J* = 8.2 Hz, 1H), 7.75-7.72 (m, 1H), 7.44-7.39 (m, 1H), 7.29-7.23 (m, 1H), 5.88-5.83 (m, 1H), 5.73-5.65 (m, 1H), 4.79 (d, *J* = 6.5 Hz, 2H), 1.99 (t, *J* = 7.0 Hz, 2H), 1.73-1.62 (m, 1H), 0.92 (s, 3H), 0.91 (s, 3H).

¹³C NMR (125 MHz, CDCl₃) δ 165.42 (e), 162.63 (e, d, ¹*J*_{CF} = 247.7 Hz), 135.99 (o), 132.67 (e, d, ³*J*_{CF} = 7.4 Hz), 130.07 (o, d, ³*J*_{CF} = 7.6 Hz), 125.46 (o), 124.73 (o), 120.04 (o, d, ²*J*_{CF} = 21.3 Hz), 116.61 (o, d, ²*J*_{CF} = 22.7 Hz), 66.22 (e), 41.72 (e), 28.20 (o), 22.40 (o).

IR (neat) 2957 (m), 2932 (w), 1871 (w), 1721 (s), 1593 (m), 1487 (m), 1447 (m), 1268 (s), 1197 (s), 1093 (m), 1066 (m) cm⁻¹.

HRMS (ESI, [M+Na]⁺) calcd for C₁₄H₁₇O₂FNa 259.1110, found 259.1098.



(2E)-5-phenylpent-2-en-1-yl 3-fluorobenzoate 29e

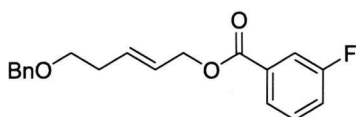
Prepared according to general synthesis of allylic carbonates outlined in chapter 2.

¹H NMR (500 MHz, CDCl₃) δ 7.88-7.86 (m, 1H), 7.77-7.74 (m, 1H), 7.47-7.43 (m, 1H), 7.33-7.27 (m, 4H), 7.24-7.21 (m, 2H), 5.96-5.91 (m, 1H), 5.76-5.70 (m, 1H), 4.79 (d, *J* = 6.4 Hz, 2H), 2.78-2.74 (m, 1H), 2.46-2.42 (m, 1H), 1.34-1.29 (m, 2H).

¹³C NMR (125 MHz, CDCl₃) δ 163.59 (e), 162.69 (e, q, ¹*J*_{CF} = 213.1 Hz), 125.96 (o), 125.39 (o), 124.30 (o), 119.98 (o, d, ²*J*_{CF} = 21.4 Hz), 135.90 (o), 132.67 (e, d, ³*J*_{CF} = 7.2 Hz), 130.09 (o, d, ³*J*_{CF} = 7.9 Hz), 128.58 (o), 128.48 (o), 116.55 (o, d, ²*J*_{CF} = 22.4 Hz), 114.59 (e), 66.00 (e), 35.41 (e), 34.19 (e).

IR (neat) 3078 (w), 3028 (w), 1934 (w), 1719 (s), 1592 (m), 1487 (m), 1446 (m), 1268 (s), 1198 (s), 1092 (m), 1066 (m) cm⁻¹.

HRMS (ESI, [M+Na]⁺) calcd for C₁₈H₁₇FNaO₂ 307.1105, found 307.1109.



(2E)-5-(benzyloxy)pent-2-en-1-yl 3-fluorobenzoate
29f

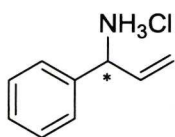
Prepared according to general synthesis of allylic carbonates outlined in chapter 2.

¹H NMR (500 MHz, CDCl₃) δ 7.89 (d, *J* = 8.0 Hz, 1H), 7.80-7.77 (m, 1H), 7.45-7.41 (m, 1H), 7.39-7.36 (m, 4H), 7.35-7.26 (m, 2H), 5.44 (ddd, *J* = 17.4, 10.0, 7.4 Hz), 5.01-4.98 (m, 1H), 4.88-4.86 (m, 1H), 4.40 (s, 2H), 3.85 (q, *J* = 7.0 Hz, 2H), 3.61-3.56 (m, 1H), 3.54-3.49 (m, 1H), 1.96-1.85 (m, 2H).

¹³C NMR (125 MHz, CDCl₃) δ 165.19 (e), 165.17 (e), 162.49 (e, d, ¹*J*_{CF} = 247.5 Hz), 138.31 (e), 132.93 (o), 132.45 (e, d, ³*J*_{CF} = 7.5 Hz), 129.99 (o, d, ³*J*_{CF} = 7.5 Hz), 128.39 (o), 127.66 (o), 127.61 (o), 125.38 (o), 119.97 (o, d, ²*J*_{CF} = 21.2 Hz), 116.50 (o, d, ²*J*_{CF} = 23.2 Hz), 72.91 (e), 69.25 (e), 65.86 (e), 32.76 (e).

IR (neat) 3063 (w), 2937 (w), 2858 (w), 1719 (s), 1592 (m), 1487 (m), 1446 (m), 1268 (s), 1197 (s), 1092 (s), 1066 (m) cm⁻¹.

HRMS (ESI, [M+Na]⁺) calcd for C₁₉H₁₉FNao₃ 337.1210, found 337.1214.

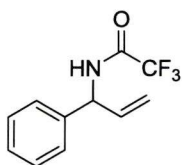


(S)-1-phenylprop-2-en-1-amine hydrochloride (S)-33^{1g, li, 20}

[α]_D²⁰ -28.7 (c = 0.9 CHCl₃), lit.²³ [α]_D²³ -36.6 (c = 1.0, CHCl₃)

¹H NMR (500 MHz, CDCl₃) δ 7.45-7.58 (m, 5H), 6.18 (ddd, *J* = 17.1, 10.3, 6.5 Hz, 1H), 5.42 (dd, *J* = 10.5, 1.1 Hz, 1H), 5.39 (d, *J* = 17.0, 1.2 Hz, 1H), 5.01 (d, *J* = 6.5 Hz, 1H), 4.77 (bs, 3H)

IR (neat) 2984 (m), 2887 (m), 2876 (w), 1600 (m), 1512 (m), 1440 (m), 1264 (w), 1197 (w) cm⁻¹.

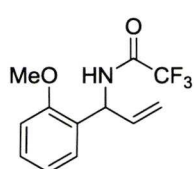


(S)-2,2,2-trifluoro-N-(1-phenylprop-2-en-1-yl)acetamide (S)-34a²¹

[α]_D²⁰ -100.9 (c = 0.88, CHCl₃); Chiral HPLC analysis (25 cm x 4.6 mm Chiralpak AD-H column, 1% isopropanol-hexane at 1.0 mL/min. flow rate, 220 nm; *t*_R (minor) 12.0 min., *t*_R (minor) 13.5 min., 97% *ee*.

¹H NMR (500 MHz, CDCl₃) δ 7.44-7.32 (m, 5H), 6.55 (bs, 1H), 6.06 (ddd, *J* = 17.2, 10.4, 5.4 Hz, 1H), 5.68-5.65 (m, 1H), 5.39 (dd, *J* = 10.4, 1.1 Hz, 1H), 5.30 (dd, *J* = 17.0, 1.4 Hz, 1H)

IR (neat) 3310 (m), 2952 (m), 2925 (s), 2855 (m), 1696 (vs), 1601 (w), 1551 (m), 1495 (m), 1465 (m), 1248 (m), 1182 (vs), 1027 (w) cm^{-1} .



(S)-2,2,2-trifluoro-N-[1-(2-methoxyphenyl)prop-2-en-1-yl]acetamide 34b

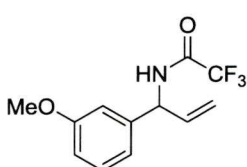
$[\alpha]_{\text{D}}^{20}$ -121.3 (c = 1.01, CHCl_3); Chiral HPLC analysis (25 cm x 4.6 mm Chiralpak AD-H column, 1% isopropanol-hexane at 1.0 mL/min. flow rate, 210 nm; t_{R} (*minor*) 47.9 min., t_{R} (*major*) 61.2 min., 74% *ee*.

^1H NMR (500 MHz, CDCl_3) δ 7.50 (bs, 1H), 7.38-7.34 (m, 1H), 7.25 (dd, J = 7.5, 1.6 Hz, 1H), 7.02-6.97 (m, 2H), 6.05 (ddd, J = 17.0, 10.3, 5.6 Hz, 1H), 5.72-5.69 (m, 1H), 5.22-5.16 (m, 2H), 3.92 (s, 3H).

^{13}C NMR (125 MHz, CDCl_3) δ 157.15 (e), 156.16 (e, q, $^2J_{\text{CF}}$ = 37.2 Hz), 135.79 (o), 129.87 (o), 129.51 (o), 126.24 (e), 121.42 (o), 116.33 (e), 116.12 (e, q, $^1J_{\text{CF}}$ = 286.2 Hz), 111.61 (o), 55.65 (o), 54.58 (o).

IR (neat) 3310 (m), 2952 (m), 2924 (s), 2854 (m), 1696 (s), 1551 (m), 1495 (m), 1465 (m), 1248 (s), 1182 (vs), 1027 (m) cm^{-1} .

HRMS (ESI, $[\text{M}-\text{H}]^-$) calcd for $\text{C}_{12}\text{H}_{11}\text{NO}_2\text{F}_3$ 258.0742, found 258.0749.



(S)-2,2,2-trifluoro-N-[1-(3-methoxyphenyl)prop-2-en-1-yl]acetamide 34c

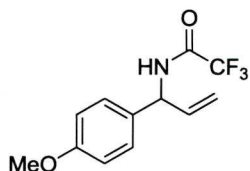
$[\alpha]_{\text{D}}^{20}$ -119.7 (c = 0.93, CHCl_3); Chiral HPLC analysis (25 cm x 4.6 mm Chiralpak AD-H column, 1% isopropanol-hexane at 1.0 mL/min. flow rate, 210 nm; t_{R} (*major*) 20.5 min., t_{R} (*minor*) 23.9 min., 94% *ee*.

^1H NMR (500 MHz, CDCl_3) δ 7.32-7.29 (m, 1H), 6.89-6.83 (m, 3H), 6.52 (bs, 1H), 6.01 (ddd, J = 17.1, 10.4, 5.5 Hz, 1H), 5.61-5.58 (m, 1H), 5.35 (dd, J = 10.4, 1.5 Hz, 1H), 5.28 (dd, J = 17.2, 1.7 Hz, 1H), 3.81 (s, 3H).

^{13}C NMR (125 MHz, CDCl_3) δ 160.22 (e), 156.30 (e, q, $^2J_{\text{CF}}$ = 37.2 Hz), 140.05 (e), 135.22 (o), 130.36 (o), 119.45 (o), 117.44 (e), 115.94 (e, q, $^1J_{\text{CF}}$ = 294.7 Hz), 113.79 (o), 113.29 (o), 55.82 (o), 55.45 (o).

IR (neat) 3295 (m), 3078 (w), 2925 (m), 2856 (w), 1702 (s), 1602 (m), 1548 (m), 1491 (m), 1267 (m), 1208 (s), 1178 (vs), 1159 (vs), 1043 (m) cm^{-1} .

HRMS (ESI, $[\text{M}-\text{H}]^-$) calcd for $\text{C}_{12}\text{H}_{11}\text{NO}_2\text{F}_3$ 258.0742, found 258.0752.



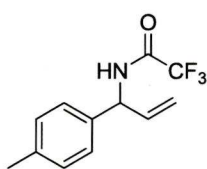
(S)-2,2,2-trifluoro-N-[1-(4-methoxyphenyl)prop-2-en-1-yl]acetamide (S)-34d²¹

$[\alpha]_{\text{D}}^{20} -103.1$ ($c = 0.85$, CHCl_3); Chiral HPLC analysis (25 cm x

4.6 mm Chiralpak AD-H column, 1% isopropanol-hexane at 1.0 mL/min. flow rate, 210 nm; t_{R} (*minor*) 28.6 min., t_{R} (*major*) 21.2 min., 95% *ee*.

¹H NMR (500 MHz, CDCl_3) δ 7.30-7.27 (m, 2H), 6.97-6.94 (m, 2H), 6.46 (bs, 1H), 6.07 (ddd, $J = 17.2, 10.5, 5.3$ Hz, 1H), 5.65-5.62 (m, 1H), 5.40-5.38 (m, 1H), 5.32-5.28 (m, 1H), 3.86 (s, 3H).

IR (neat) 3318 (m), 2952 (m), 2926 (m), 2856 (w), 1700 (s), 1545 (m), 1517 (m), 1456 (w), 1288 (m), 1192 (vs), 1178 (vs), 1160 (s), 1030 (m) cm^{-1} .



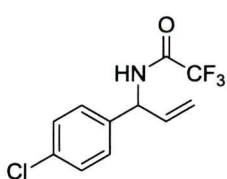
(S)-2,2,2-trifluoro-N-[1-(4-methylphenyl)prop-2-en-1-yl]acetamide 34e²¹

$[\alpha]_{\text{D}}^{20} -122.6$ ($c = 1.46$, CHCl_3); Chiral HPLC analysis (25 cm x

4.6 mm Chiralpak AD-H column, 1% isopropanol-hexane at 1.0 mL/min. flow rate, 210 nm; t_{R} (*minor*) 10.7 min., t_{R} (*major*) 12.0 min., 95% *ee*.

¹H NMR (500 MHz, CDCl_3) δ 7.25-7.17 (m, 4H), 6.47 (bs, 1H), 6.08-6.01 (m, 1H), 5.64-5.61 (m, 1H), 5.37 (d, $J = 10.4$ Hz, 1H), 5.29 (d, $J = 17.2$ Hz, 1H), 2.39 (s, 3H),

IR (neat) 3310 (m), 3083 (w), 2926 (w), 2856 (w), 1699 (vs), 1548 (m), 1366 (w), 1280 (w), 1180 (vs), 1161 (m), 998 (w) cm^{-1} .



N-[1-(4-chlorophenyl)prop-2-en-1-yl]-2,2,2-trifluoroacetamide 35f²¹

$[\alpha]_{\text{D}}^{20} -43.3$ ($c = 0.41$, CHCl_3); Chiral HPLC analysis (25 cm x

4.6 mm Chiralpak AD-H column, 1% isopropanol-hexane at 1.0 mL/min. flow rate, 220 nm; t_{R} (*minor*) 17.3 min., t_{R} (*major*) 20.2 min., 96% *ee*.

¹H NMR (500 MHz, CDCl_3) δ 7.39 (d, $J = 8.4$ Hz, 2H), 7.29-7.56 (m, 2H), 6.55 (bs, 1H), 6.03 (ddd, $J = 16.1, 10.4, 5.5$ Hz, 1H), 5.65-5.62 (m, 1H), 5.41 (d, $J = 10.5$ Hz, 1H), 5.29 (dd, $J = 16.9, 1.0$ Hz, 1H).

IR (neat) 3301 (m), 3083 (w), 2921 (w), 1702 (s), 1550 (m), 1491 (m), 1413 (w), 1326 (w), 1207 (s), 1167 (vs), 1092 (s), 1014 (m) cm^{-1} .



(S)-2,2,2-trifluoro-N-[1-[4-(trifluoromethyl)phenyl]prop-2-en-1-yl]acetamide 34g

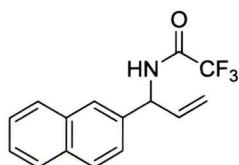
$[\alpha]_{\text{D}}^{20} -32.9$ ($c = 0.39$, CHCl_3); Chiral HPLC analysis (25 cm x 4.6 mm Chiralpak AD-H column, 1% isopropanol-hexane at 1.0 mL/min. flow rate, 210 nm; t_{R} (*minor*) 15.6 min., t_{R} (*major*) 20.9 min., 96% *ee*.

^1H NMR (500 MHz, CDCl_3) δ 7.69-7.65 (m, 2H), 7.46-7.43 (m, 2H), 6.66 (bs, 1H), 6.05 (ddd, $J = 17.0, 10.4, 5.7$ Hz, 1H), 5.73-5.70 (m, 1H), 5.44 (dd, $J = 10.5, 1.5$ Hz, 1H), 5.32 (dd, $J = 17.3, 1.6$ Hz, 1H).

^{13}C NMR (125 MHz, CDCl_3) δ 157.22 (e, q, $^2J_{\text{CF}} = 37.8$ Hz), 156.77 (e), 148.30 (e), 128.47 (e), 134.66 (o), 127.67 (o), 126.25 (o), 118.81 (e), 116.01 (e, q, $^1J_{\text{CF}} = 287.21$ Hz), 55.53 (o).

IR (neat) 3298 (w), 3073 (w), 2928 (w), 2851 (w), 1705 (s), 1621 (w), 1551 (m), 1421 (w), 1327 (vs), 1210 (s), 1164 (vs), 1128 (s), 1069 (s), 1018 (m) cm^{-1} .

HRMS (ESI, $[\text{M}-\text{H}]^-$) calcd for $\text{C}_{12}\text{H}_8\text{NOF}_6$ 296.0510, found 296.0499.



(S)-2,2,2-trifluoro-N-[1-(n-naphthyl)prop-2-en-1-yl]acetamide 34i

$[\alpha]_{\text{D}}^{20} -123.5$ ($c = 0.90$, CHCl_3); Chiral HPLC analysis (25 cm x

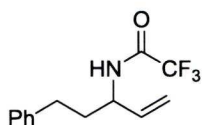
4.6 mm Chiralpak AD-H column, 1% isopropanol-hexane at 1.0 mL/min. flow rate, 215 nm; t_{R} (*minor*) 18.7 min., t_{R} (*major*) 20.9 min., 96% *ee*.

^1H NMR (500 MHz, CDCl_3) δ 7.88-7.83 (m, 3H), 7.77 (s, 1H), 7.54-7.51 (m, 2H), 7.39 (dd, $J = 8.5, 1.7$ Hz, 1H), 6.63 (bs, 1H), 6.13 (ddd, $J = 17.1, 10.5, 5.4$ Hz, 1H), 5.92-5.79 (m, 1H), 5.41 (dd, $J = 10.4, 1.0$ Hz, 1H), 5.33 (d, $J = 17.2, 1.3$ Hz, 1H).

^{13}C NMR (125 MHz, CDCl_3) δ 156.53 (e, q, $^2J_{\text{CF}} = 37.2$ Hz), 135.80 (e), 135.30 (o), 133.35 (e), 133.20 (e), 129.19 (o), 128.09 (o), 127.84 (o), 126.76 (o), 126.68 (o), 126.39 (o), 124.94 (o), 118.48 (e, q, $^1J_{\text{CF}} = 229.1$ Hz), 117.67 (e), 55.97 (o).

IR (neat) 3301 (m), 3272 (m), 2925 (w), 1700 (s), 1548 (m), 1363 (w), 1179 (vs), 1021 (m), 934 (m) cm^{-1} .

HRMS (ESI, $[\text{M}-\text{H}]^-$) calcd for $\text{C}_{15}\text{H}_{11}\text{F}_3\text{NO}$ 278.0804, found 278.0808.



(S)-2,2,2-trifluoro-N-(5-phenylpen-1-en-3-yl)acetamide 34i

$[\alpha]_D^{20} -34.7$ ($c = 0.47$, CHCl_3); Chiral HPLC analysis (25 cm x 4.6

mm Chiralpak AD-H column, 1% isopropanol-hexane at 1.0

mL/min. flow rate, 210 nm; t_R (major) 16.0 min., t_R (minor) 19.6 min., 98% ee.

^1H NMR (500 MHz, CDCl_3) δ 7.35-7.32 (m, 2H), 7.26-7.20 (m, 3H), 6.36 (bs, 1H), 5.82 (ddd, $J = 16.9, 10.7, 6.3$ Hz, 1H), 5.29-5.24 (m, 2H), 4.54 (quin, $J = 7.2$ Hz, 1H), 2.71 (t, $J = 7.8$ Hz, 2H), 2.03-1.93 (m, 2H).

^{13}C NMR (125 MHz, CDCl_3) δ 156.78 (e, q, $^2J_{\text{CF}} = 37.1$ Hz, 1C), 140.77 (e), 136.06 (o), 128.67 (o), 128.38 (o), 126.34 (o), 123.23 (o), 116.92 (e), 116.26 (e, q, $^1J_{\text{CF}} = 288.3$ Hz), 52.36 (o), 35.71 (e), 32.02 (e).

IR (neat) 3302 (w), 2089 (w), 3029 (w), 1701 (s), 1551 (m), 1455 (w), 1207 (s), 1162 (vs), 907 (vs) cm^{-1} .

HRMS (ESI, $[\text{M}-\text{H}]^-$) calcd for $\text{C}_{13}\text{H}_{13}\text{F}_3\text{NO}$ 257.1033, found 257.1032.

3.7 References

- (a) Welter, C.; Koch, O.; Lipowsky, G.; Helmchen, G. *Chem. Commun.* **2004**, 896.
 - (b) Welter, C.; Dahnz, A.; Brunner, B.; Streiff, S.; Dübon, P.; Helmchen, G. *Org. Lett.* **2005**, 7, 1239.
 - (c) Leitner, A.; Shekhar, S.; Pouy, M. J.; Hartwig, J. F. *J. Am. Chem. Soc.* **2005**, 127, 15506.
 - (d) Shi, Ce; Ojima, I. *Tetrahedron* **2007**, 63, 8563.
 - (e) Yamashita, Y.; Gopalarathnam, A.; Hartwig, J. F. *J. Am. Chem. Soc.* **2007**, 129, 7508.
 - (f) Singh, O. V.; Han, H. *Tetrahedron Lett.* **2007**, 48, 7094.
 - (g) Defieber, C.; Ariger, M. A.; Moriel, P.; Carreira, E. M. *Angew. Chem. Int. Ed.* **2007**, 46, 3139.
 - (h) Weix, D. J.; Marković, D.; Ueda, M.; Hartwig, J. F. *Org. Lett.* **2009**, 11, 2944.

- (i) Pouy, M. J.; Stanley, L. M.; Hartwig, J. F. *J. Am. Chem. Soc.* **2009**, *131*, 11312.
2. Vaska, L. *Acc. Chem. Res.* **1968**, *1*, 335.
3. Takeuchi, R.; Kashio, M. *Angew. Chem. Int. Ed.* **1997**, *36*, 263.
4. Janssen, J. P.; Helmchen, G. *Tetrahedron Letters*, **1997**, *38*, 8025.
5. Bartels, B.; Helmchen, G. *Chem. Commun.* **1999**, 741.
6. Kinoshita, N.; Marx, K. H.; Tanaka, K.; Tsubaki, K.; Kawabata, T.; Yoshikai, N.; Nakamura, E.; Fuji, K. *J. Org. Chem.* **2004**, *69*, 7960.
7. Fuji, K.; Kinoshita, N.; Tanaka, K.; Kawabata, T. *Chem. Commun.* **1999**, 2289.
8. Bartels, B.; García-Yebra, C.; Rominger, F.; Helmchen, G. *Eur. J. Inorg. Chem.* **2002**, 2569.
9. For a review on iridium-catalyzed allylic substitution reactions see: Helmchen, G.; Dahnz, A.; Dübon, Schelwies, M.; Weihofen, R. *Chem. Commun.* **2007**, 675.
10. (a) Feringa, B. L. *Acc. Chem. Res.* **2000**, *33*, 346.
(b) Tissot-Croset, K.; Polet, D.; Alexakis, A.; *Angew. Chem. Int. Ed.* **2004**, *43*, 2426.
(c) Polet, D.; Alexakis, A.; Tissot-Croset, K.; Corminboeuf, C.; Ditrach, K. *Chem. Eur. J.* **2006**, *12*, 3596.
11. (a) Bartels, B.; García-Yebra, C.; Rominger, F.; Helmchen, G. *Eur. J. Inorg. Chem.* **2002**, 2569.
(b) Kiener, C. A.; Shu, C.; Incarvito, C.; Hartwig, J. F. *J. Am. Chem. Soc.* **2003**, *125*, 14272.
(c) Leitner, A.; Shekhar, S.; Pouy, M. J.; Hartwig, J. F. *J. Am. Chem. Soc.* **2005**, *127*, 15506.
(d) Marković, D.; Hartwig, J. F. *J. Am. Chem. Soc.* **2007**, *129*, 11680.
(e) Spiess, S.; Raskatov, J. A.; Gnamm, C.; Brödnér, K.; Helmchen, G. *Chem. Eur. J.* **2009**, *15*, 11087.
(f) Madrahimov, S. T.; Markovic, D.; Hartwig, J. F. *J. Am. Chem. Soc.* **2009**, *131*, 7228.
12. Evans, P. A.; Clizbe, E. A. *Unpublished Results*.
13. Claridge, R. P.; Millar, R. W.; Sandall, J. P. B.; Thompson, C. *Tetrahedron* **1999**, *55*, 10243.
14. (a) Tillett, J. G. *Chem. Rev.* **1976**, *76*, 747.
(b) Gilchrist, T. L.; Moody, C. J. *Chem. Rev.* **1977**, *77*, 409.

15. Franz, J. A.; Martin, J. C. *J. Am. Chem. Soc.* **1975**, *97*, 583.
16. Cram, D. J.; Day, J.; Rayner, D. R.; von Schriltz, D. M.; Duchamp, D. J.; Garwood, D. C. *J. Am. Chem. Soc.*, **1970**, *92*, 7369.
17. Okamura, H.; Bolm, C.; *Org. Lett.* **2004**, *6*, 1305.
18. Lyothier, I.; Defieber, C.; Carreira, E. M. *Angew. Chem. Int. Ed.* **2006**, *45*, 6204.
19. Leitner, A.; Shu, C.; Hartwig, J. F. *Org. Lett.* **2005**, *7*, 1093.
20. Zwierzak, A.; Napieraj, A. *Synlett* **1998**, 930.
21. Pouy, M. J.; Leitner, A.; Weix, D. J.; Ueno, S.; Hartwig, J. F. *Org. Lett.* **2007**, *9*, 3949.
22. Wuts, P. G. M.; Ashford, S. W.; Anderson, A. M.; Atkins, J. R. *Org. Lett.* **2003**, *5*, 1483.
23. Buckley III, T. F.; Rappoport, H. *J. Am. Chem. Soc.* **1981**, *103*, 6157.

Chapter 4

Enantioselective Rhodium-Catalyzed Allylation of α -Alkoxy Ketone Enolates

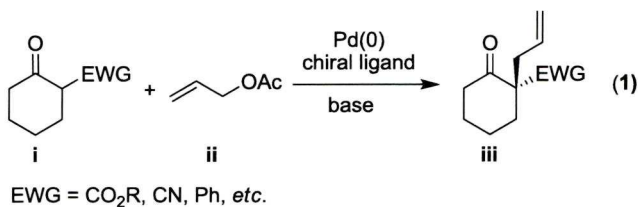
4.1 Introduction

4.1.1 Transition Metal-Catalyzed Allylation Reactions

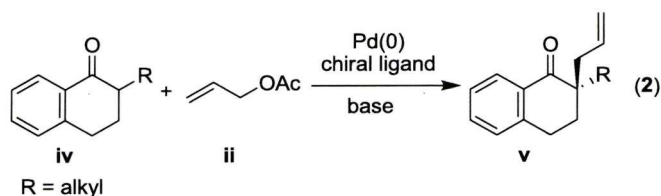
The asymmetric α -alkylation of ketone enolates represents one of the most important and challenging carbon-carbon bond forming reactions in organic synthesis.¹ This transformation has traditionally utilized chiral auxiliaries for stereoinduction; however, recent developments have been made in the enantioselective palladium-catalyzed allylic alkylation reaction using unstabilized ketone enolates. This provides a powerful method for the construction of tertiary and quaternary stereogenic centers.^{1,2}

4.1.2 Pronucleophile Scope

Frequently, a limitation in the metal-catalyzed allylic substitution reaction with ketones is the selective formation of the enolate. Several methods have been developed to circumvent this issue, including the use of symmetrical ketone pronucleophiles, blocking enolization, and the formation of silyl enols under kinetic or thermodynamic conditions.³ The groups of Hayashi,⁴ Ito,⁵ Trost,⁶ in addition to Hou and Dai⁷ have developed methods which utilize prochiral stabilized enolates (eq. 1).



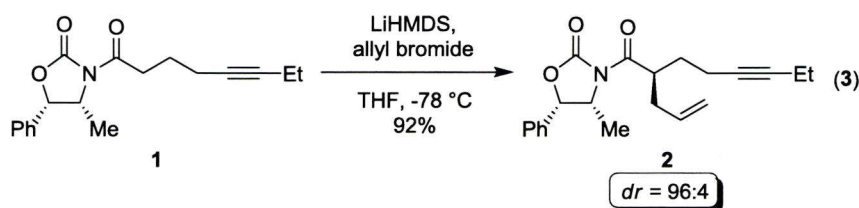
Later studies by Trost⁸ and Hou⁹ showed that unstabilized ketone enolates could be successfully employed using a weak base (eq. 2). Although both of these methods provide a solution to the issue of regioselectivity, the scope is limited to substrates where there is a large pK_a difference between the two acidic protons, or those that contain only one acidic site. The ideal transformation would allow the utilization of a wide range of pronucleophiles through the direct and *in situ* enolization of the ketone.



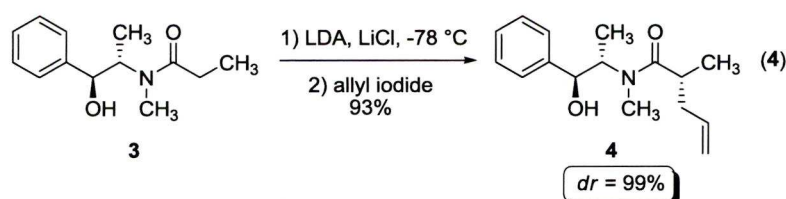
4.1.3 Non-Metal Allyl Methods for Performing Enantioselective and Diastereoselective Allylations.

4.1.3.1 Chiral Auxiliary-Based Allylations

Chiral auxiliaries have been proven effective in a number of different stereoselective reactions and have been employed extensively in total synthesis.^{1,10} The auxiliary is introduced into the substrate prior to the stereoselective step and then removed after the key reaction. In 1987, Smith and Fukui reported the total synthesis of biologically active (+)-phyllanthocin, in which the tertiary stereocenter was prepared *via* a diastereoselective auxiliary-based allylation reaction.¹¹ Treatment of imide **1** with lithium hexamethyldisilazide followed by addition of allyl bromide afforded **2** in 92% yield with excellent diastereoselectivity (eq. 3).

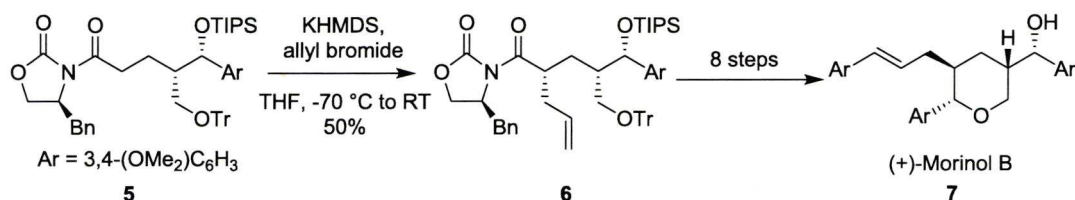


Myers and co-workers introduced pseudoephedrine as a chiral auxiliary.¹² The pseudoephedrine amides are easily prepared and generally crystalline. Treatment of the amides with base and an alkyl halide affords the α -substituted ketone products in excellent diastereoselectivity (eq. 4). Studies showed that lithium chloride was critical to accelerate the rate of alkylation and to suppress alkylation of the free hydroxyl on the auxiliary. Further examination of the reaction revealed that in all cases, the alkyl group adds *syn* to the methyl group on the pseudoephedrine chain. For example, treatment of the lithium enolate of **3** with allyl iodide affords **4** in 93% yield and with 99% diastereoselectivity. The synthetic utility of this methodology was demonstrated through further functionalization of the enantiomerically enriched alkylation products to afford enantiomerically enriched carboxylic acids, alcohols, aldehydes, and ketones.

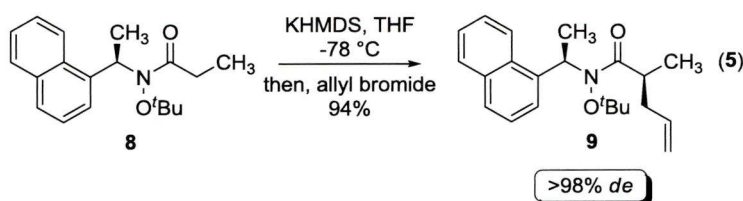


Yamauchi and co-workers have also demonstrated the synthetic utility of the auxiliary-based diastereoselective allylation reaction when determining the stereochemistry of the tetrahydropyran sesquienolignans, morinols A and B.¹³ Scheme 4.1 outlines the allylation reaction used in the synthesis of (+)-morinol B **7**. Treatment of the potassium enolate of **5** with allyl bromide afforded product **6** as a single isomer, albeit in moderate yield (50%).

Scheme 4.1 Diastereoselective allylation towards the synthesis of (+) morinol B.



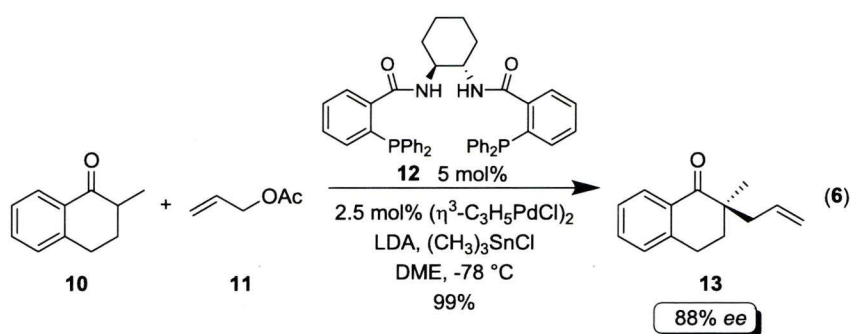
Recently, Davies reported the use of *N*-1-(1'-naphthyl-ethyl)-*O*-*tert*-butylhydroxyl-amine as a chiral Weinreb amide equivalent (eq. 5).¹⁴ Either enantiomer of the amide is easily prepared in four steps with no chromatographic purification required. Treatment of the potassium enolates with various alkyl halides afforded the alkylated products in high yield and excellent enantioselectivity (>95%). For example, treatment of ketone **8** with KHMDS, followed by allyl bromide, afforded ketone **9** in 94% yield and with >98% enantiomeric excess. To demonstrate the synthetic utility of this reaction, the alkylation products were functionalized directly into enantiomerically enriched aldehydes, ketones and iodolactones.



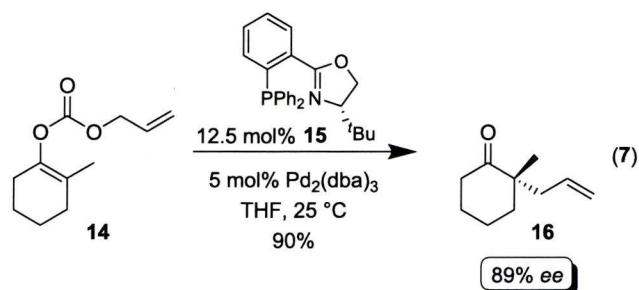
4.1.3.2 Enantioselective Palladium-Catalyzed Allylations

Although auxiliary-based methods efficiently afford enantiomerically enriched products, the added steps of introduction and removal, along with the cost of the reagents, have made this strategy less attractive. The enantioselective palladium-catalyzed allylic allylation reaction provides a catalytic method and has therefore drawn significant attention. In 1999, Trost and Schroeder described the enantioselective palladium-catalyzed asymmetric alkylation of ketone enolates (eq. 6).^{8a} Initial studies demonstrated that it was necessary to use a tin-modified lithium

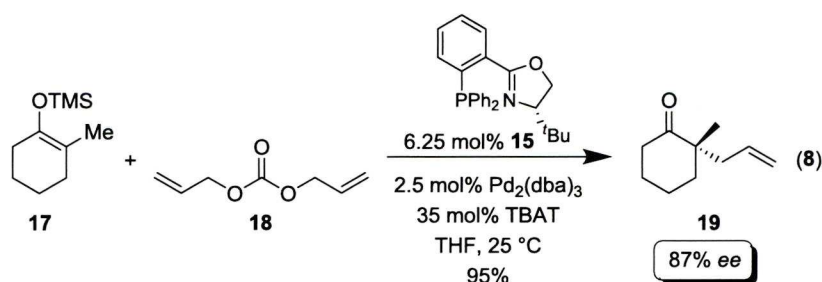
enolate in order to obtain higher enantioselectivities. The reaction was tolerant of various substituents at the 2-position, and high enantioselectivities (>80%) were obtained for all substrates except in the case of an α -substituted allyl group which afforded the product with 47% enantiomeric excess, albeit in good yield. For example, the reaction of ketone **10** under the optimized conditions afforded allylation product **13** in 99% yield and with 88% enantiomeric excess. The stereochemical outcome of the reaction was rationalized to arise from the interaction of the aromatic ring of the approaching enolate with the chiral pocket of the metal-allyl electrophile complex.



In 2004, Stoltz and Behenna reported the first example of the asymmetric Tsuji allylic alkylation using allyl enol carbonates to afford cyclohexanones with high levels of enantioselectivity.¹⁵ Preliminary ligand screening revealed chelating phosphorus/nitrogen ligands to be effective in terms of yield and enantioselectivity, with the *tert*-butyl phosphinooxazoline (*t*BuPHOX) ligand **15** being optimal (eq. 7). The reaction was tolerant of various substitution on the ring, in addition to six, seven- and eight-membered rings, to afford the products in high yield and enantioselectivity. The reaction of tetrasubstituted trimethylsilyl enol ethers underwent α -allylation with enantioselectivities up to 92%. For example, the reaction of allyl enol carbonate **14** in the presence of palladium and *t*BuPHOX afforded cyclohexanone **16** in high yield and with 89% enantiomeric excess. This method efficiently prepared highly enantiomerically enriched alpha quaternary centers with excellent regioselectivity.

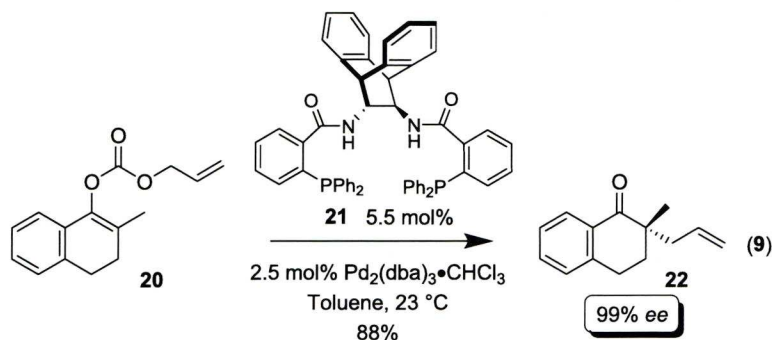


An intermolecular variant was also described utilizing a variety of silyl enol ethers and diallyl carbonate **18** (eq. 8).¹⁵ The addition of substoichiometric amounts of fluoride donor tetrabutylammonium difluorotriphenylsilicate (TBAT) was critical for the activation of the silyl enol ether. The results were comparable to those obtained when allyl enol carbonates were utilized; though, silyl enol ethers are often easier to prepare than the corresponding allyl enol carbonate. The reaction of silyl enol ether **17** under the optimized reaction conditions afforded cyclohexanone **19** in 95% yield and with 87% enantiomeric excess, compared to the 89% *ee* obtained using allyl enol carbonate **14**.

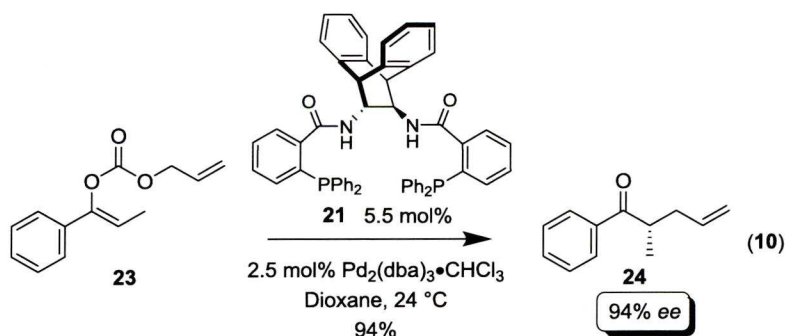


In 2005, Trost and Xu described the allylation of allyl enol carbonates utilizing bisphosphine ligand **21** (eq 9).¹⁶ The reaction afforded both tertiary and quaternary carbon centers in a highly enantioselective fashion. However, high enantioselectivity was limited to examples containing an aryl group on one side of the protected enol. For example, treatment of the allyl enol carbonate **20** under optimal conditions afforded the allylated product **22** in 88% yield and with excellent enantiomeric excess (99%). The absolute stereochemistry observed was opposite to that obtained from the palladium-catalyzed asymmetric allylic alkylation using lithium enolates. This suggests that the reaction of enol carbonates proceeds through a different mechanism. Although this reaction affords tertiary and quaternary centers

in a highly enantioselective manner, the synthetic utility of this reaction is limited by the necessity of the aryl group.

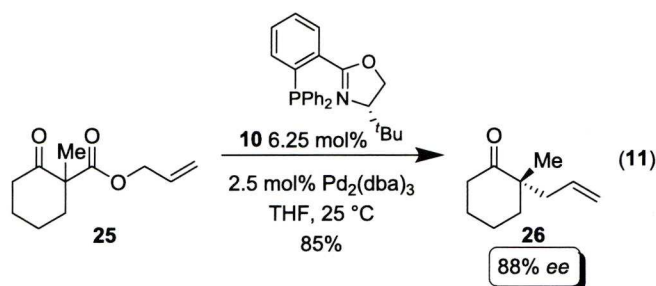


In related studies, Trost and Xu reported the first example of the palladium-catalyzed allylation reaction utilizing acyclic enolates as nucleophiles (eq. 10).¹⁷ The geometry of the enol precursor dictated both the absolute configuration of the product and the rate of reaction. This observation suggested that neither the palladium enolate nor the enol carbonate isomerize during the course of the reaction. The reaction is tolerant to a variety of aromatic ketones, affording products with enantioselectivity generally greater than 90%. For example, treatment of allyl enol carbonate **23** with palladium in the presence of bisphosphine ligand **21** afforded ketone **24** in excellent yield (94%) and enantiomeric excess (94%).



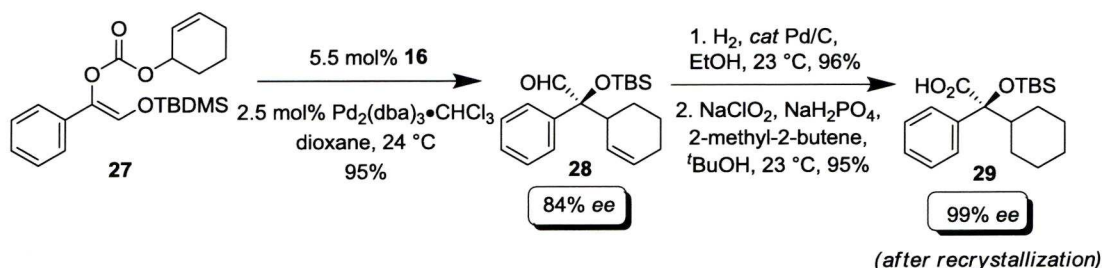
Stoltz and co-workers also described the deracemization of quaternary stereocenters *via* the palladium-catalyzed enantioconvergent decarboxylative allylation of racemic β -ketoesters (eq. 11).¹⁸ The reaction is tolerant to a wide array of substitution patterns and functionalities, including enolizable functional groups and β -heteroatoms. For example, the reaction of the methyl substituted variant **25** afforded cyclohexanone **26** in 85% yield and with 88% enantiomeric excess. All

examples proceeded regioselectively to afford products containing a quaternary center with high levels of enantioselectivity (up to 92%).

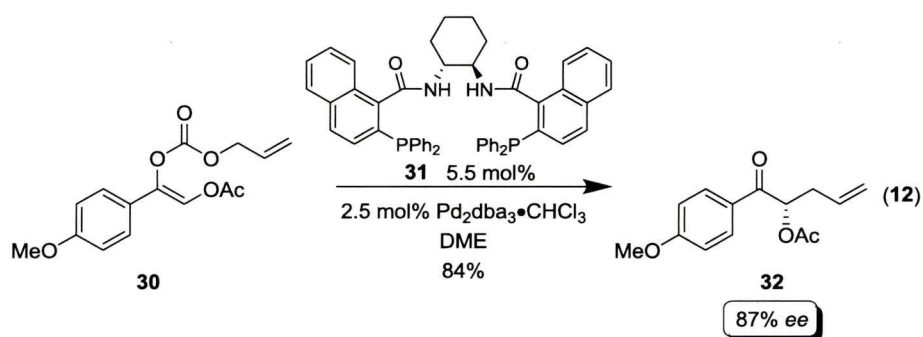


In 2007, Trost and co-workers used the palladium-catalyzed allylation to construct α -tertiary hydroxyaldehydes (Scheme 4.2).¹⁹ Protected allyl enol carbonates were used along with the analogous palladium complex previously employed to afford products with excellent enantioselectivity (up to 99%). For example, the reaction of **27** with $\text{Pd}_2(\text{dba})_3\text{CHCl}_3$ in the presence of bisphosphine ligand **16** afforded α -silyloxy hydroxyaldehyde **28** in 95% yield and with 84% enantiomeric excess. Aldehyde **28** was then further functionalized to carboxylic acid **29**, an intermediate in the synthesis of (*S*)-oxybutynin, *via* hydrogenation of the alkene and oxidation of the aldehyde. The carboxylic acid was obtained in high yield and 84% enantiomeric excess, which was increased to >99% *ee* after one recrystallization.

Scheme 4.2 Construction of (*S*)-oxybutynin intermediate **29** *via* palladium-catalyzed allylic allylation.



In 2008, Trost and co-workers described the palladium-catalyzed decarboxylative asymmetric allylic alkylation of 1,2-enediol carbonates to afford α -acyloxyketones with high regio- and enantioselectivity (eq. 12).²⁰ Initial studies showed that the use of a TBS-protected enediol affords the α -alkoxyketone in low yield, largely due to the formation of the corresponding quaternary silyloxy aldehyde. Changing the alcohol protecting group to an acetate furnished solely the α -alkoxyketones in high yield and enantioselectivity for aryl and α,β -unsaturated ketones. For instance, the reaction of substrate **30** in the presence of $\text{Pd}_2(\text{dba}_3) \cdot \text{CHCl}_3$ and ligand **31**, afforded ketone **32** in 84 % yield and with 87% enantiomeric excess. The reaction was tolerant of non-conjugated ketones; however, the products were obtained in slightly lower yield and enantioselectivity. These studies demonstrate that tuning the ligand allows for formation of either the α -alkoxyketone or the silyloxy aldehyde selectively.



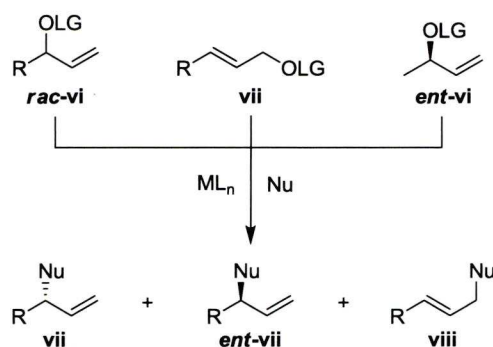
4.2 Rhodium-Catalyzed Allylic Substitution: Mechanistic Background

4.2.1 Introduction

The metal-catalyzed allylic substitution reaction has been studied using a wide array of transition metal complexes, and represents an important cross-coupling reaction for the construction of tertiary and quaternary carbon-carbon and carbon-heteroatom bonds with both stabilized and unstabilized nucleophiles (Scheme 4.3).²¹

Although the enantioselective version of this reaction dominates the field, we²² and others²³ have demonstrated the merit of the enantiospecific version. For example, many enantioselective variants employ substrates that furnish symmetrical π -allyl intermediates in order to circumvent problems with regioselectivity. There are also examples of allylic substitution reactions utilizing 3-substituted propenyl alcohol derivatives; however, high selectivities are generally only obtained with electronically biased cinnamyl derivatives.^{21b} Furthermore, depending on the metal used, π - σ - π isomerization of the π -allyl intermediate can occur, leading to racemization of unsymmetrical chiral allylic alcohol derivatives.^{24,25}

Scheme 4.3 Reaction profile for the metal-catalyzed allylic alkylation reaction with acyclic 3-substituted propenyl derivatives.



Although numerous transition-metal complexes catalyze the allylic substitution reaction, palladium-complexes have been the most widely utilized, and the majority of the metals have been proposed to proceed *via* a symmetrical π -allyl complex. The main issue with reactions proceeding through this pathway is the ability to afford secondary products through substitution at the more sterically hindered termini of the allyl system. Although the issue of regioselectivity is complex, there have been numerous reports in recent years of reactions that provide good regiocontrol and excellent enantioselectivity.²⁶

Tsuji and co-workers demonstrated that in contrast to the palladium-catalyzed version, the rhodium-catalyzed allylic alkylation reaction proceeds in a highly regioselective manner.²⁷ Subsequent work within our group demonstrated Wilkinson's catalyst modified *in situ* with triorganophosphites afforded high

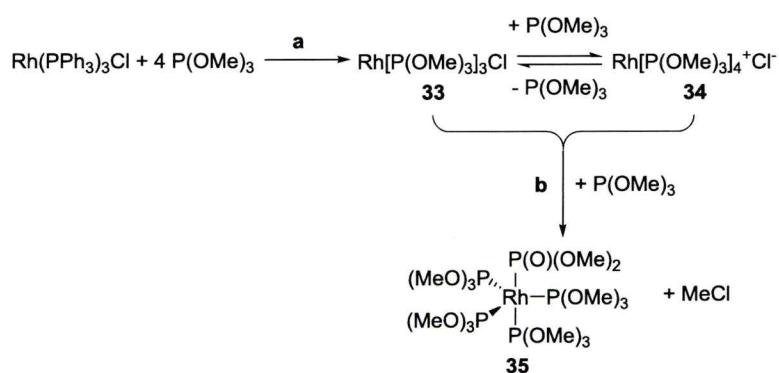
regiocontrol and enantiospecificity with a variety of nucleophiles.^{21c,28-31} The origin of this selectivity was consistent with the formation of a configurationally stable electronically *distorted* π -allyl or *enyl*^{22,32,33} ($\sigma + \pi$) organorhodium intermediate.³⁴

4.2.2 Pre-Catalyst Composition: Effect of the Trimethyl Phosphite Modifier.

NMR is a useful tool for characterizing compounds present within a reaction mixture. Specifically, $^{31}\text{P}\{^1\text{H}\}$ NMR spectroscopy is a useful tool for characterizing the complexes derived from the modification of $\text{Rh}(\text{PPh}_3)_3\text{Cl}$ with $\text{P}(\text{OMe})_3$. The identification of these complexes is possible from the coupling between ^{31}P and the 100% abundant ($I = 1/2$) ^{103}Rh . Variable temperature experiments are required in order to reduce levels of line broadening, which are due to the exchange of free phosphites with ligands bound to $\text{Rh}(\text{I})$.^{35,36}

Comprehensive NMR studies, previously performed within our group, revealed the *in situ* modification of Wilkinson's catalyst with four equivalents of trimethylphosphite resulted in complete displacement of the triphenylphosphine ligands from the rhodium.^{37,38} An initial dynamic equilibrium was observed between species **33** containing three coordinating phosphites and species **34** with four coordinating phosphites, which ultimately results in the irreversible formation of five-coordinate **35** resulting in a 1:1 mixture of **33** and **35**(Scheme 4.4).

Scheme 4.4 Results of *in situ* modification of Wilkinson's catalyst with $\text{P}(\text{OMe})_3$.

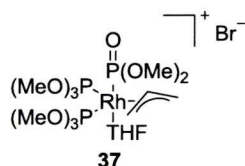


In a related study aimed at trying to understand the rhodium-*enyl* intermediate, species **33** was examined. The formation of complex **35** is more complicated than the addition of a fifth phosphite ligand, as one of the phosphites is itself modified. Reaction **b** is an example of an Arbuzov dealkylation (Scheme 4.4).³⁹⁻⁴¹ Displacement of the coordinated chloride from the rhodium metal generates the chloride anion that then acts as a nucleophile to facilitate dealkylation. After addition of a fifth phosphite ligand, the chloride anion dealkylates the methyl substituent on one of these ligands, generating the five-coordinate phosphonate complex **35** (eq. 13). It was concluded that the presence of a chloride anion is critical for this transformation to occur, since the phosphonate is only generated when the P/Rh ratio is ≥ 4 .



Treatment of $\text{Rh}[\text{P}(\text{OMe})_3]_3\text{Cl}$ with 20 equivalents of allyl methyl carbonate at 50 °C led to the formation of Rh(III) complex **37**, where one of the phosphite ligands was transformed into the phosphonate. It was hypothesized that this rhodium allyl complex could create a well defined environment for the formation of an asymmetric catalyst using a chiral phosphite ligand.

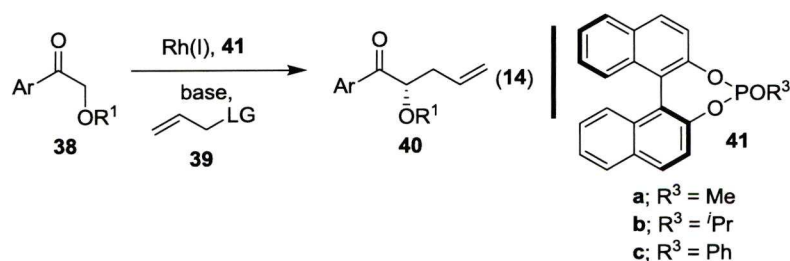
Figure 4.1 Rhodium allyl phosphonate complex by NMR.



4.3 Rhodium-Catalyzed Enantioselective Allylation

4.3.1 Hypothesis

Protected secondary homoallylic alcohols represent a class of synthetically important compounds.⁴² These compounds are generally prepared through the alkylation of chiral-auxiliary-based ketones with α -oxygenated side-chains or *via* enantioselective allylation of an aldehyde followed by protection of the newly formed hydroxyl group.⁴³ Previous work within our lab formed similar compounds *via* the rhodium-catalyzed diastereoselective and enantiospecific allylic alkylation of alkoxy ketone enolates, providing two contiguous stereocenters by means of relaying stereochemical information.^{29b} It was proposed the utility of the reaction could be expanded if the allylic substituent were removed. However, this eliminates the stereodirecting portion of the molecule and creates the necessity to develop an enantioselective rhodium-catalyzed allylic alkylation reaction. It was envisioned that chiral phosphite ligands **41** would be effective for the enantioselective rhodium-catalyzed allylation reaction (eq. 14).

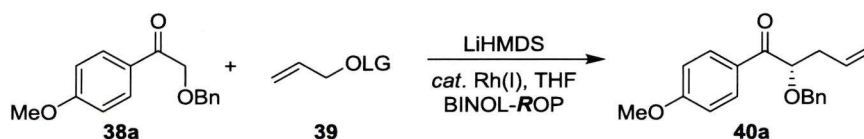


4.3.2 Reaction Optimization

Table 4.1 summarizes the development of the enantioselective rhodium-catalyzed allylic alkylation reaction using the prochiral aryl ketone **38a** (Ar = 4-MeOC₆H₄, R¹ = PhCH₂).⁴⁴ Initial studies systematically varied the R group on the chiral phosphite, in order to determine if changes to the steric environment had an effect on the catalytic activity, and also to probe the importance of the Arbuzov dealkylation.^{38,39} Under the reaction conditions, the methyl variant **41a** readily undergoes the dealkylation. In contrast, this dealkylation is very unlikely to occur for the ⁱPr version, and the phenyl substituent is unable to undergo the S_N2 attack necessary for the Arbuzov reaction. Treatment of the lithium enolate of **38a** with allyl methyl carbonate, in the presence of the chiral complex derived from the modification of Wilkinson's catalyst with the individual phosphite ligands, furnished the allylic alkylation product **40a** in low yield and with poor enantiomeric excess (entries 1-3). Although the yields and selectivities were poor in each example, the methyl substituted phosphite (BINOL-*Me*OP) provided superior enantioselectivity (entry 1 vs. 2/3) which suggests the Arbuzov dealkylation is critical to obtain high levels of enantioselectivity.

Further optimization utilizing BINOL-*Me*OP demonstrated that reducing the reaction temperature to 0 °C resulted in an increased enantioselectivity (51%), however the yield remained moderate (Table 4.1, entry 4). The effect of the leaving group was then investigated, and comparable yields were observed for both the *tert*-butyl and benzyl carbonates (entries 5 and 6), with a marginal increase in enantioselectivity in the former case (67%). Gratifyingly, the benzoate leaving group afforded a dramatic increase in both yield and enantioselectivity, affording the alkylation product in 87% and in 90% enantiomeric excess (entry 7). The yield and enantioselectivity increased further when the reaction temperature was decreased to -10 °C (entry 8).

Table 4.1 Optimization of the enantioselective rhodium-catalyzed allylic alkylation reaction.^a



Entry	LG =	BINOL- ROP	Temp (°C)	Yld (%) ^b	ee (%) ^c
1	CO ₂ Me	Me	22	44	44
2	“	<i>i</i> Pr	“	29	5 ^d
3	“	Ph	“	16	5 ^d
4	“	Me	0	41	51
5	CO ₂ ^t Bu	“	“	49	67
6	CO ₂ Bn	“	“	47	50
7	COPh	“	“	87	90
8	“	<i>Me</i>	<i>-10</i>	<i>90</i>	<i>93</i>

^aAll reactions were carried out on a 0.25 mmol reaction scale using 10 mol% RhCl(PPh₃)₃ *modified* with 10 mol% of the chiral phosphite and 2.0 equiv. of the lithium enolate in THF. ^bIsolated Yields. ^cThe enantioselectivity was determined by chiral HPLC on isolated products, using a Diacel AD-H column. ^dThe opposite enantiomer was formed.

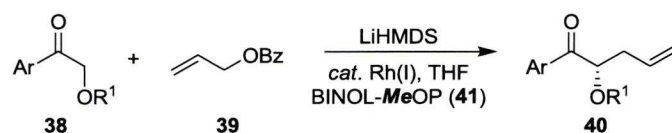
4.3.3 Substrate Scope

Table 4.2 summarizes the application of the optimized reaction conditions (Table 4.1, entry 8) to a variety of differentially protected aryl ketones. Entries 1-9 demonstrate the effect of the alkoxy substituents (R¹) of the pronucleophile. The reaction is tolerant of benzyl groups (entries 1-2), as well as linear and branched alkyl groups (entries 3-5) affording the alkylation products in high yield and excellent enantioselectivity. The electronic nature of the aryl ether was shown to impact the level of enantioselectivity (entries 6-8) with electron withdrawing groups affording products with decreased levels of enantiomeric excess. The reaction was shown to proceed efficiently with the *tert*-butylcarbonyl derivative (entry 9) to afford

homoallylic product **40i**, which is a useful intermediate for the construction of *syn*-1,3-polyols.⁴⁷

As observed with the alkoxy aryl derivatives, a similar electronic trend was observed with the aryl ketone component (Ar), where the more electron deficient derivatives provided products with lower enantioselectivities (Table 4.2, entries 6-8 vs. 10-14). The reaction of **38h** (Ar = 4-(CF₃)C₆H₄) was stopped at partial conversion to determine if epimerization was occurring throughout the course of the reaction. The product was isolated with comparable enantiomeric excess, demonstrating that epimerization was not occurring. These observations are consistent with the hypothesis that more nucleophilic enolates afford higher levels of enantioselectivity.

Table 4.2 Scope of the enantioselective rhodium-catalyzed allylic alkylation reaction with the α -alkoxy lithium enolates.^a



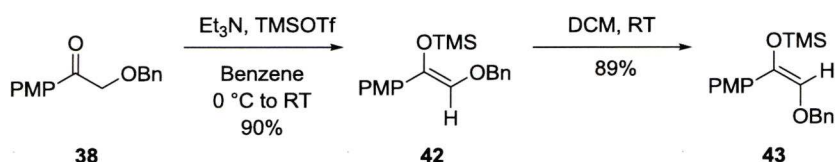
Entry	Ketone 38		Yld (%) ^b	<i>ee</i> (%) ^{c,d}
	Ar =	R ¹ =		
1	4-MeOC ₆ H ₄ -	PhCH ₂ -	a	90
2	“	4-MeOC ₆ H ₄ CH ₂ -	b	90
3	“	Me-	c	83
4	“	Allyl-	d	88
5	“	ⁱ Pr-	e	80
6	“	4-MeOC ₆ H ₄	f	85
7	“	Ph-	g	88
8	“	4-(CF ₃)C ₆ H ₄ -	h	83
9	“	^t BuOCO-	i	84
10	2,4-(MeO) ₂ C ₆ H ₃ -	PhCH ₂ -	j	81
11	Ph-	“	k	92
12	4-FC ₆ H ₄ -	“	l	86
13	4-ClC ₆ H ₄ -	“	m	81
14	4-(CF ₃)C ₆ H ₄ -	“	n	91
15	Naphthyl-	“	o	89
16	Furyl-	“	p	90

^aAll reactions were carried out on a 0.25 mmol reaction scale. ^bIsolated Yields. ^cThe enantioselectivity was determined by chiral HPLC on the purified products, using a Diacel AD-H column. ^dAbsolute configuration was assigned by analogy to **40a**.

4.3.4 Enolate Geometry

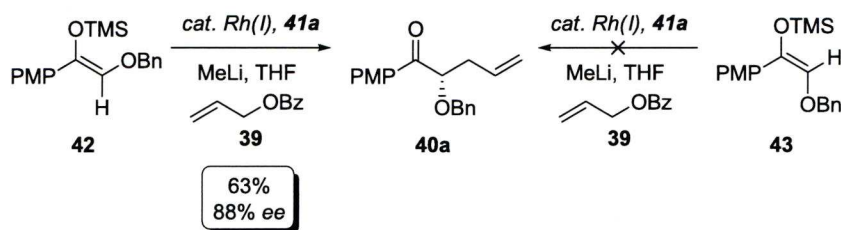
Both the *E*- and *Z*-silyl enol ethers were prepared in order to determine if the enolate geometry had any influence on the stereochemical outcome or the rate of the reaction. Deprotonation of **38a** with triethylamine, followed by trapping with TMSOTf, afforded the *Z*-silyl enol ether **42** in 90% yield (Scheme 4.5). *E*-silyl enol ether **43** was obtained through the spontaneous isomerization of **42** in wet dichloromethane overnight.

Scheme 4.5 Preparation of *E*- and *Z*-silyl enol ethers of **38**.



With both silyl enol ethers in hand, the effect of the enolate geometry could be probed. The *Z*- and *E*-lithium enolates were generated *in situ* by treating the silyl enol ether with methyllithium at -10 °C for 1 hour.⁴⁸ Once the generation of the enolate was complete, a solution of Wilkinson's catalyst *modified* with chiral phosphite ligand **41a** was added, followed by the addition of allyl benzoate **39** (Scheme 4.6). Interestingly, when the reaction was performed with the *E*-enolate generated from **43**, no reaction occurred. In contrast, when the *Z*-enolate was generated from **42**, allylation product **40a** was obtained in 63% yield and with 88% *ee*. Although the efficiency of the reaction was lower from the silyl enol ether, this study clearly demonstrates the geometry of the enolate is critical for reactivity.

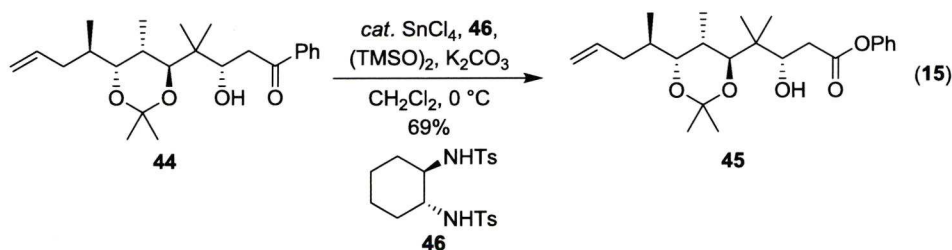
Scheme 4.6 Rhodium-allylation starting from silyl enol ethers.



4.3.5 Baeyer-Villiger

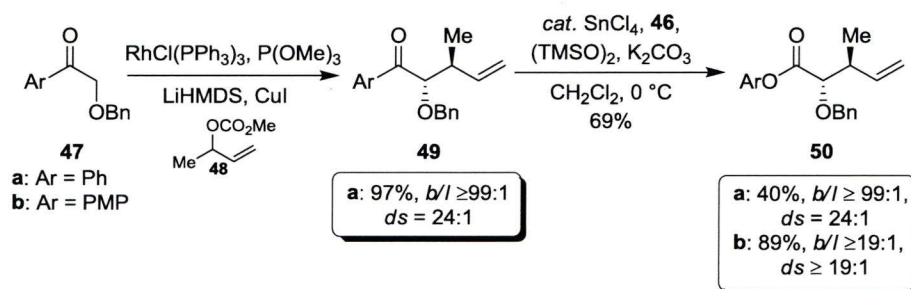
4.3.5.1 Background

The Baeyer-Villiger reaction is a convenient method to transform ketones into esters or lactones.⁴⁹ Since the discovery of the oxidation in 1899 by Adolf Baeyer and Victor Villiger, many variations have been developed. Although the applications of this method are numerous, the oxidation of a ketone in the presence of an olefin is often challenging. In 1997, Shibasaki published a selective metal-catalyzed method which utilized a catalytic amount of bissulfonamide **46** with tin tetrachloride and bistrimethylsilyl peroxide as the oxidant.⁵⁰ The reaction proved to be highly regioselective and it was hypothesized that the reaction could be tailored to substrates by varying the ligand. The reaction was later used in the total synthesis of epothilones A and B in which the oxidation was efficient in the presence of an olefin (eq. 15).⁵¹



Evans and Lawler applied this chemistry to the acyclic α -alkoxyketones afforded from the regio- and diastereoselective rhodium-catalyzed allylic substitution reaction.^{29b} Treatment of phenyl ketone **47a** under Shibasaki's conditions afforded ester **49a** in low yield (Scheme 4.7). The only isolated by-product of the reaction was an epoxide, which indicated over oxidation. It was envisioned that making the phenyl ketone **47** more electron rich would increase the rate of the Baeyer-Villiger oxidation over the olefin epoxidation. Gratifyingly, using a *p*-methoxy aryl ketone **47b** in the rhodium-alkylation reaction followed by *in situ* oxidation afforded the corresponding ester **50b** in 89% yield over the two steps with excellent regio- and diastereoselectivity.

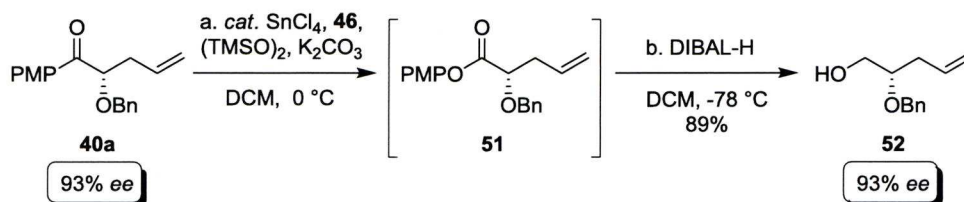
Scheme 4.7 Baeyer-Villiger oxidation of α -alkoxyketones.



4.3.5.2 Application Towards Rhodium-Catalyzed Allylation

While the enantioselective rhodium-catalyzed allylic alkylation reaction with lithium enolates is synthetically useful, the necessity for using aryl-substituted ketones may be problematic. Therefore, the ability to functionally manipulate the aryl ketone to form an alcohol would be advantageous. Gratifyingly, treatment of the aryl ketone **40a** under Baeyer-Villiger conditions afforded corresponding ester **51**.⁵² The ester intermediate was then reduced *in-situ* affording known alcohol **52**, which has been used in many synthetic applications, in 89% overall yield and with no loss of enantiomeric purity (Scheme 4.8). The synthesis of **52** allowed the confirmation of absolute stereochemistry by comparison to reported spectroscopic values.⁵³

Scheme 4.8 Preparation of alcohol **52**.



4.4 Conclusions

In conclusion, we have developed the first example of a highly enantioselective rhodium-catalyzed allylic alkylation reaction of *acyclic* α -alkoxy aryl ketone enolates using chiral monophosphite ligands. The chiral phosphite ligand study demonstrated the importance of the metal-Arbuzov reaction for the formation of the active catalyst in order to obtain high levels of enantioselectivity. We anticipate this will provide a versatile method for the enantioselective construction of acyclic protected homoallylic alcohols.

4.5 Experimental

General

Unless otherwise indicated, all reactions were carried out in flame-dried glassware, under an atmosphere of argon or nitrogen. Tetrahydrofuran (THF) was distilled from sodium benzophenone ketyl. All other starting materials were purchased from Acros, Aldrich, Alfa Aesar, or Fluorochem and used without further purification unless otherwise stated.

All acetophenone-derived ketones were prepared using literature procedures, and recrystallized as appropriate. All carbonates were prepared using literature procedures and distilled before use. Wilkinson's catalyst $[\text{RhCl}(\text{PPh}_3)_3]$ was

prepared in 5 mmol batches. Trimethyl phosphites were distilled and stored over 4Å molecular sieves.

Racemic mixtures were synthesized by alkylating the lithium enolate with allyl iodide without presence of catalyst.

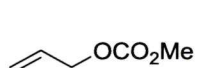
Allylic leaving groups were synthesized according to known procedures.

Thin layer chromatography (TLC) was performed on Whatman F₂₅₄ precoated silica gel plates. Visiulation was accomplished with a UV light and/or a KMnO₄ solution. Flash chromatography (FC) was performed using either Merck Silica Gel 60 (230-400 mesh) or Whatman Silica Gel Purasil[®] 60Å (230-400 mesh). Solvents for extraction and FC were technical grade. Reported solvent mixtures for TLC and FC are volume/volume mixtures. Infrared spectra were obtained on a Perkin-Elmer spectrum 100 series FTIR spectrometer peaks are reported in cm⁻¹ with the following relative intensities: vs (very strong), s (strong), m (medium) and w (weak). Mass spectra were performed at either the Indiana University Mass Spectrometry Center, the University of Liverpool Mass Spectrometry Center or the EPSRC National Mass Spectrometry Service Centre, Swansea. High-resolution electron-impact (EI, ionization voltages of 70 eV), chemical ionization (CI, reagent gas CH₄ or NH₃) were obtained on either an Autospec, ZAB 2SE, Kratos MS-80, VG 7070E double focusing magnetic sector mass spectrometer equipped with a solid probe inlet, a Quattro II, MAT 95, or MAT 900. The electrospray ionization (ESI) mass spectra were obtained on a Waters micromass LCT mass spectrometer. ¹H and ¹³C NMR were recorded on a Bruker AV 500 MHz NMR spectrometer in the indicated deuterated solvents, which were obtained from Cambridge Isotope Labs. For ¹H NMR, CDCl₃ was set to 7.26 ppm (CHCl₃ singlet). For ¹³C NMR, CDCl₃ was set to 77.16 ppm (CDCl₃ center of triplet). For ³¹P NMR, samples were externally referenced to phosphoric acid set to 0.00 ppm. ¹H data are reported in the following order: chemical shift in ppm (δ) (multiplicity, which are indicated by br (broadened), s (singlet), d (doublet), t (triplet), q (quartet), m (multiplet)); assignment of 2nd order pattern, if applicable; coupling constants (*J*, Hz); integration values for All ¹³C NMR spectra data using the descriptor *o* and *e* refer to whether the peak is odd or even respectively, and correlate to an attached proton test (ATP) experiment.

All liquid chromatographs were obtained on the Agilent 1200 series HPLC, equipped with a variable wavelength UV detector. The instrument was fitted with

either a CHIRALCEL™ AD-H column (Diacel, 4.6mm x 25cm) or CHIRALCEL™ OD column (Diacel, 4.6mm x 25nm).

All liquid chromatographs were obtained on the Agilent 1200 series HPLC, equipped with a variable wavelength UV detector. The instrument was fitted with either a CHIRALCEL™ AD-H column (Diacel, 4.6mm x 25cm) or CHIRALCEL™ OD column (Diacel, 4.6mm x 25nm).

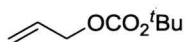


Allyl methyl carbonate 39a⁵⁴

Prepared according to general synthesis of allylic carbonates outlined in chapter 2:

¹H NMR (500 MHz, CDCl₃) δ 5.99-5.89 (m, 1H), 5.37 (dd, *J* = 17.2, 1.3 Hz, 1H), 5.28 (dd, *J* = 10.5, 1.1 Hz, 1H), 4.62 (d, *J* = 5.7 Hz, 2H), 3.79 (s, 3H).

IR (Neat) 3008 (w), 2960 (w), 1746 (s), 1444 (m), 1365 (w), 1252 (s) cm⁻¹.



Allyl *tert*-butyl carbonate 39b⁵⁵

Prepared according to general synthesis of allylic carbonates outlined in chapter 2:

¹H NMR (500 MHz, CDCl₃) δ 5.96-5.88 (m, 1H), 5.37-5.31 (m, 1H), 5.27-5.22 (m, 1H), 4.62 (d, *J* = 4.7 Hz, 1H), 4.54 (d, *J* = 4.8 Hz, 1H) 1.46 (s, 9H)

IR (Neat) 2982 (w), 2937 (w) 1739 (s), 1455 (w), 1369 (m), 1273 (s), 1248 (s) cm⁻¹.



Allyl benzyl carbonate 39c⁵⁶

Prepared according to general synthesis of allylic carbonates outlined in chapter 2:

¹H NMR (500 MHz, CDCl₃) δ 7.41-7.33 (m, 5H), 5.98-5.90 (m, 1H), 5.36 (dd, *J* = 17.2, 1.3 Hz, 1H), 5.27 (dd, *J* = 10.4, 1.3 Hz, 1H), 5.18 (s, 2H), 4.65 (dt, *J* = 2.5, 1.6 Hz, 2H)

IR (Neat) 3035 (w), 2955 (w), 1742 (s), 1456 (m), 1386 (m), 1240 (s) cm⁻¹.



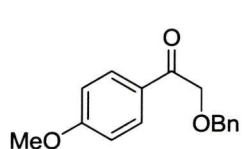
Allyl benzoate 39d⁵⁷

Prepared according to general synthesis of allylic carbonates outline in chapter 2:

¹H NMR (500 MHz, CDCl₃) δ 8.08-8.06 (m, 2H), 7.58-7.55 (m, 1H), 7.46-7.43 (m, 2H) 6.05 (ddt, *J* = 17.2, 10.6, 5.4 Hz, 1H), 5.42 (dd, *J* = 17.2, 1.5 Hz, 1H), 5.29 (dd, *J* = 10.5, 1.2 Hz, 1H), 4.83 (dt, *J* = 5.6, 1.3 Hz, 2H).

IR (Neat) 3073 (w), 2945 (w), 1718 (s), 1452 (m), 1361 (m), 1266 (s) cm^{-1} .

General procedure for preparation of aryl ketones:



2-(Benzyloxy)-1-(4-methoxyphenyl)ethanone 38a

Benzyloxyacetic acid⁵⁸ (21.65 g, 130 mmol) was dissolved in dichloromethane (600 mL) in a 2 liter round-bottom flask equipped with a magnetic stir-bar. 2-Chloro-1-methylpyridinium iodide (39.90 g, 156 mmol) was added in portions along with N,O-dimethylhydroxylamine hydrochloride (13.29 g, 135 mmol). The flask was flushed with argon and cooled on an ice bath for 15 minutes. Triethylamine (61.57 mL, 442 mmol) was injected over 10 minutes and the reaction was slowly brought to a gentle reflux overnight. The flask was then cooled and quenched with water (300 mL). The layers were separated, and the aqueous layer washed with dichloromethane (300 mL). The organic layers were combined, dried over magnesium sulphate, filtered, and concentrated. The resulting crude oil was preabsorbed onto silica gel and flushed through a short plug of silica gel using 40% ethyl acetate/hexanes to afford 20.92g (75%) of semi-purified weinreb amide, which was used in the next step with no further purification.

Flame-dried magnesium metal (3.01 g, 124 mmol) was suspended in tetrahydrofuran (125 mL) under argon in a 1 liter flask equipped with a condenser and an addition funnel. One crystal of iodine added to the magnesium suspension and 4-bromoanisole (18.6 mL, 124 mmol) was added to the addition funnel. Approximately 1 mL 4-bromoanisole was added to the round bottom flask, and the solution was heated to activation, detected by the solution going colorless, at which point the remaining 4-bromoanisole was slowly added to maintain a gentle reflux. The grignard solution was allowed to cool to room temperature for 1 hour.

The semi-pure weinreb amide (20.92 g, 100 mmol) was dissolved in dry tetrahydrofuran (700 mL) under argon in a 2 liter flask. The flask was then cooled on an ice-bath for 30 minutes. The previously prepared grignard solution was then carefully transferred *via* Teflon cannula into the weinreb amide solution over 10 minutes and the entire solution was warmed to room temperature. The reaction was then cooled on an ice-bath and slowly quenched with saturated aqueous ammonium chloride solution (300 mL) and diethyl ether (300 mL). The layers were separated and the aqueous layer was extracted with diethylether (2 x 200 mL). The organic

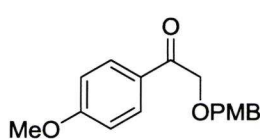
layers were combined and dried using magnesium sulphate, filtered, and concentrated. The resultant oil (which may solidify) was taken up in 60 mL ethyl acetate and heated. 300 mL hexanes was slowly added while maintaining gentle heating. The flask was allowed to slowly cool to room temperature and then placed in the refrigerator for several hours yielding large needle-like crystals of **32a**, which were isolated *via* vacuum filtration and washed with chilled hexanes (60 mL) to afford white crystals.

¹H NMR (500 MHz, CDCl₃) δ 7.93-7.90 (m, 2H), 7.40-7.29 (m, 5H), 6.94-6.91 (m, 2H), 4.72 (s, 2H), 4.68 (s, 2H), 3.86 (s, 3H).

¹³C NMR (125 MHz, CDCl₃) δ 194.87 (e), 163.85 (e), 137.47 (e), 130.35 (o), 128.57 (o), 128.12 (o), 127.07 (e), 128.03 (o), 113.92 (o), 73.13 (e), 72.56 (e), 55.55 (o).

IR (Neat) 3010 (w), 2937 (w), 2846 (w), 1685 (s), 1602 (m), 1576 (m), 1420 (m), 1232 (m), 1182 (m), 1031 (m) cm⁻¹.

HRMS (EI, M-H) calcd for C₁₆H₁₅O₃ 255.1016, found 255.1021.



2-[(4-Methoxybenzyl)oxy]-1-(4-methoxyphenyl)ethanone
38b

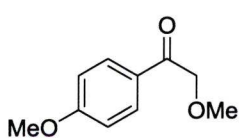
Prepared according to general synthesis of aryl ketones:

¹H NMR (500 MHz, CDCl₃) δ 7.99-7.97 (m, 2H), 6.95-6.93 (m, 2H), 6.89 (d, *J* = 9.3 Hz, 2H), 6.81 (d, *J* = 7.4 Hz, 2H), 5.15 (s, 2H), 5.14 (s, 2H), 3.74 (s, 3H), 3.78 (s, 3H).

¹³C NMR (125 MHz, CDCl₃) δ 193.47 (e), 164.07 (e), 154.45 (e), 152.37 (e), 130.57 (o), 127.73 (e), 115.99 (o), 114.74 (o), 114.05 (o), 71.68 (e), 71.64 (e), 55.74 (o), 55.59 (o).

IR (Neat) (neat) 2932 (w), 2852 (w), 1686 (s), 1600 (m), 1510 (m), 1422 (m), 1235 (s), 1175 (m), 1027 (m) cm⁻¹.

HRMS (CI, M-H) calcd for C₁₇H₁₇O₄ 285.1121, found 285.1130.



2-Methoxy-1-(4-methoxyphenyl)ethanone 38c

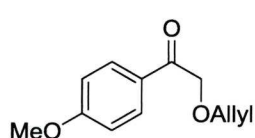
Prepared according to general synthesis of aryl ketones:

¹H NMR (500 MHz, CDCl₃) δ 7.94-7.92 (m, 2H), 6.95-6.93 (m, 2H), 4.66 (s, 2H), 3.87 (s, 3H), 3.52 (s, 3H).

^{13}C NMR (125 MHz, CDCl_3) δ 194.53 (e), 163.65 (e), 129.97 (o), 127.70 (e), 113.71 (o), 75.01 (e), 59.17 (o), 55.29 (o).

IR (Neat) 2935 (w), 2921 (w), 1683 (s), 1575 (m), 1510 (m), 1238 (s), 1170 (m), 1031 (m) cm^{-1} .

HRMS (CI, M^+) calcd for $\text{C}_{10}\text{H}_{12}\text{O}_3$ 180.0781, found 180.0786.



2-(Allyloxy)-1-(4-methoxyphenyl)ethanone 38d

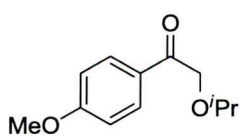
Prepared according to general synthesis of aryl ketones:

^1H NMR (500 MHz, CDCl_3) δ 7.94-7.91 (m, 2H), 6.94-6.92 (m, 2H), 6.0-5.91 (m, 1H), 5.32 (d, $J = 17.4$ Hz, 1H), 5.24 (d, $J = 10.3$ Hz, 1H), 4.69 (m, 2H), 3.86 (m, 3H).

^{13}C NMR (125 MHz, CDCl_3) δ 194.75 (e), 163.74 (e), 134.04 (o), 130.18 (o), 127.92 (e), 127.04 (o), 118.00 (e), 113.83 (o), 72.42 (e), 72.34 (e), 55.44 (o).

IR (Neat) 2937 (w), 2840 (w), 1689 (m), 1599 (s), 1575 (m), 1510 (m), 1257 (s), 1234 (s), 1172 (m), 1025 (m) cm^{-1} .

HRMS (CI, $\text{M}+\text{H}$) calcd for $\text{C}_{12}\text{H}_{15}\text{O}_3$ 207.1016, found 207.1015.



2-Isopropoxy-1-(4-methoxyphenyl)ethanone 38e

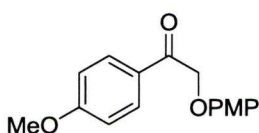
Prepared according to general synthesis of aryl ketones:

^1H NMR (500 MHz, CDCl_3) δ 7.92-7.89 (m, 2H), 6.90-6.87 (m, 2H), 4.63 (s, 2H), 3.81 (s, 3H), 11.20 (s, 3H), 11.18 (s, 3H).

^{13}C NMR (125 MHz, CDCl_3) δ 195.48 (e), 163.66 (e), 130.35 (o), 128.14 (e), 113.78 (o), 72.56 (o), 71.22 (e), 55.46 (o), 21.90 (o).

IR (Neat) 2972 (m), 2841 (w), 1691 (m), 1599 (s), 1575 (m), 1510 (m), 1256 (s), 1235 (s), 1171 (s), 1124 (s) cm^{-1} .

HRMS (CI, $\text{M}+\text{H}$) calcd for $\text{C}_{12}\text{H}_{17}\text{O}_3$ 209.1172, found 209.1174.



2-(4-Methoxyphenoxy)-1-(4-methoxyphenyl)ethanone 38f

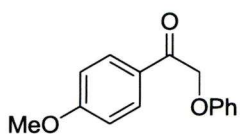
Prepared according to general synthesis of aryl ketones:

^1H NMR (500 MHz, CDCl_3) δ 7.99-7.97 (m, 2H), 6.95-6.80 (m, 6H), 5.14 (s, 2H), 3.85 (s, 3H), 3.73 (s, 3H).

^{13}C NMR (125 MHz, CDCl_3) δ 193.47 (e), 164.07 (e), 154.45 (e), 152.37 (e), 130.57 (o), 127.73 (e), 115.99 (o), 114.74 (o), 114.05 (o), 71.68 (e), 55.73 (o), 55.59 (e).

IR (Neat) 3009 (w), 2895 (w), 1697 (m), 1601 (m), 1508 (s), 1436 (m), 1264 (m), 1226 (s), 1168 (s) cm^{-1} .

HRMS (CI, M^+) calcd for $\text{C}_{16}\text{H}_{16}\text{O}_4$ 272.1043, found 272.1039.



1-(4-Methoxyphenyl)-2-phenoxyethanone 38g

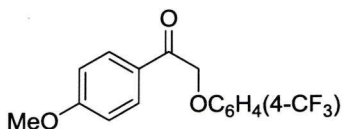
Prepared according to general synthesis of aryl ketones:

^1H NMR (500 MHz, CDCl_3) δ 8.01-7.98 (m, 2H), 7.30-7.25 (m, 2H), 6.99-6.93 (m, 5H), 5.21 (s, 2H), 3.87 (s, 3H).

^{13}C NMR (125 MHz, CDCl_3) δ 193.04 (e), 163.99 (e), 158.06 (e), 130.50 (o), 129.50 (o), 127.61 (e), 121.50 (o), 114.75 (o), 113.96 (o), 70.66 (e), 55.47 (o).

IR (Neat) 3058 (w), 3006 (w), 2933 (w), 1685 (s), 1598 (s), 1494 (m), 1263 (s), 1220 (s), 1168 (s) cm^{-1} .

HRMS (CI, M^+) calcd for $\text{C}_{15}\text{H}_{14}\text{O}_3$ 242.0937, found 242.0928.



1-(4-Methoxyphenyl)-2-[4-(trifluoromethyl)

phenoxy]ethanone 38h

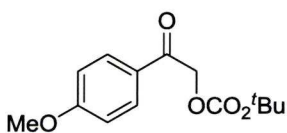
Prepared according to general synthesis of aryl ketones:

^1H NMR (500 MHz, CDCl_3) δ 8.00-7.97 (m, 2H), 7.53 (d, $J = 8.7$ Hz, 2H), 6.99-6.96 (m, 4H), 5.28 (s, 2H), 3.88 (s, 3H).

^{13}C NMR (125 MHz, CDCl_3) δ 192.21 (e), 164.38 (e), 160.62 (e), 130.58 (o), 130.58 (o), 127.38 (e), XXX, 114.86 (o), 114.26 (o), 70.49 (e), 55.68 (o).

IR (Neat) 3085 (w), 2944 (w), 2846 (w), 1690 (m), 1615 (m), 1593 (m), 1512 (m), 1333 (m), 1106 (s), 1068 (m) cm^{-1} .

HRMS (CI, M^+) calcd for $\text{C}_{16}\text{H}_{13}\text{O}_3\text{F}_3$ 310.0811 found 310.0820.



tert-Butyl 2-(4-methoxyphenyl)-2-oxoethyl carbonate 38i

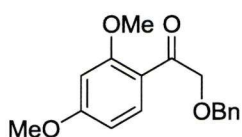
Prepared according to general synthesis of aryl ketones:

^1H NMR (500 MHz, CDCl_3) δ 8.05-8.03 (m, 2H), 7.91-7.88 (m, 2H), 5.25 (s, 2H), 3.87 (s, 3H), 1.52 (s, 9H).

^{13}C NMR (125 MHz, CDCl_3) δ 190.62 (e), 164.01 (e), 153.33 (e), 129.83 (o), 127.10 (e), 113.95 (o), 82.79 (e), 67.62 (e), 55.45 (o), 27.62 (o).

IR (Neat) 2981 (w), 2897 (w), 1747 (s), 1695 (m), 1610 (m), 1460 (m), 1310 (m), 1241 (s), 1174 (s), 1027 (m) cm^{-1} .

HRMS (CI, M^+) calcd for $C_{14}H_{18}O_5$ 266.1149 found 266.1156.



2-(Benzyloxy)-1-(2,4-dimethoxyphenyl)ethanone 38j

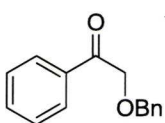
Prepared according to general synthesis of aryl ketones:

1H NMR (500 MHz, $CDCl_3$) δ 7.98 (d, J = 8.8 Hz, 1H), 7.38-7.21 (m, 5H), 6.56 (dd, J = 8.8, 2.3 Hz, 1H), 6.42 (d, J = 2.3 Hz, 1H), 4.68 (s, 4H), 3.85 (s, 3H), 3.84 (s, 3H).

^{13}C NMR (125 MHz, $CDCl_3$) δ 195.64 (e), 165.11 (e), 165.00 (e), 161.17 (e), 138.10 (e), 132.82 (o), 128.39 (o), 128.02 (o), 127.70 (o), 105.68 (o), 98.08 (o), 76.48 (e), 73.22 (e), 55.60 (o), 55.46 (o).

IR (Neat) 3027 (w), 2965 (w), 2900 (w), 2857 (w), 1675 (m), 1594 (s), 1570 (m), 1474 (m), 1251 (s), 1219 (s), 1209 (s), 1165 (s), 1108 (s), 1014 (s) cm^{-1} .

HRMS (CI, $M+H$) calcd for $C_{17}H_{19}O_4$ 287.1278 found 287.1270.



2-(Benzyloxy)-1-phenylethanone 38k

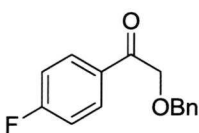
Prepared according to general synthesis of aryl ketones:

1H NMR (500 MHz, $CDCl_3$) δ 7.93-7.91 (m, 2H), 7.57 (t, J = 7.4 Hz, 1H), 7.47-7.44 (m, 2H), 7.41-7.30 (m, 5H), 4.76 (s, 2H), 4.70 (s, 2H).

^{13}C NMR (125 MHz, $CDCl_3$) δ 194.89 (e), 163.85 (e), 137.47 (e), 130.35 (o), 128.57 (o), 128.12 (o), 128.03 (o), 113.92 (o), 73.40 (e), 72.56 (e), 55.55 (o).

IR (Neat) 3028 (w), 2942 (w), 1692 (s), 1580 (m), 1449 (m), 1390 (m), 1226 (m), 1216 (m), 1127 (m), 1078 (m) cm^{-1} .

HRMS (CI, $M+H$) calcd for $C_{15}H_{15}O_2$ 227.1067 found 227.1068.



2-(Benzyloxy)-1-(4-fluorophenyl)ethanone 38l

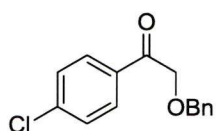
Prepared according to general synthesis of aryl ketones:

1H NMR (500 MHz, $CDCl_3$) δ 7.97-7.93 (m, 2H), 7.39-7.29 (m, 5H), 7.12-7.08 (m, 2H), 4.70 (s, 2H), 4.67 (m, 2H).

^{13}C NMR (125 MHz, $CDCl_3$) δ 194.80 (e), 166.90 (e), 164.86 (e), 137.18 (e), 130.72 (d, J_{CF} = 10.0 Hz, 2C), 128.53 (o), 128.05 (o), 115.90 (o), 115.72 (o), 73.39 (e), 72.63 (e).

IR (Neat) 3028 (w), 2945 (w), 2860 (w), 1692 (s), 1593 (m), 1508 (m), 1412 (m), 1228 (m), 1211 (m), 1126 (m) cm^{-1} .

HRMS (CI, M+H) calcd for C₁₅H₁₄O₂F 245.0972 found 245.0961.



2-(Benzyloxy)-1-(4-chlorophenyl)ethanone 38m

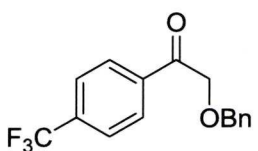
Prepared according to general synthesis of aryl ketones:

¹H NMR (500 MHz, CDCl₃) δ 4.89-4.86 (m, 2H), 7.43 (d, *J* = 8.6 Hz, 2H), 7.39-7.30 (m, 5H), 4.70 (s, 2H), 4.68 (s, 2H).

¹³C NMR (125 MHz, CDCl₃) δ 195.38 (e), 140.12 (e), 137.23 (e), 133.33 (e), 129.14 (o), 128.69 (o), 128.23 (o), 128.20 (o), 73.57 (e), 72.75 (e).

IR (Neat) 3029 (w), 2944 (w), 2883 (w), 1692 (s), 1589 (m), 1402 (m), 1228 (m), 1216 (m), 1133 (m), 1093 (m) cm⁻¹.

HRMS (CI, M+H) calcd for C₁₅H₁₄O₂Cl 261.0677 found 261.0672.



2-(Benzyloxy)-1-[4-(trifluoromethyl)phenyl]ethanone 38n

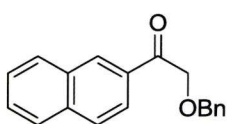
Prepared according to general synthesis of aryl ketones:

¹H NMR (500 MHz, CDCl₃) δ 8.05-8.02 (m, 2H), 7.76-7.72 (m, 2H), 7.41-7.35 (m, 5H), 4.77 (s, 2H), 4.70 (s, 2H).

¹³C NMR (125 MHz, CDCl₃) δ 195.60 (e), 137.57 (e), 136.90 (e), 134.89-134.58 (m, 1C), 130.50-122.11 (m, 1C), 128.57 (o), 128.43 (o), 128.15 (o), 128.07 (o), 125.70 (d, *J*_{CF} = 3.8 Hz, 2C), 73.52 (e), 72.83 (e).

IR (Neat) 2911 (w), 2859 (w), 1698 (s), 1411 (m), 1328 (s), 1227 (m), 1169 (s), 1112 (vs), 1066 (s) cm⁻¹.

HRMS (CI, M+H) calcd for C₁₆H₁₄O₂F₃ 295.0940 found 295.0941.



2-(Benzyloxy)-1-(2-naphthyl)ethanone 38o

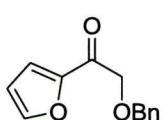
Prepared according to general synthesis of aryl ketones:

¹H NMR (500 MHz, CDCl₃) δ 8.43 (s, 1H), 8.01-7.99 (m, 1H), 7.94-7.86 (m, 3H), 7.57-7.53 (m, 2H), 7.42-7.33 (m, 5H), 4.90 (s, 2H), 4.76 (s, 2H).

¹³C NMR (125 MHz, CDCl₃) δ 196.15 (e), 137.35 (e), 135.72 (e), 132.17 (e), 129.55 (o), 129.55 (o), 128.65 (o), 128.55 (o), 128.09 (o), 128.02 (o), 127.80 (o), 126.86 (o), 123.51 (o), 73.39 (e), 72.70 (e).

IR (Neat) 3056 (w), 2937 (w), 2889 (w), 1691 (s), 1467 (m), 1370 (m), 1255 (m), 1216 (m), 1134 (s), 1119 (s) cm⁻¹.

HRMS (CI, M+H) calcd for C₁₉H₁₇O₂ 277.1223 found 277.1225.



2-(Benzyloxy)-1-(2-furyl)ethanone 38p

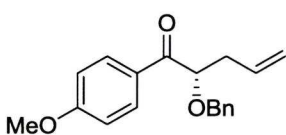
Prepared according to general synthesis of aryl ketones:

¹H NMR (500 MHz, CDCl₃) δ 7.58-7.57 (m, 1H), 7.40-7.30 (m, 6H), 6.54 (dd, *J* = 3.6, 1.7 Hz, 1H), 4.68 (s, 2H), 4.59 (s, 2H).

¹³C NMR (125 MHz, CDCl₃) δ 184.99 (e), 150.70 (e), 146.48 (o), 137.01 (e), 128.27 (o), 128.05 (o), 127.85 (o), 118.03 (o), 112.09 (o), 73.34 (e), 72.03 (e).

IR (Neat) 3064 (w), 2887 (w), 1694 (s), 1572 (s), 1471 (s), 1374 (m), 1254 (m), 1135 (m), 1032 (m) cm⁻¹.

HRMS (CI, M+H) calcd for C₁₃H₁₃O₃ 217.0859 found 217.0863.



(2S)-2-(Benzyloxy)-1-(4-methoxyphenyl)pent-4-en-1-one 40a.

Representative Procedure for the Rhodium-Catalyzed Allylic Allylation: A suspension of chiral phosphite **41a** (35.9 mg, 0.10 mmol) and Wilkinson's catalyst (23.6 mg, 0.026 mmol) in anhydrous tetrahydrofuran (1.0 mL) was stirred under an atmosphere of argon at room temperature for *ca.* 10 minutes resulting in a light yellow homogeneous solution. In a separate flask, lithium *bis*(trimethylsilyl)amide (485 mL, 0.49 mmol), 1.0M solution in tetrahydrofuran) was added dropwise to a solution of aryl ketone **38a** (128.7 mg, 0.50 mmol) in anhydrous tetrahydrofuran (1.5 mL) at -10 °C, and the anion allowed to form over *ca.* 5 minutes resulting in a light yellow homogeneous solution. The catalyst solution was then added *via* Teflon® cannula to the enolate solution followed by addition of allyl benzoate (41.4 mg, 0.26 mmol) *via* a tared gas-tight syringe and allowed to stir for *ca.* 14 hours (t.l.c. control). The reaction was quenched with saturated aqueous ammonium chloride solution (2 mL) and partitioned between diethyl ether and saturated aqueous ammonium chloride. The combined organic phases were dried using magnesium sulfate, filtered and concentrated *in vacuo* to afford a crude oil. Purification by flash chromatography (eluting with 5 % ethyl acetate/hexanes) furnished the α-alkoxy allyl ketone **40a** (68.1 mg, 90%; 93% *ee*) as a colorless oil.

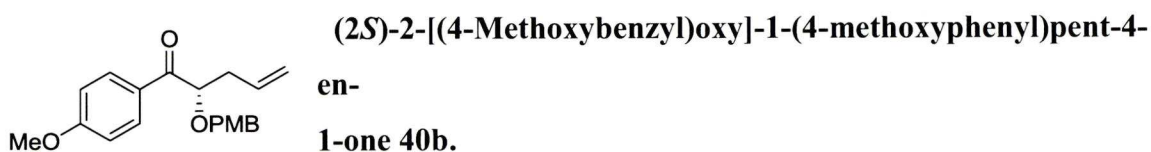
[α]_D²⁰ -57.5 (*c* = 1.01, CHCl₃); Chiral HPLC analysis (25 cm x 4.6 mm Chiralpak AD-H column, 7% isopropanol-hexane at 0.8 mL/min. flow rate, 210 nm; *t_R* (*major*) 11.3 min., *t_R* (*minor*) 19.7 min., 93% *ee*).

¹H NMR (500 MHz, CDCl₃) δ 8.09-8.06 (m, 2H), 7.34-7.26 (m, 5H), 6.95-6.92 (m, 2H), 5.87 (ddt, *J* = 17.0, 10.3, 6.9 Hz, 1H), 5.11-5.07 (m, 2H), 4.66 (d, A of AB, *J*_{AB} = 11.8 Hz, 1H), 4.66-4.63 (m, 1H), 4.41 (d, B of AB, *J*_{AB} = 11.7 Hz, 1H), 3.87 (s, 3H), 2.68-2.57 (m, 2H).

¹³C NMR (125 MHz, CDCl₃) δ 198.55 (e), 163.88 (e), 137.75 (e), 133.69 (o), 131.38 (o), 128.52 (o), 128.26 (e), 128.12 (o), 127.95 (o), 117.84 (e), 113.94 (o), 82.30 (o), 71.86 (e), 55.63 (o), 37.95 (e).

IR (neat) 3068 (w), 3028 (w), 3008 (w), 2977 (w), 2948 (w), 2836 (w), 1765 (m), 1597 (w), 1505 (s), 1455 (m), 1441 (m), 1190 (s), 1166 (m), 1118 (s), 1101(s), 1033 (m) cm⁻¹.

HRMS (EI, M+H⁺) calcd for C₁₉H₂₀O₃ 296.1407, found 296.1401.



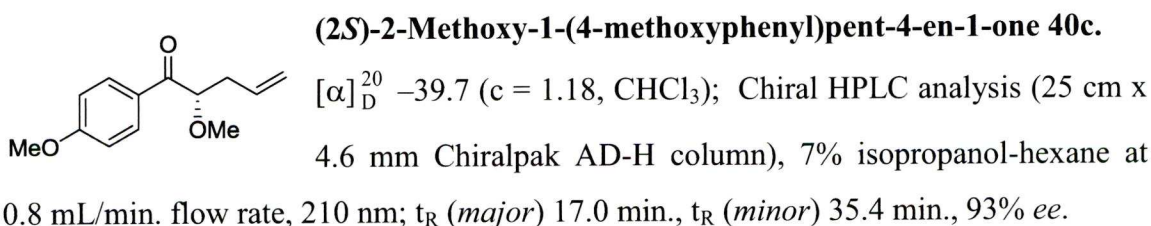
[α]_D²⁰ -57.5 (c = 1.01, CHCl₃); Chiral HPLC analysis (25 cm x 4.6 mm Chiralpak AD-H column), 7% isopropanol-hexane at 0.8 mL/min. flow rate, 210 nm; *t*_R (*major*) 11.3 min., *t*_R (*minor*) 19.7 min., 93% *ee*.

¹H NMR (500 MHz, CDCl₃) δ 8.09-8.06 (m, 2H), 7.34-7.26 (m, 5H), 6.95-6.92 (m, 2H), 5.87 (ddt, *J* = 17.0, 10.3, 6.9 Hz, 1H), 5.11-5.07 (m, 2H), 4.66 (d, A of AB, *J*_{AB} = 11.8 Hz, 1H), 4.66-4.63 (m, 1H), 4.41 (d, B of AB, *J*_{AB} = 11.7 Hz, 1H), 3.87 (s, 3H), 2.68-2.57 (m, 2H).

¹³C NMR (125 MHz, CDCl₃) δ 198.55 (e), 163.88 (e), 137.75 (e), 133.69 (o), 131.38 (o), 128.52 (o), 128.26 (e), 128.12 (o), 127.95 (o), 117.84 (e), 113.94 (o), 82.30 (o), 71.86 (e), 55.63 (o), 37.95 (e).

IR (neat) 3068 (w), 3028 (w), 3008 (w), 2977 (w), 2948 (w), 2836 (w), 1765 (m), 1597 (w), 1505 (s), 1455 (m), 1441 (m), 1190 (s), 1166 (m), 1118 (s), 1101(s), 1033 (m) cm⁻¹.

HRMS (EI, M+H⁺) calcd for C₁₉H₂₀O₃ 296.1407, found 296.1401.

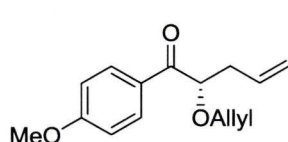


¹H NMR (500 MHz, CDCl₃) δ 8.08-8.05 (m, 2H), 7.23-7.20 (m, 2H), 6.94-6.92 (m, 2H), 6.86-6.83 (m, 2H), 5.89-5.80 (m, 1H), 5.08-5.05 (m, 2H), 4.61 (dd, *J* = 7.9, 5.5 Hz, 1H), 4.58 (d, A of AB, *J*_{AB} = 11.4 Hz, 1H), 4.34 (d, B of AB, *J*_{AB} = 11.3 Hz, 1H), 3.88 (s, 3H), 3.80 (s, 3H), 2.65-2.54 (m, 2H).

¹³C NMR (125 MHz, CDCl₃) δ 198.70 (e), 163.83 (e), 159.42 (e), 133.72 (o), 131.34 (o), 129.82 (o), 129.76 (e), 128.24 (e), 117.73 (e), 113.88 (o), 81.88 (o), 71.50 (e), 55.60 (o), 55.38 (o), 37.91 (e).

IR (neat) 3008 (w), 2962 (w), 2937 (w), 2966 (w), 2838 (w), 1680 (m), 1598 (s), 1511 (s), 1463 (m), 1421 (m), 1304 (m), 1246 (s), 1171 (s), 1093 (m), 1032 (s) cm⁻¹.

HRMS (CI, M-H⁺) calcd for C₂₀H₂₁O₄ 325.1434, found 325.1426.



(2S)-2-(Allyloxy)-1-(4-methoxyphenyl)pent-4-en-1-one 40d.

[α]_D²⁰ -31.9 (c = 1.10, CHCl₃); Chiral HPLC analysis (25 cm x 4.6 mm Chiralpak AD-H column), 7% isopropanol-hexane at

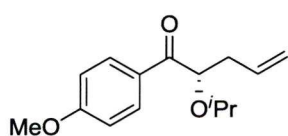
0.8 mL/min. flow rate, 210 nm; *t*_R (*major*) 8.2 min., *t*_R (*minor*) 10.8 min., 87% *ee*.

¹H NMR (500 MHz, CDCl₃) δ 8.09-8.06 (m, 2H), 6.95-6.93 (m, 2H), 5.93-5.82 (m, 2H), 5.25 (dq, *J* = 17.3, 1.5 Hz, 1H), 5.18-5.16 (m, 1H), 5.10-5.06 (m, 2H), 4.61 (dd, *J* = 7.5, 5.6 Hz, 1H), 4.10 (ddt, A of ABMX, *J*_{AB} = 12.9 Hz, *J*_{AM} = 5.4 Hz, *J*_{AX} = 1.4 Hz, 1H), 3.91 (ddt, B of ABMX, *J*_{AB} = 12.8 Hz, *J*_{BM} = 6.1 Hz, *J*_{BX} = 1.2 Hz, 1H), 3.88 (s, 3H), 2.63-2.54 (m, 2H).

¹³C NMR (125 MHz, CDCl₃) δ 198.58 (e), 163.85 (e), 134.36 (o), 133.70 (o), 131.33 (o), 128.30 (e), 117.81 (e), 117.76 (e), 113.93 (o), 82.26 (o), 71.02 (e), 55.62 (o), 37.96 (e).

IR (neat) 3079 (w), 3008 (w), 2981 (w), 2937 (w), 2840 (w), 1677 (m) 1599 (s), 1574 (m), 1509 (m), 1421 (m), 1310 (m), 1257 (s), 1172 (s), 1100 (m), 1031 (m) cm⁻¹.

HRMS (CI, M+H⁺) calcd for C₁₅H₁₉O₃ 247.1329, found 247.1339.



(2S)-2-Isopropoxy-1-(4-methoxyphenyl)pent-4-en-1-one 40e.

[α]_D²⁰ -50.5 (c = 0.99, CHCl₃); Chiral HPLC analysis (25 cm x 4.6 mm Chiralpak AD-H column), 4% isopropanol-hexane at 0.8

mL/min. flow rate, 280 nm; *t*_R (*major*) 7.7 min., *t*_R (*minor*) 10.2 min., 89% *ee*.

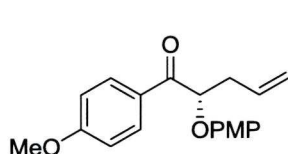
¹H NMR (500 MHz, CDCl₃) δ 8.13-8.10 (m, 2H), 6.95-6.92 (m, 2H), 5.85 (ddt, *J* = 17.1, 10.2, 6.9 Hz, 1H), 5.09-5.05 (m, 2H), 4.56 (dd, *J* = 8.2, 5.4 Hz, 1H), 3.87 (s, 3H),

3.59 (septet, $J = 6.1$ Hz, 1H), 2.59-2.48 (m, 2H), 1.16 (d, 6.1 Hz, 3H), 1.11 (d, $J = 6.2$ Hz, 3H).

^{13}C NMR (125 MHz, CDCl_3) δ 199.79 (e), 163.71 (e), 134.04 (o), 131.60 (o), 128.12 (e), 117.57 (e), 113.77 (o), 81.76 (o), 71.83 (o), 55.60 (o), 38.65 (e), 23.08 (o), 21.66 (o).

IR (neat) 3078 (w), 2972 (w), 2932 (w), 2841 (w), 1687 (m), 1668 (m), 1598 (s), 1574 (m), 1509 (m), 1463 (w), 1310 (m), 1254 (s), 1171 (s), 1117 (m), 1088 (m), 1028 (m) cm^{-1} .

HRMS (CI, $\text{M}+\text{H}^+$) calcd for $\text{C}_{15}\text{H}_{21}\text{O}_3$ 249.1485, found 249.1495.



(2S)-2-(4-Methoxyphenoxy)-1-(4-methoxyphenyl)pent-4-en-1-one 40f.

$[\alpha]_{\text{D}}^{20} -13.5$ ($c = 1.11$, CHCl_3); Chiral HPLC analysis (25 cm x

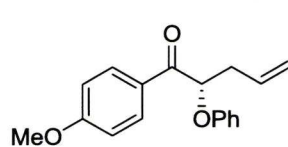
4.6 mm Chiralpak AD-H column, 7% isopropanol-hexane at 0.8 mL/min. flow rate, 210 nm; t_{R} (*major*) 23.9 min., t_{R} (*minor*) 36.5 min., 90% *ee*.

^1H NMR (500 MHz, CDCl_3) δ 8.11-8.07 (m, 2H), 6.95-6.92 (m, 2H), 6.82-6.79 (m, 2H), 6.76-6.73 (m, 2H), 5.94 (ddt, $J = 17.1, 10.2, 6.9$ Hz, 1H), 5.19 (dd, $J = 8.0, 5.2$ Hz, 1H), 5.18-5.11 (m, 2H), 3.87 (s, 3H), 3.71 (s, 3H), 2.83-2.71 (m, 2H).

^{13}C NMR (125 MHz, CDCl_3) δ 197.23 (e), 164.04 (e), 154.42 (e), 151.98 (e), 133.21 (o), 131.47 (o), 127.56 (e), 118.33 (e), 116.60 (o), 114.78 (o), 114.07 (o), 81.81 (o), 55.76 (o), 55.63 (o), 37.90 (e).

IR (neat) 3073 (w), 3008 (w), 2936 (w), 2906 (w), 2838 (w), 1680 (m), 1597 (s), 1510 (s), 1462 (m), 1304 (m), 1245 (s), 1171 (s), 1094 (m), 1029 (m), cm^{-1} .

HRMS (CI, $\text{M}+\text{H}^+$) calcd for $\text{C}_{19}\text{H}_{21}\text{O}_4$ 313.1434, found 313.1427.



(2S)-1-(4-Methoxyphenyl)-2-phenoxy-pent-4-en-1-one 40g.

$[\alpha]_{\text{D}}^{20} +4.7$ ($c = 1.14$, CHCl_3); Chiral HPLC analysis (25 cm x

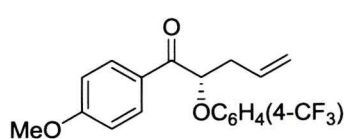
4.6 mm Chiralpak AD-H column, 4% isopropanol-hexane at 0.8 mL/min. flow rate, 210 nm; t_{R} (*major*) 16.0 min., t_{R} (*minor*) 23.6 min., 87% *ee*.

^1H NMR (500 MHz, CDCl_3) δ 8.11-8.08 (m, 2H), 7.23-7.20 (m, 2H), 6.95-6.90 (m, 3H), 6.87-6.85 (m, 2H), 5.95 (ddt, $J = 17.1, 10.2, 6.9$ Hz, 1H), 5.29 (dd, $J = 8.0, 5.1$ Hz, 1H), 5.18-5.12 (m, 2H), 3.87 (s, 3H), 2.85-2.73 (m, 2H).

^{13}C NMR (125 MHz, CDCl_3) δ 196.85 (e), 164.08 (e), 157.81 (e), 133.12 (o), 131.45 (o), 129.69 (o), 127.44 (e), 121.58 (o), 118.39 (e), 115.36 (o), 114.10 (o), 80.83 (o), 55.64 (o), 37.84 (e).

IR (neat) 3073 (w), 3013 (w), 2918 (w), 2850 (w), 1686 (m), 1597 (s), 1573 (m), 1509 (m), 1493 (m), 1421 (m), 1309 (m), 1258 (m), 1227 (s), 1171 (s), 1071 (m), 1027 (m) cm^{-1} .

HRMS (CI, $\text{M}+\text{H}^+$) calcd for $\text{C}_{18}\text{H}_{19}\text{O}_3$ 283.1329, found 283.1323.



(2S)-1-(4-Methoxyphenyl)-2-[4-(trifluoromethyl)phenoxy]pent-4-en-1-one 40h.

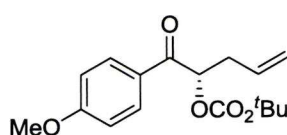
$[\alpha]_{\text{D}}^{20}$ +19.04 (c = 1.11, CHCl_3); Chiral HPLC analysis (25 cm x 4.6 mm Chiralpak AD-H column, 4% isopropanol-hexane at 0.8 mL/min. flow rate, 230 nm; t_{R} (*major*) 15.9 min., t_{R} (*minor*) 23.4 min., 78% *ee*.

^1H NMR (500 MHz, CDCl_3) δ 8.07 (d, J = 8.8 Hz, 2H), 7.47 (d, J = 8.7 Hz, 2H), 6.97-6.94 (m, 2H), 6.91 (d, J = 8.7 Hz, 2H), 5.93 (ddt, J = 17.1, 10.2, 6.9 Hz, 1H), 5.36 (dd, J = 7.7, 5.2 Hz, 1H), 5.20-5.14 (m, 2H), 3.88 (s, 3H), 2.87-2.76 (m, 2H).

^{13}C NMR (125 MHz, CDCl_3) δ 195.78 (e), 164.34 (e), 160.21 (e), 132.65 (o), 131.35 (o), 127.16 (o, q, $^3J_{\text{CF}}$ = 3.7 Hz), 125.46 (e, q, $^1J_{\text{CF}}$ = 270.7 Hz), 123.71 (e, q, $^2J_{\text{CF}}$ = 33.1 Hz), 118.75 (e), 115.25 (o), 114.28 (o), 80.68 (o), 55.68 (o), 37.72 (e).

IR (neat) 3078 (w), 3013 (w), 2957 (w), 2936 (w), 2841 (w), 1936 (w), 1686 (m), 1615 (m), 1598 (s), 1512 (m), 1422 (w), 1326 (s), 1310 (m), 1239 (s), 1171 (s), 1161 (s), 1109 (s), 1063 (s), 1029 (m) cm^{-1} .

HRMS (CI, $\text{M}+\text{H}^+$) calcd for $\text{C}_{19}\text{H}_{18}\text{O}_3\text{F}_3$ 351.1203, found 351.1202.



***tert*-Butyl (2S)-1-(4-methoxyphenyl)-1-oxypent-4-en-2-yl carbonate 40i.**

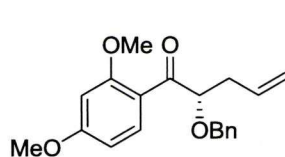
$[\alpha]_{\text{D}}^{20}$ +42.50 (c = 0.55, CHCl_3); Chiral HPLC analysis (25 cm x 4.6 mm Chiralpak AD-H column, 7% isopropanol-hexane at 0.8 mL/min. flow rate, 270 nm; t_{R} (*major*) 12.8 min., t_{R} (*minor*) 42.8 min., 94% *ee*.

^1H NMR (500 MHz, CDCl_3) δ 7.95-7.92 (m, 2H), 6.96-6.93 (m, 2H), 5.84 (ddt, J = 17.1, 10.2, 7.0 Hz, 1H), 5.72 (dd, J = 8.1, 4.6 Hz, 1H), 5.13-5.09 (m, 2H), 3.87 (s, 3H), 2.67-2.55 (m, 2H), 1.46 (s, 9H).

^{13}C NMR (125 MHz, CDCl_3) δ 194.54 (e), 164.00 (e), 153.10 (e), 132.41 (o), 130.93 (o), 127.67 (e), 118.72 (e), 114.12 (o), 83.07 (e), 76.77 (o), 55.65 (o), 36.10 (e), 27.81 (o).

IR (neat) 3079 (w), 3013 (w), 2981 (w), 2937 (w), 2840 (w), 1677 (m), 1599 (s), 1574 (m), 1509 (m), 1421 (m), 1310 (m), 1257 (s), 1172 (s), 1100 (m), 1031 (m) cm^{-1} .

HRMS (EI, M^+) calcd for $\text{C}_{17}\text{H}_{22}\text{O}_5$ 306.1462, found 306.1464.



(2S)-2-(Benzyloxy)-1-(2,4-dimethoxyphenyl)pent-4-en-1-one 40j.

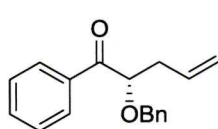
$[\alpha]_{\text{D}}^{20}$ -57.69 ($c = 1.04$, CHCl_3); Chiral HPLC analysis (25 cm x 4.6 mm Chiralpak AD-H column, 7% isopropanol-hexane at 0.8 mL/min. flow rate, 210 nm; t_{R} (major) 20.2 min., t_{R} (minor) 25.4 min., 98% *ee*.

^1H NMR (500 MHz, CDCl_3) δ 7.85 (d, $J = 8.8$ Hz, 1H), 7.38-7.32 (m, 4H), 7.29-7.26 (m, 1H), 6.56 (dd, $J = 8.8$, 2.1 Hz, 1H), 6.44 (d, $J = 2.1$ Hz, 1H), 5.93 (ddt, $J = 16.8$, 9.7, 7.1 Hz, 1H), 5.07-5.04 (m, 2H), 4.98 (dd, $J = 8.1$, 3.5 Hz, 1H), 4.76 (d, A of AB, $J_{\text{AB}} = 11.9$ Hz, 1H), 4.42 (d, B of AB, $J_{\text{AB}} = 11.9$ Hz, 1H), 3.87 (s, 3H), 3.81 (s, 3H), 2.56-2.51 (m, 1H), 2.41-2.36 (m, 1H).

^{13}C NMR (125 MHz, CDCl_3) δ 199.47 (e), 164.83 (e), 160.42 (e), 138.56 (e), 134.91 (o), 133.32 (o), 128.32 (o), 128.03 (o), 127.59 (o), 119.74 (e), 116.92 (e), 105.66 (o), 98.41 (o), 83.37 (o), 71.94 (e), 55.71 (o), 55.54 (o), 37.10 (e).

IR (neat) 3068 (w), 3008 (w), 2977 (w), 2942 (w), 2839 (w), 1670 (m), 1598 (s), 1572 (m), 1498 (m), 1455 (m), 1417 (m), 1295 (m), 1252 (m), 1211 (s), 1162 (m), 1103 (s), 1025 (m) cm^{-1} .

HRMS (CI, $\text{M}+\text{H}^+$) calcd for $\text{C}_{20}\text{H}_{23}\text{O}_4$ 327.1591, found 327.1590.



(2S)-2-(Benzyloxy)-1-phenylpent-4-en-1-one 40k.

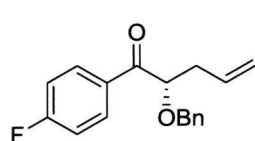
$[\alpha]_{\text{D}}^{20}$ -58.43 ($c = 1.02$, CHCl_3); Chiral HPLC analysis (25 cm x 4.6 mm Chiralpak AD-H column, 4% isopropanol-hexane at 0.8 mL/min. flow rate, 210 nm; t_{R} (major) 7.93 min., t_{R} (minor) 11.01 min., 90% *ee*.

^1H NMR (500 MHz, CDCl_3) δ 8.05-8.03 (m, 2H), 7.60-7.57 (m, 1H), 7.48-7.45 (m, 2H), 7.35-7.28 (m, 5H), 5.92-5.84 (m, 1H), 5.11-5.07 (m, 2H), 4.73-4.71 (m, 1H), 4.68 (d, A of AB, $J_{\text{AB}} = 11.7$ Hz, 1H), 4.43 (d, B of AB, $J_{\text{AB}} = 11.7$ Hz, 1H), 2.65-2.61 (m, 2H).

^{13}C NMR (125 MHz, CDCl_3) δ 200.07 (e), 137.59 (e), 135.30 (e), 133.57 (o), 133.45 (o), 128.87 (o), 128.77 (o), 128.52 (o), 128.12 (o), 127.98 (o), 117.99 (e), 81.99 (o), 71.94 (e), 37.66 (e).

IR (neat) 3065 (w), 3030 (w), 2922 (w), 2856 (w), 1693 (s), 1676 (s), 1597 (m), 1578 (w), 1448 (m), 1242 (m), 1207 (m), 1098 (s), 1077 (m), 1027 (m), 1001 (m) cm^{-1} .

HRMS (CI, $\text{M}+\text{H}^+$) calcd for $\text{C}_{18}\text{H}_{19}\text{O}_2$ 267.1380, found 267.1393.



(2S)-2-(Benzyloxy)-1-(4-fluorophenyl)pent-4-en-1-one 40l.

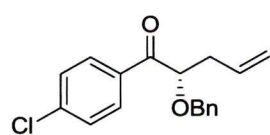
$[\alpha]_{\text{D}}^{20}$ -46.33 ($c = 1.14$, CHCl_3); Chiral HPLC analysis (25 cm x 4.6 mm Chiralpak AD-H column, 4% isopropanol-hexane at 0.8 mL/min. flow rate, 210 nm; t_{R} (major) 7.6 min., t_{R} (minor) 10.3 min., 87% *ee*.

^1H NMR (500 MHz, CDCl_3) δ 8.12-8.09 (m, 2H), 7.34-7.28 (m, 5H), 7.14-7.11 (m, 2H), 5.89-5.81 (m, 1H), 5.11-5.09 (m, 1H), 5.08-5.06 (m, 1H) 4.78 (d, A of AB, $J_{\text{AB}} = 11.6$ Hz, 1H), 4.62-4.60 (m, 1H), 4.43 (d, B of AB, $J_{\text{AB}} = 11.7$ Hz, 1H), 2.69-2.56 (m, 2H).

^{13}C NMR (125 MHz, CDCl_3) δ 198.63 (e), 165.99 (e, d, $^1J_{\text{CF}} = 255.6$ Hz), 137.41 (e), 133.28 (o), 131.79 (o, d, $^3J_{\text{CF}} = 9.3$ Hz), 131.60 (e), 131.58 (e), 128.56 (o), 128.14 (o), 128.08 (o), 118.14 (e), 115.88 (o, d, $^2J_{\text{CF}} = 21.9$ Hz), 82.62 (o), 72.06 (e), 37.69 (e).

IR (neat) 3084 (w), 3013 (w), 2925 (w), 2861 (w), 1691 (m), 1676 (m), 1598 (s), 1506 (m), 1455 (w), 1410 (w), 1233 (s), 1157 (m), 1097 (m), 1014 (w) cm^{-1} .

HRMS (CI, $\text{M}+\text{H}^+$) calcd for $\text{C}_{18}\text{H}_{18}\text{O}_2\text{F}$ 285.1285, found 285.1293.



(2S)-2-(Benzyloxy)-1-(4-chlorophenyl)pent-4-en-1-one 40m.

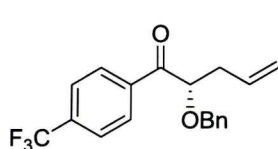
$[\alpha]_{\text{D}}^{25}$ -22.7 ($c = 1.08$, CHCl_3); Chiral HPLC analysis (25 cm x 4.6 mm Chiralpak AD-H column, 4% isopropanol-hexane at 0.8 mL/min. flow rate; t_{R} (major) 7.7 min., t_{R} (minor) 10.9 min., 90% *ee*.

^1H NMR (500 MHz, CDCl_3) δ 8.02-7.99 (m, 2H), 7.44-7.41 (m, 2H), 7.35-7.27 (m, 5H), 5.88-5.80 (m, 1H), 5.09 (t, $J = 1.1$ Hz, 1H), 5.08-5.05 (m, 1H), 4.63 (d, A of AB, $J_{\text{AB}} = 12.0$ Hz, 1H), 4.60 (dd, $J = 7.9, 5.8$ Hz, 1H), 4.43 (d, B of AB, $J_{\text{AB}} = 11.7$ Hz, 1H), 2.68-2.56 (m, 2H).

^{13}C NMR (125 MHz, CDCl_3) δ 199.10 (e), 140.06 (e), 137.36 (e), 133.48 (e), 133.19 (o), 130.50 (o), 129.09 (o), 128.60 (o), 128.17 (o), 128.13 (o), 118.24 (e), 82.63 (o), 71.12 (e), 37.66 (e).

IR (neat) 3067 (w), 3033 (w), 2922 (w), 2867 (w), 1680 (s), 1587 (s), 1488 (m), 1455 (m), 1400 (m), 1271 (m), 1208 (m), 1176 (m), 1091 (s), 1013 (m) cm^{-1} .

HRMS (CI, $\text{M}+\text{H}^+$) calcd for $\text{C}_{18}\text{H}_{18}\text{O}_2^{35}\text{Cl}$ 301.0990, found 301.0992.



(2S)-2-(Benzyloxy)-1-[4-(trifluoromethyl)phenyl]pent-4-en-1-one 40n.

$[\alpha]_{\text{D}}^{20} -35.30$ ($c = 1.00$, CHCl_3); Chiral HPLC analysis (25 cm x

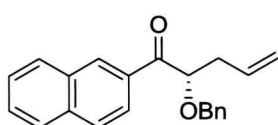
4.6 mm Chiralpak AD-H column, 4% isopropanol-hexane at 0.8 mL/min. flow rate, 230 nm; t_{R} (major) 7.6 min., t_{R} (minor) 10.3 min., 79% *ee*.

^1H NMR (500 MHz, CDCl_3) δ 8.15 (d, $J = 8.3$ Hz, 2H), 7.72 (d, $J = 8.4$ Hz, 2H), 7.35-7.26 (m, 5H), 5.70 (ddt, $J = 17.2, 10.3, 6.9$ Hz, 1H), 5.11-5.06 (m, 2H), 4.65 (dd, $J = 5.6, 1.8$ Hz, 1H), 4.64 (d, $J = 10.4$ Hz, 1H), 4.47 (d, $J = 11.7$ Hz, 1H), 2.70-2.58 (m, 2H).

^{13}C NMR (125 MHz, CDCl_3) δ 199.44 (e), 137.94 (e), 137.19 (e), 134.67 (e, q, $^2J_{\text{CF}} = 32.7$ Hz), 132.95 (o), 129.38 (o), 128.61 (o), 128.19 (o), 125.79 (o), 123.66 (e, q, $^1J_{\text{CF}} = 273.1$ Hz), 125.75 (o, q, $^3J_{\text{CF}} = 3.6$ Hz), 118.42 (e), 82.71 (o), 72.25 (e), 37.45 (e).

IR (neat) 2962 (m), 2924 (m), 2856 (m), 1699 (m), 1687 (m), 1510 (w), 1456 (m), 1410 (m), 1324 (s), 1270 (m), 1169 (s), 1130 (s), 1112 (s), 1067 (s), 1016 (m) cm^{-1} .

HRMS (CI, $\text{M}+\text{H}^+$) calcd for $\text{C}_{19}\text{H}_{18}\text{O}_2\text{F}_3$ 335.1253, found 335.1250.



(2S)-2-(Benzyloxy)-1-(2-naphthyl)pent-4-en-1-one 40o.

$[\alpha]_{\text{D}}^{20} -46.85$ ($c = 1.19$, CHCl_3); Chiral HPLC analysis (25 cm x

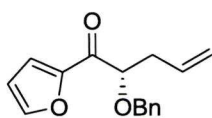
4.6 mm Chiralpak AD-H column, 7% isopropanol-hexane at 0.8 mL/min. flow rate, 210 nm; t_{R} (major) 10.09 min., t_{R} (minor) 12.46 min., 88% *ee*.

^1H NMR (500 MHz, CDCl_3) δ 8.63 (s, 1H), 8.07 (dd, $J = 8.6, 1.7$ Hz, 1H), 7.95 (d, $J = 8.1$ Hz, 1H), 7.92-7.88 (m, 2H), 7.64-7.61 (m, 1H), 7.58-7.55 (m, 1H), 7.34-7.27 (m, 5H), 5.95-5.87 (m, 1H), 5.12-5.09 (m, 2H), 4.84 (dd, $J = 7.5, 5.6$ Hz), 4.72 (d, A of AB, $J_{\text{AB}} = 11.7$ Hz, 1H), 4.48 (d, B of AB, $J_{\text{AB}} = 11.7$ Hz, 1H), 2.76-2.66 (m, 2H).

^{13}C NMR (125 MHz, CDCl_3) δ 200.07 (e), 137.62 (e), 135.85 (e), 133.50 (o), 132.62 (e), 132.59 (e), 130.80 (o), 129.89 (o), 128.86 (o), 128.65 (o), 128.57 (o), 128.22 (o), 128.04 (o), 127.92 (o), 126.95 (o), 124.51 (o), 118.07 (e), 82.23 (o), 72.02 (e), 37.88 (e).

IR (neat) 3062 (w), 3028 (w), 2923 (m), 2855 (m), 1686 (s), 1627 (m), 1464 (m), 1455 (m), 1278 (m), 1188 (m), 1098 (s) cm^{-1} .

HRMS (CI, $\text{M}+\text{H}^+$) calcd for $\text{C}_{22}\text{H}_{21}\text{O}_2$ 317.1536, found 317.1534.



(2S)-2-(Benzyloxy)-1-(2-furyl)pent-4-en-1-one 40p

$[\alpha]_D^{20}$ -51.08 ($c = 1.20$, CHCl_3); Chiral HPLC analysis (25 cm x 4.6 mm Chiralpak AD-H column, 7% isopropanol-hexane at 0.8 mL/min.

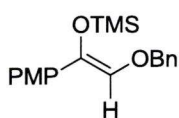
flow rate, 280 nm; t_R (major) 9.0 min., t_R (minor) 11.7 min., 85% *ee*.

^1H NMR (500 MHz, CDCl_3) δ 7.63 (s, 1H), 7.43 (d, $J = 3.6$ Hz, 1H), 7.35-7.28 (m, 5H), 6.55-6.54 (m, 1H), 5.85 (ddt, $J = 17.1, 10.2, 7.0$ Hz, 1H), 5.12-5.07 (m, 2H), 4.67 (d, A of AB, $J_{AB} = 11.7$ Hz, 1H), 4.48-4.45 (m, 1H), 4.45 (d, B of AB, $J_{AB} = 11.8$ Hz, 1H), 2.66-2.56 (m, 2H).

^{13}C NMR (125 MHz, CDCl_3) δ 189.23 (e), 150.92 (e), 147.16 (o), 137.50 (e), 133.25 (o), 128.54 (o), 128.07 (o), 128.03 (o), 119.80 (o), 118.15 (e), 112.43 (o), 82.19 (o), 72.31 (e), 37.92 (e).

IR (neat) 3134 (w), 3068 (w), 3032 (w), 2925 (w), 2861 (w), 1668 (s), 1567 (m), 1463 (s), 1391 (m), 1100 (m), 1084 (m), 1014 (s) cm^{-1} .

HRMS (CI, $\text{M}+\text{H}^+$) calcd for $\text{C}_{16}\text{H}_{17}\text{O}_3$ 257.1172, found 257.1181.



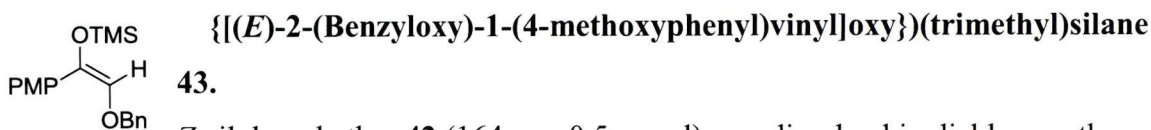
42. {[(Z)-2-(Benzyloxy)-1-(4-methoxyphenyl)vinyl]oxy}(trimethyl)silane

A solution of Ketone **38a** (263.7 mg, 1.0 mmol) in benzene (10 mL) was cooled to 0 °C under an atmosphere of argon. Triethylamine (217 μL , 1.5 mmol) was slowly added followed by trifluoromethanesulfonate (260 μL , 1.4 mmol). The reaction was then warmed to ambient temperature. After 4 hours, the reaction was quenched with water (2 mL) and partitioned between diethyl ether (5 mL) and saturated aqueous ammonium chloride solution (10 mL). Organic layers were dried using magnesium sulfate, filtered and concentrated *en vacuo*. Product was purified *via* flash chromatography with 2% ethylacetate/hexanes to afford 305 mg of **42** (90%) as a colorless oil.

^1H NMR (500 MHz, CDCl_3) δ 7.42-7.31 (m, 7H), 6.85-6.81 (m, 2H), 6.30 (s, 1H), 4.87 (s, 2H), 3.80 (s, 3H), 0.21 (s, 9H).

^{13}C NMR (125 MHz, CDCl_3) δ 158.73 (e), 137.46 (e), 134.78 (e), 129.69 (e), 129.37 (o), 128.59 (o), 128.07 (o), 127.86 (o), 125.10 (o), 113.75 (o), 74.27 (e), 55.37 (o), 0.71 (o).

IR (neat) 3034 (w), 2956 (w), 2901 (w), 2866 (w), 2836 (w), 1661 (m), 1607 (m), 1510 (s), 1455 (m), 1343 (m), 1299 (m), 1245 (vs), 1152 (s), 1135 (s), 1077 (s), 1031 (s) cm^{-1} .

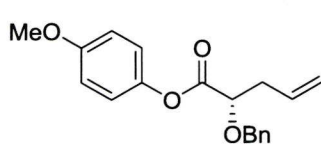


Z-silyl enol ether **42** (164 mg, 0.5 mmol) was dissolved in dichloromethane (2 mL) with water (10 μ L) under an atmosphere of argon and let stir at ambient temperature for *ca.* 14 hours. Reaction mixture concentrated *en vacuo* to afford crude oil which was purified via column chromatography on silica gel with 2.5% ethyl acetate/hexanes to afford 146 mg of **36** (89%) as a colorless oil.

¹H NMR (500 MHz, CDCl₃) δ 8.19-8.16 (m, 2H), 7.36-7.32 (m, 4H), 7.31-7.27 (m, 1H), 6.93-6.90 (m, 2H), 5.48 (s, 1H), 4.77 (d, A of AB, J_{AB} = 11.8 Hz, 1H), 4.63 (d, B of AB, J_{AB} = 11.7 Hz, 1H), 3.87 (s, 3H), 0.17 (s, 9H).

¹³C NMR (125 MHz, CDCl₃) δ 193.32 (e), 163.81 (e), 137.27 (e), 132.61 (o), 128.53 (o), 128.05 (o), 127.95 (o), 126.39 (e), 113.62 (o), 98.14 (o), 69.16 (e), 55.54 (o), 0.34 (o).

IR (Neat) 3068 (w), 3033 (w), 2958 (w), 2901 (w), 2841 (w), 1725 (m), 1682 (m), 1599 (s), 1575 (m), 1511 (m), 1456 (m), 1254 (s), 1173 (m), 1152 (m), 1044 (m), 1028 (m).



4-Methoxyphenyl (2S)-2-(benzyloxy)pent-4-enoate **51**

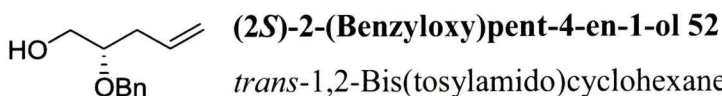
$[\alpha]_D^{20}$ -55.1 (c = 1.00, CHCl₃). Chiral HPLC analysis (25 cm x 4.6 mm Chiralpak AD-H column), 1% isopropanol-hexane at 0.8 mL/min. flow rate, 210 nm; t_R (*minor*) 14.8 min., t_R (*major*) 16.4 min., 93% *ee*.

¹H NMR (500 MHz, CDCl₃) δ 7.43-7.31 (m, 5H), 7.00 (d, J = 8.9 Hz, 2H), 6.90 (d, J = 9.0 Hz, 2H), 5.95 (ddt, J = 17.2, 10.1, 7.1 Hz, 1H), 5.24 (d, J = 17.1 Hz, 1H), 5.19 (d, J = 10.2 Hz, 1H), 4.83 (d, A of AB, J_{AB} = 11.3 Hz, 1H), 4.58 (d, B of AB, J_{AB} = 12.4 Hz, 1H), 4.25 (t, J = 6.2 Hz, 1H), 3.81 (s, 3H), 2.73-2.71 (m, 2H).

¹³C NMR (125 MHz, CDCl₃) δ 171.10 (e), 157.47 (e), 143.89 (e), 137.35 (e), 132.87 (o), 128.58 (o), 128.20 (o), 128.09 (o), 122.25 (o), 118.51 (e), 114.57 (o), 77.68 (o), 72.60 (e), 55.69 (o), 37.56 (e).

IR (neat) 3073 (w), 2942 (w), 2912 (w), 2866 (w), 2835 (w), 1765 (m), 1642 (w), 1597 (w), 1505 (vs), 1464 (m), 1455 (m), 1248 (m), 1191 (s), 1167 (m), 1115 (s), 1102 (s), 1030 (m) cm⁻¹.

HRMS (ESI, [M + Na]⁺) calcd for C₁₉H₂₀O₄²³Na 335.1259, found 335.1254.



trans-1,2-Bis(tosylamido)cyclohexane **46** (19.4 mg, 0.046 mmol) and potassium carbonate (63.5 mg, 0.46 mmol) were suspended in anhydrous dichloromethane (1.0 mL) at room temperature. Tin(IV) chloride (45.9 mL, 0.046 mmol, 1M in dichloromethane) was added, and the reaction cooled to 0 °C, prior to the addition of *bis*-trimethylsilyl peroxide (81.9 mg, 0.46 mmol) *via* tared syringe. The mixture was stirred for *ca.* 10 minutes at 0 °C, then a solution of the aryl ketone **40a** (68.0 mg, 0.23 mmol) in anhydrous dichloromethane (200 mL) was added *via* Teflon[®] cannula. The resulting reaction was stirred at 0 °C for *ca.* 15 minutes, (t.l.c. control), and then cooled to -78 °C and diisobutylaluminum hydride (810 µL, 1M in hexanes) was slowly injected. The reaction was stirred for 45 minutes and quenched with 1M hydrochloric acid solution (2 mL) and partitioned between dichloromethane and diluted hydrochloric acid solution. The combined organic phases were dried (MgSO₄), filtered and concentrated *in vacuo* to afford a crude oil. Purification by flash chromatography (eluting with 15% ethyl acetate/hexanes) furnished the primary alcohol **52** (36.0 mg, 92%) as a colorless oil: Chiral HPLC analysis (25 cm x 4.6 mm Chiralpak AD-H column, 4% isopropanol-hexane at 0.8 mL/min. flow rate, 254 nm; *t_R* (*major*) 12.09 min., *t_R* (*minor*) 13.13 min., 93% *ee*.

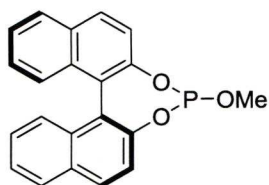
$[\alpha]_{\text{D}}^{20} +24.3$ (*c* = 0.55, CH₂Cl₂), lit.⁵³ $[\alpha]_{\text{D}}^{24} +21.7$ (*c* = 0.55, CH₂Cl₂). Chiral HPLC analysis (25 cm x 4.6 mm Chiralpak AD-H column), 4% isopropanol-hexane at 0.8 mL/min. flow rate, 254 nm; *t_R* (*major*) 12.09 min., *t_R* (*minor*) 13.13 min., 93% *ee*.

¹H NMR (500 MHz, CDCl₃) δ 7.40-7.34 (m, 4H), 7.33-7.29 (m, 1H) 5.83 (ddt, *J* = 17.3, 10.1, 7.3 Hz, 1H), 5.15-5.08 (m, 2H), 4.67 (d, A of AB, *J*_{AB} = 11.6 Hz, 1H), 4.55 (d, B of AB, *J*_{AB} = 11.5 Hz, 1H), 3.69 (d, *J* = 8.8 Hz, 1H), 3.61-3.54 (m, 2H), 2.44-2.40 (m, 1H), 2.39-2.30 (m, 1H), 2.08 (br s, 1H).

¹³C NMR (125 MHz, CDCl₃) δ 138.39 (e), 134.16 (o), 128.62 (o), 127.93 (o), 127.91 (o), 117.71 (e), 79.24 (o), 71.68 (e), 64.16 (e), 35.45 (e).

IR (neat) 3360 (m), 3078 (w), 3033 (w), 2938 (w), 1509 (vs), 1454 (m), 1440 (m), 1232 (s), 1100 (m), 1021 (m), 1035 (s) cm⁻¹.

HRMS (CI, M⁺) calcd for C₁₂H₁₆O₂ 192.1145, found 192.1143.



(S)-4-Methoxydinaphtho[1,2-*f*:2',1'-*d*][1,3,2]dioxaphosphine 41a.

S-(-)-1,1'-Bi-2-naphthol (1.09 g, 3.76 mmol) was suspended in anhydrous dichloromethane (10 mL) under an atmosphere of argon. Triethylamine (1.31 mL, 9.40 mmol) was slowly added with stirring at room temperature. The reaction mixture was then cooled to 0 °C and neat MeOPCl₂ (436 µL, 4.5 mmol) added slowly *via* tared syringe. The reaction mixture was then allowed to warm to room temperature and stirred for *ca.* 30 minutes (t.l.c. control). The reaction was then concentrated *in vacuo* and filtered through a plug of silica gel (eluting with 20% dichloromethane/hexanes) to afford the BINOL-*MeOP* (1.00 g, 77%) as a white crystalline solids, which was further purified by crystallization from dichloromethane/hexanes: $[\alpha]_D^{20} +705$ (*c* = 1.1, CHCl₃).

¹H NMR (500 MHz, CDCl₃) δ 8.02-7.94 (m, 4H), 7.55 (d, *J* = 8.7 Hz, 1H), 7.50-7.29 (m, 7H), 3.59 (d, *J* = 9.8 Hz, 3H).

¹³C NMR (125 MHz, CDCl₃) δ 132.96 (e), 132.74 (e), 131.66 (e), 131.13 (e), 130.57 (o), 130.25 (o), 128.51 (o), 128.43 (o), 127.11 (o), 126.42 (o), 126.40 (o), 125.20 (o), 125.06 (o), 121.96 (o), 121.68 (o), 52.13 (o).

³¹P NMR (125 MHz, CDCl₃) δ 140.03 (s, 1P).

IR (neat) 3058 (w), 3008 (w), 2947 (w), 2846 (w), 1618 (w), 1590 (m), 1505 (m), 1460 (m), 1325 (m), 1227 (s), 1200 (m), 1030 (vs), 947 (vs) cm⁻¹.

HRMS (CI, M⁺) calcd for C₂₁H₁₅O₃P 346.0753, found 346.0760.

4.6 References

1. Seyden-Penne, J. in *Chiral Auxiliaries and Ligands in Asymmetric Synthesis*, Wiley: New York, 1995; Ch. 5, pp. 157-207.
2. For a short review on enantioselective palladium-catalyzed decarboxylative allylic alkylations, see: You, S.-L.; Dai, L.-X. *Angew. Chem. Int. Ed.* **2006**, *45*, 5246.
3. For a short review on enantioselective Tsuji allylations, see: Mohr, J. T.; Stoltz, B. M. *Chem. Asian J.* **2007**, *2*, 1476.
4. Hayashi, T.; Kanehira, K.; Hagihara, T.; Kumada, M. *J. Org. Chem.* **1988**, *53*, 113.
5. (a) Sawamura, M.; Nagata, H.; Sakamoto, H.; Ito, Y. *J. Am. Chem. Soc.* **1992**, *114*, 2586.
(b) Sawamura, M.; Sudoh, M.; Ito, Y. *J. Am. Chem. Soc.* **1996**, *118*, 3309.
(c) Kuwano, R.; Ito, Y. *J. Am. Chem. Soc.* **1999**, *121*, 3236.
(d) Kuwano, R.; Uchida, K.; Ito, Y. *Org. Lett.* **2003**, *5*, 2177.
6. (a) Trost, B. M.; Radinov, R.; Grenzer, E. M. *J. Am. Chem. Soc.* **1997**, *119*, 7879.
(b) Trost, B. M.; Ariza, X. *Angew. Chem. Int. Ed.* **1997**, *36*, 2635.
(c) Trost, B. M.; Schroeder, G. M.; Kristensen, J. *Angew. Chem. Int. Ed.* **2002**, *41*, 3492.
7. You, S.-L.; Hour, X.-L.; Dai, L.-X.; Cao, B.-X.; Sun, J. *Chem. Commun.* **2000**, 1933.
8. (a) Trost, B. M.; Schroeder, G. M. *J. Am. Chem. Soc.* **1999**, *121*, 6759.
(b) Trost, B. M.; Schroeder, G. M. *Chem. Eur. J.* **2005**, *11*, 174.
9. You, S.-L.; Hour, X.-L.; Dai, L.-X.; Zhu, X.-Z. *Org. Lett.* **2001**, *3*, 149.
10. Gnas, Y.; Glorius, F. *Synthesis* **2006**, 1899.
11. Smith, A. B., III; Fukui, M. *J. Am. Chem. Soc.* **1987**, *109*, 1269.
12. (a) Myers, A. G.; Yang, B. H.; Chen, H.; Gleason, J. L. *J. Am. Chem. Soc.* **1994**, *116*, 9361.
(b) Myers, A. G.; Yang, B. H.; Chen, H.; McKinsty, L.; Kopecky, D. J.; Gleason, J. L. *J. Am. Chem. Soc.* **1997**, *119*, 6496.
13. Yamauchi, S.; Sugahara, T.; Akiyama, K.; Maruyama, M.; Kishida, T. *J. Nat. Prod.* **2007**, *70*, 549.

14. Chernega, A. N.; Davies, S. G.; Goodwin, C. J.; Hepworth, D.; Kurosawa, W.; Robers, P. M.; Thomson, J. E. *Org. Lett.* **2009**, *11*, 3254.
15. Behenna, D. C.; Stoltz, B. M. *J. Am. Chem. Soc.* **2004**, *126*, 15044.
16. Trost, B. M.; Xu, J. *J. Am. Chem. Soc.* **2005**, *127*, 2846.
17. Trost, B. M.; Xu, J. *J. Am. Chem. Soc.* **2005**, *127*, 17180.
18. Mohr, J. T.; Behenna, D. C.; Harned, A. M.; Stoltz, B. M. *Angew. Chem. Int. Ed.* **2005**, *44*, 6924.
19. Trost, B. M.; Xu, J.; Reichle, M. *J. Am. Chem. Soc.* **2007**, *129*, 282.
20. Trost, B. M.; Xu, J.; Schmidt, T. *J. Am. Chem. Soc.* **2008**, *130*, 11852.
21. (a) Tsuji, J. in *Palladium Reagents and Catalysts*; Wiley: New York, 1996; Ch. 4, p 290.
- (b) Trost, B. M.; Lee, C. in *Catalytic Asymmetric Synthesis*, 2nd ed.; Ojima, I., Ed.; Wiley-VCH: New York, 2000; Ch. 8, p 593.
- (c) Leahy, D. K.; Evans, P. A. in *Modern Rhodium-Catalyzed Organic Reactions*, Evans, P. A., Ed.; Wiley-VCH: Weinheim, 2005; Ch. 10, p 191 and pertinent references cited therein.
22. Evans, P. A.; Nelson, J. D. *J. Am. Chem. Soc.* **1998**, *120*, 5581.
23. For other examples of enantiospecific allylic substitution reactions, see:
- (a) *Fe*: Zhou, B.; Xu, Y. *J. Org. Chem.* **1988**, *53*, 4419.
- (b) *Ir*: Bartels, B.; Helmchen, G. *Chem. Commun.* **1999**, 741.
- (c) *Ru*: Trost, B. M.; Fraisse, P. L.; Ball, Z. T. *Angew. Chem. Int. Ed.* **2000**, *41*, 1059.
- (d) *Mo*: Faller, J. W.; Sarantopoulos, N. *Organometallics* **2004**, *23*, 2179. And pertinent references cited therein.
24. Hayashi, T.; Yamamoto, A.; Hagihara, T. *J. Org. Chem.* **1986**, *51*, 723.
25. Hayashi, T.; Okada, A.; Suzuka, T.; Kawatsura, M. *Org. Lett.* **2003**, *5*, 1713.
26. For examples of transition metal-catalyzed regio- and enantioselective allylic alkylation reactions of alkyl substituted allylic alcohol derivatives with stabilized carbon nucleophiles, see:
- (a) *Mo*: Glorius, F.; Pfaltz, A. *Org. Lett.* **1999**, *1*, 141.
- (b) *Ir*: Lipowsky, G.; Miller, N.; Helmchen, G. *Angew. Chem. Int. Ed.* **2004**, *43*, 4595.
- (c) *Pd*: Hayashi, T.; Kawatsura, M.; Uozumi, Y. *J. Am. Chem. Soc.* **1998**, *120*, 1681. And pertinent references cited therein.

27. (a) Tsuji, J.; Minami, I.; Shimizu, I. *Tetrahedron Lett.* **1984**, 25, 5157.
 (b) Mini, I.; Shimizu, I.; Tsuji, J. *J. Organomet. Chem.* **1985**, 296, 269.
28. (a) Evans, P. A.; Nelson, J. D. *Tetrahedron Lett.* **1998**, 39, 1725.
 (b) Evans, P. A.; Kennedy, L. J. *J. Org. Lett.* **2000**, 2, 2213.
 (c) Evans, P. A.; Kennedy, L. J. *J. Am. Chem. Soc.* **2001**, 123, 1234.
 (d) Evans, P. A.; Kennedy, L. J. *Tetrahedron Lett.* **2001**, 42, 7015.
29. (a) Evans, P. A.; Leahy, D. K. *J. Am. Chem. Soc.* **2003**, 125, 8974.
 (b) Evans, P. A.; Lawler, M. J. *J. Am. Chem. Soc.* **2004**, 126, 8642.
30. (a) Evans, P. A.; Robinson, J. E.; Nelson, J. D. *J. Am. Chem. Soc.* **1999**, 121, 6761.
 (b) Evans, P. A.; Robinson, J. E. *Org Lett.* **1999**, 1, 1929.
 (c) Evans, P. A.; Robinson, J. E.; Moffett, K. K. *Org. Lett.* **2001**, 3, 3269.
 (d) Evans, P. A.; Clizbe, E. A. *J. Am. Chem. Soc.* **2009**, 131, 8722.
31. (a) Evans, P. A.; Leahy, D. K. *J. Am. Chem. Soc.* **2000**, 122, 5012.
 (b) Evans, P. A.; Leahy, D. K. *J. Am. Chem. Soc.* **2002**, 124, 7882.
 (c) Evans, P. A.; Leahy, D. K.; Sleiker, L. M. *Tetrahedron Asymmetry*, **2003**, 14, 3613.
 (d) Evans, P. A.; Leahy, D. K.; Andrews, W. J.; Uraguchi, D. *Angew. Chem. Int. Ed.* **2004**, 43, 4788.
32. Enyl complexes are, by definition, those that have a discrete σ - and π -metal carbon component within a single ligand. Sharp, P. R. in *Comprehensive ORGANOMETALLIC Chemistry II*, Abel, E. W.; Stone, F. G. A.; Wilkinson, G., Eds.; Pergamon Press: New York, 1995, Ch. 2, p 272.
33. Tanaka, I.; Jin-no, N.; Kushida, T.; Tsutsui, N.; Ashida, T.; Suzuki, H.; Sakurai, J.; Moro-oka, Y.; Ikawa, T. *Bull. Chem. Soc. Jpn.* **1983**, 56, 657.
34. For some related examples of rhodium-catalyzed allylic substitution reactions, see:
 - (a) Takeuchi, R.; Kitamura, N. *New J. Chem.* **1998**, 22, 659.
 - (b) Fagnou, K.; Lautens, M. *Org. Lett.* **2000**, 2, 2319.
 - (c) Muraoka, T.; Matsuda, I.; Itoh, K. *Tetrahedron Lett.* **2000**, 41, 8807.
 - (d) Ashfeld, B. L.; Miller, K. A.; Martin, S. F. *Org. Lett.* **2004**, 6, 1321.
 - (e) Ha, J. D.; Shin, E. Y.; Kang, S. K.; Ahn, J. H.; Choi, J.-K. *Tetrahedron Lett.* **2004**, 45, 4193.
35. Jesson, J. P.; Meakin, P. *J. Am. Chem. Soc.* **1974**, 96, 5760.

36. English, A. D.; Meakin, P.; Jesson, J. P. *J. Am. Chem. Soc.* **1976**, *98*, 7590.
37. Caulton, K. G.; Evans, P. A.; Lawler, M. J.; Leahy, D. K.; Watson, L. A.
Unpublished Results.
38. Lawler, M. J. *The Development of New Rhodium-Catalyzed Allylic Alkylation Reactions and their Application Towards the Total Synthesis of Marinomycin A*. Ph. D. Dissertation, Indiana University, Bloomington, IN, 2008.
39. Brill, T. B.; Landon, S. J. *Chem. Rev.* **1984**, *84*, 577.
40. Koelle, U.; Ruether, T.; Kläui, W. *J. Organomet. Chem.* **1992**, *426*, 99.
41. Stockland, R. A.; Maher, D. L.; Anderson, G. K.; Rath, N. P. *Polyhedron* **1999**, *18*, 1067.
42. Seyden-Penne, J. in *Chiral Auxiliaries and Ligands in Asymmetric Synthesis*, Wiley: New York, 1995; Ch. 5, p 157-207.
43. (a) Frost, C. G.; Howarth, J.; Williams, J. M. J. *Tetrahedron: Asymmetry* **1992**, *3*, 1089.
(b) Trost, B. M.; Van Vranken, D. L. *Chem. Rev.* **1996**, *96*, 395.
(c) Tsuji, J. *Palladium Reagents and Catalysts: Innovations in Organic Synthesis*; Wiley & Sons: Chichester., New York: **1995**.
(d) Trost, B. M.; Less, C. in *Catalytic Asymmetric Synthesis*, 2nd ed.; Ojima, I.; Ed.; Wiley-VCH: New York, 2000, Ch. 8, p 593-649.
44. Evans, P. A.; Clizbe, E. A.; Lawler, M. J. *Unpublished Results*
45. Reetz, M. T.; Mehler, G. *Angew. Chem. Int. Ed.* **2000**, *39*, 3889.
46. For a review on Arbuzov dealkylative reactions involving transition metal phosphite complexes, see: Brill, T. B.; Landon, S. J. *Chem. Rev.* **1984**, *84*, 577.
47. Duan, J. J.-W.; Sprengeler, P. A.; Smith, A. B. *Tetrahedron Lett.* **1992**, *33*, 6439.
48. NMR studies showed no change in enolate formation after 30 minutes.
49. For reviews on Baeyer-Villiger oxidation reactions see:
(a) Renz, M.; Meunier, B. *Eur. J. Org. Chem.* **1999**, 737.
(b) Katsuki, T. *Russ. Chem. Bull. Int. Ed.*, **2004**, *53*, 1859.
(c) Mihovilovic, M. D.; Rudroff, F.; Grötzl, B. *Curr. Org. Chem.* **2004**, *8*, 1057.
50. Göttlich, R.; Yamakoshi, K.; Sasai, H.; Shibasaki, M. *Synlett*, **1997**, 971.
51. Sawada, D.; Kanai, M.; Shibasaki, M. *J. Am. Chem. Soc.* **2000**, *122*, 10521.
52. The ester can be isolated in 83% yield.
53. Crimmins, M. T.; DeBaillie, A. C. *J. Am. Chem. Soc.* **2006**, *128*, 4936.
54. Commercially available.

55. Stoner, E. J.; Peterson, M. J.; Allen, M. S.; DeMattei, J. A.; Haight, A. R.; Leanna, M. R.; Patel, S. R.; Plata, D. J.; Premchandran, R. H.; Rasmussen, M. *J. Org. Chem.* **2003**, *48*, 8847.
56. Bertolini, G.; Pavich, G.; Vergani, B. *J. Org. Chem.* **1998**, *63*, 6031.
57. Iranpoor, N.; Firouzabadi, H.; Khalili, D.; Motevalli, S. *J. Org. Chem.* **2008**, *73*, 4882.
58. Banfi, L.; Basso, A.; Guanti, G.; Paravidino, M.; Riva, R.; Scapolla, C. *Arkivoc* **2006** *vi*, 15.